AD_____

Award Number: DAMD17-99-1-9505

TITLE: Chemoprevention of Ovarian Cancer

PRINCIPAL INVESTIGATOR: David Gershenson, M.D.

CONTRACTING ORGANIZATION: The University of Texas
M.D. Anderson Cancer Center
Houston, TX 77030

REPORT DATE: October 2006

TYPE OF REPORT: Final

PREPARED FOR: U.S. Army Medical Research and Materiel Command
Fort Detrick, Maryland 21702-5012

DISTRIBUTION STATEMENT: Approved for Public Release;
Distribution Unlimited

REPORT DOCUMENTATION PAGE

Form Approved
OMB No. 0704-0188

1. REPORT DATE	2. REPORT TYPE	3. DATES COVERED
01-10-2006	Final	1 Oct 1999 – 30 Sep 2006

4. TITLE AND SUBTITLE

Chemoprevention of Ovarian Cancer

5a. CONTRACT NUMBER

5b. GRANT NUMBER
DAMD17-99-1-9505

5c. PROGRAM ELEMENT NUMBER

6. AUTHOR(S)

David Gershenson, M.D.

E-Mail:

5d. PROJECT NUMBER

5e. TASK NUMBER

5f. WORK UNIT NUMBER

7. PERFORMING ORGANIZATION NAME(S) AND ADDRESS(ES)

The University of Texas
M.D. Anderson Cancer Center
Houston, TX 77030

8. PERFORMING ORGANIZATION REPORT NUMBER

9. SPONSORING / MONITORING AGENCY NAME(S) AND ADDRESS(ES)
U.S. Army Medical Research and Materiel Command
Fort Detrick, Maryland 21702-5012

10. SPONSOR/MONITOR'S ACRONYM(S)

11. SPONSOR/MONITOR'S REPORT NUMBER(S)

12. DISTRIBUTION / AVAILABILITY STATEMENT
Approved for Public Release; Distribution Unlimited

13. SUPPLEMENTARY NOTES
Original contains colored plates: ALL DTIC reproductions will be in black and white.

14. ABSTRACT

The overarching hypothesis of this program project has been that 4-HPR (a synthetic vitamin A) and oral contraceptives (OCP) induce apoptosis, possibly through induction of TGFß production by stromal cells, as well as by direct interaction with the surface epithelial cells, and these two cell types may act synergistically. In Project 1, 19 adult Rhesus monkeys were given 4-HPR, OCP, the combination, or no medication for 3 months. There were consistent differences in the absolute fluorescence intensities and relative contributions noted between pre- and post-drug measurements in each drug group. A second study involving 30 Cynomolgus macaques and using a crossover design has been completed; immunohistochemical analysis of several biomarkers and analysis of the fluorescence spectroscopy data are ongoing. Project 2 was transferred to the University of Arizona with the relocation of Dr. Molly Brewer in 2001. This project was not able to be completed related to multiple regulatory issues and inadequate patient accrual. In Project 3, we have focused on understanding the mechanism of action of 4-HPR in tissue culture using both normal and immortalized epithelial cells. Studies are now complete.

15. SUBJECT TERMS
Ovarian Cancer

16. SECURITY CLASSIFICATION OF:			17. LIMITATION OF ABSTRACT	18. NUMBER OF PAGES	19a. NAME OF RESPONSIBLE PERSON
a. REPORT	b. ABSTRACT	c. THIS PAGE			USAMRMC
U	U	U	UU	110	19b. TELEPHONE NUMBER *(include area code)*

TABLE OF CONTENTS

INTRODUCTION

Ovarian cancer is the second most common malignancy of the female genital tract in the United States. No effective screening tool exists. Consequently, over 70% of cases are diagnosed after the cancer has already spread beyond the ovary. For women with stage III epithelial ovarian cancer—the most common stage—the 5-year survival is no higher than 20%. Clearly, early detection and prevention of this disease are critical issues. The overall goals of this program project are: 1) to develop innovative strategies for prevention of ovarian cancer through the assessment of the potential effect of oral contraceptives (OCP) and retinoids (Vitamin A derivatives) on the ovary and identification of molecular markers and mechanisms associated with the chemopreventive activity of these compounds, and 2) to assemble a multidisciplinary team that will become a world leader in the field of ovarian cancer prevention. A large body of epidemiologic evidence supports the fact that OCP can reduce a woman's risk of ovarian cancer as much as 50%. Similarly, preliminary data from a large Italian randomized chemoprevention trial for secondary breast cancers suggests that retinoids may have preventive activity against ovarian cancer. In addition, retinoids have been shown to induce apoptosis in normal ovarian surface epithelial cells in the laboratory. The major overarching hypothesis of this program project is that 4-HPR and OCP induce apoptosis, possibly through induction of TGFβ production by stromal cells, as well as by direct interaction with the surface epithelial cells, and may act synergistically.

BODY

Project 1

Chemoprevention of Ovarian Cancer Using a *Rhesus* Primate Model

Task 1 Completion of the primate trial and biomarker analysis

Months 1-6

a) Perform pre trial surgery and biopsies;
b) Perform fluorescence and reflectance spectroscopy;
c) Initiate randomization and treatment;
d) Assess markers in histopathology core for biopsies;
e) Analyze fluorescence and reflectance spectroscopy.

Months 6-9

a) Complete treatment;
b) Perform post-trial surgery and biopsies;
c) Perform fluorescence and reflectance spectroscopy;
d) Assess markers in histopathology core for biopsies;
e) Analyze fluorescence and reflectance spectroscopy.

Months 9-12

a) Assess markers in histopathology core for biopsies;
b) Analyze fluorescence and reflectance spectroscopy;
c) Complete analysis of data;
d) Prepare manuscripts and reports for agency;
e) Present data at annual meeting.

All tasks in Project 1 have been completed. Five manuscripts have been submitted for publication; four have been published and one is under revision. All in press and published manuscripts are included in the Appendix.

Nineteen female adult *Rhesus macaques* were included in this study[1,2,3]. This protocol was approved by the Animal Care Use Committee at The University of Texas M. D. Anderson Cancer Center. The animals were given either 4HPR, oral contraceptive (OCP), the combination of

4HPR+OCP, or no medication for 3 months. Exploratory laparotomy was done to assess intermediary biomarkers and to perform fluorescence spectroscopy and a visual analytic tool was developed to explore fluorescence differences grouped by monkey, drug, and time (pre and post-drug): emission spectra were plotted for each group pre and post-drug at each excitation wavelength measured. Means were calculated and overlaid on these plots to view the relationship. The data were examined in 2 methodologies: first, the raw intensities were compared; and, second, emission spectra were normalized to a common wavelength to enhance relative spectral contributions. Using this information, we compared all fluorescence measurements between the first and second measurements using the 2-tailed Student's t test. Significance level was between 0.1 and 0.01 for this exploratory study. Areas where statistically significant differences were observed between the first (pre-drug) and second (post-drug) measurements were identified in the EEM and p values between 0.01 and 0.1 were plotted as contour lines.

Results: The pilot study showed that the animals tolerated the drugs and 2 surgeries without difficulty[(1)]. Rhesus ovaries are easily accessible through a midline laparotomy incision and are 1-1.5 cm in length and 0.75-1 cm in the other two dimensions. There were consistent differences in the absolute fluorescence intensities and relative contributions noted between the pre and post-drug measurements in each drug group as well as the controls. However, the differences noted in the control group attributable to a time effect, were much smaller than those seen in the 3 drug groups. Two main areas of change can be identified. The center of the first area is located at 450nm excitation and 550nm emission wavelength, consistent with the FAD emission peak. This area of fluorescence intensity is increased in the 3 post-drug groups, which correlates with increased FAD presence and decreased FADH. The 4HPR group ($p=0.01$) shows a larger area of difference in pre and post-drug intensity than the OCP group ($p=0.05$-0.07), while the combination group is in between the 4HPR and OCP groups. There are no differences attributable to time seen in the control group in this area of the EEM. The second area is located in the 350nm excitation, 450nm emission which is consistent with the NAD(P)H emission peak. All 4 groups show a decrease in these intensities, which correlates with a decreased NAD(P)H presence and thus an increase in NAD(P) (the oxidized form). However, the OCP group shows the largest change ($p<0.01$) followed by the 4HPR and OCP group, and the control shows the smallest change (very small area of significant change)[(2)].

The markers were not consistently different but there were trends noted. Visual examination of the markers in 2X2 Chi square tables show that EGFR was consistently present, both pre and post-

measurements. Her-2, P21, and P53 were rarely present while BAX was usually present. Estrogen receptors were absent while progesterone receptors were usually present. There were some non-consistent trends in the OCP group with apoptosis and TGFβ more frequently declining after exposure to drug. However, there were no consistent trends attributable to a drug effect, so if trends were actually present, they were not large enough, given our numbers, to have adequate power to detect a difference. In addition, surface epithelium was denuded in 40% of the samples. This loss was attributed to handling of the ovary during the operative procedure and handling in the processing phase. These problems are felt to be corrected in the current study, which has just been started, by minimal handling of the ovary at the time of biopsy, then placing the biopsies directly into formalin rather than wrapping it in gauze as was done in this study.[3]

A second study was done which included 30 monkeys in a crossover study design. Three manuscripts have resulted. Biomarker modulation has been evaluated in immunohistochemistry[3,5] as well as RNA analysis for marker expression.[5] A fifth paper resulting from the second portion of this study showed that there was a significant difference between groups based on chemometric analysis.[5] This manuscript has been provisionally accepted and has been resubmitted with revisions.

Conclusions: The non-human primate is an excellent model for ovarian cancer chemoprevention. Fluorescence spectroscopy may be the best biomarker for following changes from chemopreventive agents optically, but a larger study needs to be done to further evaluate biomarkers.

Project 2

Chemoprevention of Ovarian Cancer: Modulation of Biomarkers in Women at Low- and High-Risk for Ovarian Cancer Using Fenretinide (4-HPR) and Oral Contraceptives

We tried to begin the clinical study on this project while Dr. Brewer was still located at The University of Texas M. D. Anderson Cancer Center. However, approval of the clinical trial was delayed with IRB issues. During the first 3 years of the grant, the protocol underwent several cycles of revision. In 2000, based on a version of the Surgeon General's Human Subject Review Board (HRSSB), a final set of revisions was drafted. Later in 2000, another major revision included the reintroduction of premenopausal women into the 4-HPR group to better balance the final analysis. In 2001, Dr. Molly Brewer relocated to the University of Arizona. After extensive discussions between Dr. Gershenson and Dr. Brewer, Dr. Gershenson and Drs. Howard and Pursley at HRSSB, and Dr. Gershenson and

Dr. Mishra at the DOD, it was decided that Project 2, along with the remaining UT-Austin subcontract, should be transferred to the University of Arizona. This transfer was necessary to accomplish the following goals: 1) The protocol would be more likely to be completed in an expeditious manner because of the greater availability of patients undergoing surgery for benign conditions at that site; 2) Only through this transfer would we be able to accomplish the spectroscopy portion of the trial since Dr. Brewer's and Dr. Utzinger's expertise was required; and 3) Such a transfer would allow Dr. Brewer to complete the work begun at M.D. Anderson Cancer Center and thus enhance her career trajectory.

After the protocol was approved in 2004, we were required to submit the protocol for FDA approval and the protocol was modified to reflect their recommendations. They were hesitant to approve the use of the oral contraceptive immediately prior to surgery. By the time the FDA approved the study, the oral contraceptive that Dr. Brewer negotiated with Ortho-McNeil to formulate had expired. We then had to work with the local drug representative to find adequate amounts of drug for the study. We accrued one patient to the study and had several patients interested in participating. However, our 4HPR expired, and when Dr. Brewer contacted the Division of Cancer Prevention (DCP) at NCI to replace the drug, we were told there was minimal drug available. Dr. Brewer hired a research assistant to accrue patients from the low risk population and that assistance identified 10 patients interested in participating, but by the time Dr. Brewer received their names, they had already scheduled their oophorectomy.

Fox Chase Cancer Center has had a prevention trial using 4-HPR for 5 years and has not accrued many patients due to the regulatory difficulties and the difficulties in convincing patients to postpone their surgery. Dr. Brewer participated in the NCI sponsored trial led by Baylor and accrued 3 patients in the last 4 months of the grant. This project had significant regulatory difficulties and was finally approved by both the University of Arizona and the NCI in April 2006 after 7 years of no accrual. We have learned a significant amount about how to successfully conduct prevention trials for ovarian cancer and they are extremely difficult to do. Identifying the population is time consuming and difficult; convincing healthy patients to delay their surgery and take a drug is difficult. However, the biggest roadblock has been regulatory issues, and in many institutions, the requirements change from year to year. Meeting new requirements for re-approval required 3-6 months of time before the trial was re-approved. With the drug availability problems, these regulatory issues became a major roadblock. We discussed requesting another extension, but when Dr. Brewer decided to relocate to the

University of Connecticut in the fall of 2006, we decided to terminate the project because of poor patient accrual and difficult regulatory issues.

List of personnel receiving partial salary support from this research effort:

Molly Brewer, MD, DVM
Urs Utzinger, PhD
Changping Zou
Kathy Schmidt
Xiomei Li
Brandy Parker
Patricia Konarski
Jean Neukam Feugang
Lourdes Velasco
Carole Meyer
William Brands
Vive Chandrasekharan
Katherine Hunt
Ellen Datena
Jian Wang

Project 3

Chemoprevention of Ovarian Cancer: Molecular Mechanisms and Markers Laboratory Investigations of 4HPR and OCP

Task 1 (Months 1-48)

a) Study the effect of 4-HPR, norethindrone and estradiol, individually and in combination, on explants of normal human ovaries to determine induction of TGFβ in stroma and of apoptosis in the epithelium;
b) Determine the role of TGFβ~ in explants, quantiating the peptide factor and blocking its activity with antibody;
c) Compare 4-HPR to specific RAR and RXR ligands;
d) Study the interaction of TGFβ with 4-HPR, norethindrone and estradiol in normal ovarian surface epithelial cells;
e) Explore expression of proteins that regulate apoptosis in normal ovarian epithelial cells treated with TGFβ, OCP components and 4-HPR;
f) Measure signaling in normal ovarian epithelial cells and in cancer cells treated with TGFβ, 4-HPR and OCP components.

We were not successful with inducing any changes with TGFβ or OCP components. Thus this portion of the work was never published because all results were negative.

Task 2 (Months 3-48)

a) Prepare RNA from normal ovarian epithelial cells treated with TGFβ, 4-HPR, norethindrone or estradiol;
b) Perform clontech arrays;
c) Collaborate with Millenium for EST array analysis;
d) Confirm modulation of gene expression;
e) In situ expression studies with markers for TGFβ response;
f) Functional studies of genes induced by TGFβ;
g) Differential expression of genes before and after TGFβ treatment of normal ovarian epithelial cells and OVCA 420 ovarian cancer cells;
h) Functional studies of response genes that protect against the induction of apoptosis in OVCA 420 cells.

Task 3 (Months 1-20)

a) Determination of the sensitivity and specificty of spectroscopic changes in apoptosis and transformation;
b) Use of fluoresceinated reagents to enhance sensitivity.

All tasks have been completed except for the TGFβ, norethindrone, estradiol, clontech arrays and collaboration with Millenium for EST array analysis.

Task 1

Methods/ Design: We grew NOE cells using the methods described by Nellie Auersberg. Apoptosis is measured with both Tunel (Apoptag®) assay and cell cycle analysis (Apo-Direct®). In attempting to reproduce our data that we reported last year on our first 2 experiments with NOE cells, we have found that the NOE cells do not produce reliable data. Cells from passage # 3 or 4 show excellent induction of apoptosis with both 2 and 5 uM 4HPR with an additive/synergistic effect with 10ng TGFβ. When these cells are cultured at passage 8 they have become relatively resistant to 4HPR and do not show the additive effect from TGFβ. We have then undertaken identification of these cells, staining for cytokeratin, a reliable marker for epithelial cells and vimentin, a marker expressed consistently by stromal or mesenchymal cells and inconsistently by epithelial cells.

IOSE 029 and IOSE 029 cells were established by Nellie Ausberg and her group from British Columbia. NOE cells were collected by scraping the ovary with a scalpel prior to disruption of the blood supply. A piece is then removed and scraped for further harvesting. In the last year we have also experimented with different ways of harvesting cells and find that scraping the surface of the ovary gives the maximal number of epithelial cells; increasing the numbers of cells at the time of initial culture increases the growth rate. Ovaries are handled carefully to avoid disrupting the surface epithelial cells. OVCA 420 cells were used for the positive control. This cell line is an established ovarian cancer cell line that was originally isolated from malignant ascites in the Knapp laboratory by Dr. Robert Bast. The OVCA 420 cells are maintained in MEM medium supplemented with 5% FBS, MEM Non-Essential Amino Acids, 2mM Glutamine, 50ug/ml Gentamicin.

Results: 4-HPR alone induced a high level of apoptosis in some NOE cells but not in others. 4HPR and TGFß combination induced a synergistic rate of apoptosis in some NOE cells but not in others.[3,4]

Table I. Percent Apoptosis

	NOE72	NOE71	NOE95	NOE88 p4	NOE88 p7
Control	5.4	5.2	3.9	5.3	4.5
TGF(10ng/ml)	12	9.3	5	8.1	3
4HPR2uM	38.6	31.5	9.6	7.8	4.3
4HPR5uM	96.3	81	10.4	22.7	3.6
4HPR10uM	98.7	90.4	75.8	48.8	97.1
4HPR(2uM)+TGF	84	96	16.46	9.2	3.2
4HPR(5uM)+TGF	95.5	92.5	9.05	40.9	2.4
4HPR(10uM)+TGF	97.1	89.5	39.5		82.7

Legend: In comparing the sensitivity of NOE, IOSE, and OVCA 420 cells grown with and without TGFβ in varying concentrations of 4HPR normal cells are more sensitive than genetically altered cells which in turn are more active than cells transformed into cancer.

Task 2

Growth inhibitory effects of 4-HPR in NOE, IOSE, and ovarian cancer cells NOE, IOSE, and the three ovarian cancer cell lines were grown in monolayer cultures and treated with different concentrations of 4-HPR (1–10 AM) for 3 days. SkOV3, OVCA420, and OCC-1 were studied to determine which ovarian cancer cell line would serve as the best model for comparison between the normal, premalignant and malignant models. OVCA420 was chosen because it had the most sensitivity to 4-

HPR and, thus, could be evaluated most comparably to the NOE and IOSE cell lines. We first compared low concentrations from 1 to 5 μM of 4-HPR in NOE, IOSE, and OVCA420. Concentrations from 2 to 10 μM 4-HPR were used on the ovarian cancer cells; 10 μM 4-HPR had greater growth inhibitory effects than the lower doses on the cancer cell lines. OVCA420 cells were the most sensitive cell line compared with other two cell lines. The NOE and IOSE cells were very sensitive to 10 μM 4-HPR; almost all cells were killed by day 3. Morphological changes consistent with differentiation (cells become more elongated) were observed along with cell death.

Apoptosis induction by 4-HPR [3,4,6]

To assess other possible mechanisms of 4-HPR in ovarian cells, we analyzed the effects of 4-HPR on the induction of apoptosis in primary culture and cell lines by TdT labeling and flow cytometry. NOE and IOSE cells were treated with 5 μM 4-HPR. DNA content and apoptosis induction were analyzed. The results showed that the apoptotic cell population did not change at this concentration, but a population of cells with hypodiploid (HD) DNA content increased 2- to 8-fold with increasing time of incubation with 5 μM 4-HPR in these cells. NOE, IOSE, and OVCA420 cells were treated with 2, 5, and 10 μM 4-HPR. Apoptosis induction was analyzed at different concentrations and different time points. Results demonstrated that 4-HPR-induced apoptosis was dose dependent in the NOE and OVCA420 cells; apoptosis was less marked in the IOSE cells than in the NOE and OVCA420 cells. 4-HPR-induced apoptosis was also time dependent in ovarian cells. A time course of apoptosis induction was carried out in the NOE, IOSE, and OVCA420 cells when treated with 4-HPR at 10 μM.

Effect of 4-HPR on caspase-3 activity. The 4-HPR effect on caspase-3 activation at different concentrations and different lengths of incubation was measured in NOE, IOSE, and OVCA420 cells. Cells were treated with 2, 5, and 10 μM 4-HPR, and caspase-3 activity was measured at 12, 24, 48, and 72 hours after treatment. The patterns of caspase-3 activity were different in the all three cell types, and 2 μM 4-HPR had little effect on caspase-3 activity in any of the cells. After 24 hours of treatment, an increase in caspase-3 activity was detected in IOSE and OVCA420 cells treated with 10 μM 4 HPR. Caspase-3 activity increased when NOE cells were incubated for 3 days with 10 μM 4-HPR.

Mitochondrial permeability transition (MPT) changes are associated with apoptosis [4,6]

To investigate the mechanism of 4-HPR-induced apoptosis in ovarian cancer cells, experiments were carried out to determine the effect of 4-HPR on MPT in NOE, IOSE and OVCA420 cells. OVCA420 cells had a 4-HPR decreased mitochondrial inner membrane potential, which increased MPT in these cells. An inverse relationship in mitochondrial potential correlated in a dose-dependent manner with both the increase in apoptosis and growth inhibition by 4-HPR in all three cell types.

Modulation of p53 and other gene expressions by 4-HPR in NOE, IOSE, and OVCA420 cells. [4,6]
The effect of 4-HPR on the expression of the apoptosis associated genes p53, p21, and p16 was examined in NOE, IOSE, and OVCA420 cells; p53 expression was detected in the NOE, IOSE, and OVCA420 cells. 4-HPR increased p53 expression in the NOE cells in a dose-dependent manner, but not in IOSE and OVCA420 cells. The expression of the p21 gene was increased in NOE and IOSE cells but was not detectable in OVCA420 cells. The expression of p16 was modulated by 4-HPR in all three cell types.

Task 3 [3,6,7]

Cells are grown and treated as described in Task 1. Fluorescence spectroscopy was measured on a fluorimeter measuring fluorescence emission at 290nm (tryptophane), 350nm (NADH) and 460nm (FAD) excitation. Redox potentials are calculated using FAD/FAD+NADH.

The mechanism of action of 4-HPR's cancer chemoprevention is unclear. It may act partly through modulation of gene expression via retinoid receptors although modulation of retinoid receptors is still controversial. Retinoid receptors are members of the steroid hormone receptor superfamily. Two types of receptors have been identified: retinoic acid receptors (RARs) and retinoid X receptors (RXRs). Each type includes 3 subtypes with distinct amino- and carboxyl-terminal domains. The RARs bind to all trans- retinoic acid (ATRA) and 9-cis-retinoic acid (9cRA), a natural retinoic acid isomer, whereas the RXRs bind only to 9cRA.15–18 RARs can form heterodimers with RXRs and bind to retinoic acid response elements (RAREs), specific DNA sequences that are characterized by direct repeats of (A/G)GGTCA separated by 2 or 5 nucleotides that act as ligand-dependent transcriptional regulators for retinoic acid-responsive genes. Some investigators hypothesize that both ATRA and 4-HPR bind to RARE and regulate gene expression (Zou and Lotan, unpublished data). DNA microarray is widely used in identifying gene expression in normal and cancer cells, and in evaluating molecular changes before and after treatment with drugs. Use of array technology

allows simultaneous evaluation of expression of many (up to thousands) genes. The challenge of such a powerful technique is to develop rigorous, quantitative methods for interpretation of such a wealth of data to identify the expression profile providing maximal biologic information. Techniques based on quantitative optical fluorescence spectroscopy have shown promise to improve detection of epithelial lesions in the colon, cervix, bladder, head and neck, esophagus and other epithelial surfaces. Certain molecules within a cell can be excited using light in the visible and UV range. This principle can be used to optically interrogate endogenous fluorophores with quasi monochromatic excitation light. Natural intracellular fluorophores include electron carriers nicotinamide adenine dinucleotide (NADH) and flavin adenine dinucleotide (FAD) and the aromatic amino acids tryptophan, tyrosine and phenylalanine, as well as structural proteins, each of which have a characteristic wavelength for excitation with an associated characteristic emission. In particular, FAD and NADH can provide an estimate of mitochondrial metabolic activity through an estimate of cellular redox. Fluorescence spectroscopy of endogenous fluorophores has been used as a marker for both early detection and chemoprevention.

Expression of genes altered by 4-HPR in IOSE and OVCA433 cells detected by microarray [5]-
Microarray analysis was performed using total RNA purified from treated and untreated cells. The expression of genes modulated by 4-HPR was evaluated. Genes with a change of expression >2-fold were recorded. In IOSE cells, there was up-regulation of apoptotic related genes and differentiation genes, as well as genes on chromosome 3 and 9. Cancer cells showed upregulation of fewer genes associated with apoptosis and showed similar effects on up-regulation of the antioncogene segment on chromosome 9. Mitochondrial, NAD, NADH and NADPH genes were modulated by 4-HPR in both IOSE and OVCA433 cells. Growth inhibition and apoptosis induction by 4-HPR in ovarian cell lines IOSE and OVCA433 cells treated with different concentrations of 4-HPR, the growth inhibitory effect were compared in monolayer culture. Increasing the concentration of 4-HPR resulted in dose-dependent growth inhibition.

Effect of 4-HPR on Caspase 3 activity and Caspase 3 and 9 protein expression [3,5]
Caspase 3 activity, a central mediator of apoptosis, was measured in IOSE and OVCA433 cells at different time points with different concentration of 4-HPR. Caspase 3 enzyme activity was slightly increased at day 3 in the different concentration groups in OVCA433 cells, which correlated with maximal apoptosis and growth inhibition in these cells. However, Caspase 3 and Caspase 9 protein were not changed by 4-HPR in either IOSE or OVCA433 cells. Effect of 4-HPR on mitochondrial

permeability transition MPT changes are associated with mitochondrial mediated apoptosis. To investigate the mechanism of 4-HPR induced apoptosisin ovarian cancer cells, experiments were carried out to investigate the effect of 4-HPR in mitochondrial potential in IOSE and OVCA433 cells. 4-HPR decreased mitochondrial inner-membrane potential, which increased MPT in IOSE and OVCA433 cells. An inverse relationship in mitochondrial potential correlated in a dose-dependent manner with the increase in apoptosis and growth inhibition by 4-HPR in IOSE and OVCA433 cells, suggesting that these activities were mediated by changes in the mitochondrial membrane.

Expression of apoptosis-associated genes modulated by 4-HPR The effect of 4-HPR on the expression of the apoptosis-associated genes p53, p21, p16 and Rb were examined along with BRCA genes with Western blot and real-time PCR method. The expression of these genes was detected in both IOSE and OVCA433 cells. 4-HPR increased expression after 3 days of treatment in a dose dependent manner in OVCA433 cells, which correlated with the microarray results, showing an increase in human p53 binding protein mRNA in these cells. 4-HPR modulating retinoid receptors and BRCA genes detected by Q-RT-PCR Microarray data showed that retinoid receptors were modulated by 4-HPR. Some receptors were induced by 4-HPR and others were suppressed by 4-HPR. We verified the effect of 4-HPR on receptor expression and induction by Q-RT-PCR. RARs were not significantly changed by 4-HPR in either cell line; however, RXRs were modulated by 4-HPR in IOSE cells. 4-HPR increased RXRa and RXRb expression and decreased RXRg expression in IOSE cells. The expression of RARs and RXRs were not altered by 4-HPR in cancer cells. BRCA1 and BRCA2 gene expressions were decreased by 4-HPR in both IOSE and OVCA433 cells. Real time RT-PCR result was consistent with these results. The IOSE cell line exhibited a highly variable redox related fluorescence ratio compared to the OVCA433 cell line in which the estimated redox increased in a linear fashion. The OVCA433 cells demonstrated a strong sensitivity to 4-HPR treatment and[(6)] illustrates that dose dependence as a linear increase with a slope of 0.0059/lM 4-HPR ($p < 0.001$). An increased redox ratio suggests less oxidative metabolism indicating that the cells may be entering quiescence. When considering the relative ratios to untreated cells, the OVCA433 cells had a higher value at each drug dosage. At higher concentrations of 4-HPR the redox related fluorescence ratio increased for the IOSE cells but never reached the level of the OVCA433 cells. This is consistent with the result that the IOSE cell line was variable in response to 4-HPR treatment.

Administrative Core

The responsibilities of the Administrative Core include provision of leadership and general administration of all activities related to the grant. Dr. David Gershenson, Core Director and Dr. Gordon Mills, Core Co-Director, direct all projects and cores. The administrative assistant works closely with Dr. Gershenson to schedule all meetings, ensure communication between all investigators and prepare required reports and publications.

Task 1 – Months 1-48

Coordinate and schedule all grant-related meetings;

a) Weekly meetings of administrative personnel
b) Monthly meetings of the Executive Committee
c) Monthly research meetings
d) Research retreats (twice annually)
e) Meetings of the Internal Scientific Advisory Committee

Task 2 – Months 1-48

Facilitate interactions and communications between investigators;

a) Ensure interactions between Project Directors and collaborators
b) Ensure interactions between Project Directors
c) Ensure interactions between Project Directors and Core Facility Directors

Task 3 – Months 1-48

Evaluate and track the direction and progress of each project and core;

a) Through daily communications with Project and Core Directors
b) Through monthly meetings of the Executive Committee
c) Through monthly research meetings
d) Through research retreats
e) Through meetings of the Internal Scientific Advisory Committee

Task 4 – Months 1-48

Coordinate quality control and quality assurance;

a) Ensure timely submission of case report forms
b) Audit case report forms for completeness and accuracy Maintain data in central location within the Administrative Core

Task 5 – Months 1-48

Maintain fiscal control;

a) Monitor accounts for expenditures on a periodic basis
b) Communicate any problem or discrepancy with Project or Core Director

Task 6 – Months 11-48

Prepare interim and final reports;

a) Ensure timely submission of all reports to the Administrative Core
b) Edit reports and prepare final drafts in conjunction with Department of Scientific Publications
c) Ensure timely submission of all reports to granting agency
d) Assist -in editing and preparation of all abstracts and manuscripts arising from grant-related research

All tasks in the Administrative Core have been completed.

Histopathology Core

Task 1
A. Project 1 (months 1-12)

a) Process tissue for routine histology (processing, paraffin blocks, H&E stained slides) when received from the investigator over the 12 month period of the project; 160 specimens
b) Evaluate the histomorphology of the specimens (160).
c) Perform immunohistochemistry as the specimens are received over the 12 month period of the project; 1,600 stains (160 specimens x 10 antibodies)
d) Evaluate and quantify the immunohistochemical results; 1600 stains
e) Perform TUNEL assay for apoptosis as the specimens are received over the 12 month period of the project; 160 assays
f) Evaluate and quantify the results of the TUNEL assays; 160 assays
g) Perform in-situ hybridization studies for RARI3 on the specimens from the first five primates during the first six months (20 hybridizations)
h) Evaluate and quantify the in-situ hybridization studies and compare to the IHC results during the first six months.

All tasks have been completed.

B. Project 2 (months 1-48)

a) Process patient specimens for routine histology (processing, paraffin blocks, H&E stained slides) as they are received following surgery over the over the 48 months of the project; 258 specimens each years X3 years (43 patients X 6 specimens each) and 126 specimens in year 4 (21 patients X 6 specimens each) = 900 specimens total
b) Evaluate the histomorphology of the specimens; 258 specimens each year x 3 years and 126 specimens year 4 = 900 total
c) Perform immunohistochemistry as the specimens are received following patient surgery over the 48 months of the project; approximately 2,580 stains each year (258 specimens x 10 stains each) x 3 years and 1260 stains year 4 (126 specimens x 10 stains) = 9000 stains total

d) Evaluate and quantify the immunohistochemical results; 2580 stains each year x 3 years and 1260 stains year 4 = 9,000 total
e) Perform TUNEL assay for apoptosis as the specimens are received over the 48 months of the project; 258 assays each year x 3 years and 126 assays year 4 = 900 . total
f) Evaluate and quantify the results of the TUNEL assays; 258 assays each year x 3 years and 126 assays year 4 = 900 total
g) Perform in-situ hybridization studies for RARI3 on the specimens from the first five patients during the first six months (30 hybridizations)
h) Evaluate and quantify the in-situ hybridization studies and compare to the IHC results during the first six months.

The purpose of the histopathology core is to provide central and uniform histopathologic, immunohistochemical, in-situ hybridization, and apoptosis assay support to the projects in this grant. Histopathologic evaluation, immunohistochemistry, in-situ hybridization, and evaluation of apoptosis have a central role in the design of these projects. The Histopathology Core, in using one central lab for this purpose, will promote uniformity of results by controlling variables associated with specimen handling, and with the technical performance and interpretations of these tests.

For Project 1, biopsies from 19 Rhesus monkeys before treatment and after treatment (for a total of 53 specimens) were fixed, processed, and embedded in paraffin blocks. These blocks were sectioned and stained with hematoxylin and eosin for histologic evaluation. A pathologist associated with the core (M.D.) reviewed these H&E slides. Immunohistochemical staining was then performed on all of the specimens. The markers included BAX, BCL-X, EGFR, ER, Her-2, Ki-67, p21, p53, PR, TGF beta, TGF beta-RI, TGF beta-RII. The 636 immunohistochemical stains were then evaluated and quantified. These results were then given to the investigator. Next the 53 specimens were evaluated for apoptosis using APO-TAG. These assays were reviewed and evaluated with the results forwarded to the investigator. In-situ hybridization for RAR-beta on these specimens is pending.

As Project 2 had just started recruiting patients and no specimens have been processed by the Histopathology Core, this study has now been closed.

In support of the Idea Grant, immunohistochemical staining was reviewed and evaluated on seven cell lines. These cell lines included NOE 71, 72, 78, 79, 80, 83, and 86. Cytospins and smears from each of these lines were stained with AE1/AE3 and vimentin immunohistochemistry. The stains were reviewed and evaluated with the results forwarded to the investigator.

KEY RESEARCH ACCOMPLISHMENTS

Project 1

Chemoprevention of Ovarian Cancer Using a *Rhesus* Primate Model

- Pilot study completed as outlined in the grant
- Fluorescence spectroscopy data analyzed
- Marker data evaluated with statistician
- Second primate trial completed

Project 2

Chemoprevention of Ovarian Cancer: Modulation of Biomarkers in Women at Low- and High-Risk for Ovarian Cancer Using Fenretinide (4-HPR) and Oral Contraceptives

- Poor progress was made on this project due to significant difficulty with regulatory issues and difficulty in accruing patients.

Project 3

Chemoprevention of Ovarian Cancer: Molecular Mechanisms and Markers Laboratory Investigations of 4HPR and OCP

- Development of NOE cell harvest and growth requirements
- Increased experience with handling NOE and IOSE cells
- Development of methods of assaying for apoptosis
- Large amount of data gathered on differential degrees of induction of apoptosis by 4HPR
- Gene modulation from cell exposure to 4-HPR analyzed and published.
- Significant data on fluorescence spectra of cells undergoing apoptosis

REPORTABLE OUTCOMES

Project 1

Chemoprevention of Ovarian Cancer Using a *Rhesus* and Cynomolgus Primate Model

Five manuscripts have been submitted; 4 have been published and 1 is in revision.

I. The Non-Human Primate Model for Ovarian Cancer Chemoprevention, published in Comparative Medicine, outlines the primate as a model.

II. Biomarker Modulation in the Non-Human Rhesus Primate Model for Ovarian Cancer Chemoprevention, published in Cancer Epidemiology Biomarkers and Prevention, evaluates fluorescence spectroscopy as a biomarker for drug activity.

III. Fluorescence Spectroscopy as a Biomarker in a Cellculture and in a Nonhuman Primate Model for Ovarian Cancer Chemopreventive Agents, published in the Journal of Biomedical Optics, evaluates the combination of fluorescence signatures and immunohistochemistry.

IV. Combination of 4-HPR and Oral Contraceptives in Monkey Model of Chemoprevention of Ovarian Cancer, published in Frontiers of BioScience, evaluates gene expression and immunohistochemistry in response to 4HPR and the OCP.

V. Characterization of Chemopreventive Drug Activity in a Non-Human Cynomolgus (Macaca Fascicularis) Primate Model Using Fluorescence Spectroscopy and Chemometric Analysis, in revision and provisionally accepted in Journal of Biomedical Optics.

Project 2

Chemoprevention of Ovarian Cancer: Modulation of Biomarkers in Women at Low- and High-Risk for Ovarian Cancer Using Fenretinide (4-HPR) and Oral Contraceptives

This project underscored the difficulty in regulatory issues and patient accruals in chemoprevention trials. One manuscript has been published:

I. Prevention of Ovarian Cancer: Intraepithelial Neoplasia, published in Clinical Cancer Research.

Project 3

Chemoprevention of Ovarian Cancer: Molecular Mechanisms and Markers Laboratory Investigations of 4HPR and OCP

We have substantial data on cell response to 4HPR and on optical markers as biomarkers for chemoprevention.

Four manuscripts were published.

I. Endogenous Fluorescence Spectroscopy of Cell Suspensions for Chemopreventive Drug Monitoring, published in Photochemistry and Photobiology.
II. In Vitro Model of Normal, Immortalized Ovarian Surface Epithelial Cells and Ovarian Cancer Cells for Chemoprevention of Ovarian Cancer, published in Gynecologic Oncology.
III. 4-HPR Modulates Gene Expression in Ovarian Cells, published in the International Journal of Cancer.
IV. Prevention of Ovarian Cancer: Intraepithelial Neoplasia, published in Clinical Cancer Research.

CONCLUSIONS

In conclusion, the project was ambitious and covered all aspects of investigating prevention modalities with 4HPR, a synthetic retinoid, and the OCP. We evaluated the effect in a primate model with 2 major studies resulting in multiple publications. We are the first to develop fluorescence signatures as a biomarker for drug activity which could serve as a non invasive marker for drug activity. We also correlated these signatures with the effects seen in cells. Our cell work was also novel in that it evaluated the effects of the synthetic retinoid on normal, immortalized, and ovarian cancer cells. We also evaluated gene expression which is instrumental in our understanding of the effect of retinoids on the ovary. Some of the activity is receptor dependent and some is receptor independent which is contrary to other origins of cells.

We were not able to see any effect from the progestin even with 1000X the physiological dose and despite reports to the contrary. These results suggest that the stroma may be essential to the effect of the progestin on the surface epithelial cells. In Projects 1 and 3, we accomplished more that we had proposed doing and had multiple manuscripts. Despite intensive efforts to complete Project 2, the regulatory issues and drug supply of a drug that is not made commercially, nor is it being produced at all, proved a major roadblock. We do, however, plan a follow up study using a commercially available retinoid which will have less regulatory issues. We have also learned through multiple pitfalls, how to best accomplish a clinical prevention trial and will use this information in subsequent trials.

REFERENCES

1. Brewer MA, Baze W, Hill L, Utzinger U, Follen M, Khan-Dawood F, Satterfield W,: Rhesus Macaque model for ovarian cancer chemoprevention, Comparative Medicine 2001; 51:424-29.

2. Brewer MA, Utzinger U, Satterfield W, Gershenson DM, Bast RC, Richards-Kortum R,: Biomarker modulation in a nonhuman Rhesus primate model for ovarian cancer chemoprevention, Cancer Epidemiol Biomarkers Prev 2001; 10: 889-93.

3. Brewer MA, Utzinger U, Li Y, Atkinson EN, Satterfield W, Auersperg N, Richards-Kortum R, Follen M, Bast RC,: Fluorescence spectroscopy as a biomarker in a cell culture and in a nonhuman Rhesus primate model for ovarian cancer chemopreventive agents, Journal of Biomedical Optics 2002; 7:20-26.

4. Brewer MA, Wharton JT, Wang J, McWatters A, Auersperg N, Gershenson DM, Bast RC, Zou CP,: In vitro model of normal, immortalized ovarian surface epithelial and ovarian cancer cells for chemoprevention of ovarian cancer, Gynecol Oncol 2005; 98:182-92.

5. Brewer MA, Ranger-Moore J, Satterfield W, Hao Z, Wang J, Brewer E, Wharton JT, Bast RC, Zou C,: Combination of 4-HPR and oral contraceptive in monkey model of chemoprevention of ovarian cancer, Front Biosci 2007; 12:2260-68.

6. Brewer MA, Kirkpatrick ND, Wharton JT, Wang J, Hatch H, Auersperg N, Utzinger U, Gershenson DM, Bast RC, Zou C,: 4-HPR modulates gene expression in ovarian cells, Int J Cancer 2006; 119:1005-13.

7. Kirkpatrick ND, Zou C, Brewer MA, Brands WR, Drezek RA, Utzinger U,: Endogenous fluorescence spectroscopy of cell suspensions for chemopreventive drug monitoring, Photochem Photobiol 2005; 81:125-34.

8. Brewer MA, Johnson K, Follen M, Gershenson DM, Bast RC,: Prevention of ovarian cancer: intraepithelial neoplasia, Clinical Cancer Research 2003; 9:20-30.

APPENDIX

1. Brewer MA, Baze W, Hill L, Utzinger U, Follen M, Khan-Dawood F, Satterfield W. Rhesus Macaque Model for Ovarian Cancer Chemoprevention. Comparative Medicine 51:424-429, 2001.

2. Brewer MA, Utzinger U, Satterfield W, Gershenson DM, Bast RC, Richards-Kortum R, Follen M. Biomarker Modulation in a Nonhuman Rhesus Primate Model for Ovarian Cancer Chemoprevention. Cancer Epidemiology Biomarkers Prevention 10: 889-93, 2001.

3. Brewer MA, Utzinger U, Li Y, Atkinson EN, Satterfield W, Auersperg N, Richards-Kortum R, Follen M, Bast RC. Fluorescence Spectroscopy as a Biomarker in a Cell Culture and in a Nonhuman Rhesus Primate Model for Ovarian Cancer Chemopreventive Agents. Journal of Biomedical Optics 7:20-26, 2002.

4. Brewer MA, Johnson K, Follen M, Gershenson DM, Bast RC. Prevention of Ovarian Cancer: Intraepithelial Neoplasia. Clinical Cancer Research 9:20-30, 2003.

5. Kirkpatrick ND, Zou C, Brewer MA, Brands WR, Drezek RA, Utzinger U. Endogenous Fluorescence Spectroscopy of Cell Suspensions for Chemopreventive Drug Monitoring. Photochemistry and Photobiology 81:125-134, 2005.

6. Brewer MA, Wharton JT, Wang J, McWatters A, Auersperg N, Gershenson DM, Bast RC, Zou CP. In Vitro Model of Normal, Immortalized Ovarian Surface Epithelial and Ovarian Cancer Cells for Chemoprevention of Ovarian Cancer. Gynecologic Oncology 98:182-192, 2005.

7. Brewer MA, Kirkpatrick ND, Wharton JT, Wang J, Hatch H, Auersperg N, Utzinger U, Gershenson DM, Bast RC, Zou C. 4-HPR Modulates Gene Expression in Ovarian Cells. International Journal of Cancer 119:1005-1013, 2006.

8. Brewer MA, Ranger-Moore J, Satterfield W, Hao Z, Wang J, Brewer E, Wharton JT, Bast RC, Zou C. Combination of 4-HPR and Oral Contraceptive in Monkey Model of Chemoprevention of Ovarian Cancer. Frontiers in Bioscience 12, 2260-2268, 2007.

Comparative Medicine
Copyright 2001
by the American Association for Laboratory Animal Science

Vol 51, No 5
October 2001
Pages 424-429

Rhesus Macaque Model for Ovarian Cancer Chemoprevention

Molly Brewer, DVM, MD,[2,3*] Wallace Baze, DVM, PhD,[1] Lori Hill, DVM,[1] Urs Utzinger, PhD,[4] J. Taylor Wharton, MD,[2] Michele Follen, MD,[2,3] Firyl Khan-Dawood, PhD,[3] and William Satterfield, DVM[1]

Purpose: **The objective of the study reported here was to explore whether a nonhuman primate model could be developed for chemoprevention of ovarian cancer.**

Methods: **An initial feasibility trial was done with three monkeys to determine tolerance for these drugs and for acquisition of surgical ovarian biopsy specimens. In the study, 19 female adult *Macacca mulatta* (rhesus macaques) were given fenretinide (4HPR) oral contraceptive (OCP), the combination of 4HPR+OCP, or no medication for three months. Laparotomy was performed before and after drug administration, and ovarian biopsy specimens were obtained to evaluate the potential for this animal as a model for ovarian cancer chemoprevention, as well as evaluating fluorescence spectroscopy and other potential biomarkers for ovarian cancer prevention studies.**

Results: **The monkeys tolerated the drugs, surgeries, and acquisition of multiple ovarian biopsy specimens with resultant minimal morbidity. On initial data analysis, fluorescence spectroscopy was the marker that appeared the most promising.**

Conclusions: **On the basis of results of this study, this model merits further investigation. The rhesus monkey is an excellent candidate for a nonhuman primate model for ovarian cancer chemoprevention.**

Epithelial ovarian cancer has the highest mortality of any of the gynecologic cancers, with a five-year survival rate ≤ 30% despite aggressive treatment. Seventy percent of diagnosed ovarian cancers are associated with widespread intra-abdominal disease or distant metastases, which accounts for their dismal prognosis. Even cancers limited to the pelvis have a five-year survival rate of only 50% (1). Thus, prevention, including use of chemoprevention agents, merits at least as much attention as does treatment of this disease.

Chemoprevention involves administering medications to normal or undiseased hosts to prevent or delay the onset of cancer (2). Intermediary biomarkers are measured to determine markers for prevention, as well as gain knowledge about the mechanism of drug action. Limitations to studying chemoprevention agents in humans include the difficulty in accessing the ovaries in their intraperitoneal location, and, unlike the uterine cervix or endometrium, the necessity for an anesthetic and an operative procedure to biopsy the ovaries. Invasive procedures performed on women without disease raise ethical concerns that excess risks are not outweighed by potential benefits; thus, animal prevention models in which these procedures can be performed are needed. Animal models are developed to reconcile biologic phenomena between species (3) and to allow extrapolation of knowledge from one species to another, usually animal to human. An appropriate model should include: the ability to accurately mimic the desired function or disease of humans in the animal; the availability of the animal to many investigators; an animal that is easily handled; an animal that can survive sufficiently long for studies to be completed; an animal that can fit into available housing facilities; an animal of sufficient size to provide multiple samples; and an animal who can produce enough offspring to maintain availability of the species (3).

Use of tissue culture and small animal models can help elucidate molecular mechanisms and develop end-point biomarkers for chemoprevention studies. However, limitations exist to both of these models. Cell culture, although an environment which can be maximally manipulated, lacks the cell interactions present in most tissues, such as the interaction between the ovarian epithelial and stromal cells and the ovarian epithelial cells and the mesothelial cells in the peritoneal cavity. With increasing passage of time, ovarian epithelial cells more closely resemble mesenchymal cells morphologically and lose the expression of cell surface markers (cytokeratin). In addition, they have a different sensitivity to retinoids (Brewer: unpublished data). Small animal models are useful for understanding basic mechanisms, but they have different hormonal pathways and histochemical markers in the ovary than do humans; thus, histochemical and optical markers may differ substantially from those of women. The nonhuman primates are the mammals with the most similar reproductive anatomy and menstrual pattern as the human (3-5), and the primate ovary behaves in a manner histochemically and hormonally similar to the human ovary (6, 7). Use of an animal model is ideal to understand the mechanism of action, the optimal dose, and the optimal duration, because it avoids the pitfalls of tissue culture in the laboratory and clinical trials in humans.

We chose to study the rhesus macaque because of its availability, cost, and ease of handling. We treated the monkeys with oral contraceptives (OCP) and the retinoid N-(4-hydroxyphenyl) retinamide (4HPR), both of which may prevent ovarian cancer in women, and we examined biomarkers in ovarian biopsy specimens to assess the animals as a nonhuman primate model for the chemoprevention of ovarian cancer.

Received: 3/02/01. Revision requested: 4/20/01. Accepted: 7/26/01.
[1]Department of Veterinary Sciences Science Park and [2]Department of Gynecologic Oncology, The University of Texas M. D. Anderson Cancer Center, Houston, Texas, 77030,[3]Department of Obstetrics, Gynecology and Reproductive Science, The University of Texas Medical School, Houston Texas 77030, and [4]Biomedical Engineering Program, The University of Texas at Austin, Austin, Texas, 78712.
**Corresponding author.*

Materials and Methods

Animal Care. Twenty-one female adult rhesus monkeys were assembled for the study from monkeys that had been culled from the specific-pathogen-free (SPF) breeding colony at the Department of Veterinary Sciences, (Bastrop, Tex.) due to their viral status, reproductive history, or social incompatibilities (Table 1). The animals were examined and determined to be in good physical condition. All animals had been reproductively capable and had one or more offspring. The protocol was approved by the Animal Care Use Committee at The University of Texas M. D. Anderson Cancer Center and was conducted at the Department of Veterinary Sciences campus, an approved facility of the Association for the Assessment and Accreditation of Laboratory Animal Care International. Experiments were performed in accordance with the *Guide for the Care and Use of Laboratory Animals* (8). Monkeys were housed individually in open-air cages. Handlers cared for all animals twice daily and recorded their menstrual cycle (Table 2). Three animals were initially used for a feasibility study to develop techniques for animal handling and tissue handling. The remaining 19 animals were used in a three-month pilot study to assess whether a chemoprevention model could be established.

Table 1. Reproductive history and reasons for culling of monkeys from the specific-pathogen-free (SPF) colony

Monkey No. Treated	Age	No. of Offspring	Comments
L749	11	4	Birthing problems
L923	10	4	Prior viral exposure
J377	5	0	Diarrhea
L967	9	3	HBV indeterminate
J261	6	2	HBV indeterminate
J153	7	4	Social problem
J55	8	4	2 stillborn infants—social problem
J243	6	2	Diarrhea
L753	11	5	No baby for 3 years
J189	7	1	No baby for 3 years
L783	11	5	Diarrhea
L581	13	2	No baby for 3 years
L785	11	4	Obese — no baby in 3 years
L809	11	2	Poor breeder
J571	3	2	HBV positive
Controls			
J465	4	1	STLV indeterminate
J371	5	2	HBV indeterminate
J269	6	3	HBV indeterminate
L937	10	6	HBV indeterminate

HBV = Herpes B Virus; STLV = Simian T cell Lymphotrophic Virus.

Table 2. Monkey demographics of the study

Monkey	Drug	Weight (kg)	No. of menses	Herpesvirus status
J153	4HPR	5.3	2	Negative
J243	4HPR	5.8	1	Negative
L753	4HPR	6.3	1	Negative
J189	4HPR	8.1	3	Negative
L967	OCP	5.1	1	Indeterminate
J261	OCP	5.2	3	Indeterminate
L749	OCP	6.8	1	Negative
L923	OCP	5.9	2	Negative
J377	OCP	4.6	3	Negative
J465	Control	2.06	2	Indeterminate
J371	Control	5.6	2	Indeterminate
J269	Control	5.6	1	Indeterminate
J937	Control	5.8	4	Indeterminate
L783	4HPR+OCP	6.3	2	Negative
L581	4HPR+OCP	6.2	3	Negative
L785	4HPR+OCP	10.5	2	Negative
L809	4HPR+OCP	5.8	3	Negative
J511	4HPR+OCP	6.3	1	Negative

4HPR = Fenretinide; OCP = Ortho-Novum.

Drug administration. Animals were fed medication once daily that was formulated into a palatable treat by a veterinary pharmacist. Doses of 4HPR (Fenretide: RW Johnson Pharmaceutical Research Institute, San Diego, Calif.) and OCP (Ortho-McNeil Pharmaceuticals, Rareton, N.J.) were calculated by use of allometric scaling involving a dose based on body weight and basal metabolic rate of the subject (9). The OCP was Ortho-Novum 1/35 with 1 mg of Norethindrone and 35 μg of ethinyl estradiol in each pill, based on a human dose of one pill daily. With allometric scaling, the monkeys on OCP received 0.2 mg of Norethindrone and 0.07 mg of ethinyl estradiol. The 4-HPR dose, 35 μg, was calculated in similar manner from the standard human dose of 200 mg daily, which is well tolerated with minimal side effects.

Fluorescence emission. Fluorescence emission was measured from each site prior to biopsy. Characterization of the fluorescence properties of an unknown sample requires measurement of a fluorescence excitation and emission matrix (EEM), with the fluorescence intensity recorded as a function of excitation and emission wavelengths (10). Our fast EEM system consists of a Xenon arc lamp coupled to a scanning spectrometer and a 295-nm long-pass filter that provide broadband illumination. A fiber optic probe that directs monochromatic light to the tissue, collects emitted fluorescence light and delivers it to an imaging spectrograph and a charge couple device (CCD) camera. Fluorescence emission spectra were collected sequentially at 18 excitation wavelengths ranging from 350 to 500 nm and were assembled into fluorescence EEM's.

Laparotomy and biopsy. Prior to starting medication and after either 60-90 days on medication, monkeys underwent laparotomy with spectroscopy and ovarian biopsy. Food was withheld from monkeys for 12 h prior to surgery. They were then anesthetized by intramuscular administration of tiletamine HCl/zolazepam HCl (5 mg/kg of body weight; Telazol, Fort Dodge Laboratories, Inc., Fort Dodge, Iowa). Once sedated, monkeys were intubated and maintained on 2.0 to 2.5% isoflurane gas. (IsoFlo, USP, Abbott Laboratories, North Chicago, Ill.) delivered by a precision vaporizer with oxygen (Fortec, Fraser Harlake, Orchard Park, N.Y.). All animals recovered without complication from the surgery and anesthesia. Several 2-mm biopsy specimens were taken from the area optically imaged from the left ovary (pre-drug laparotomy) and from the right ovary (post-drug laparotomy).

Biopsy and analysis. Biopsy specimens were fixed in neutral-buffered 10% formalin, embedded in paraffin, cut into 4-mm sections, stained with hematoxylin and eosin (H&E), and examined under light microscopy by a board-certified veterinary pathologist (WB). Sections were evaluated for morphologic characteristics, pathologic changes, and biomarkers. Biomarkers chosen for this trial include markers of neoplastic phenotype (p53), proliferative markers (Ki67), markers of intact response pathways (estrogen, progesterone and nuclear retinoid receptors), or inducible growth-regulatory molecules (apoptosis, TGFβ, and receptors, HER-2, BAX, BCLx). Apoptosis was evaluated by use of Apotag (Phoenix Flow Systems, Inc., San Diego, Calif.). The remainder of the markers were either mouse or rabbit antibodies that were evaluated by use of immunohistochemical analysis in standard manner. The choice of these markers was based on results of prior studies (apoptotic, proliferative, neoplastic, and retinoid markers), known pathways (retinoid markers), and hypothesized mechanisms (TGF and receptors, p21).

Optical spectroscopy was measured as a marker that identifies metabolic changes.

Estimates were made of the numbers of ova, developing and atretic follicles, corpora lutea, corpora albicans, and surface epithelial cells. Previous surgical biopsies have adequately documented the parenchyma of the ovary to include the cortex, medulla, and vasculature. However, of particular interest, has been evaluation (e.g., apoptosis index) of the surface epithelium of the ovary. To date, biopsy specimens have inconsistently contained these cells; thus, in developing this model in primates, we needed to further investigate techniques of ovarian surface epithelial cell preservation. To do so, we performed imprints and scrapings of ovaries from sheep, as this was the most available animal for necropsy. Clean glass microscope slide were touched to blood- and tissue fluid-free surfaces of the ovaries, and one or multiple imprints were taken. Imprints were then fixed with a cytologic fixative containing alcohol, acetone, and Carbowax 1540. They were air dried, and stained with Diff-Quik, Giemsa, or H&E. Scrapings were collected, using a clean scalpel blade pulled across the ovary perpendicular to the surface. The collected material was then transferred to a clean glass microscope slide and fixed and stained as described for imprints.

Results

During the two-month feasibility study and the three-month pilot study, all monkeys took their medication daily in the formulated treat and tolerated both surgical procedures without complications. In the feasibility study, ovarian biopsy specimens taken after two months of medication had ovulatory activity in various stages that ranged from developing follicles to resolving corpus lutea. One monkey receiving OCP and one receiving OCP+4HPR had evidence of recent ovulation, with a corpus luteum being present. Although it is unclear from human literature whether ovulation suppression is necessary to prevent ovarian cancer, we assumed that suppression of ovulation is one of the mechanisms by which prevention occurs. We also assumed that the primate ovary would receive approximately the same dose of drug as would the human ovary, so either a longer duration or a higher dose of OCP was needed to suppress ovulation. Rather than change the dose on the basis of such small sample size, duration of the study was changed. The larger study was extended to three months, and paired samples for determination of progesterone concentration were taken two weeks apart to help determine whether ovulation was occurring. All monkeys in the control group had an increase in progesterone concentration (> 2 ng/ml), which suggests that ovulation was occurring in all monkeys (Table 3). In the combination group, one of five monkeys did not experience an increase in progesterone concentration, and in the OCP group, two of five monkeys did not have an increase, suggesting that these animals did not ovulate. Menses did not appear to be a predictable way of determining ovulation as it was sporadic in all groups, possibly attributable to the poor breeding status of these monkeys (Table 1).

Table 3. Paired samples taken two weeks apart for progesterone determination. A twofold change is thought to indicate ovulation in women

Monkey	Group	Progesterone (1 ng/dl)	Progesterone (2 ng/dl)
L967	OCP	< 0.2	6.03
J261	OCP	0.48	4.97
L749	OCP	0.32	4.77
L923	OCP	< 0.2	< 0.2
J377	OCP	< 0.2	1.22
J465	Control	4.26	0.45
J371	Control	2.78	0.94
J269	Control	0.22	2.83
J937	Control	< 0.2	4.47
L783	4HPR+OCP	0.48	< 0.2
L581	4HPR+OCP	< 0.2	9.58
L785	4HPR+OCP	< 0.2	2.32
L809	4HPR+OCP	0.21	4.96
J511	4HPR+OCP	7.49	0.2

See Table 2 for key.

Some biopsy specimens had nicely preserved surface epithelium (Fig. 1a), whereas others lacked appreciable areas of epithelium (Fig. 1b). It is difficult to evaluate the surface epithelium in women because its presence on pathology specimens is sporadic. Therefore, we undertook a pilot study to determine the best handling and processing of ovaries to preserve their surface epithelium. Scraping the surface of the ovary prior to biopsy was the most reliable method of harvesting ovarian surface epithelial cells, although they lost their orientation to the remainder of the ovary and any proliferation of the epithelium would not be apparent. Biopsy of the ovary without rubbing off the surface epithelium requires minimal contact with the ovary and careful handling by the surgeon and the pathologist. Thus, due to poor preservation of the surface epithelium, we modified the biopsy technique by placing specimens immediately into formalin without handling by either the surgeon or pathologist; both techniques added to the preservation of the surface epithelium. These techniques will be important as we further develop this model.

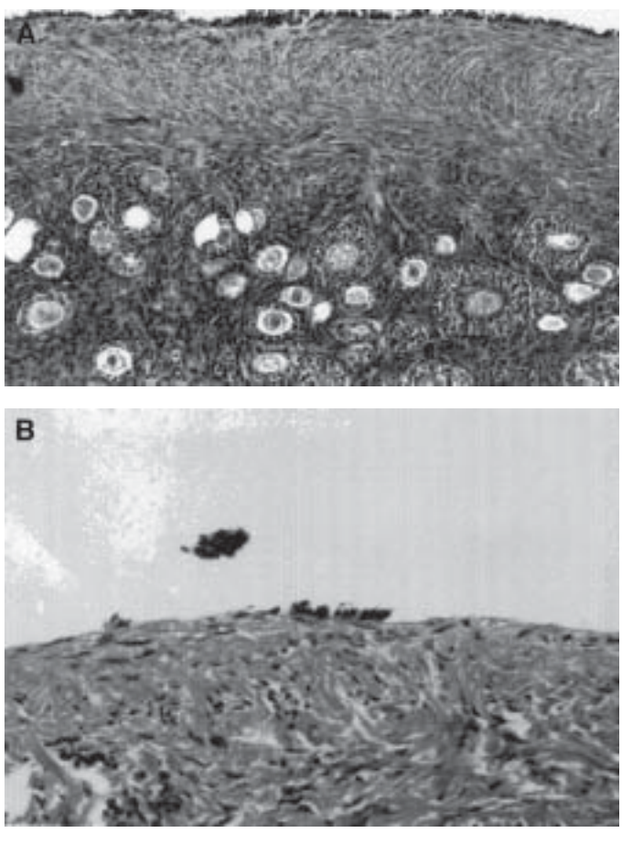

Figure 1. Photomicrographs of sections of rhesus ovaries: (A) well preserved ovarian surface epithelium and (B) poorly preserved ovarian surface epithelium. Hemotoxylin and Eosin (H & E). ×7.6 magnification.

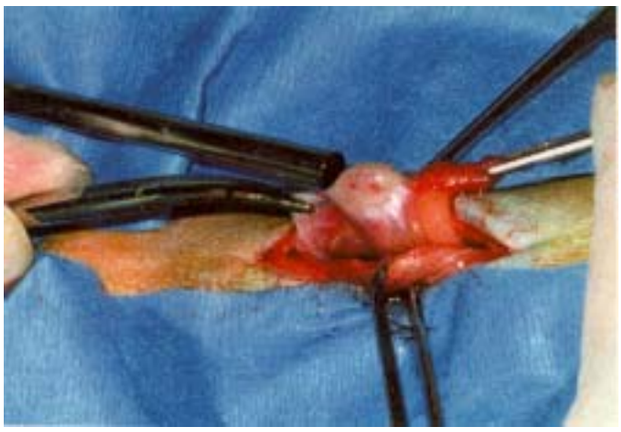

Figure 2. Healed defect in ovary three months after biopsy. Spectroscopy probe is located adjacent and to the left of the ovary.

For biopsy specimens with surface epithelium, cell counts averaged 100 to 200 cells. Likewise, other morphologic characteristics of the ovaries (e.g., follicle formation, corpora lutea) were not significantly different among groups. Rhesus ovaries were easily accessible through a midline laparotomy incision and were 1.0 to 1.5 cm long by 0.75 to 1 cm in the other two dimensions. At the time of the second surgery, the scar from the previous biopsy was completely healed, and there was a small visible area < 1 mm where the defect had filled in (Fig. 2) Biopsy of this area revealed some disorganization of the underlying stroma, but otherwise microscopic he aling of the defect was observed. Areas of viable follicular activity were found adjacent to the defect, suggesting that the ovary healed well after a small biopsy specimen had been taken.

Markers were evaluated visually in a 2 × 2 table. Missing data in the 4HPR as well as the OCP group precluded any data analysis as there were only two monkeys with histochemical marker data in the 4HPR and 4 in the OCP group due to difficulties in slide preparation. The markers did not indicate consistent changes in response to drug, but there were trends in marker expression. Endothelial growth factor receptor (EGFR, whose overexpression is associated with neoplasia) was consistently present in pre- and post-drug measurements, Her-2 (proto-oncogene), p21 (growth inhibitor), and p53 (G1 arrest) were rarely present in either group; however, BAX (pro-apoptotic) was usually present and did not change in response to drug exposure. Estrogen receptors were absent, but progesterone receptors were usually present and did not change in response to drug exposure. Apoptosis was present in two monkeys of the OCP group, and TGFβ values decreased after exposure to drug. However, two other 2 monkeys did not have either marker present before or after drug exposure. Therefore, if trends were actually present, they were not sufficiently large, given our numbers, to have adequate power to detect a difference statistically.

The spectroscopy data is presented in more detail in a separate publication (11). There were consistent differences in the absolute fluorescence intensities, and relative contributions were noted between the pre- and post-drug measurements in each drug group as well as the controls. Two main areas of change can be identified. The first area was located in the 350-nm excitation, 450-nm emission wavelength, which is consistent with

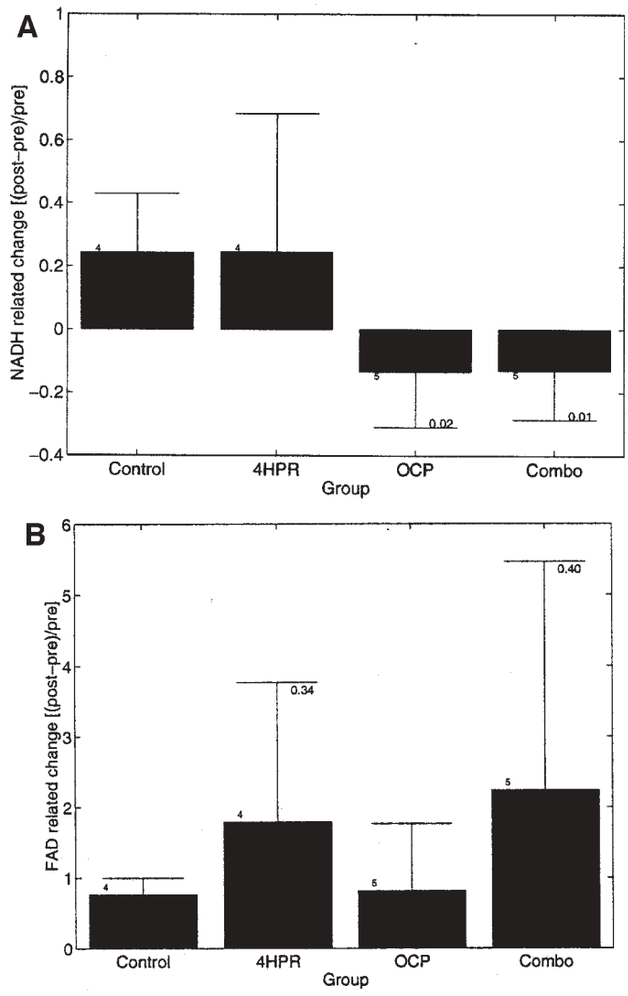

Figure 3. Ovaries with an NADH-related change intensity at 330 nm excitation, 460 emission (A) and an FAD-related change intensity at 460nm emission, 520 emission (B) 4HPR = Fenretinide; OCP = Ortho-Novum.

the NAD(P)H emission peak (Fig. 3a). The 4HPR and the control groups both had the same mean increase in intensity in the NAD(P)H area of the spectrum. The OCP and combination groups had decreased intensity corresponding to an increase in NAD(P) (the oxidized form).

The second area was located at 450-nm excitation, 550-nm emission wavelength, consistent with the FAD emission peak. The intensity in this area of the EEM was increased in all four groups (Fig. 3b). However, the control and the OCP groups had minimal change, compared with that of the 4HPR and the combination groups, suggesting a different effect from these two drugs.

Discussion

Results of this study indicate that the nonhuman primate is a viable model for developing a better understanding of the drugs involved in the study and other potential agents to prevent ovarian cancer. Because there are no ethical constraints on study design, drug doses and duration, and numbers and extent of procedures, the study can be tailored to optimize scientific meth-

ods. These monkeys easily tolerated two surgeries, and the ovaries healed between biopsies. In addition, promising results were observed by us of spectroscopy and preservation of the surface epithelium has been optimized.

Chemoprevention studies require a normal host to be given a drug to prevent a disease (2). Models with compromised immune systems, such as the transgenic mouse, cannot approximate normal hosts and are better used to understand cancer development. Nonhuman primates have numerous biological similarities to humans, reflecting a close genetic relationship, and can be manipulated by doing a before-and-after drug study, which has the advantage of controlling for intra-species variation and the time effect, something for which historical control or separate control groups cannot account. Cost of procuring and caring for these animals, low reproductive rates, long developmental periods, and relative scarcity of these animals limit their use as animal models for human diseases. However, the close genetic similarity and, thus, the high probability of producing results that can be extrapolated to humans more than overcomes the aforementioned limitations (3). The rhesus macaque was chosen because of its availability, cost, and ease of handling.

Epithelial ovarian cancers arise from the surface epithelial cells, particular those lining the crypts or the inclusion cysts within the ovarian stroma (11). The cancers are thought to arise from a neoplastic process that develops as a series of mutations in these cells. If a mutation occurs in the apoptotic pathway, mutated cells would retain the ability to divide and further mutate; this is one of the hypothesized mechanisms for these cancers to develop. Thus, characterization of the epithelial cells is a critical part of this model and, in this study, we overcame the difficulties of preserving the epithelial cells. We also developed a technique of scrapings followed by freezing the cells to allow further evaluation of markers as new techniques emerge.

Results of epidemiologic and experimental studies suggest that oral contraceptives (OCP) (12-14) and N-(4-hydroxyphenyl) retinamide (4HPR) (15) may reduce the risk of ovarian cancer, but mechanisms underlying the chemopreventive activity of these agents are not well understood. One in vivo study indicated the rate of apoptosis of ovarian surface epithelial cells to be significantly different in OCP (14.5%)- and progestin (24.9%)-treated monkeys, compared with controls (3.8%), suggesting that one of the mechanisms of OCP prevention of ovarian cancer may be induction of apoptosis (16). The retinoids constitute another family of chemopreventive agents that can induce apoptosis, inhibit proliferation, modulate differentiation, and prevent progression of carcinoma in-situ (17, 19). However, in vivo biomarker development is an integral part of development of any chemopreventive agents because the duration necessary to prevent disease is so long. These, however, are difficult to develop in the human ovary, because of the inherent difficulty in accessing the ovary to obtain pre- and post-drug specimens. The histochemistry of the nonhuman primate ovary and the human ovary indicates remarkable similarities (22, 23) and these non human primate models will be more useful than human models for investigation of the action of these drugs. Although marker development is not the focus of this report, all immunohistochemical techniques that are used in women were technically feasible in the monkey. It is unclear at the present time which markers are important in cancer prevention of the ovary. Optics is a promising procedure (11, 20, 21), with fluorescence intensity results indicating a difference between drug groups. Study of apoptosis is also promising (20), but depends on preservation of surface epithelium; techniques developed in this pilot study will improve preservation of surface epithelium. Generally, proliferation markers might be expected to be reduced in prevention trials as these are usually up-regulated in cancers. Retinoid markers are being studied in cell culture in our laboratory and will be adapted to further primate trials as more information is available. A second primate trial has been started with larger numbers in each group to overcome the statistical limitations evident in this pilot study.

The rhesus macaque could serve as an excellent model for the study of chemoprevention of ovarian cancer. These monkeys are close to humans in their cyclic menstrual pattern and ovarian function, structure, histochemistry, and response to hormones. Their ovaries are readily accessible and continue to function after multiple biopsies, and the monkeys tolerate the drugs and combination of drugs without apparent toxicosis. In addition, spectroscopy is being developed (11) as a biomarker for chemoprevention, and may prove helpful in assessing drug response. The ability to develop a nonhuman primate model for chemoprevention of ovarian cancer will allow us to make substantial progress in understanding how chemopreventive drugs affect the ovary and how to develop rational chemoprevention strategies for this devastating disease.

Acknowledgments

The authors thank Gerald Costello for preparation of the tissues used in the study, as well the valuable assistance of the animal care staff of the Department of Veterinary Science, MD Anderson Cancer Center. This work was supported by funding from the Sandra G. Davis Ovarian Cancer Research Program, Department of Defense CDRMP, J. Taylor Wharton.

References

1. **Hoskins, W. J.** 1995. Prospective on ovarian cancer: Why prevent? J. Cell Biochem. Suppl. **23:**189-199.
2. **Kelloff, G. J., C. W. Boone, J. A. Crowell, S. G. Nayfield, E. Hawk, V. E. Steele, R. A. Lubet, and C. C. Sigman.** 1995. Strategies for phase II cancer chemoprevention trials: cervix, endometrium, and ovary. J. Cellular Biochem. Suppl. **23:**1-9.
3. **Lewis, S. M., and J. H. Carraway.** 1992. Large animal models of human disease. Lab Animal **21:**22-29.
4. **Hendrickx, A. G., and W. R. Dukelow.** 1995. Reproductive biology. *In* B. T. Bennet, C. Abee, R. Hendrickson (ed.), Nonhuman primates in biomedical research: biology and management. Academic Press Inc., San Diego, Calif., N.Y., London, Tokyo, Toronto.
5. **Ford, E. W., J. A. Roberts, J. L. Suthers.** 1998. Genital system. *In* B. T. Bennet, C. Abee, R. Hendrickson (ed.), Nonhuman primates in biomedical research: diseases. Academic Press Inc., San Diego, Calif., N.Y., London, Tokyo, Toronto.
6. **Pauerstein, C. J., C. A. Eddy, H. D. Croxatto, R. Hess, T. M. Siler-Khodr, and H. B. Croxatto.** 1978. Temporal relationships of estrogen, progesterone and luteinizing hormone levels to ovulation in women and infrahuman primates. Am. J. Obstet. Gynecol.**130:** 876-886.
7. **Walker, M. L., T. P. Gordon, and M. E. Wilson.** 1983. Menstrual cycle characteristics of seasonally breeding rhesus monkeys. Biol. Reprod. **29:**841-848.
8. **Koering, M. J., D. R. Danforth, and G. D. Hodgen.** 1991. Early folliculogenesis in primate ovaries: testing the role of estrogen. Biol. Reprod. **45:**890-897.
9. **Guide for the Care and Use of Laboratory Animals.** 1996. Appendix A. Institute of Laboratory Animal Resources, National Academy Press, Washington.

10. **Sedgwick, C. J., and M. A. Pokras.** 1988. Extrapolating rational drug doses and treatment by allometric scaling, p. 156-157. Proc. Annu. Meet. Am. Anim. Hosp. Assoc.
11. **Brewer, M., U. Utzinger, W. Satterfield, L. Hill, D. Gershenson, R. Bast, J. T. Wharton, R. Richards-Kortum, and M. Follen.** Biomarker modulation in a nonhuman rhesus primate model for ovarian cancer chemoprevention. Cancer Epidemiol. Biomarkers Prev. Accepted for publication 2001.
12. **Zuluaga, A. F., U. Utzinger, A. Durkin, H. Fuchs, A. Gillenwater, R. Jacob, B. Kemp, J. Fan, and R. Richards-Kortum.** 1998. Fluorescence excitation emission matrices of human tissue: a system for in vivo measurement and method of data analysis. Appl. Spectrosc. **53(3) 3:**11.
13. **Scully, R. E.** 1995. Pathology of ovarian cancer precursors. J. Cell Biochem. (S) **23:**208-218.
14. **Rosenberg, L., S. Shapiro, D. Slone, D. W. Kaufman, S. P. Helmrich, O. S. Miettinen, P. D. Stolley, N. B. Rosenshein, D. Schottenfeld, and R. L. Engle, Jr.** 1982. Epithelial ovarian cancer and combination oral contraceptives. J. A. M. A. **247(23):** 3210- 3212.
15. **Rosenberg, L., J. R. Palmer, A. G. Zauber, B. L. Strom, S. Harlap, and S. Shapiro.** 1994. A case-control study of oral contraceptive use and invasive epithelial ovarian cancer. Am. J. Epidemiol. **139:** 654-661.
16. **Whittemore, A. S., R. Harris, and J. Itnyre, and Collaborative Ovarian Cancer Group.** 1992. Characteristics relating to ovarian cancer risk: collaborative analysis of 12 U.S. case-control studies. II. Invasive epithelial ovarian cancers in white women. Am. J. Epidemiol.**136:**1184-1120.
17. **De Palo, G, U. Veronesi, T. Camerini, F. Formelli, G. Mascotti, C. Boni, V. Fosser, M. Del Vecchio, T. Campa, and A. Costa.** 1995. Can fenretinamide protect women against ovarian cancer. J. Natl. Cancer Inst. **87(2):**146-147.
18. **Hong, W. K., and L. M. Itri.** 1994. Retinoids and human cancer. *In* M. B. Sporn, A. B. Roberts, D. S. Goodman (ed). The retinoids: biology, chemistry, and medicine, 2nd edition. Raven Press, Ltd., N.Y.
19. **Rodriguez, G. C., D. K. Walmer, M. Cline, H. Krigman, B. A. Lessey, R. S. Whitaker, R. Dodge, and C. L. Hughes.** 1998. Effect of progestin on the ovarian epithelium of macaques: cancer prevention through apoptosis? J. Soc. Gynecol. Invest. **5:**271-276.
20. **Bigio, I. J., and J. R. Mourant.** 1997. Ultraviolet and visible spectroscopies for tissue diagnostics: fluorescence spectroscopy and elastic-scattering spectroscopy. Phys. Med. Biol. **42(5):**803-814.
21. **Richards-Kortum, R., and E. Sevick-Muraca.** 1996. Quantitative optical spectroscopy for tissue diagnosis. Annu. Rev. Phys. Chem. **47:**555-606.
22. **Khan-Dawood, F. S., M. Y. Dawood, and S. Tabibzadeh.** 1996. Immunohistochemical analysis of the microanatomy of primate ovary. Biol. Reprod. **54:**734-742.
23. **Hild-Petito, S., R. L. Stouffer, and R. M. Brenner.** 1988. Immunocytochemical localization of estradiol and progesterone receptors in the monkey ovary throughout the menstrual cycle. Endocrinology **123:**2896-2905.

Journal of Biomedical Optics 7(1), 20–26 (January 2002)

Fluorescence spectroscopy as a biomarker in a cell culture and in a nonhuman primate model for ovarian cancer chemopreventive agents

Molly Brewer
University of Texas M.D. Anderson Cancer Center
Houston, Texas 77030
and
University of Arizona
Division of Gynecologic Oncology
Tucson, Arizona 85718

Urs Utzinger
University of Texas at Austin
Biomedical Engineering Program
Austin, Texas 78712
and
University of Arizona
Division of Gynecologic Oncology
Tucson, Arizona 85718

Yang Li
E. Neely Atkinson
William Satterfield
Nelly Auersperg
University of Texas M.D. Anderson Cancer Center
Houston, Texas 77030

Rebecca Richards-Kortum
University of Texas at Austin
Biomedical Engineering Program
Austin, Texas 78712

Michele Follen
University of Texas M.D. Anderson Cancer Center
Houston, Texas 77030
and
University of Texas Medical School
Department of Obstetrics, Gynecology
and Reproductive Science
Houston, Texas 77030

Robert Bast
University of Texas M.D. Anderson Cancer Center
Houston, Texas 77030

Abstract. Objective: The objective of this study was to compare the effects of chemopreventive agents on natural fluorescence emission of ovarian cells in a cell culture and in a primate model as a feasibility trial to monitor drug activity. **Methods:** Fluorescence emission spectra were collected from normal (NOE) and immortalized ovarian surface epithelial cells at 290, 360, and 450 nm excitation. Redox potentials were calculated and compared to % apoptosis and cell survival. Fluorescence emission spectra were collected from 18 female rhesus macaques receiving fenretinide [N-(-hydroxyphenyl)retinamide (4-HPR)] orally and/or oral contraceptive pills (OCP) or no medication. Fluorescence intensities and redox ratios were compared using a two-tailed Student's t test. **Results:** Apoptosis and cell survival correlated with fluorescence emission consistent with metabolically active proteins [flavin adenine dinucleotide (FAD) and nicotinamide adenine dinucleotide (NAD(P)H)] and the resulting redox ratio in cells grown with 4-HPR. The 4-HPR consistently inhibited cell survival in a dose dependent manner. Degree of correlation varied between different cell lines. In primates receiving 4-HPR, fluorescence emission was increased at 450 nm excitation, 550 nm emission consistent with FAD presence, whereas those receiving OCP showed decreased emission at 350 nm excitation, 450 nm emission consistent with decreased NAD(P)H presence. Redox ratios were increased by both drugs. **Conclusions:** Fluorescence intensity and redox ratio appear to be altered by 4-HPR treatment *in vivo* and in cell culture and by OCP *in vivo*. Fluorescence intensity may be useful to monitor chemopreventive agents in clinical trials. [DOI: 10.1117/1.1427672]

Keywords: primate and cell culture models; fluorescence spectroscopy.

Paper 102127 received May 18, 2001; revised manuscript received Oct. 3, 2001; accepted for publication Oct. 5, 2001.

1 Introduction

Epithelial ovarian cancer has the highest mortality rate of any of the gynecologic cancers. Only 40% of patients survive five years, despite aggressive treatment, due, in part, to the fact that 70% of patients are diagnosed after metastases have already occurred.[1] Given our inability to cure ovarian cancer, strategies for prevention merit at least as much attention as does treatment of disease. Cancer chemoprevention refers to the administration of chemical agents that prevent or delay the development of cancer in healthy people. Biomarkers that are likely to be affected by the preventive agent and whose modulation supports the postulated chemopreventive activity[2,3] are one of the most important components for prevention studies. Identification of these predictive biomarkers would shorten the time necessary for prevention studies by assessing drug activity rather than following patients for the years that it takes for cancers to develop.[3] However, development of biomarkers is the most difficult and time consuming aspect of prevention studies and usually requires an invasive biopsy. The ability to noninvasively monitor drug activity wold be a major advancement in the prevention of ovarian cancer and could potentially be extended to other organ sites, thus reducing the morbidity of preventing disease.

Retinoids, vitamin A derivatives, have been studied as cancer chemopreventive agents[4–7] based on epidemiologic data showing that diets high in vitamin A are associated with lower odds of epithelial cancers. An Italian trial that evaluated N-(4-hydroxyphenyl) retinamide (4-HPR) for prevention of secondary breast cancers incidentally demonstrated a decreased inci-

Address all correspondence to Dr. Molly Brewer. Tel: 520-626-9283; Fax: 520-626-9287; E-mail: mbrewer@azcc.arizona.edu

1083-3668/2002/$15.00 © 2002 SPIE

dence of ovarian cancer in the women receiving 4-HPR, suggesting that retinoids prevented the development of ovarian cancer.[4] After cessation of 4-HPR treatment, new ovarian cancers occurred in the treatment group, suggesting that the prevention was not durable. Experimental studies have demonstrated that retinoids can affect human ovarian cancer cell growth by inhibiting proliferation and inducing apoptosis,[5–7] which are thought to be important mechanisms in cancer prevention.[8] Retinoids, particularly 4-HPR, have been shown to increase aerobic glycolysis by increasing mitochondrial permeability to the co-enzymes nicotinamide adenine dinucleotide (NAD(P)H) and flavin adenine dinucleotide (FAD), as well as activity of the electron transport chain characterized by an increase in reactive oxygen species and cytochrome oxidase.[9,10] Thus, retinoids are drugs whose activities are potentially amenable to surveillance with fluorescence spectroscopy. Other chemopreventive agents are also of interest in the ovary. Multiple epidemiologic studies have shown that the oral contraceptive pill (OCP) use for at least five years is associated with a 50% or greater reduction in the odds of developing ovarian cancer.[11–15] The mechanism of this prevention is unclear; one factor may be suppression of ovulation, but other mechanisms are hypothesized. A single prospective study has shown that OCP and progesterone increased the rate of apoptosis of ovarian surface epithelial cells in primates.[16]

In the last decade, there has been substantial research to develop optical methods as early diagnostic tools for cancers.[17–20,27] Current diagnostic techniques lack sufficient predictive value to diagnose preinvasive cancers when they might be prevented from progressing or to diagnose small invasive cancers that might be cured with minimal morbidity. Novel optical techniques can aid in the early, near real-time diagnosis by localizing abnormal areas without a visible lesion for biopsy. This paper describes the use of fluorescence spectroscopy as a marker for the action of drugs that may prevent cancers by inducing quiescence of those cells destined to develop into cancer or by reversing preinvasive changes that have not yet developed into a cancer.

Natural fluorophores in tissue include NAD(P)H, FAD, structural proteins such as collagen, elastin, and their cross-links, and the aromatic amino acids tryptophan, tyrosine, and phenylalanine, each of which has a characteristic wavelength for excitation with an associated characteristic emission. Fluorescence collected on the tissue surface is also affected by absorption and scattering. Fluorescence spectroscopy is being used to detect cancers noninvasively in many organ systems, including the cervix, head, and neck and the lungs.[17–20] Fluorophore concentrations change as normal tissues progress to cancer.[21] Different changes in the fluorescence signature may occur in response to an agent that arrests cell growth or induces apoptosis. In this study, we evaluated fluorescence spectroscopy as a marker for drug activity in the ovary in the monkey and as a measure of metabolic activity in cell culture.

A redox ratio can be calculated as the ratio of the FAD fluorescence intensity to that of the sum of FAD and NAD(P)H intensities, and is a measure of aerobic glycolysis in tissue.[21] An increasing redox ratio signifies that either FAD fluorescence intensity has increased, NAD(P)H fluorescence intensity has decreased, or both changes have occurred. In a prior pilot study in women,[22] differences in excitation-emission matrices (EEMs) from normal ovaries and invasive cancer were observed with peaks at 350 nm excitation and 460 nm emission wavelengths that represent both collagen and NAD(P)H. These peaks were higher in the cancers suggesting increased NAD(P)H signal. In tumors, these co-enzymes are thought to exist in their reduced state (NAD(P)H,FADH) with a unique fluorescence signature (NAD(P)H high, FAD low) as a result of alterations in blood flow, decreased *p*H of the tissue, abnormal mitochondria, and abnormal transport of electron carrier molecules into the mitochondria[21] where the electron transport chain takes place.

This study is a feasibility study to explore fluorescence spectroscopy as a biomarker for drug activity. In the present study we have used three different human ovarian epithelial cell lines to explore whether apoptosis and growth inhibition induced by 4-HPR are correlated with changes in NAD(P)H and FAD fluorescence intensity and the resultant redox potentials. We have further explored the changes in fluorescence spectra in response to chemopreventive agents in a primate model that allows us to evaluate the response of the ovary *in situ* to these drugs where the surface epithelial cells are in contact with stromal cells. The cell model has permitted evaluation of several different combinations and doses of drugs, whereas the primate provides an *in vivo* model that can provide a bridge for human clinical studies due to similarities in reproductive function between primates and women. These studies have permitted us to evaluate the potential role of fluorescence spectroscopy as a biomarker for chemopreventive drug activity in the ovary.

2 Materials and Methods

2.1 Cell Culture

2.1.1 *Experimental Design*

Three different cell lines were incubated with different doses of 4-HPR (0, 2, 5, 10 μM) to evaluate sensitivity to 4-HPR. TGF-β1 has been shown to have additive effects in some cell lines in the induction of apoptosis, but had no effect in these cultures. Primary cultures of normal ovarian epithelial (NOE) cells were established from surgical specimens of normal ovaries as previously described.[23] They were maintained in a 1:1 mixture of cell culture media MCDB 105 and Medium 199 supplemented with 5% fetal bovine serum, 2 mM L-glutamine, 100 units/ml penicillin and 100 μg/mL streptomycin. Simian virus 40-immortalized ovarian surface epithelium cell lines IOSE-29 and IOSE-261 were established as immortalized cell lines. They were maintained in a 1:1 mixture of MCDB 105 and Medium 199 supplemented with 5% fetal bovine serum and 50 μg/mL gentamycin sulfate.

2.1.2 *Fluorescence*

NOE, IOSE 29, and IOSE 261 were the three cell lines used. After three days of treatment with 4-HPR or diluent, cells were harvested. Since the media itself shows a strong autofluorescence the cells were washed three times with phosphate buffered saline (PBS) before optical studies were performed. For the spectroscopic studies, all cells were diluted in sterile buffered isotonic saline solution (PBS) with 5% glucose. The cell suspension was centrifuged at 400 g for 10 min. then washed three times. Fluorescence emission was measured us-

ing a scanning spectrofluorimeter (Hitachi Ltd., F-4010, Tokyo, Japan). Excitation light was generated at three wavelengths to probe for fluorescence consistent with tryptophan, the co-factors NAD(P)H and FAD. Because of the design of the fluorimeter and the inherently weak signal of the autofluorescence of the cell suspension, additional optical components were placed into the excitation and emission beam path. Dielectric bandpass filters (Omega, Brattleboro, VT) reduced the out-of-band light of the excitation monochromator and long pass filters (colored glass filters, Schott Glass Technologies, Duryea, PA) prevented stray light generated in the sampling chamber from reaching the detector. For each of the three excitation wavelengths a different filter set was used. At 290 nm excitation, emission spectra were recorded from 300 to 570 nm, at 365 nm excitation from 375 to 720 nm emission, and at 460 nm excitation from 470 to 800 nm emission. In all measurements at 290 nm excitation, emission peaks were observed at 340 nm consistent with tryptophan. At 365 nm excitation emission peaks were located at 450 nm consistent with NAD(P)H and at 420 nm consistent with water Raman scattering. At 460 nm excitation, emission peaks were located at 520 nm consistent with FAD emission and at 540 consistent with water Raman scattering.

Studies were conducted using a microcuvette with a volume of 200 μL. The cells were repeatedly stirred with a pipette to prevent settling between the measurements. A fluorescence standard was measured each measurement day at all three excitation wavelengths to monitor system drift. The standard solution was 2 mg/L Rhodamine 610 (Exciton, Dayton, OH) in ethylene glycol.

2.1.3 *Cell Treatment*

4-HPR was obtained from Sigma Chemicals (St. Louis, MO). A 10 mM stock solution was made in 100% DMSO and stored at $-20\,^{\circ}$C. Recombinant human TGF-β1 was obtained from R&D Systems (Minneapolis, MN). A 10 μg/mL stock solution was made using 4 mM HCL containing 1 mg/m*l* BSA (HCL-BSA) and stored at $-70\,^{\circ}$C. Immediately prior to use, 4-HPR (2, 5, and 10 μM) and TGF-β1 (10 ng/mL) stock solutions were diluted in culture medium, 10^6 exponentially growing cells were incubated for three days with the different concentrations of 4-HPR (2, 5, 10 μM/mL) and/or TGF-β1 (10 ng/m*l*).

2.1.4 *DNA Fragmentation Assay*

Cells were harvested after three days of treatment and analyzed for the presence of DNA fragments using the APO-DIRECT Kit (Phoenix-Flow Systems, Inc., San Diego, CA). Briefly, this involves terminal deoxynucleotidyl transferase [TdT]-mediated (TUNEL) labeling of the 3′-hydroxyl ends of DNA fragments formed during apoptosis with fluorescein-tagged dUTP which reveals % apoptosis using flow cytometry.

2.1.5 *Cell Survival (Growth Inhibition) Assay*

Cells were seeded in 96 well dishes at densities ranging from 1000 to 3000 cells per well and allowed to attach overnight. The exponentially growing cells were treated in triplicate with TGF-β1(10 μg/mL), 4-HPR (2, 5, 10 μg) or medium alone for three days. Cell numbers were estimated using a modified sulforhodamine B (SRB) assay. A 0.4% (w/v) solution of SRB (Sigma Chemicals, St. Louis, MO) was made in 1% acetic acid. The medium was aspirated and the cells fixed *in situ* with 100 μL per well of 10% TCA for 60 min. at 4 °C. The plates were rinsed five times with de-ionized water and air dried. The plates were incubated for 10 min at room temperature with 50 μL per well of SRB. Unbound SRB was solubilized with 100 μL per well of unbuffered 10 mM Tris base. The optical densities were determined using a microtiter plate reader set at 492 nm. Percent cell survival was calculated and ID_{50} was determined by inspection of dose response curves.

2.1.6 *Data Analysis*

For further analysis of the spectra, intensities were measured at 290 nm excitation, 340 nm emission, at 365 nm excitation, 420 nm emission, and at 460 nm excitation, 520 nm emission. These locations correspond to tryptophan, NAD(P)H and FAD emission and lay outside the range of Raman scattering of water. The emission from the supernatant of the third wash was subtracted from all other measurements as the background. Redox ratio was then calculated. Growth inhibition, apoptosis, and fluorescence intensities at the three wavelengths and the resultant redox ratios were then evaluated statistically using the Spearman rank correlation test to evaluate correlation between variables. Interactions were explored using regression analysis. The studies that included TGF-β1 were included with the 4-HPR group either 0, 2, 5, or 10 μM 4-HPR for analysis because there was consistently no effect from TGF-β1 on FAD, NAD(P)H, cell survival or apoptosis; the correlation was 0.

2.2 Primate

2.2.1 *Experimental Design*

Eighteen female adult rhesus macaques were used in this exploratory study. This protocol was approved by the Animal Care and Use Committee at The University of Texas M.D. Anderson Cancer Center and was conducted at the Department of Veterinary Sciences in Bastrop, Texas, where all animals were caged separately. The animals were given 4-HPR (four monkeys), OCP (five monkeys), the combination of 4-HPR+OCP (five monkeys), or no medication (four monkeys) daily for three months. Doses of 4-HPR and OCP were calculated by allometric scaling[26] and given orally. The OCP used was Ortho-Novum 1/35, a medium-dose oral contraceptive with 1 mg norethindrone and 35 μg ethinyl estradiol in each pill. The 4-HPR dose was calculated in the same manner from the accepted human dose of 200 mg daily. Prior to starting medication and following 90 days of medication, monkeys underwent laparotomy, spectroscopy, and ovarian biopsies.

2.2.2 *Fluorescence*

Fluorescence excitation-emission matrices (EEMs), which contain the fluorescence intensity as a function of both excitation and emission wavelengths, were measured. The spectroscopic system for *in vivo* use records EEMs in less than 1.5 min and consists of a xenon arc lamp coupled to a scanning spectrometer that provides excitation light. A fiberoptic probe directs excitation light to the tissue, collects emitted fluores-

cence light, and delivers it to an imaging spectrograph and charge coupled device camera. The interrogated tissue area is 2 mm in diameter. Fluorescence emission spectra ranging from 320 to 850 nm were collected sequentially at 19 excitation wavelengths ranging from 300 to 480 nm in 10 nm steps. Before assembling the data into fluorescence EEMs, system dependent response and background signals were removed. Tissue exposure to broadband UV radiation from this device is below the total exposure limits developed by the American Conference of Governmental Industrial Hygienists (ACGIH) for epithelial tissues. Initially the left ovary was optically interrogated and biopsied. Following three months of drug, the right ovary was optically interrogated and biopsied. Base line fluorescence measurements were collected from the contra lateral ovary (the ovary that was not biopsied). Only one ovary was biopsied due to the concern that a biopsy would affect the subsequent fluorescence measurement due to collagen formation as the ovary healed.

2.2.3 *Data Analysis*

From the fluorescence measurements, values were extracted which may relate to NAD(P)H and FAD fluorescence. Signals were averaged at 450 nm excitation and 535 nm emission which is consistent with FAD and collagen emission and at 365 nm excitation and 450 nm emission which is consistent with NAD(P)H and collagen emission NAD(P)H. Although these wavelength ranges include contributions from both structural proteins as well as FAD and NAD(P)H, drugs should only modulate cell fluorescence and not collagen matrix. Therefore, we expect changes to be attributable to the effect of the drugs on the epithelial cells or stromal cells in the regions of NAD(P)H and FAD, rather than to an effect on the collagen matrix, because these drugs are receptor mediated and should not affect collagen. However, both epithelial and stromal cells may be affected.

For each monkey, data was available from three measurement sites. The three spectra were averaged yielding between four and five averaged measurements for each drug group. Using this information, we compared all fluorescence measurements between the first and second measurements using the two-tailed Student's t test. Group means and standard errors were calculated and plotted. From the three sites per measurement, two were biopsied on the same ovary pre drug treatment and two were biopsied posttreatment on the opposite ovary. This allowed us to visually compare posttreatment data from ovaries which had been previously biopsied and ovaries which had not been biopsied.

3 Results

3.1 Fluorescence Measurements

3.1.1 *Cells*

The Spearman rank correlation test was used to determine the correlation between apoptosis, growth inhibition, and fluorescence measurements. The presence or absence of TGF-β1 did not affect either survival, apoptosis, or redox ratio in this set of experiments (data not shown). Results varied between cell lines. There is a strong correlation between redox ratio and cell survival ($p=0.0274$), FAD and apoptosis ($p<0.001$), and redox ratio and apoptosis ($p=0.0045$) in the regression model (Table 1). There is consistent interaction with the cell line in the regression model, suggesting a different response with the different cell types. NOE cells showed a strong correlation between NAD(P)H fluorescence intensity and survival ($p=0.04$), between redox ratio and survival ($p=0.018$), and redox ratio and NADH fluorescence intensity ($p=0.005$). Figure 1 shows the relationship between cell survival and redox ratio in the three cell lines. Redox ratio increased in all three cell lines as cell survival decreased, (or growth inhibition increased). As the dose of 4-HPR increased, the cell survival decreased in all three experiments, but the sensitivity of the cells varied. IOSE 261 showed a slightly different response. The association between NAD(P)H fluorescence intensity and survival ($p=0.02$) persisted, but there was not an association with the other variables. IOSE 29 showed a correlation between NAD(P)H fluorescence intensity and survival ($p<0.0001$), between NAD(P)H fluorescence intensity and apoptosis ($p=0.0002$), FAD and apoptosis ($p=0.04$), redox ratios and survival ($p=0.0002$), and redox ratio and NAD(P)H fluorescence intensity ($p=0.0001$), suggesting that IOSE 261 is more sensitive to 4-HPR than IOSE 29.

Table 1 Multivariate regression analysis.

Variables	*p* value
Redox/apoptosis	$P=0.0045$
Redox/survival	$P=0.0274$
FAD/apoptosis	$P<0.001$

Percent apoptosis, as visualized in Figure 2, varied between cell lines and dose of 4-HPR. NOE and IOSE 261, respectively, did not show significant changes in apoptosis with 2 and 5 μM 4-HPR. However, they still showed an increase in redox ratio with increasing doses of 4-HPR. The IOSE 29 did have an increase in apoptosis at the 5 μM dose which correlated with an increase in redox ratio. The 10 μM dose of 4-HPR was used on this cell line and induced a higher apoptosis than the 5 μM dose. The higher rate of apoptosis correlated with a higher redox ratio. Both apoptotic rates and redox ratios varied between cell lines which was consistent with different sensitivities of the cell lines to 4-HPR.

3.1.2 *Primates*

Consistent differences in the absolute fluorescence intensities and relative contributions were noted between the pre- and postdrug measurements in each drug group as well as the controls. The advantage of this model is that variability due to time can be evaluated as well as variability due to drug effect. The differences observed in the control group were much smaller than those seen in the three groups receiving drugs. Changes observed in the control group could be attributed to natural fluctuations of the optical signal. When the average change within each group was compared, the NAD(P)H related signal decrease was statistically significant for the OCP ($p=0.02$) and the combination group (OCP+4-HPR) compared to the control group ($p=0.01$) [Figure 3(a)]. In the 4-HPR and control group, this signal increased but the change

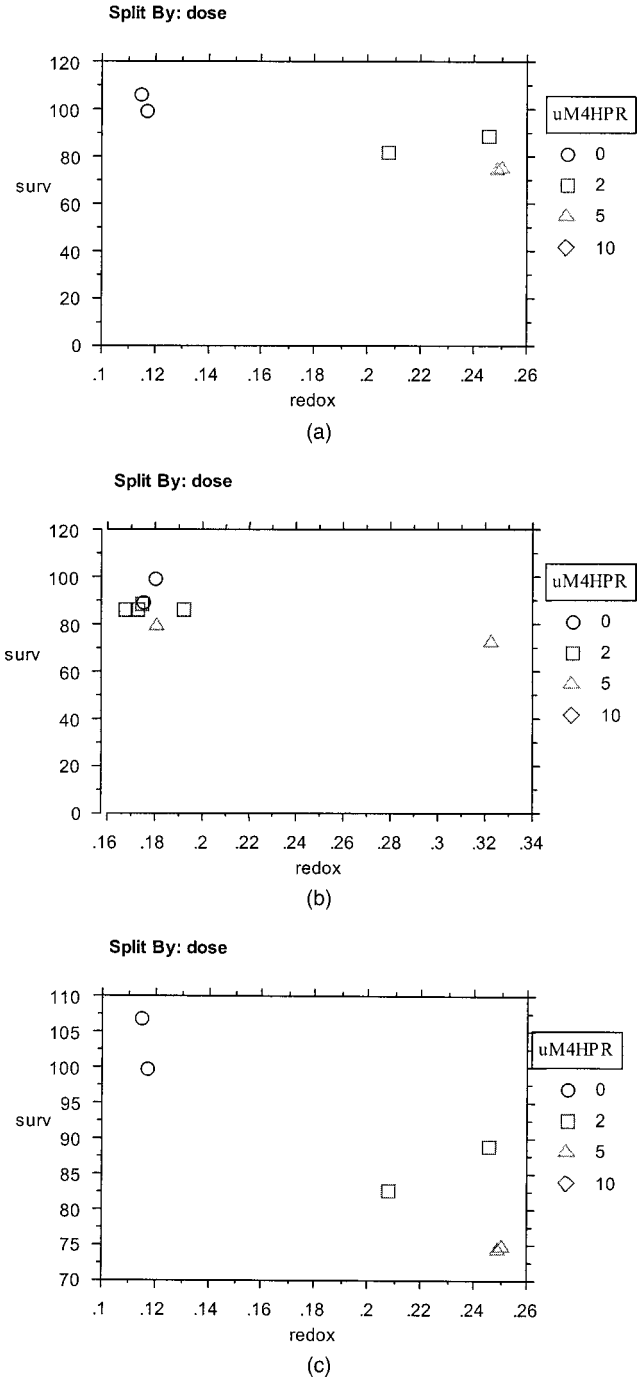

Fig. 1 Cell survival compared to redox potential in three cell lines NOE (a), IOSE 261 (b), and IOSE 29 (c). Increasing doses of 4-HPR show a decreased rate of cell survival.

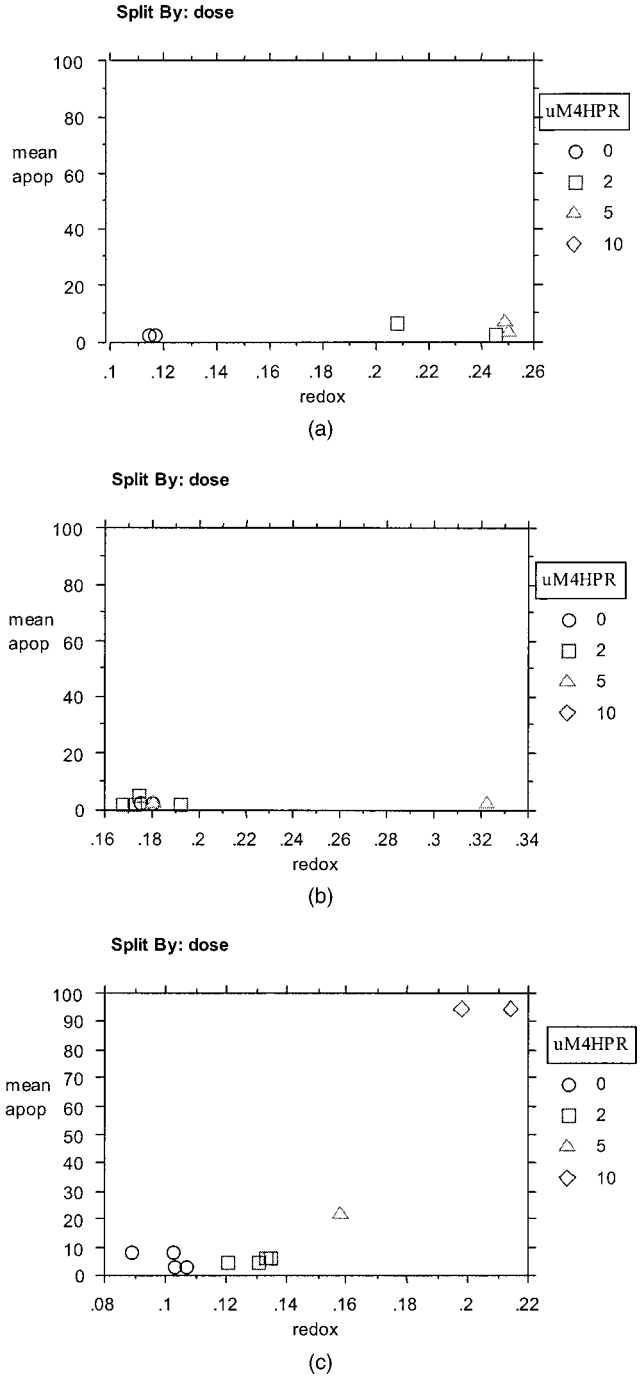

Fig. 2 Percent apoptosis compared to redox potential in three cell lines NOE (a), IOSE 261 (b), and IOSE 29 (c). Increasing doses of 4-HPR show an increased rate of apoptosis in the IOSE 29.

in the 4-HPR was not statistically different from the control group. The largest increase in the FAD related signal was found in the combination group and the 4-HPR group [Figure 3(b)]. The standard deviation was large and the number of samples small, yielding p values too large to be significant. However, the greatest effect was found in the 4-HPR group.

Redox ratios increased in each group [Figure 3(c)]. The change in the control group was the smallest. The 4-HPR group changed the redox potential due to its contribution from increasing FAD, while the OCP group changed the redox potential due to its relative decrease in NADH. The combination group showed contribution from both increased FAD and decreased NADH. Although these differences did not achieve statistical significance related to small numbers within groups and large variances, there appears to be a trend of increasing redox potentials with both drugs. The visual comparison of data from ovaries that had been previously biopsied to data from ovaries which had not been biopsied showed no notice-

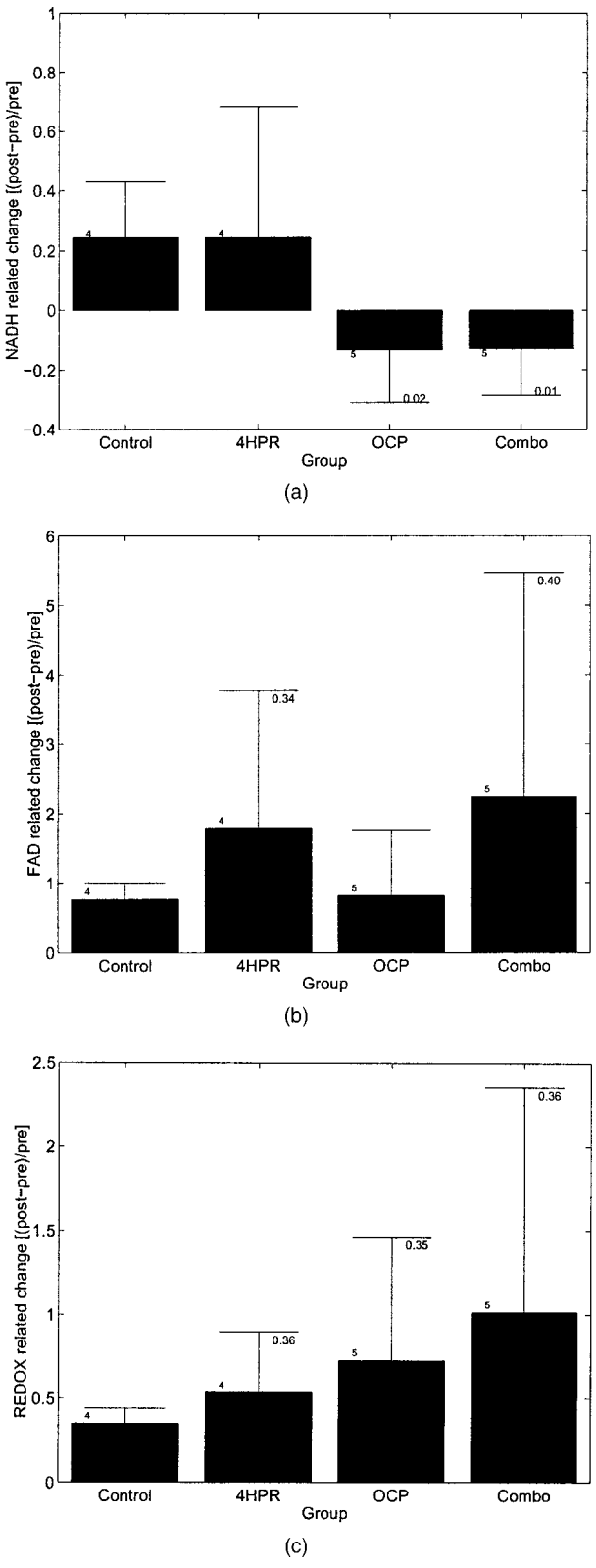

Fig. 3 (a) Compares % NADH increase between three drug groups and control group, OCP ($p=0.02$) and combination $p=0.01$ significant when compared to control group. (b) Compares % FAD increase between drug groups and control group, p values not significant. (c) Compares redox potentials between drug groups and control group, p values not significant.

able difference. This implies that healing response did not dramatically alter fluorescence.

4 Discussion

Fluorescence spectroscopy is being used to detect cancers noninvasively in many organ systems.[17–20,24] In this study, we evaluated it as a method to detect drug activity in the ovary in primates and to measure metabolic activity in human cell culture. In our prior pilot study in women[22] differences in EEMs were found in the area of NAD(P)H fluorescence and hemoglobin absorption. These changes were attributed to increased NAD(P)H and hemoglobin presence. In tumors, NADH and FADH are postulated to increase as a result of alterations in blood flow, decreased pH of the tissue, and abnormal mitochondria as well as abnormal transport of electron carrier molecules into the mitochondria[28,29] where the electron transport takes place. Intriguingly, this study suggests that these chemopreventive agents alter the metabolism of normal tissue in a direction opposite to that of cancer.

TGFβ has been found to induce apoptosis in ovarian cancer cell lines and has been hypothesized to be a primitive surveillance mechanism for abnormal cells.[25] However, data from our laboratory have shown inconsistent results with TGFβ and in this study it had no effect.

Limitations of the cell data include the lack of interaction of epithelial cells with the stroma, which may account for the differences seen between primate ovaries and the isolated human ovarian epithelial cells. They both, however, are strongly associated with an increased redox ratio. No cell line can approximate the behavior of tissue *in vivo* in humans, but mechanistic studies can be done on cells to understand the potential application to *in vivo* systems. The cell line data suggest that redox ratios are useful to evaluate biologic activity of these drugs.

Limitations of our primate study include too few numbers to reach significance due to large inter-animal variances; however, there appears to be a relationship between increasing redox ratios and treatment with 4-HPR and OCP. Effects of 4-HPR and OCP appear additive or potentially synergistic when the two drugs are combined, consistent with different mechanisms of action for these drugs. The primate results also suggest that redox values may correlate with drug effects.

The 4-HPR activity in the mitochondria may be evaluated with fluorescence spectroscopy, because natural fluorophores in cells, NAD(P)H and FAD are affected by 4-HPR. Although the mechanism of the OCP prevention of ovarian cancer is poorly understood, and has not yet been validated in the laboratory, there is a different signal seen with the monkeys receiving 4-HPR and those receiving OCP. Use of both the cell model and the primate model are powerful tools for studying the biologic activity of these drugs. Areas for future research include a study with larger numbers of monkeys to attain additional statistical significance as well as further laboratory work to elucidate the mechanism of OCP and 4HPR activity in cell culture. Ultimately, this work will be extended to monitoring clinical trials in chemoprevention.

References

1. American Cancer Society. www.cancer.org
2. G. Kelloff, C. W. Boone, J. A. Crowell, S. G. Nayfield, E. Hawk, V.

A. Steele, R. A. Lubet, and C. C. Sigman, ''Strategies for phase II cancer chemoprevention trials: Cervix, endometrium, and ovary,'' *J. Cell Biochem. Suppl.* **23**, 1–9 (1995).
3. K. Dhingra, ''A phase II chemoprevention trial design to identify surrogate endpoint biomarkers in breast cancer,'' *J. Cell Biochem. Suppl.* **23**, 19–24 (1995).
4. G. De Palo, U. Veronesi, T. Camerini, F. Formelli, G. Mascotti, C. Boni, V. Fooser, M. Del Vecchio, T. Campa, and A. Costa, ''Can fenretinamide protect women against ovarian cancer,'' *J. Natl. Cancer Inst.* **87**, 146–147 (1995).
5. S. Y. Sun, J. M. Kurie, P. Yue, M. I. Dawson, B. Shroot, R. A. S. Chandraratna, W. K. Hong, and R. Lotan, ''Differential responses of normal, premalignant and malignant human bronchial epithelial cells to receptor-selective retinoids,'' *Clin. Cancer Res.* **5**, 431–437 (1999).
6. S. Y. Sun, W. Li, P. Yue, S. M. Lippman, W. K. Hong, and R. Lotan, ''Mediation of N-(4-Hydoxyphenyl) retinamide-induced apoptosis in human cancer cells by different mechanisms,'' *Cancer Res.* **59**, 2943–98 (1999).
7. D. D. Taylor, C. G. Taylor, P. H. Black, C. G. Jiang, and I. N. Chou, ''Alterations of cellular characteristics of a human ovarian teratocarcinoma cell line after in vitro treatment with retinoids,'' *Differentiation* **43**, 123–130 (1990).
8. A. H. Wyllie, ''Apoptosis and carcinogenesis,'' *Eur. J. Cell Biol.* **73**, 189–197 (1997).
9. R. Dabal, C. M. Boyer, A. Berchuck, A. Roberts, N. Roche, M. Sporn, and R. Bast, ''Synergistic inhibition of ovarian cancer cell proliferation by TGFβ and retinoic acid (RA) derivatives,'' *Proc. American Association of Cancer Research* **36**, 635 (1995).
10. R. Supino, M. Crosti, M. Clerici, A. Warlters, L. Cleris, F. Zunino, and F. Formelli, ''Induction of apoptosis by fenretinide (4-HPR) in human ovarian carcinoma cells and its association with retinoic acid receptor expression,'' *Int. J. Cancer* **65**, 491–497 (1996).
11. X. Liu, C. N. Kim, J. Yang, R. Jemmerson, and X. Wang, Induction of apoptotic program in cell-free extracts, ''Requirement for dATP and cytochrome c,'' *Cell* **86**, 147–157 (1996).
12. S. Suzuki, M. Higuchi, R. J. Proske, N. Oridate, W. K. Hong, and R. Lotan, ''Implication of mitochondria-derived reactive oxygen species, cytochrome C and caspace-3 in N-(4-Hydroxyphenyl) retinamide-induced apoptosis in cervical carcinoma cells,'' *Oncogene* **18**, 6380–6387 (1999).
13. A. S. Whittemore, R. Harris, J. Itnyre, and Collaborative Ovarian Cancer Group, ''Characteristics relating to ovarian cancer risk: Collaborative analysis of 12 U.S. case-control studies. II. Invasive epithelial ovarian cancers in white women,'' *Am. J. Epidemiol.* **136**, 1184–1203 (1992).
14. S. Franceschi, F. Parazzini, E. Negri, M. Booth, C. La Vecchia, V. A. Beral, and D. Trichopoulos, ''Pooled analysis of 3 European case-control studies. III. Oral contraceptive use,'' *Int. J. Cancer* **49**, 61–65 (1991).
15. Centers for Disease Control cancer and steroid hormone study, ''Oral contraceptive use and the risk of ovarian cancer,'' *J. Am. Med. Assoc.* **249**, 1596–1599 (1983).
16. J. Rosenberg, S. Shapiro, D. Slone, D. W. Kaufman, S. P. Helmrich, O. S. Miettinen, P. D. Stolley, N. B. Rosenshein, D. Schottenfeld, and R. L. Engle, ''Epithelial ovarian cancer and combination oral contraceptives,'' *J. Am. Med. Assoc.* **243**(23), 3210–3212 (1982).
17. R. Marchesini, M. Brambilla, E. Pignoli, G. Bottiroli, A. C. Croce, M. Dal Fante, P. Spinelli, and S. di Palma, ''Light-induced fluorescence spectroscopy of adenomas, adenocarcinmas and non-neoplastic mucose in human colon,'' *Photochem. Photobiol.* **14**(3), 219–230 (1992).
18. R. M. Cothren, R. R. Richards-Kortum, R. P. Rava, G. A. Boyce, M. Doxtader, R. Blackman, T. B. Ivanc, and G. B. Hayes, ''Gastrointestinal tissue diagnosis by LIF spectroscopy at endoscopy,'' *Gastrointest. Endosc.* **36**, 105–111 (1990).
19. J. Hung, S. Lam, J. C. LeRiche, and B. Palcic, ''Autofluorescence of normal and malignant bronchial tissue,'' *Lasers Surg. Med.* **11**(2), 99–105 (1991).
20. S. Lam, J. Y. C. Hung, S. M. Kennedy, J. C. LeRiche, R. Vedal, B. Nelems, C. E. Macaulay, and B. Palcic, ''Detection of dysplasia and carcinoma in situ by ratio fluorometry,'' *Am. Rev. Respir. Dis.* **146**, 1458–1461 (1992).
21. B. Chance, ''Metabolic heterogeneities in rapidly metabolizing tissues,'' *J. Appl. Cardiol.* **4**, 207–221 (1989).
22. M. Brewer, U. Utzinger, E. Silva, D. Gershenson, R. C. Bast, M. Follen, and R. Richards-Kortum, ''Fluorescence spectroscopy for *in vivo* characterization of ovarian tissue,'' *Lasers Surg. Med.* (in press).
23. P. A. Kruk, S. L. Maines-Bandiera, and N. Auersperg, ''A simplified method to cuture human ovarian surface epithelium,'' *Lab. Invest.* **63**, 132–136 (1990).
24. G. C. Rodriguez, D. K. Walmer, M. Cline, H. Krigman, B. A. Lessey, R. S. Whitaker, R. Dodge, and C. L. Hughes, ''Effect of progestin on the ovarian epithelium of macaques: Cancer prevention through apoptosis?'' *J. Soc. Gynecol. Investig.* **5**, 271–276 (1998).
25. A. Berchuck, G. Rodriquez, G. Olt, R. Whitaker, M. Boente, B. Arrick, D. Clarke-Pearson, and R. Bast, ''Regulation of growth of normal epithelial cells and ovarian cancer cell lines by transforming growth factor-β,'' *Am. J. Obstet. Gynecol.* **166**, 676–684 (1992).
26. C. J. Sedgwick and M. A. Pokras, ''Extrapolating rational drug doses and treatment by allometric scaling,'' *AAHA's 55th Annual Meeting Proceedings* (1988).
27. A. Gillenwater, R. Jacob, and R. Richards-Kortum, ''Fluorescence spectroscopy: A technique with potential to improve the early detection of aerodigestive tract neoplasia,'' *Head Neck* **20**, 556–562 (1998).
28. C. J. Gulledge and M. W. Dewhirst, ''Tumor oxygenation: A matter of supply and demand,'' *Anticancer Res.* **16**, 741–750 (1996).
29. C. Richter and M. Schweizer, ''Oxidative stress in mitochondria,'' *Oxidative Stress and the Molecular Biology of Antioxidant Defenses* (1997).

Available online at www.sciencedirect.com

SCIENCE DIRECT®

Gynecologic Oncology 98 (2005) 182 – 192

Gynecologic Oncology

www.elsevier.com/locate/ygyno

In vitro model of normal, immortalized ovarian surface epithelial and ovarian cancer cells for chemoprevention of ovarian cancer

Molly Brewer[a,d,*], J. Taylor Wharton[a], Jian Wang[d], Amanda McWatters[a], Nelly Auersperg[c], David Gershenson[a], Robert Bast[b], Changping Zou[d]

[a]*Department of Gynecologic Oncology, University of Texas, The M. D. Anderson Cancer Center, Houston, TX 77030, USA*
[b]*Experimental Therapeutics, University of Texas, The M. D. Anderson Cancer Center, Houston, TX 77030, USA*
[c]*University of British Columbia, Vancouver, British Columbia, Canada*
[d]*Department of Obstetrics and Gynecology, Division of Gynecologic Oncology, University of Arizona, Tucson, AZ 85724, USA*

Received 9 July 2004
Available online 23 May 2005

Abstract

Background. Epithelial ovarian cancer has the highest mortality rate among the gynecologic cancers. The synthetic retinoid, N-(4-hydroxyphenyl) retinamide (4-HPR), has been used in the chemoprevention of ovarian cancer. However, the effectiveness of its application for different populations has been questioned because of the genetic differences among normal, high risk, and women with cancer.

Objective. To explore the similarities and the differences in 4-HPR effects on different ovarian epithelial cells which mimic different populations of women, normal ovarian surface epithelium to represent the normal population of women, immortalized ovarian surface epithelium to represent premalignant changes, and cells derived from ovarian cancer cells to represent malignant changes were used as in vitro models.

Methods. Normal ovarian surface epithelial cells, immortalized ovarian surface epithelial cells, and ovarian cancer cells were incubated for different intervals with increasing concentrations of 4-HPR. Growth inhibition, the fraction of apoptotic cells, the expression of apoptosis-related genes, including p53, p16, p21, and caspase-3, and mitochondrial permeability transition were measured before and after 4-HPR treatment.

Results. Treatment with 4-HPR produced growth inhibition and apoptosis in a dose-dependent manner for all 3 cell types. 4-HPR produced the strongest activation of the p53 pathway in normal ovarian epithelial (NOE) cells, while it caused the largest increase in MPT in the cancer cells, suggesting a different mechanism for growth inhibition and/or apoptosis in these cell lines. 4-HPR, at a concentration of 10 μM, had a maximal effect on caspase-3 activity at 72 h in normal cells and at 48 h in immortalized and cancer cells, although the effects were modest.

Conclusions. Normal ovarian surface epithelial cells, immortalized ovarian surface epithelial cells, and ovarian cancer cells showed a differential response to 4-HPR. Although the same endpoints of growth inhibition and apoptosis induction were present in response to 4-HPR, these endpoints may be regulated through different pathways.

Implications. Clinical trials with higher concentrations of 4-HPR should prove beneficial.

Keywords: Retinoids; Growth inhibition; Apoptosis; Cancer prevention

Introduction

Epithelial ovarian cancer has the highest mortality rate among the gynecologic cancers. Only 30–40% of patients survive 5 years despite aggressive treatment, in part, due to the advanced stage at diagnosis, with 70% of patients

* Corresponding author. Department of Obstetrics and Gynecology, Division of Gynecologic Oncology, Arizona Cancer Center, 1515 N. Campbell Avenue, Room 1968, Tucson, AZ 85724-5024, USA. Fax: +1 520 626 9287.
E-mail address: mbrewer@azcc.arizona.edu (M. Brewer).

0090-8258/$ - see front matter © 2005 Elsevier Inc. All rights reserved.
doi:10.1016/j.ygyno.2005.01.051

having widespread metastases [1]. Given our inability to consistently cure ovarian cancer, strategies for prevention merit at least as much attention as does treatment of the disease. Cancer chemoprevention is the administration of chemical agents to prevent or delay the development of cancer in healthy people. Biomarkers that are likely to be affected by the preventive agent and whose modulation supports the postulated chemopreventive activity [2,3] are important components of prevention studies.

N-(4-hydroxyphenyl) retinamide (4-HPR), a synthetic analog of Vitamin A, has been shown to have anti-neoplastic activity in both experimental models and clinical trials [4–12], particularly in the skin [5]. It has also been found to coincidentally decrease the risk of ovarian cancer in a breast cancer chemoprevention trial [13–15]. In both the skin [5] and the ovary [15], the response lasted for the duration of drug ingestion, suggesting that the use of retinoids may need to be longer than previously thought. This study, as well as others [16–20], shows activity by 4-HPR against tumor cell lines with increasing rates of apoptosis, suggesting that this drug has the potential for preventing and treating ovarian cancer. This is the first study to explore the effect of 4-HPR on normal ovarian epithelial cells and cells immortalized with viral T-antigen which are compared to ovarian cancer cell lines. Normal cells were used to mimic normal woman who carried no increased risk for ovarian cancer, and immortalized cells to mimic high-risk women who may harbor cells that have undergone various mutations. The in vitro model was chosen to evaluate the effect of 4-HPR on different cell types and to study the dose response in these cells because the efficacy of 4-HPR in clinical prevention trials has been contradictory for the high-risk population [3–15,21]. Early investigators using 4-HPR for prevention limited the dose to 200 mg due to safety concerns: 200 mg/day of 4-HPR was used in the breast cancer prevention trial for prevention of secondary breast cancers [14]; although there was no effect on the incidence of breast cancer, 4-HPR was found to decrease the risk of ovarian cancer at this concentration [15]. However, Dr. Follen's group found that 200 mg 4-HPR, which corresponds to 2 μM concentration in vitro [21], was not effective in inducing the regression of cervical pre-neoplasia in vivo. Moreover, their in vitro model showed that the higher dose of 10 μM concentration was needed to induce growth inhibition or apoptosis in both dysplastic and cervical cancer cells [22]. These studies have helped establish a relevant biologically active dose for clinical trials for premalignant lesions in the cervix, corresponding to >2 μM tissue concentration [21,22]. This study investigates the molecular and cellular events that occur in conjunction with exposure to different concentrations of 4-HPR.

Our research determines how 4-HPR inhibits growth and promotes apoptosis in normal ovarian surface epithelial cells, in immortalized ovarian surface epithelial cells, and in ovarian cancer cell lines at different concentrations. These results suggest that different doses of 4-HPR may be necessary for different populations of women to prevent and treat ovarian cancer.

Materials and methods

Cell lines, retinoids, and normal ovarian epithelial (NOE) cells

Surface epithelial cells were harvested at the time of oophorectomy for benign gynecological conditions. Primary cultures were established from the surgical specimens of normal ovaries [23], from patients without any increased risk for ovarian cancer based on their personal or family history of cancer, nor did any of these women have a known BRCA mutation. Prior to disruption of the blood supply, and without handling the ovaries, the ovary was gently scraped with a scalpel and the scalpel rinsed with sterile culture medium. Cells were maintained in a 1:1 mixture of MCDB 105 and medium 199 supplemented with 5% fetal bovine serum, 100 units/ml penicillin, 2 mM L-glutamine, and 100 μg/ml streptomycin. Six different NOE primary cell lines were used in this study.

Immortalized ovarian surface epithelial (IOSE) cells were obtained from Nelly Auersperg (University of British Columbia, Vancouver, British Columbia). IOSE and ovarian cancer cells, OVCA420, SKOV3, and OCC-1 cells were grown in a 1:1 (volume/volume) mixture of Dulbecco's modified Eagle's medium (DMEM), and Ham's F12, with 10% fetal bovine serum, at 37°C in a humidified atmosphere of 95% air and 5% CO_2. N-(4-hydroxyphenyl) retinamide (4-HPR) purchased from Sigma Chemical Co. (St. Louis, MO) was dissolved in dimethyl sulfoxide (DMSO) at stock solutions of 0.1 mM and stored in an atmosphere of N_2 at −80°C.

Effects of 4-HPR on cell proliferation in monolayer cultures

Cells were plated in 96-well plates at a concentration of 10^5 cells per well and grown for 24 h. The NOE, IOSE, and OVCA420 cells were incubated with 1, 2, and 5 μM concentrations of 4-HPR and the ovarian cancer cells (OVCA420, SkOV3, and OCC-1) were incubated for 5 days with 2, 5, and 10 μM concentrations of 4-HPR. Control cultures contained DMSO, and the medium was replaced every 2 days. Growth inhibition was determined using the crystal violet method as previously reported [17]. After a 5-day treatment, cells were fixed with 5% glutaraldehyde in phosphate-buffered saline, rinsed with distilled water, and air dried. Cells were incubated with 1:1 (volume/volume) 200 mM (3-[cyclohexylamino]-1-propanesulfonic acid (CAPS) buffer (pH 9.5), and 0.2% CV at 25°C for 30 min, then washed and air dried. The intracellular dye was solubilized with 10% glacial acetic acid and the absorbance at 590 nm was determined using a

microtiter plate reader. Growth inhibition was calculated according to the equation: inhibition = $(1 - Nt/Nc) \times 100$, where Nt and Nc are the number of cells in treated and control cultures, respectively. All experiments were performed in triplicate and the means ± standard deviations calculated.

Analysis of apoptosis induced by 4-HPR

Terminal deoxynucleotidyl transferase (TdT)-mediated fluorescein-deoxyuridine-triphosphate (dUTP) nick-end labeling (TUNEL) assay was used [17]. Following incubation for 24, 48, and 72 h with different concentrations of 4-HPR, cells were fixed in 1% formaldehyde in PBS (pH 7.4) for 15 min at 4°C. The cells were washed twice with PBS. Cells were then resuspended in 70% ice-cold ethanol and stored in a −2°C freezer. For the assay, cells were first suspended in 1 ml wash buffer containing cacodylic acid, Tris–HCl-buffered solution and sodium azide (Phoenix flow cytometry kit, Phoenix Flow Systems, San Diego, CA). Approximately 10^6 cells were resuspended in 50 μl staining buffer containing Tris–HCl, TdT, and fluorescein-12-dUTP (Phoenix flow cytometry kit). Cells were incubated at 37°C for 60 min, rinsed twice with PBS, stained with 500 μl of propidium iodide/RNase A solution in the dark for 30 min at room temperature, then analyzed by flow cytometry using a FACScan flow cytometer, the Epics Profile (Coulter Corp, Hialeah, FL) with a 15-mW argon laser for excitation at 488 nm. Fluorescence was measured at 480 nm. The Phoenix flow cytometry kit included suspensions of cells that served as negative and positive controls for apoptosis. Computer analysis of the data provided information on the percentage of apoptotic cells, as well as the proportion of cells in the hypodiploid, G_1, S, and G_2 phases of the cell cycle.

Caspase-3 activity assay

The cells were plated in 96-well tissue culture plates at densities ranging from 0.5 to 1×10^5 cells per well and treated with 2, 5, or 10 μM 4-HPR for 12, 24, 48, or 72 h. Control cultures received the same amount of DMSO. Following culture, the 96-well plate was spun at $500 \times g$ for 5 min, and the supernatant removed. The extraction buffer (EB) and assay buffer (AB) caspase-3 activity assay fluorometric kit (Oncogene Research Products) was prepared by adding 10 μl of 1 M DTT/ml EB and 10 μl of 1 M DTT/ml AB. Positive and negative controls were provided with the fluorometric kit, and 50 μl EB/well were added to each assay and mixed gently. The plate was incubated for 30 min at 4°C; 50 μl AB/well was added to each assay well, and the plate was incubated for 30 min at 37°C. The plate was read immediately after adding 10 μl/well of caspase-3 fluorescent substrate using a fluorescent plate reader at 400 nm excitation, 505 nm emission. Maximal caspase-3 activity was determined at different interval, and the remainder of the experiment was carried out when maximal activity was observed.

Mitochondrial permeability transition (MPT)

NOE, IOSE and OVCA420 cells were treated with 2, 5 and 10 μM 4-HPR for 12, 24, 48, and 72 h to determine the time of maximal mitochondrial permeability transition. Cells were then washed and resuspended in 40 nM MitoFluor® medium, incubated for 30–45 min at 3°C, and visualized under the fluorescent microscope at 490 nm excitation, 516 nm emission. Using a photo-amplifier connected to the epifluorescent microscope, a field of 20–30 cells was chosen to measure light intensity.

Western blot analysis of apoptosis-related genes and other gene expressions modulated by 4-HPR

Nuclear and cytoplasmic extracts were prepared from control and 2, 5, and 10 μM 4-HPR-treated NOE, IOSE and OVCA420 cells. Nuclear or cytoplasmic protein (80 μg/lane) were electrophoresed on 8% polyacrylamide gels in the presence of 0.1% SD, and transferred to a nitrocellulose membrane. The membrane was incubated with mouse IgG monoclonal antibodies against p53 (which recognizes both wild type and mutant), p21 and p16 (Santa Cruz Biotech, Santa Cruz, CA), then washed and incubated with a peroxidase-conjugated anti-mouse antibody (Amersham Biosciences, Piscataway, NJ). Immunoreactive bands were developed using an enhanced chemiluminescence reagent (Amersham Biosciences). The blots were stripped and then re-incubated with mouse anti-β-actin antibody (Sigma Chemical Co.) to normalize for loading differences. The quantization of the expression level relative to that of β-actin was calculated by using arbitrary units obtained from the densitometry.

Results

Growth inhibitory effects of 4-HPR in NOE, IOSE, and ovarian cancer cells

NOE, IOSE, and the three ovarian cancer cell lines were grown in monolayer cultures and treated with different concentrations of 4-HPR (1–10 μM) for 3 days. SkOV3, OVCA420, and OCC-1 were studied to determine which ovarian cancer cell line would serve as the best model for comparison between the normal, premalignant and malignant models. OVCA420 was chosen because it had the most sensitivity to 4-HPR and, thus, could be evaluated most comparably to the NOE and IOSE cell lines. We first compared low concentrations from 1 to 5 μM of 4-HPR in NOE, IOSE, and OVCA420 (Fig. 1a). Concentrations from 2 to 10 μM 4-HPR were used on the ovarian cancer cells (Fig. 1b); 10 μM 4-HPR had greater growth inhibitory

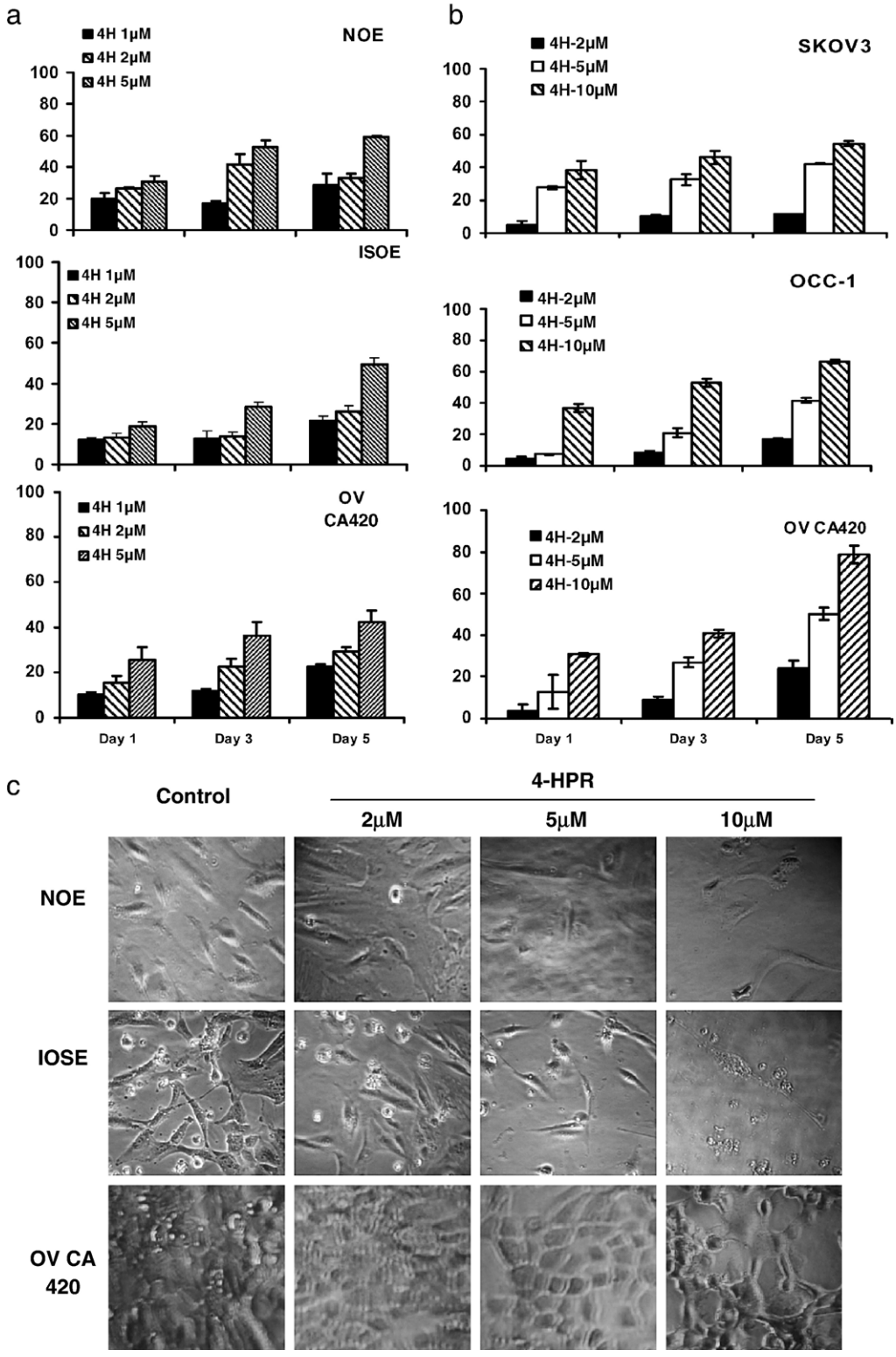

Fig. 1. Effect of 4-HPR on the growth inhibition of NOE, IOSE, and ovarian cancer cells. Cells were grown in the absence (control) or presence of 1, 2, 5, or 10 μM 4-HPR for 5 days, and stained with crystal violet on day 5 for analysis of growth inhibition. The percentage of growth inhibition was calculated as described in Materials and methods. (a) NOE* (average from 6 different NOE cells), IOSE, and OVCA420 cells were treated with 1, 2, or 5 μM 4-HPR. (b) Ovarian cancer cells, SkOV3, OCC-1, and OVCA420 cells, were treated with 2, 5, or 10 μM 4-HPR. (c) Morphologic change of 2, 5, or 10 μM 4-HPR in normal and ovarian cancer cells.

effects than the lower doses on the cancer cell lines. OVCA420 cells were the most sensitive cell line compared with other two cell lines (Fig. 1b). The graphical representations for the percentage of growth inhibition are shown in Figs. 1a and b. The morphologic changes of 1–10 μM 4-HPR in normal and ovarian cancer cells are shown in Fig. 1c. The NOE and IOSE cells were very sensitive to 10 μM 4-HPR; almost all cells were killed by day 3. Morphological changes consistent with differentiation (cells become more elongated) are observed along with cell death (Fig. 1c).

Apoptosis induction by 4-HPR

To assess other possible mechanisms of 4-HPR in ovarian cells, we analyzed the effects of 4-HPR on the induction of apoptosis in primary culture and cell lines by TdT labeling and flow cytometry. NOE and IOSE cells were treated with 5 μM 4-HPR. DNA content and apoptosis induction were analyzed (Fig. 2). The results showed that the apoptotic cell population did not change at this concentration, but a population of cells with hypodiploid (HD) DNA content increased 2- to 8-fold with increasing time of incubation with 5 μM 4-HPR in these cells (Fig. 2). The increase in hypodiploid cell population was shown as a population shift to the left (Fig. 2).

NOE, IOSE, and OVCA420 cells were treated with 2, 5, and 10 μM 4-HPR. Apoptosis induction was analyzed at different concentrations and different time points (Figs. 3a and b). Results demonstrated that 4-HPR-induced apoptosis was dose dependent in the NOE and OVCA420 cells (Fig. 3a); apoptosis was less marked in the IOSE cells than in the NOE and OVCA420 cells (Fig. 3a). 4-HPR-induced apoptosis was also time dependent in ovarian cells. A time course of apoptosis induction was carried out in the NOE, IOSE, and OVCA420 cells when treated with 4-HPR at 10 μM (Fig. 3b).

Effect of 4-HPR on caspase-3 activity

The 4-HPR effect on caspase-3 activation at different concentrations and different lengths of incubation was measured in NOE, IOSE, and OVCA420 cells (Fig. 4). Cells were treated with 2, 5, and 10 μM 4-HPR, and caspase-3 activity was measured at 12, 24, 48, and 72 h after treatment. The patterns of caspase-3 activity were different in the all three cell types, and 2 μM 4-HPR had little effect

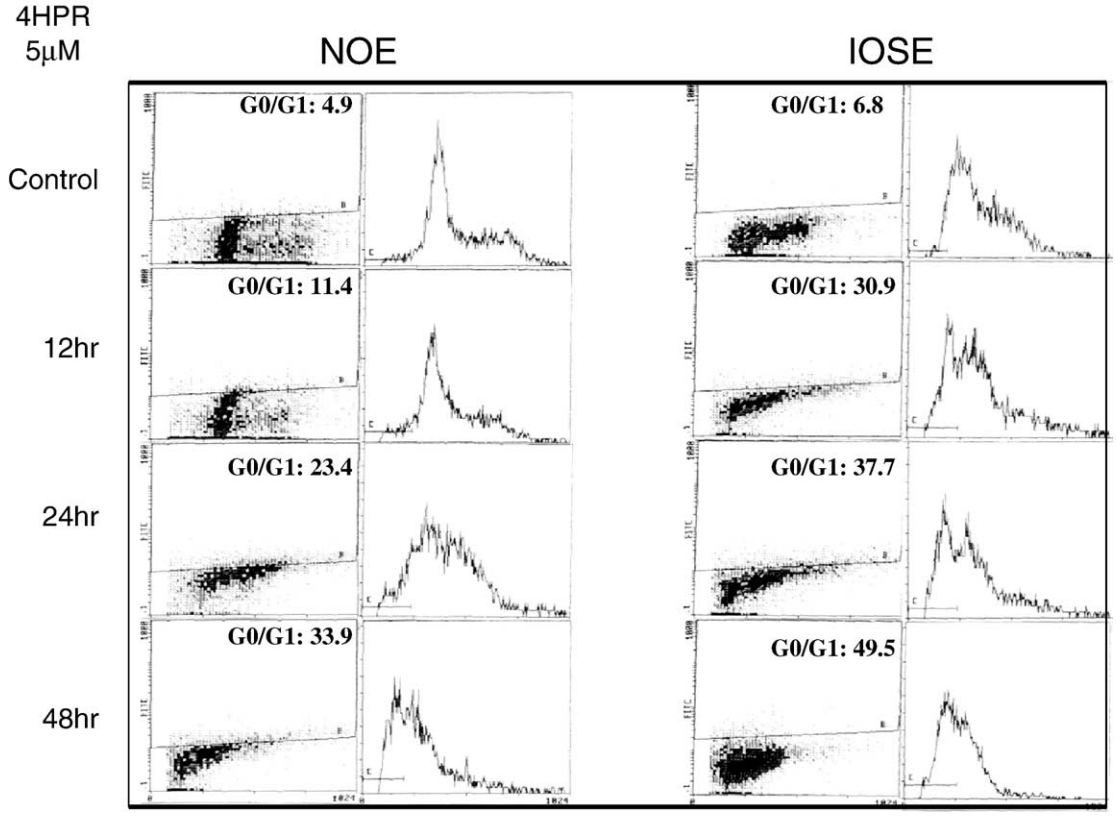

Fig. 2. Effect of 5 μM 4-HPR in NOE and IOSE cells. Cells were treated with 5 μM 4-HPR for 12, 24, and 48 h. The cells were harvested and then stained with propidium iodide for DNA content analysis and with fluorescein-labeled dUTP to label DNA fragments by the TUNEL method, as described in Materials and methods. The fluorescence of cells labeled by the TUNEL method is presented in the left columns, which fluorescence of viable and apoptotic cells represented by the dark dots below and above a demarcation line determined by a standard cell line provided with the labeling kit. The data on DNA content distribution are presented in the left column. The percentage of cell populations in the G0/G1 phase were labeled in the right corner at each time interval.

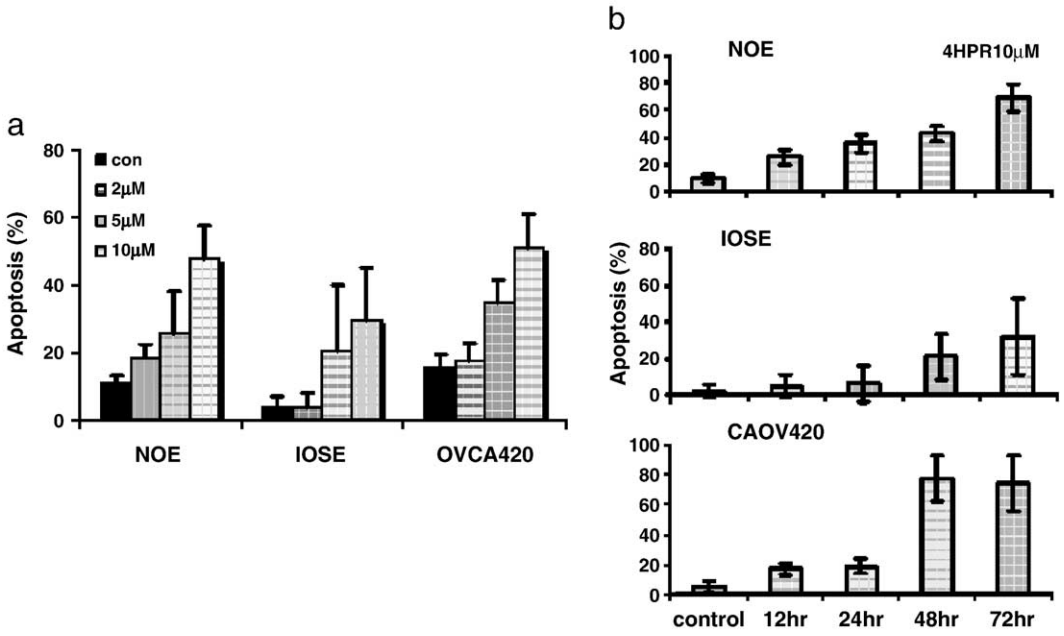

Fig. 3. Effect of 4-HPR on apoptosis induction in NOE, IOSE, and OVCA420 cells. (a) Dose response of 4-HPR in apoptosis induction. Effect of different concentration of 4-HPR on ovarian cells. Cells were treated with 2, 5, and 10 μM 4-HPR for 3 days. The apoptosis were determined by the TUNEL assay. The percentage of apoptotic cells is indicated in the right corner of each treatment analysis. (b) Time-course of 10 μM 4-HPR on apoptosis induction. Cells were treated with 10 μM 4-HPR for 12, 24, 48, and 72 h. The percentage of apoptotic cells was determined by the TUNEL assay. Data are presented as the mean ± SE of triplicate assays.

on caspase-3 activity in any of the cells. After 24 h of treatment, an increase in caspase-3 activity was detected in IOSE and OVCA420 cells treated with 10 μM 4-HPR. Caspase-3 activity increased when NOE cells were incubated for 3 days with 10 μM 4-HPR (Fig. 4).

Effect of 4-HPR on mitochondrial permeability transition

Mitochondrial permeability transition (MPT) changes are associated with apoptosis. To investigate the mechanism of 4-HPR-induced apoptosis in ovarian cancer cells, experiments were carried out to determine the effect of 4-HPR on MPT in NOE, IOSE and OVCA420 cells. OVCA420 cells had a greater change in MPT than did the NOE and IOSE cells after treatment with 4-HPR (Figs. 5a and b). 4-HPR decreased mitochondrial inner membrane potential, which increased MPT in these cells (Figs. 5a and b). An inverse relationship in mitochondrial potential correlated in a dose-dependent manner with both the increase in apoptosis and growth inhibition by 4-HPR in all three cell types (Figs. 1, 2, 5b).

Modulation of p53 and other gene expressions by 4-HPR in NOE, IOSE, and OVCA420 cells

The effect of 4-HPR on the expression of the apoptosis-associated genes p53, p21, and p16 was examined in NOE, IOSE, and OVCA420 cells; p53 expression was detected in the NOE, IOSE, and OVCA420 cells. 4-HPR increased p53 expression in the NOE cells in a dose-dependent manner, but not in IOSE and OVCA420 cells (Figs. 6a and b). The expression of the p21 gene was increased in NOE and IOSE cells but was not detectable in OVCA420 cells. The expression of p16 was modulated by 4-HPR in all three cell types (Figs. 6a and b).

Discussion

Retinoids have been studied as cancer chemopreventive agents [4–7] based on epidemiologic data, showing that diets high in Vitamin A are associated with lower odds of epithelial cancers [24]. An Italian trial that evaluated 4-HPR for the prevention of secondary breast cancers [14] demonstrated a decreased incidence of ovarian cancer in women receiving 4-HPR, suggesting that retinoids prevented the development of ovarian cancer [13,15]. Experimental studies have demonstrated that retinoids can affect human ovarian cancer cell growth by inhibiting proliferation and inducing apoptosis, which are thought to be important mechanisms in cancer prevention [12].

Programmed cell death is a physiological mechanism by which organisms eliminate cells during embryonic development and counterbalance cell division for homeostatic regulation of tissue mass in the adult. The term apoptosis was coined by Kerr et al. to describe this process, which is characterized by cell shrinkage, chromatin condensation, nuclear segmentation, and internucleosomal degradation of DNA [25]. Apoptosis can be induced by a variety of external and intracellular signals including those that induce

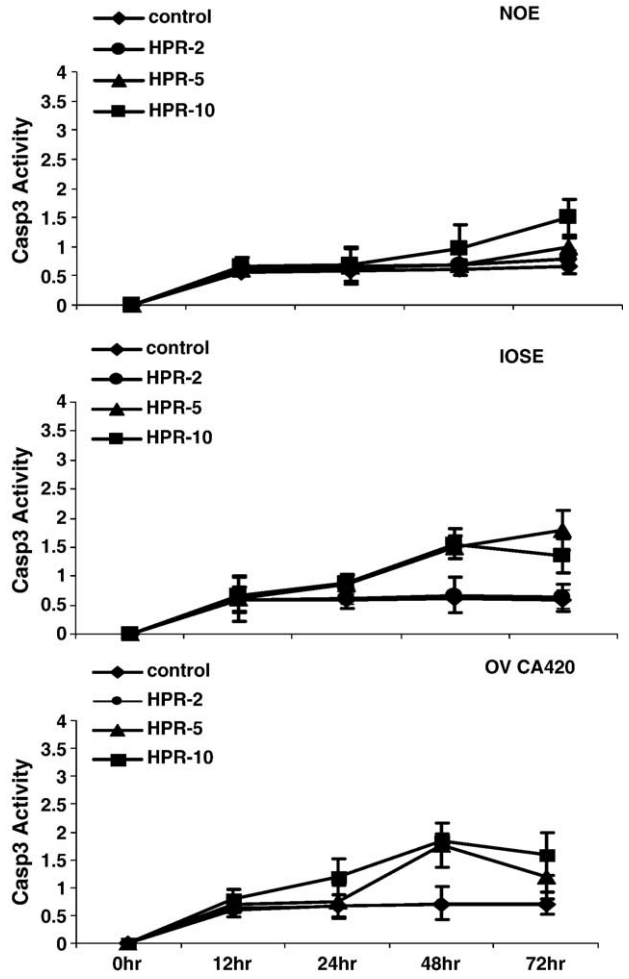

Fig. 4. Effect of 4-HPR on caspase-3 activity in NOE, IOSE, and OVCA420 cells. Cells were grown in 96-well plates in the absence (control) or presence of 4-HPR (2, 5 and 10 μM) for 12, 24, 48 and 72 h, and incubated in caspase-3 activity assay buffer, as described in Materials and methods. The intensity of staining was read using a fluorescent plate reader at 400 nm excitation, 505 nm emission, immediately after adding caspase-3 fluorescent substrate conjugate.

terminal differentiation or DNA-damage. This induction may constitute a protective anti-neoplastic mechanism to eliminate DNA-damaged cells and repair mutations [26]. Carcinogenesis is often associated with a decreased tendency to undergo apoptosis in response to certain physiological stimuli and cytotoxic agents. Therefore, agents that can induce apoptosis or restore the ability to undergo apoptosis in premalignant and malignant cells are expected to be effective in cancer prevention and treatment [26,27]. Several reports have demonstrated that certain retinoids, in addition to exerting cytostatic effects on tumor cells in vitro [28], also induce apoptosis in various cell types during normal development and in cultured normal and tumor cells [29–33].

This study is the first to use normal ovarian surface epithelial cells, immortalized epithelial cells, and cancer cells to investigate the effect of 4-HPR on growth and apoptosis. Different cell types showed different responses to 4-HPR in a dose-dependent manner. The normal cells harvested from normal women's ovaries were used to mimic normal ovarian surface cells. The immortalized cells were used to mimic epithelial cells from high-risk women. Although T-antigen immortalized cells may not bear a resemblance to preneoplastic cells, this is the best model currently available, and immortalized cells have been extensively studied in cervical [22] and lung epithelial cells [17,18] as premalignant models. Since the doses of 4-HPR were contradictory in human trials [13–15,21], we tested different concentrations of 4-HPR, ranging from 1 to 10 μM in these cell models, to determine an optimal concentration depending on cell type. The immortalized ovarian cells, which may correspond to what is present in high risk women, were not sensitive to 4-HPR compared to normal and cancer cells, and less apoptosis was detected by TUNEL assay, suggesting that cells containing mutations may be less sensitive to chemopreventive agents. This phenomenon has also been observed in immortalized lung epithelial cells in which these cells exhibit less sensitivity than lung adenocarcinoma cells in response to 4-HPR [17,18]. 4-HPR was thought to act mainly through induction of differentiation which takes 2–4 days in cell culture; however, Kelloff et al [34] as well as other groups have shown that this drug acts thorough induction of apoptosis and growth inhibition which occurs within 12–24 h, earlier and stronger than differentiation [7–9]. Dr. Follen's group reported that in both in vivo and in vitro, a higher 4-HPR dose may be needed to treat a premalignant lesion [21,22]. There are clinical trials currently being conducted with 4-HPR treatment for ovarian cancer in doses as high as 1800 mg/day without reported toxicity. Thus, the higher dose corresponding to the 5–10 μM in vitro concentration may be achievable without major toxicity and therefore merits intensive in vitro study.

Retinoids, particularly 4-HPR, have been shown to increase aerobic glycolysis by increasing mitochondrial permeability to the co-enzymes nicotinamide adenine dinucleotide (NAD(P)H) and flavin adenine dinucleotide (FAD), as well as activity of the electron transport chain characterized by an increase in reactive oxygen species and cytochrome oxidase [8,9]. There has been increased interest in mitochondrial function in both normal and cancer cells. In particular, the mitochondria are thought to be the site of induction of apoptosis for many of the chemopreventive agents. Retinoids were initially thought to act through nuclear receptors. However, 4-HPR has been shown to be receptor independent in many cells lines [35–39] and induces a change in the mitochondrial permeability of the membrane [29]. The permeability of the inner mitochondrial membrane, also called membrane permeability transition, can be increased by thiol agents and oxidative stress-inducing agents that are thought to be dependent on the opening of a non-selective pore [40–44]. A shift towards a more oxidized condition increases membrane permeability, while the opposite occurs with reducing agents [41].

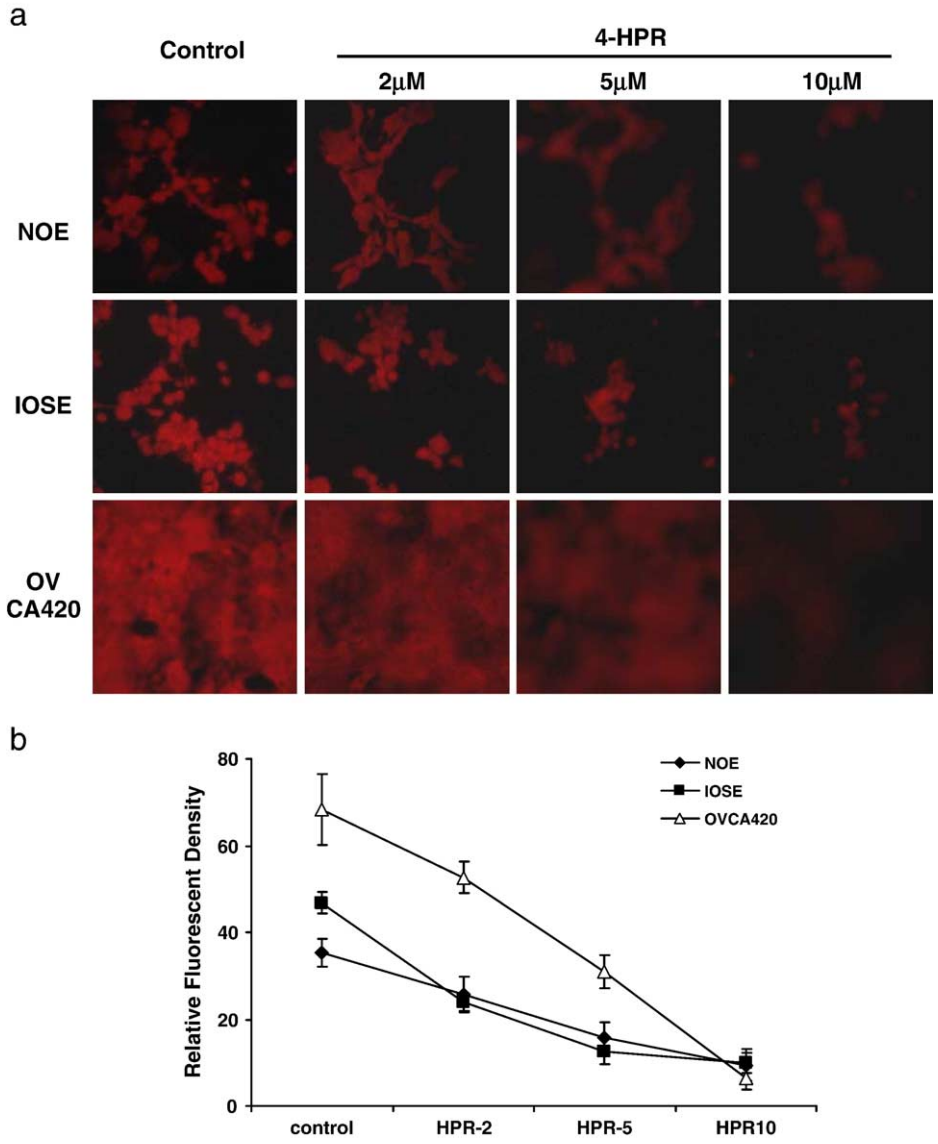

Fig. 5. (a) Effect of 4-HPR on mitochondrial permeability transition (MPT) in NOE, IOSE, and OVCA420 cells. Cells were treated with 2, 5, and 10 μM 4-HPR for 3 days and then resuspended in 40 nM MitoFluor medium. Cells were visualized under the fluorescent microscope. (b) Quantitative changes in relative fluorescent density which corresponds to change in mitochondrial permeability transition.

Mitochondrial dysfunction, in particular the induction of the mitochondrial membrane permeability transition (MPT), has been implicated in the cascade of events involved in the induction of apoptosis. Inhibition of the mitochondrial electron-transport chain reduces the mitochondrial transmembrane potential ($\Delta\Psi_m$), which induces the formation of the mitochondrial permeability transition pore and the subsequent MPT. Disruption or collapse of the $\Delta\Psi_m$ and the induction of the MPT results in the loss of matrix Ca^{2+} and glutathione, increased oxidation of thiols, and further depolarization of the inner mitochondrial membrane, which increase the gating potential for the MPT pore. The MPT is thought to function as a self-amplifying "switch" that, once activated, irreversibly commits the cell to apoptosis. We have clearly shown that treatment with increasing doses of 4-HPR has a major effect on the MPT, inducing formation of this non-selective pore and allowing dissipation of the dye that is sequestered inside the mitochondria inner membranes. These findings, which are the first to be reported in ovarian cells, suggest that these agents act through changes in the membrane potential by uncoupling the electron transport chain and inducing formation of the MPT which allows dissipation of not only the mitochondrial dye but also the small ions and molecules inherent in the functioning of the mitochondria.

Cancers are thought to create a more hypoxic environment which may affect mitochondrial function [45,46]. Growth in the presence of retinoids may alter the mitochondrial function by inducing growth arrest and apoptosis and thus create a more oxidized environment, or alternatively, retinoids may increase the oxidized condition and the mitochondrial permeability which may induce apoptosis.

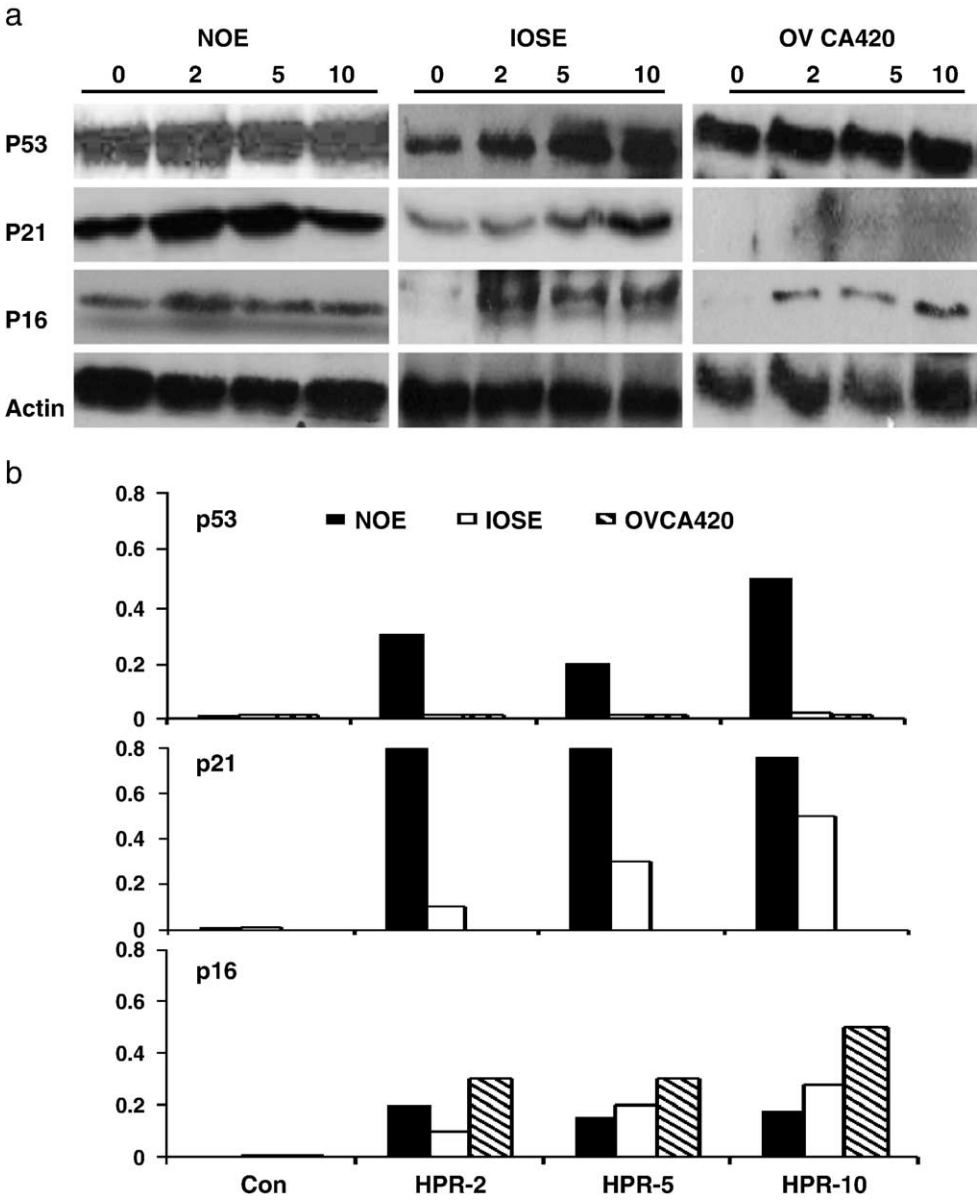

Fig. 6. (a) Effect of 4-HPR on p53, p21, and p16 expression in NOE, IOSE and OVCA420 cells. Nuclear proteins were extracted from cells treated with 5 μM 4-HPR for 3 days. Eighty microgram/lane of nuclear proteins were subjected to SDS-PAGE. The p53, p21, and p16 proteins were identified by blotting with monoclonal antibodies. Immunoreactive bands were visualized using enhanced chemiluminescence, as described in Materials and methods. The blots were stripped and reblotted to mouse anti-β-actin antibody for assessment of loading in each lane. (b) This graph shows the quantitative changes in p53, p21, and p16 in NOE, IOSE, and OVCA420 at 2, 5, and 10 μM 4-HPR.

In our study, all three cell types showed an increase in mitochondrial permeability, most notable in the ovarian cancer cell line, suggesting that 4-HPR induces apoptosis and inhibits growth, in part, by increasing mitochondrial permeability. Our work with fluorescence spectroscopy suggests a change in the oxidative state in cells treated with 4-HPR due to an increased generation of FAD and decreased generation of NADH [47]. The redox potential increased as both growth inhibition and apoptosis increased [47].

P53, a tumor suppressor protein and transcription factor, increases G_1, induces cell growth arrest, and allows cells to repair DNA damage or undergo apoptosis [47–49]. The binding of p53 to DNA induces cell cycle-related genes, the mechanism by which growth inhibition occurs. P53 binding is redox sensitive and is inhibited by oxidizing conditions, which decreases the growth inhibition or apoptotic effect of p53 while reducing conditions enhance the binding of p53 to DNA [48], increasing the response to some retinoids [49]. In addition, p53 has been hypothesized to induce apoptosis by stimulating the production of reactive oxygen species (ROS), causing mitochondrial damage, which is suggested by the change in the mitochondrial permeability that occurred [50,51]. In our study, 4-HPR induced apoptosis

and increased p53 expression in NOE cells. These results suggest that 4-HPR partially stimulates the p53 pathway with downstream markers p21 and p16 being activated, particularly in normal cells.

The NOE cells showed the most activation of the p53 pathway, while the cancer cells showed the most effect on the MPT, suggesting a different mechanism for the end result of growth inhibition and/or apoptosis. Caspase-3 is one of the effector caspases and may be p53 dependent or independent. The effect on caspase-3 activation was modest and occurred maximally at 72 h in the normal and immortalized cells and maximally at 48 h in the ovarian cancer cells with the higher concentration (10 μM 4-HPR), suggesting that the effect of 4-HPR may be through multiple pathways, including p53, and by a direct effect on the mitochondria. Different concentrations of retinoid may act in a different manner, with the lower doses inducing more growth arrest and the higher doses inducing more apoptosis. In addition, using these models of normal, premalignant and cancer cells may reflect some differences in vivo and may help determine which populations might benefit the most from these concentration.

These finding have implications for the approaches for chemopreventive recommendations. Women with normal, low-risk ovaries may be amenable to lower doses of retinoid and the higher-risk women with potentially more mutations (analogous to the immortalized cells) may respond to a higher dose of 4-HPR. One of the limitations of any study is the lack of a true premalignant ovarian surface epithelial cell line. However, it is a model that represents a cell that has undergone a mutation which could conceivably be a precursor to a premalignant lesion. Our results suggest that different concentrations of 4-HPR may be needed in different populations of women for prevention of ovarian cancer.

Acknowledgments

This study was supported by a grant from the Arizona Disease Control Research Commission (ADCRC), RFP 1-700 (Brewer and Zou). Drs. Brewer, Gershenson, and Bast were supported by a grant from the Department of Defense, DAMD 17-99-1-9505. Dr. Zou was supported by a grant from the NIH-NCI, KO7-CA75966 and Ovarian Cancer Research Fund, NY, NY.

References

[1] Hoskins WJ. Prospective on ovarian cancer: why prevent? J Cell Biochem Suppl 1995;23:189–99.
[2] Kelloff GJ, Boone CW, Crowell JA, Nayfield SG, Hawk E, Steele VE. Strategies for Phase II cancer chemoprevention trials: cervix, endometrium, and ovary. J Cell Biochem Suppl 1995;23:1–9.
[3] Dhingra K. A Phase II chemoprevention trial design to identify surrogate endpoint biomarkers in breast cancer. J Cell Biochem Suppl 1995;23:19–24.
[4] Moon TE, Levine N, Cartmel B, Bangert JL, Rodney S, Dong Q, et al. Effect of retinol in preventing squamous cell skin cancer in moderate-risk subjects: a randomized, double-blind, controlled trial. Southwest Skin Cancer Prevention Study Group. Cancer Epidemiol Biomarkers Prev 1997;6:949–56.
[5] Levine N, Moon TE, Cartmel B, Bangert JL, Rodney S, Dong Q, et al. Trial of retinol and isotretinoin in skin cancer prevention: a randomized, double-blind, controlled trial. Southwest Skin Cancer Prevention Study Group. Cancer Epidemiol Biomarkers Prev 1997;6:957–61.
[6] Kurie JM, Lee JS, Khuri FR, Mao L, Morice RC, Lee JJ, et al. N-(4-hydroxyphenyl) retinamide in the chemoprevention of squamous metaplasia and dysplasia of the bronchial epithelium. Clin Cancer Res 2000;6:2973–9.
[7] Clifford JL, Sabichi AL, Zou C, Yang X, Steele VE, Kelloff GJ, et al. Effects of novel phenylretinamides on cell growth and apoptosis in bladder cancer. Cancer Epidemiol Biomarkers Prev 2001;10:391–5.
[8] Suzuki S, Higuchi M, Proske RJ, Oridate N, Hong WK, Lotan R. Implication of mitochondria-derived reactive oxygen species, cytochrome C and caspase-3 in N-(4-hydroxyphenyl) retinamide-induced apoptosis in cervical carcinoma cells. Oncogene 1999;18:6380–7.
[9] Oridate N, Suzuki S, Higuchi M, Mitchell MF, Hong WK, Lotan R. Involvement of reactive oxygen species in N-(4-hydroxyphenyl)retinamide-induced apoptosis in cervical carcinoma cells. J Natl Cancer Inst 1997;89:1191–8.
[10] Sharp RM, Bello-DeOcampo D, Quader ST, Webber MM. N-(4-hydroxyphenyl) retinamide (4-HPR) decreases neoplastic properties of human prostate cells: an agent for prevention. Mutat Res 2001;496:163–70.
[11] Thaller C, Shalev M, Frolov A, Eichele G, Thompson TC, Williams RH, et al. Fenretinide therapy in prostate cancer: effects on tissue and serum retinoid concentration. J Clin Oncol 2000;18:3804–8.
[12] Supino R, Crosti M, Clerici M, Warlters A, Cleris L, Zunino F, et al. Induction of apoptosis by Fenretinide (4-HPR) in human ovarian carcinoma cells and its association with retinoic acid receptor expression. Int J Cancer 1996;65:491–7.
[13] De Palo G, Veronesi U, Camerini T, Formelli F, Mascotti G, Boni C. Can Fenretinide protect women against ovarian cancer? J Natl Cancer Inst 1995;87:146–7.
[14] Veronesi U, De Palo G, Marubini E, Costa A, Formelli F, Mariani L, et al. Randomized trial of fenretinide to prevent second breast malignancy in women with early breast cancer. J Natl Cancer Inst 1999;91:1847–56.
[15] De Palo G, Mariani L, Camerini T, Marubini E, Formelli F, Pasini B, et al. Effect of fenretinide on ovarian carcinoma occurrence. Gynecol Oncol 2002;86:24–7.
[16] Dabal R, Boyer CM, Berchuck A, Roberts A, Roche N, Sporn M, et al. Synergistic inhibition of ovarian cancer cell proliferation by TGFβ and retinoic acid (RA) derivatives. Proc Am Assoc Cancer Res 1995;36:635.
[17] Zou CP, Kurie JM, Lotan D, Zou CC, Hong WK, Lotan R. Higher potency of N-(4-hydroxyphenyl) retinamide than all-trans-retinoic acid in induction of apoptosis in non-small cell lung cancer cell lines. Clin Cancer Res 1998;4:1345–55.
[18] Kim Y-H, Dohi DF, Han G-R, Zou CP, Oridate N, Walsh GL, et al. Retinoid refractoriness occurs during lung carcinogenesis despite functional retinoid receptors. Cancer Res 1995;55:5603–10.
[19] Wu S, Zhang D, Soprano D, Soprano K. Effects of conformationally restricted synthetic retinoids on ovarian tumor cell growth. J Cell Biochem 1998;68:378–88.
[20] Zhang D, Holmes WF, Wu S, Soprano DR, Soprano KJ. Retinoids and ovarian cancer. J Cell Physiol 2000;185:1–20.
[21] Follen M, Atkinson EN, Schottenfeld D, Malpica A, West L, Lippman S, et al. A randomized clinical trial of 4-hydroxyphenylretinamide for high-grade squamous intraepithelial lesions of the cervix. Clin Cancer Res 2001;7:3356–65.
[22] Zou C, Vlastos AT, Yang L, Wang J, Brewer M, Follen M. Effect of 4-

hydroxyphenyl retinamide on human cervical epithelial and cancer cell lines. J Soc Gynecol Invest 2003;10:41–8.
[23] Berchuck A, Rodriquez G, Olt G, Whitaker R, Boente MP, Arrick BA, et al. Regulation of growth of normal ovarian epithelial cells and ovarian cancer cell lines by transforming growth factor-beta. Am J Obstet Gynecol 1992;166:676–84.
[24] Mori M, Harabuchi I, Miyake H, Casagrande JT, Henderson BE, Ross RK. Reproductive, genetic, and dietary risk factors for ovarian cancer. Am J Epidemiol 1998;128:771–7.
[25] Kerr JF, Wyllie AH, Currie AR. Apoptosis: a basic biological phenomenon with wide-ranging implications in tissue kinetics. Br J Cancer 1972;26:239–57.
[26] Thompson HJ, Strange R, Schedin PJ. Apoptosis in the genesis and prevention of cancer. Cancer Epidemiol Biomarkers Prev 1992;1: 597–602.
[27] Dive C, Wyllie AH. Apoptosis and cancer chemotherapy. In: Hickman JA, Tritton TT, editors. Frontiers in Pharmacology: Cancer Chemotherapy. Oxford: Blackwell Scientific; 1993. p. 21–56.
[28] Lotan R. Cellular biology of the retinoids. In: Degos L, Parkinson DR, editors. Retinoids in Oncology. Berlin: Springer; 1995. p. 27–42.
[29] Kochhar DM, Jiang H, Harnish DC, Soprano DR. Evidence that retinoic acid-induced apoptosis in the mouse limb bud core mesenchymal cells is gene-mediated. Prog Clin Biol Res 1993; 383B:815–25.
[30] Benito A, Grillot D, Nunez G, Fernandez-Luna JS. Regulation and function of Bcl-2 during differentiation-induced cell death in HL-60 promyelocytic cells. Am J Pathol 1995;146:481–90.
[31] Nagy L, Thomazy VA, Chandraratna RAS, Heyman RA, Davies PJA. Retinoid-regulated expression of Bcl-2 and tissue transglutaminase during the differentiation and apoptosis of human myeloid leukemia (HL-60) cells. Leukemia Res 1996;20:499–505.
[32] Okazawa H, Shimizu J, Kamei M, Imafuku I, Hamada H, Kanazawa I. Bcl-2 inhibits retinoic acid-induced apoptosis during the neural differentiation of embryonal carcinoma stem cells. J Cell Biol 1996;132:955–68.
[33] Dipietrantonio A, Hsieh T-C, Wu JM. Differential effects of retinoic acid (RA) and N-(4-hydroxyphenyl)retinamide (4-HPR) on cell growth, induction of differentiation, and changes in p34cdc2, Bcl-2, and actin expression in the human promyelocytic HL-60 leukemic cells. Biochem Biophys Res Commun 1996;224:837–42.
[34] Kelloff GJ. N-(4-hydroxyphenyl)retinamide (4HPR): clinical development plan. J Cell Biochem Suppl 1994;20:176–96.
[35] Hail Jr N, Lotan R. Mitochondrial permeability transition is a central coordinating event in N-(4-hydroxyphenyl) retinamide-induced apoptosis. Cancer Epidemiol Biol Prev 2000;9:1293–301.
[36] Sun SY, Li W, Yue P, Lippman SM, Hong WK, Lotan R. Mediation of N-(4-hydoxyphenyl) retinamide-induced apoptosis in human cancer cells by different mechanisms. Cancer Res 1999;59:2943–98.
[37] Marchetti P, Zanzani N, Joseph B, Maschke S, Mereau-Richard C, Costantine AP, et al. The novel retinoid 6-[3-(1-adamantyl)-4-hydroxyphenyl]-2-napthalene carboxylic acid cancer trigger apoptosis through a mitochondrial pathway independent of the nucleus. Cancer Res 1999;59:6257–66.
[38] Sun SY, Yue P, Lotan R. Induction of apoptosis by N-(4-hydroxyphenyl) retinamide and its association with reactive oxygen species, nuclear retinoic acid receptors, and apoptosis-related genes in human prostate carcinoma cells. Am Soc Pharmacol Exp Ther 1999;55:403–10.
[39] Suzicki S, Higuchi M, Proske R, Oridate N, Hong WK, Lotan R. Implication of mitochondria-derived reactive oxygen species, cytochrome C and caspase-3 in N-(4-hydroxyphenyl) retinamide-induced apoptosis in cervical cancer cells. Oncogene 1999;18: 6380–7.
[40] Tafani M, Schneider TG, Pastorino JG, Farber JL. Cytochrome *c*-dependent activation of caspase-3 by tumor necrosis factor requires induction of the mitochondrial permeability transition. Am J Pathol 2000;156:2111–21.
[41] Halestrap AP, McStay GP, Clarke SJ. The permeability transition pore complex: another view. Biochimie 2002;84:153–66.
[42] Tiwari BS, Belenghi B, Levine A. Oxidative stress increased respiration and generation of reactive oxygen species, resulting in ATP depletion, opening of mitochondrial permeability transition, and programmed cell death. Plant Physiol 2002;128:1271–81.
[43] Hail Jr N, Youssef EM, Lotan R. Evidence supporting a role for mitochondrial respiration in apoptosis induction by the synthetic retinoid CD437. Cancer Res 2001;61:6698–702.
[44] Higuchi M, Proske RJ, Yeh ET. Inhibition of mitochondrial respiratory chain complex I by TNF results in cytochrome *c* release, membrane permeability transition, and apoptosis. Oncogene 1998;17: 2515–24.
[45] Walenta S, Snyder S, Haroon ZA, Braun RD, Amin K, Brizel D, et al. Tissue gradients of energy metabolites mirror oxygen tension gradients in a rat mammary carcinoma model. Int J Radiat Oncol Biol Phys 2001;51:840–8.
[46] Chance B. Metabolic heterogeneities in rapidly metabolizing tissue. J Appl Cardiol 1989;4:207–21.
[47] Brewer M, Utzinger U, Li Y, Atkinson EN, Satterfield W, Auersperg N, et al. Fluorescence spectroscopy as a biomarker in a cell culture and in a nonhuman rhesus primate model for ovarian cancer chemopreventive agents. J Biomed Opt 2002;7:20–6.
[48] Berchuck A, Elbendary A, Havrilesky L, Rodriquez G, Bast R. Pathogenesis of ovarian cancers. J Soc Gynecol Invest 1994;1: 181–90.
[49] Wu Q, Kirschmeier P, Hockenberry T, Yang TY, Brassard DL, Wang L, et al. Transcriptional regulation during p21WAF1/CIP1-induced apoptosis in human ovarian cancer cells. J Biol Chem 2002;277: 36329–37.
[50] Shin D, Xu X, Lippma S, Lee JL, Lee JS, Batsakis J, et al. Accumulation of p53 protein and retinoid acid receptor ß in retinoid chemoprevention C1. Cancer Res 1997;3:875–80.
[51] Polyak K, Xia Y, Zweier JL, Kinzler KW, Vogelstein B. A model for p53-induced apoptosis. Nature 1997;389:300–5.

[Frontiers in Bioscience 12, 2260-2268, January 1, 2007]

Combination of 4-HPR and oral contraceptive in monkey model of chemoprevention of ovarian cancer

Molly Brewer [1], James Ranger-Moore[2], William Satterfield[3], Zengping Hao[1], Jian Wang [1], Emily Brewer [1], J. Taylor Wharton [4], Robert Bast [4] , Changping Zou [1]

[1] Department of OB/GYN, University of Arizona, College of Medicine, Tucson, AZ 85724, [2] University of Arizona, College of Public Health, Tucson, AZ 85724, [3] Department of Veterinary Sciences Park, M. D. Anderson Cancer Center, Houston, TX, 77030, [4] Gynecologic Oncology, M. D. Anderson Cancer Center, Houston, TX, 77030

TABLE OF CONTENTS

1. ABSTRACT

4-(N-hydroxyphenyl) retinamide (4-HPR) and the oral contraceptives (OCP) are currently being used alone, and in combination, for the prevention of ovarian cancer. However, the mechanism of their effects has not been studied. Non-human primate models are ideal for studying the role of these and other drugs for cancer chemoprevention because of the genetic similarity between primates and humans in respect to hormone regulation and menstrual cycle. 4-HPR and OCP were administered to sixteen female adult *Macacca mulatta* (Rhesus macaques) for three months alone and in combination. Laparotomy was performed before and after treatment, and ovarian biopsies were obtained to evaluate the expression of retinoid and hormone receptors, and apoptosis. ERα was undetectable, but ERβ, PR, RXRα, and RXRγ were constitutively expressed in the ovaries. 4-HPR induced RXRα and RXRγ expression at a low level and, OCP induced expression of ERβ. However, the combination of 4-HPR with OCP had a larger effect on expression of retinoid receptors. Apoptosis was detected in the 4-HPR group (equivalent dose: 200 mg/day). The results provide a rationale for the use of the Rhesus macaque as a model for ovarian cancer chemoprevention.

2. INTRODUCTION

Ovarian cancer is the most common cause of death from gynecologic cancer. There are 23,400 new cases and 13,900 deaths estimated in 2003 in the US (1). Despite aggressive treatment, this cancer has the highest mortality of all gynecologic cancers with a 5 year survival rate for stage III and IV (the most commonly diagnosed stage) of 5-30% (1,2). Over 70% of ovarian cancers are diagnosed after the cancer has spread beyond the ovary (2), partially because there is no acceptable screening test or biomarkers to identify women destined to develop ovarian cancer or identify ovarian cancer at a premalignant or early stage. Late stage disease has an extremely poor prognosis. Given these characteristics, one rationale to reduce the mortality from ovarian cancer is prevention.

Retinoids have been used extensively in laboratory and clinical studies to prevent several human malignancies (3-8). Retinoids, especially the synthetic retinoid 4-HPR, have been shown to reduce ovarian cancer in a large scale clinical trial in Italy (5-8) and is now being used in combination with Tamoxifen in a phase II breast cancer prevention trial (9). It has been proposed that the anticarcinogenic and antitumor effects of retinoids are the result of retinoid-induced changes in cell growth and differentiation caused by changes in the expression of specific genes, such as oncogenes, growth factors, and growth factor receptors. Retinoids exert their effects on gene expression by activating a signal transduction pathway in which nuclear retinoid receptors play a pivotal role (10-16). These receptors are members of the steroid hormone receptor super family (10-16).

From a combined analysis of case control studies, observational data suggest that the oral contraceptive (OCP) reduces ovarian cancer risk by

approximately 10% for each year of use (17) leading to a total reduction around 40% after 4 to 5 years of use. (18,19)**.** It is hypothesized that the biological prevention activity is related to the progestational component of the OCP.

Animal models are developed to reconcile biologic phenomena between species (20) and allow for extrapolation of knowledge from one species to another, usually animal to human. Humans are difficult to study as experimental models because of ethical limitations, cost limitations, and lack of volunteers. Institutional Review Boards (IRB) has limited the scope of chemoprevention trials because the targeted population does not have cancer and thus the tolerance for side-effects is less than if cancer were present. Development of an animal model to mimic a human disease allows experimentation in a strictly controlled laboratory environment, in which experimental subjects can be manipulated in ways that can never be done in humans. Animal models are ideal for developing strategies based on mechanistic understanding of how these agents or interventions work. By understanding mechanisms of action, we can not only develop better strategies for intervention**,** but also target the most appropriate population. The non-human primate model is ideal for developing strategies because of the genetic similarity between monkey and humans, such as hormone regulation and menstrual cycle, which are lacking in small animal models such as the chicken and rodent.

Multi-targeted therapies or combination of retinoids and hormonal therapies**,** including OCP**,** may have an advantage in cancer chemoprevention because they may combine different mechanisms of prevention with a synergistic effect. This is the first study to combine 4-HPR and OCP in chemoprevention of ovarian cancer *in vivo*. Our results will provide important information for human trials.

3. MATERIAL AND METHOD

3.1. Monkeys

Sixteen female adult (age) Macacca mulatta (rhesus macaques) were used in the study as previously described (21). Monkeys used in this study were culled from the specific pathogen free rhesus colony because they developed herpes-B-indeterminate status, they were poor breeders, or they had chronic diarrhea. The monkeys were prevented from eating for 12 hr before surgery. Anesthesia was induced with an intramuscular injection of tiletamine HCl/zolazepam HCl (Telazol; Fort Dodge Laboratories, Inc., Fort Dodge, IA). The monkey was sedated, removed from the cage and intubated, and anesthesia was maintained on 2–2.5% isoflurane gas with oxygen. After each initial procedure, monkeys were maintained in separate housing and were fed the drug in a flavored treat. Menses were recorded daily, and progesterone levels were measured 2 weeks apart to evaluate ovulatory status.

Monkeys were given 35 mg 4-HPR/day, OCP 0.2 mg norethindrone/0.07 mg of ethinyl estradiol/day, combination of 4-HPR+OCP, or no medication for three months as previously reported (21). Laparotomy was performed before and after drug administration, and ovarian biopsy specimens were obtained. Doses of 4-HPR and OCP were calculated by allometric scaling, which calculates a dose based on both weight and basal metabolic rate (21). This is derived from the equation $Y + K(W_{kg}^{0.75})$, where Y is the resting animal's energy output in kcal/24 h (also termed the minimum energy cost), K is a constant based on core temperature, which is specific for each species, and W is mass in kilograms. Doses were calculated for a 7 kg monkey.

3.2. Immunohistochemistry (IHC)

Paraffin-embedded monkey slides were deparaffininzed in xylene, rehydrated through graded alcohols to water, then incubated for 10 min in PBS. The slides were blocked for 30 min with 3% horse serum diluted in PBS, the sections were then blotted and incubated with primary antibody of RARs and RXRs, ERα, β, and PR (Santa Cruse) for 1 hr at room temperature. For immunoperoxidase staining, the avidin-biotin-peroxidase complex (ABC) technique was used (Vector Laboratories). For this technique, the endogenous peroxidase was inactivated by incubation for 30 min in 0.015% peroxide in methanol, then rehydrated for 10 min in PBS. The slides were then incubated with biotinylated horse antibody to the appropriate species, depending on the primary antibody, for 1 hr at room temperature, washed in PBS, then incubated with ABC for 30 min at room temperature. The slides were then washed and the peroxidase reaction developed with diaminobenzidine and peroxide. The slides were then washed in water, counterstained with hemotoxylin, mounted in Aqua-mount, and evaluated on a light microscopy. Appropriate positive and negative antibodies and tissues were included in each assay as controls.

3.3. Real-Time Quantitative RT-PCR

Real time Q RT-PCR was performed utilizing the 7700 Sequence Detector (Applied Biosystems, CA). Specific quantitative assays for RARα, β, γ, and RXRα, β, γ were developed using Primer Express software (Applied Biosystems). Total RNA was extracted from monkey ovary by Tri-reagent. The RT-PCR resulting data were analyzed using SDS software (Applied Biosystems). The final data were normalized to GAPDH (housekeeping gene) and are presented as the molecules of transcript/molecules of GADPH x 100 (% GAPDH). For this type of analysis, it is critical that the housekeeping gene does not change across experimental conditions. Calculate ΔCt for each gene by Excel according to the equations as: ΔCt = Cttreatment condition - Ctcontrol condition. 2^(- ΔΔCt) = Fold Change, which "Ct" means: the cycle at which the reaction crossed the threshold. If fold change > 1.0, the gene is up-regulated

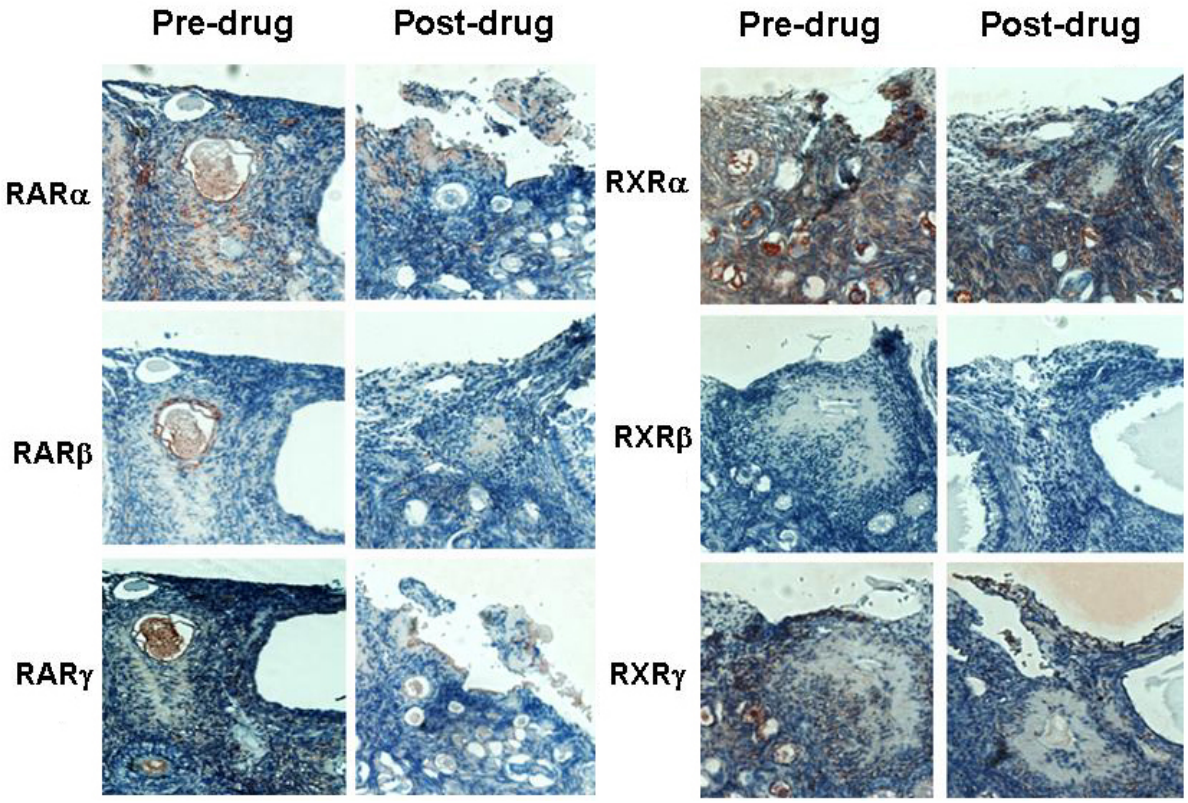

Figure 1. Immunohistochemical staining of retinoid receptors in control group (J465). Monkeys received no medication for three months. Left panel was stained for RAR receptors, and right panel was stained for RXR receptors.

relative to the control (equal to 1). If fold change is <1.0, the gene is down-regulated relative to the control.

3.4. *In situ* Cell Death Detection

Paraffin-embedded monkey slides were deparaffininzed in xylene, rehydrated through graded alcohols to water, then incubated for 10 min in PBS. The slides were then labeled with *In situ* Cell Death Detection kit (Boehringer Mannheim). Briefly, the slides were incubated in 0.5 % triton X100 for 10 min, then washed, and followed by proteinase K digestion in 37°C for 15 min. Following this incubation, 0.3 U/μl TDT and 20 mM biotinylated dUTP in TDT buffer was applied to the slides and incubated for 1 hr at 37°C. Counter staining was done using Avidin-Biotin-peroxidase Complex.

3.4. Statistical Analysis

Results of immunohistochemical analysis were semi-quantitatively scored as 0 (no staining), 1+ (weak staining), 2+ moderate staining), or 3+ (strong staining). The results were ordered using a rank sum test. The equality of the population was tested with Kruschal Wallis and Chi Square where appropriate. Histograms were prepared to visually evaluate differences between groups.

4. RESULTS

4.1. Comparing RARs and RXRs Expression and Induction by 4-HPR, OCP and Combination *in vivo*

The expression of RARs and RXRs were examined in tissue sections. RXRα and RXRγ were found to be consistently present in all monkeys (Figure 1, Table 1). Treatment with 4-HPR alone consistently increased RXRα expression from a 1+ to 2+ expression. RXRγ expression was increased from 1+ to 2+ in 2/3 monkeys but decreased expression in one monkey from 1+ to 0 (Figure 2 and Table 2). Treatment of OCP alone had little effect on retinoid receptors expression (Figure 3 and Table 3) except for a modest decrease in RARα in two-thirds of monkeys from 1+ to 0. The combination of 4-HPR and OCP increased RXRα significantly, p=0.04 (Figure 4, and Table 4). The combination of 4-HPR and OCP also modulated 4 of the retinoid receptors RARα, RARβ, RARγ, and RXRα expression. RARβ increased consistently (p=0.01). RXRα expression increased in three-fourths of monkeys from 1+ to 3+ (1 monkey) 1+ to 2+ (2 monkeys) and did not change in one monkey (2+). The retinoid receptor RXRγ was found to be increased in 2 monkeys treated with 4-HPR alone and 1 monkey treated with the combination of 4-HPR and OCP (Tables 2 and 4) and increased in 1 monkey treated with the combination.

4.2. Hormone Receptor Expression and Induction by OCP and Combination of 4-HPR and OCP *in vivo*

Hormone receptors ERα, ERβ, and PR were examined in monkeys. ERα expression was not detected in the monkey ovaries which were studied (not shown). PR expression was detected in all monkeys (Table 1), and treatment did not change PR expression significantly; however, 4-HPR treatment decreased PR expression in one monkey (Table 2) and OCP increased PR expression in 2 monkeys (Table 3).

Table 1. Semi-quantitative assessment of immunohistochemical staining of receptor expression in control animal group.

Control group	Pre-drug J465-L	Post-drug J465-R1	Pre-drug J937-L	Post-drug J937-R1	Pre-drug J371-L	Post-drug J371-R1
RARα	+	+	++	++	-	-
RARβ	-	-	-	-	-	-
RARγ	-	-	-	-	-	-
RXRα	+	+	++	++	++	++
RXRβ	-	-	-	-	-	-
RXRγ	+	+	++	+	+	+
ER β	+	++	++	++	++	++
PR	++	++	++	++	++	++
EGF	-	-	-	-	-	-
EGF-R	++	++	++	++	++	++

Table 2. Semi-quantitative assessment of immunohistochemical staining of receptor expression in 4-HPR-treated animal group

4HPR Group	Pre-drug J243-L	Post-drug J243-R1/R2	Pre-drug J753-L	Post-drug J753-R2	Pre-drug J153-L	Post-drug J153-L1/L2
RARα	+	++	+	+	+	+
RARβ	-	-	+	++	-	-
RARγ	-	-	-	-	-	-
RXRα	+	++	+	++	+	++
RXRβ	-	-	-	-	-	-
RXRγ	+	++	+	-	+	++
ER β	++	++	+	++	+++	+++
PR	++	-	++	++	++	++
EGF	++	+	+	-	-	+
EGF-R	++	++	++	++	++	++

Table 3. Semi-quantitative assessment of immunohistochemical staining of receptor expression in OCP-treated animal group

OCP group	Pre-drug J261-L	Post-drug J261-R1	Pre-drug J269-L	Post-drug J269-R2	Pre-drug L976-L	Post-drug L976-R1
RARα	+	-	+	-	+	+
RARβ	-	-	+	-	-	-
RARγ	-	-	-	-	-	-
RXRα	++	++	+	+	++	++
RXRβ	-	-	-	-	-	-
RXRγ	++	-	+	+	+	++
ER β	+	++	++	+++	++	+++
PR	++	++	+	++	+	++
EGF	-	-	-	-	-	-
EGF-R	++	++	++	++	++	++

Table 4. Semi-quantitative assessment of immunohistochemical staining of receptor expression in combination treatment animal group

Combin group	Pre-drug J511-L	Post-drug J511-R1	Pre-drug L783-L	Post-drug L783-R2	Pre-drug L581-L	Post-drug L581-R2	Pre-drug L809-L	Post-drug L809-R2
RARα	-	++	-	-	+	+	+	++
RARβ	-	++	-	+	_	++	-	++
RARγ	-	+	-	+	-	-	-	-
RXRα	+	+++	+	++	++	+	+	++
RXRβ	-	-	-	-	-	-	+	+
RXRγ	+++	++	+	+	++	++	+	++
ER β	++	++++	++	++++	+++	+++	++	+++
PR	++	+	+	-	+	++	++	-
EGF	-	-	++	+++	-	+	-	++
EGF-R	++	++	++	++	++	++	+	++

The result from combination group was shown in Table 4. ERβ were found to be expressed in untreated and treated monkeys (Figure 5, Table 1). The control group and the 4-HPR group had no change in ERβ expression ($p = 1.0$), ERβ showed an increase in expression in the OCP group (Figure 3 and Table 3) and in the combination of 4-HPR and OCP (Figure 4 and Table 4) ($p = 0.01$). P53 and p21 were not expressed and did not change between groups except for minimal expression in one or two samples (data not shown). EGF and EGF-R expression, the epidermal growth factor receptor, approached significant expression in the combination group with a p value of 0.09.

4.3. Modulation of Retinoid Receptors Expression Detected by Real Time Q RT-PCR

Real-time Q RT-PCR results showed 4-HPR and the OCP/4-HPR combination treatment increased 4 out of 6 retinoid receptors expression, RARα, β, γ, and RXRα (Figure 6). The real-time PCR results are consistent with the IHC result. However, RXR β and γ expression were decreased by exposure to 4-HPR, RXR γ expression was increased in two-thirds of monkeys and decreased in 1 monkey by IHC (Figure 6 and Tables 2 and 4). OCP treatment increased RXRα and decreased RARα expression which were also similar to the IHC result (Figure 6 and Table 3). 4-HPR modulated RARα, β, γ, and RXRα receptor expression; OCP

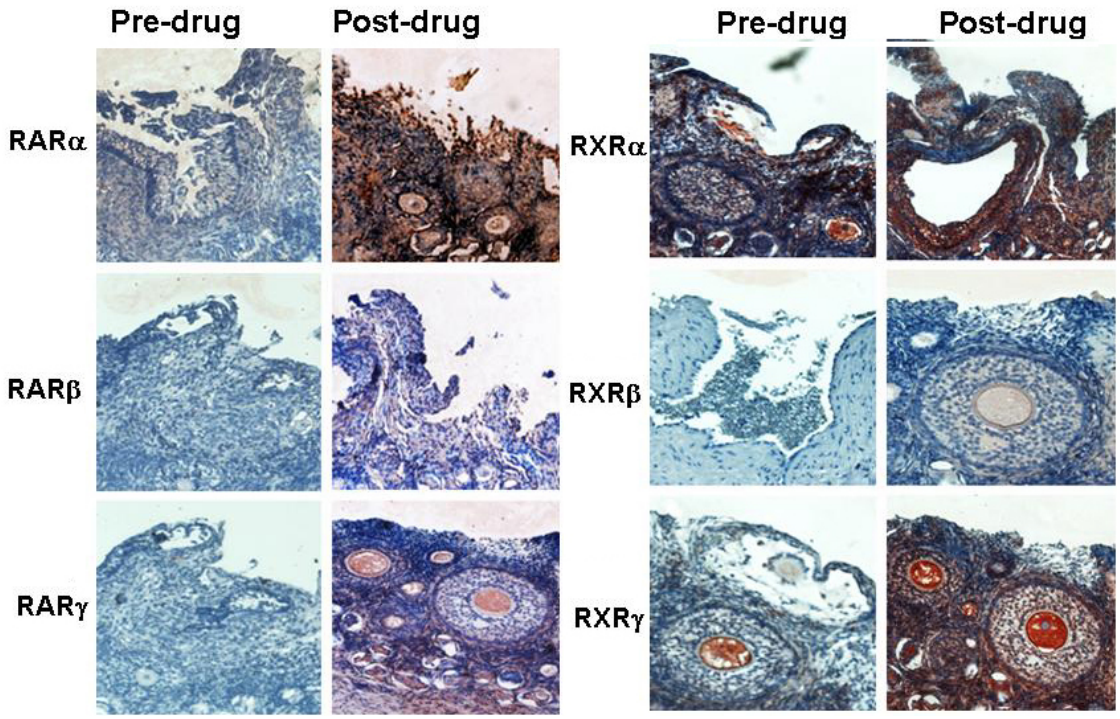

Figure 2. Immunohistochemistry staining of retinoid receptors in 4-HPR treatment group (J243). This group of monkey received 35 mg 4HPR/day for three months. Left panel was stained for RAR receptors, and right panel was stained for RXR receptors. The receptors expression was examined before and after 4-HPR treatment.

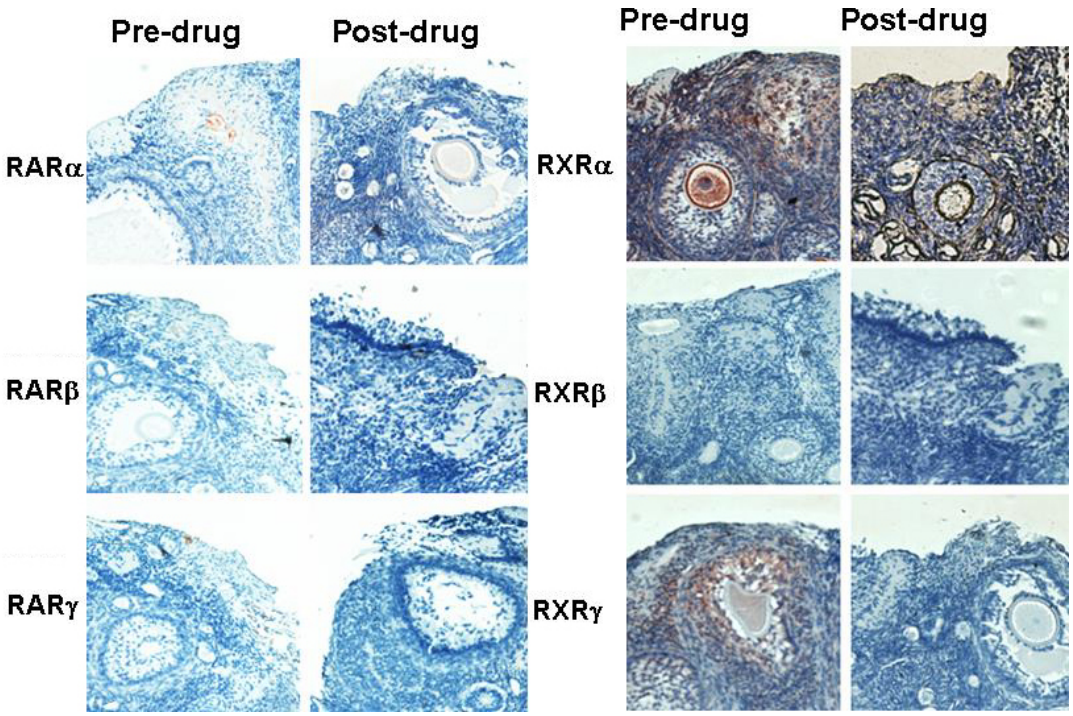

Figure 3. Immunohistochemistry staining of retinoid receptors in OCP treatment group (J261). Monkeys received OCP 0.2 mg norethindrone/0.07 mg of ethinyl estradiol/day. Left panel was stained for RAR receptors, and right panel was stained for RXR receptors. The receptor expression was examined before and after OCP treatment.

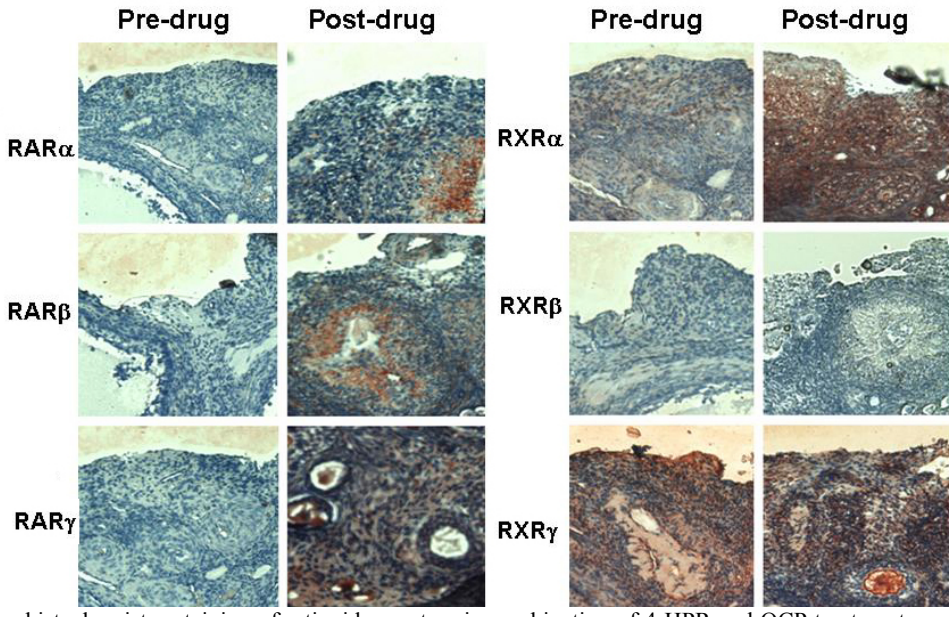

Figure 4. Immunohistochemistry staining of retinoid receptors in combination of 4-HPR and OCP treatment group (J511). Left panel was stained for RAR receptors, and right panel was stained for RXR receptors. The receptor expression was examined before and after combination of 4-HPR and OCP treatment.

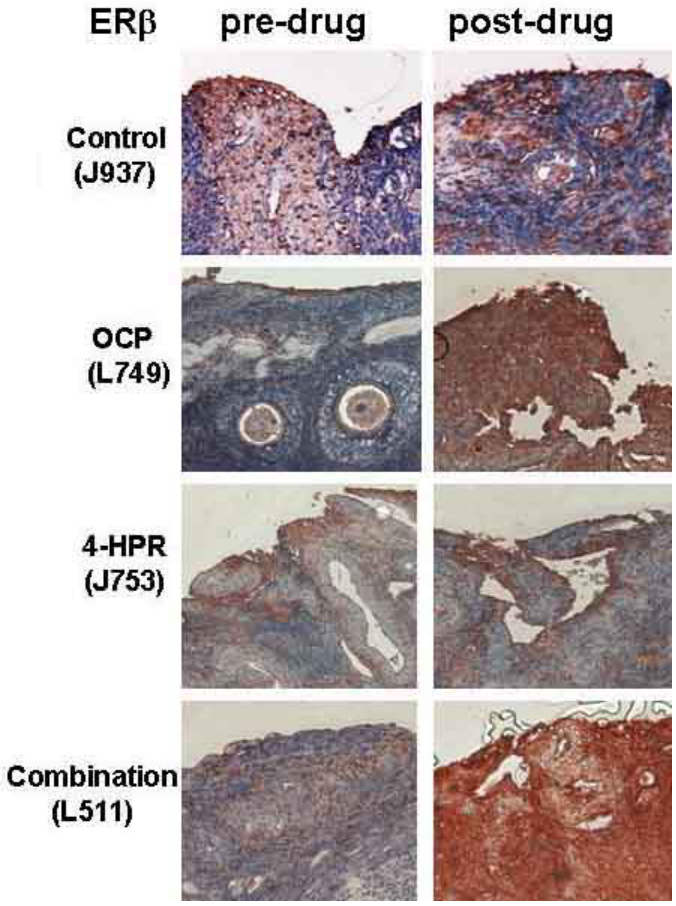

Figure 5. Immunohistochemistry staining of ERβ before and after treatments. Left panel was prior to treatment, and right panel was after treatment.

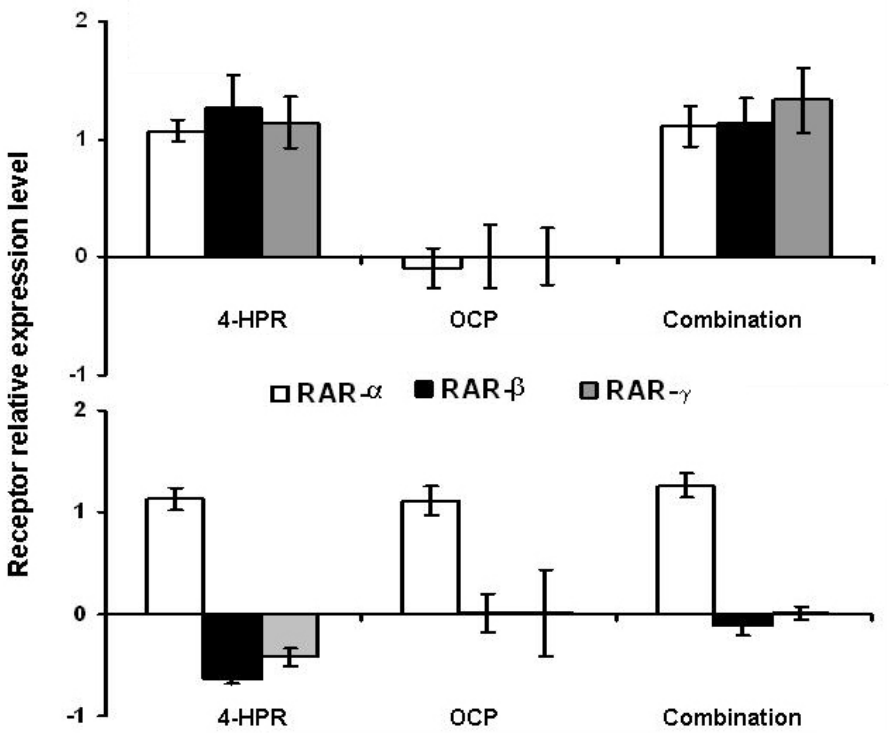

Figure 6. The total RNA was extracted from monkey ovaries and real time Q RT-PCR were analyzed for expression of retinoid receptors. The result represented the fold changes. If fold change > 1.0, the gene is up-regulated relative to the control (equal to 1). If fold change is <1.0, the gene is down-regulated relative to the control.

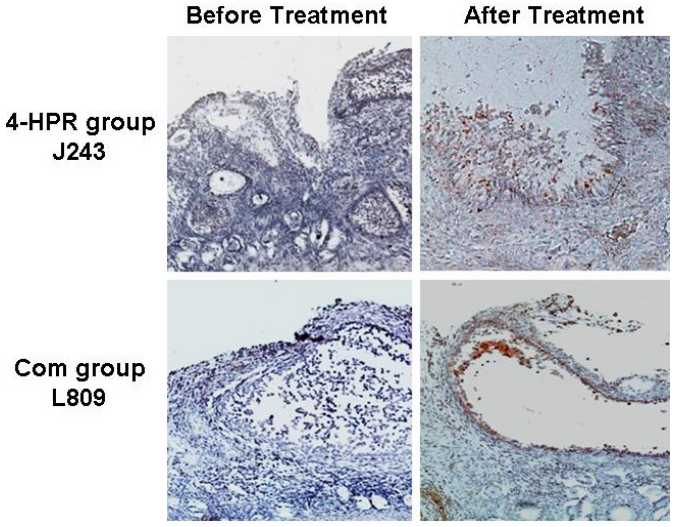

Figure 7. *In-situ* apoptosis staining in 4-HPR and combination treatment animal group. Apoptosis could not be detected in ovarian epithelial. Apoptosis was detected after 4-HPR and combination of 4-HPR and OCP treatment. Apoptotic cell staining was stronger in the combination-treated group than that in the 4-HPR-treated group.

increased RXRα expression; the combination of the two treatments did not show any synergistic or additive effects.

4.4. Apoptosis Induction by 4-HPR and Combination of 4-HPR and OCP *in vivo*

4-HPR at the equivalent human dose of 200mg/day concentration induced apoptosis in monkey ovaries *in vivo* using *in-situ* cell death detection kit staining (Figure 7).

5. DISCUSSION

This is the first report on the combination of retinoid and OCP induced modulation of retinoid

receptors *in vivo* detected by both IHC and real-time Q RT-PCR. A prior human study in oral pre-malignant and cancer of the head and neck showed induction of RARβ by 4-HPR (15, 16) which is consistent with our findings. It is also the first report on the induction of apoptosis *in vivo* using 4-HPR at 200mg/day.

Epidemiologic and laboratory data suggest that retinoids may have a role as preventive or therapeutic agents for ovarian cancer (4-5, 12-14). It has been proposed that the anticarcinogenic and antitumor effects of retinoids are the result of retinoid-induced changes in cell growth and differentiation caused by changes in the expression of specific genes, such as oncogenes, growth factors, and growth factor receptors. Retinoids exert their effects on gene expression by activating a signal transduction pathway in which nuclear retinoid receptors play a pivotal role (9-15). Nuclear retinoid receptors are the proximate mediators of many of the effects of retinoids on gene expression; therefore, it is plausible to assume that changes in their expression and function may cause aberrations in the response of cells to retinoids and thereby alter the regulation of cell growth, differentiation, and expression of the transformed phenotype.

Oral contraceptives (OCP) are well known in their ability to prevent ovarian cancer. Much of the preventive effect is thought to correspond to apoptosis induction, a process that removes cells at risk of undergoing subsequent malignant transformation. This hypothesis is supported by the observation that apoptosis is induced in up to 25% of cells in the ovarian epithelium in cynamolgus monkeys receiving levonorgestrel as a single agent (22). In the macaque setting, the level of apoptosis is associated with progestin-related changes in TGF-β isoforms; *i.e.*, a decrease in TGF-β1 accompanied by an increase in TGF-β2/3. In the human setting, additional support for the activity of progestin is provided by an analysis of data from the Cancer and Steroid Hormone Study (CASH) (23), showing a dose-response relationship. Data from the CASH Study suggests that ovarian cancer risk reduction increases with exposure to progestins of higher potency even for a short duration (24). Dose-response is a question that needs to be further explored in preclinical settings. Historically, there has been wide variation in OCP formulations from the 1960's particularly with regard to androgenicity of the progesterone component, but such changes over time did not appear to affect the ovarian cancer risk reduction associated with oral contraceptives (25, 26). The result from our study showed OCP can induce RXRα as well as ER expression, RXRα could form herterodimer with the ER receptor to regulate gene expression. The preventive capabilities are unclear in high risk women with one study showing a benefit and one study showing an increased risk of breast cancer. For women at no additional risk of breast cancer over the general population, it is an appealing alternative for prevention: however, it is unlikely that a woman is at substantial risk of ovarian cancer without being at risk for breast cancer.

This study suggests that the combination of 4-HPR and OCP may increase the modulation of epithelial cell growth through both the retinoid receptor RXRα and through the ERβ receptor. The retinoid receptors are thought to be associated with the activity of the retinoid. A prior study (27, 28) explored the fluorescence signatures of these drugs on the monkey ovary and found that 4-HPR increased the expression of FAD and OCP decreased the expression NADH associated emission, while the combination had an additive but not synergistic effect. In fact, the combination had a decrease in its effect on both the increased FAD and decreased NADH associated signature suggesting that the combination had less effect than each drug individually. These cofactors of the electron chain are strongly associated with the energy potential of tissue. This study suggests that the combination had more effect on markers associated with growth inhibition and apoptosis. A study with colon cancer cells showed that upregulation of ERβ was associated with inhibition of proliferation in colon cancer cells. A possible mechanism by which ERβ over-expression inhibits proliferation is by modulation of key regulators of the cell cycle; there was a decrease in cyclin E and an increase in the cdk inhibitor p21CIP1. Flow cytometry blocked the G1-S phase progression induced by ERβ over-expression. ERβ modulation is intriguing and bears further study.

6. CONCLUSION

This study evaluates the potential for using the Rhesus monkey as a model for ovarian cancer chemoprevention by using combination of 4-HPR and OCP. It also serves as an initial evaluation of potential intermediate biomarkers for ovarian cancer chemoprevention trials using these drugs. The results of this monkey study suggest that the combination of 4-HPR and OCP up-regulated 4 out of 6 retinoid receptors and ERβ expression, providing a potential mechanism for the effect of these drugs on the ovary. Although numbers of animals were extremely small, this pilot trial supports further study of potential intermediate biomarkers in the Rhesus monkey as a model for human ovarian chemoprevention studies.

7. ACKNOWLEDGMENT

Supported by grants from Department of Defense, DAMD 17-99-1-9505 (MB), Arizona Disease Control Research Commission (ADCRC), RFP 1-700 (MB and CZ), and grant from Ovarian Cancer Research Foundation, NY (CZ).

8. REFERENCES

1. Cancer Statistics 2004. American Cancer Society, Inc. 2004.
2. Hoskins, W.J. Prospective on ovarian cancer: Why prevent? *J Cell Biochem Suppl* 23, 189-199 (1995)
3. Kelloff, G.J., Boone, C.W., Crowell, J.A., Nayfield, S.G., Hawk, E., Steele, V.E., Lubet, R.A., Sigman, CC. Strategies for phase II cancer chemoprevention trials:

cervix, endometrium, and ovary. *J Cell Biochem Suppl* 23, 1-9 (1995)
4. Supino, R., Crosti, M., Clerici, M., Warlters, A., Cleris, L., Zunino, F., Formelli, F. Induction of apoptosis by fenretinide (4HPR) in human ovarian carcinoma cells and its association with retinoic acid receptor expression. *Int J Cancer* 65, 491-497 (1996)
5. Brewer, M., Wharton, J.T., Wang, J., Auersperg, N., Gershenson, D., Bast, R., and Zou, CP. *In vitro* model of normal, immortalized ovarian surface epithelium cells and ovarian cancer cells for chemoprevention of ovarian cancer. *Gyn Oncology* 98(2), 182-92 (2005)
6. Veronesi, U., De Palo, G., Marubini, E., Costa, A., Formelli, F., Mariani, L., Decensi, A., Camerini, T., Del Turco, M.R., Di Mauro, M.G., Muraca, M.G., Del Vecchio, M., Pinto, C., D'Aiuto, G., Boni, C., Campa, T., Magni, A., Miceli, R., Perloff, M., Malone, W.F., Sporn, M.B. Randomized trial of fenretinide to prevent second breast malignancy in women with early breast cancer. *J Natl Cancer Inst* 91, 1847-1856 (1996)
7. De Palo, G., Mariani, L., Camerini, T., Marubini, E., Formelli, F., Pasini, B., Decensi, A., Veronesi, U. Effect of fenretinide on ovarian carcinoma occurrence. *Gynecol Oncol* 86, 24-27 (2002)
8. De Palo, G., Veronesi, U., Camerini, T., Formelli, F., Mascotti, G., Boni, C., Fosser, V., Del Vecchio, M., Campa, T., Costa, A. Can fenretinide protect women against ovarian cancer? *J Natl Cancer Inst* 87, 146-147 (1995)
9. Minton, S.E. Chemoprevention of breast cancer in the older patient. *Hematol Oncol Clin North Am.* 14(1), 113-130 (2000)
10. Zou, CP., Kurie, J.M., Lotan, D., Zou, CC., Hong, W.K., Lotan, R. Higher potency of N-(4-hydroxyphenyl) retinamide than all-trans-retinoic acid in induction of apoptosis in non-small cell lung cancer cell lines. *Clin. Cancer Res* 4, 1345-1355 (1998)
11. Sun, S.Y., Kurie, J.M., Yue, P., Dawson, M.I., Shroot, B., Chandraratna, R.A., Hong, W.K., Lotan, R. Differential responses of normal, premalignant, and malignant human bronchial epithelial cells to receptor-selective retinoids. *Clin. Cancer Res* 5, 431-437 (1999)
12. Wu, S., Zhang, D., Donigan, A., Dawson, M.I., Soprano, D.R., Soprano, K.J. Effects of conformationally restricted synthetic retinoids on ovarian tumor cell growth. *J Cell Biochem* 68, 378-388 (1998)
13. Zhang, D., Holmes, W.F., Wu, S., Soprano, D.R., Soprano, K.J. Retinoids and ovarian cancer. *J Cell Physiol* 185, 1-20 (2000)
14. Sabichi, A.L., Hendricks, D.T., Bober, M.A., Birrer, M.J. Retinoic acid receptor beta expression and growth inhibition of gynecologic cancer cells by the synthetic retinoid N-(4-hydroxyphenyl) retinamide. *J Natl Cancer Inst* 90, 597-605 (1998)
15, Sun, S.Y., Li, W., Yue, P., Lippman, S.M., Hong, W.K., Lotan, R. Mediation of N-(4-hydoxyphenyl) retinamide-induced apoptosis in human cancer cells by different mechanisms. *Cancer Res* 59, 2493-2498 (1999)
16. Clifford, J.L., Menter, D.G., Wang, M., Lotan, R., Lippman, S.M. Retinoid receptor-dependent and -independent effects of N-(4-hydroxyphenyl)retinamide in F9 embryonal carcinoma cells. *Cancer Res* 59, 14-18 (1999)
17. Gnagy, S., Ming, E.E., Devesa, S.S., Hartge, P., Whittemore, A.S. Declining ovarian cancer rates in U.S. women in relation to parity and oral contraceptive use. *Epidemiology*11(2), 102-5 (2000)
18. Whittemore AS, Harris R, Itnyre J, Halpern J. Characteristics relating to ovarian cancer risk: collaborative analysis of 12 US case-control studies. I. Methods. Collaborative Ovarian Cancer Group. *Am J Epidemiol* 15;136(10), 1175-1183 (1992)
19. Whittemore AS, Harris R, Itnyre J. Characteristics relating to ovarian cancer risk: collaborative analysis of 12 US case-control studies. II. Invasive epithelial ovarian cancers in white women. Collaborative Ovarian Cancer Group. *Am J Epidemiol* 15;136(10), 1184-1203 (1992)
20. Zupp J. Concern at animal research should not be dismissed. *Nature* 20;437(7062), 1089 (2005)
21. Brewer M, Baze W, Hill L, Utzinger U, Wharton JT, Follen M, Khan-Dawood F, Satterfield W. Rhesus macaque model for ovarian cancer chemoprevention. *Comp Med* 51(5), 424-9 (2001)
22. Rodriguez GC, Nagarsheth NP, Lee KL, Bentley RC, Walmer DK, Cline M, Whitaker RS, Isner P, Berchuck A, Dodge RK, Hughes CL. Progestin-induced apoptosis in the Macaque ovarian epithelium: differential regulation of transforming growth factor-beta. *J Natl Cancer Inst* 2;94(1), 50-60 (2002)
23. Cancer and Steroid Hormone Study (CASH), Centers for Disease Control Cancer and Steroid Hormone Study. The reduction in risk of ovarian cancer associated with oral contraceptive use. *N Eng J Med* 316, 650–655 (1987)
24. Schildkraut, J. M., B. Calingaert, P. A. Marchbanks, P. G. Moorman, and G. C. Rodriguez. Impact of progestin and estrogen potency in oral contraceptives on ovarian cancer risk. *J. Natl. Cancer Inst. (Bethesda)* 94, 32–38 (2002).
25. Risch, HA. Hormonal etiology of epithelial ovarian cancer, with a hypothesis concerning the role of androgens and progesterone. *J Natl Cancer Inst* 2;90(23), 1774-86 (1998)
26. Risch, HA. Oral-contraceptive use, anovulatory action, and risk of epithelial ovarian cancer. *Epidemiology* 11(5), 614-5 (2000)
27. Brewer, M., U. Utzinger, E. Silva, D. Gershenson, R. C Bast, M. Follen, Jr., J. T. Wharton, and R. Richards-Kortum. Biomarker modulation in a nonhuman rhesus primate model for ovarian cancer chemoprevention. *Cancer Epidemiol Biomark Prev* 10, 889–893 (2001)
28. M. Brewer, U. Utzinger, Y. Li, E. N. Atkinson, W. Satterfield, N. Auersperg, N. Auersperg, R. Richards-Kortum, M. Follen, and R. Bast, "Fluorescence spectroscopy as biomarker in a cell culture and in a nonhuman primate model for ovarian cancer chemopreventive agents," *J. Biomed. Opt.* 7, 20-26 (2002)

Abbreviations: 4-HPR: N-4-hydroxyphenyl-retinamide, OCP: oral contraceptive

Key Words: 4-HPR, OCP, Ovarian cancer, Monkey

Send correspondence to: Molly Brewer, MD, DVM, The University of Arizona, 1515 N Campbell Ave., Box 245024, Tucson, AZ 85724, Tel: 520-626-9280, Fax: 520-626-9287, E-mail: mbrewer@azcc.arizona.edu

http://www.bioscience.org/current/vol12.htm

4-HPR Modulates Gene Expression in Ovarian Cells

Molly Brewer, Nathaniel D. Kirkpatrick, J. Taylor Wharton, Jian Wang, Kenneth Hatch, Nelly Auersperg, Urs Utzinger, David Gershenson, Robert Bast, and Changping Zou

Department of Obstetrics and Gynecology, Division of Gynecologic Oncology, Arizona Cancer Center, Tucson, AZ 85724 (Molly Brewer, Kenneth Hatch, Jian Wang, Urs Utzinger and Changping Zou); Biomedical Engineering, University of Arizona (Molly Brewer, Nathaniel Kirkpatrick, Urs Utzinger); University of British Columbia, Vancouver, British Columbia (Nelly Auersperg), Department of Gynecologic Oncology (J. Taylor Wharton and David Gershenson), and Experimental Therapeutics (Robert Bast), The University of Texas M.D. Anderson Cancer Center, Houston, TX 77030.

Running title: **Effect of 4-HPR on ovarian cells**

Key words: retinoids,4-HPR, apoptosis, ovarian cancer cells

Correspondence and Reprint Requests to:
Changping Zou, MD, PhD
Department of Obstetrics and Gynecology
Arizona Cancer Center
University of Arizona
1515 N. Campbell Avenue
Tucson, AZ 85724-5024
Tel: 520-626-8883
Fax: 520-626-9287
E-mail: czou@azcc.arizona.edu

Ovarian cancer has a high rate of recurrence and subsequent mortality following chemotherapy despite intense efforts to improve treatment outcomes. Recent trials have suggested that retinoids, especially 4-(*N*-hydroxyphenyl) retinamide (4-HPR), play an important role as a chemopreventive agent and are currently being used in clinical trials for ovarian cancer chemoprevention as well as treatment. This study examines the mechanism of its activity in premalignant and cancer cells. We investigated the modulation of gene expression by 4-HPR in immortalized ovarian surface epithelial (IOSE) cells and ovarian cancer (OVCA433) cells with DNA microarray. Real time RT-PCR and western blotting were used to confirm the microarray results and metabolic changes were examined with optical fluorescence spectroscopy. 4-HPR resulted in an up-regulation of expression of pro-apoptotic genes and mitochondrial uncoupling protein in OVCA433 cells and modulation of the RXR receptors in IOSE cells, and down-regulation of mutant BRCA genes in both IOSE and OVCA433 cells. 4HPR had a larger effect on the redox in the 433 cells compared to IOSE. These findings suggest that 4-HPR acts through different mechanisms in premalignant ovarian surface cells and cancer cells, with a preventive effect in premalignant cells and a treatment effect in cancer cells.

Introduction

Epithelial ovarian cancer is the leading cause of death from the gynecologic cancers.[1] In 2003, an estimated 25,400 women were diagnosed with ovarian cancer, and 14,300 women died from the disease.[1] It is most commonly diagnosed in Stage III or IV where the mortality rate is 70% or greater. [2] Currently, there is no generally accepted screening test in which sensitive and reliable biomarkers can be used to identify women destined to develop ovarian cancer. Although initial treatment for ovarian cancer has an excellent response rate, the recurrence rate is high following chemotherapy and drug resistance is a common problem. Better strategies for prevention and treatment of ovarian cancer are thus strongly warranted.

Retinoids have been intensively investigated as chemopreventive agents and have been shown to inhibit ovarian carcinogenesis based on both laboratory data and clinical trials. [3-7] The potential of the synthetic retinoid 4-HPR to prevent ovarian cancer was recognized in a large Italian breast cancer chemoprevention clinical trial. [5-7] Patients on the 4-HPR arm demonstrated a decreased incidence of ovarian cancer [7], with 6 patients developing ovarian cancer in the control group for the duration of drug ingestion but none in the 4-HPR group ($p=0.0327$) [6]. After cessation of the clinical trial, 6 patients in the 4-HPR group developed ovarian cancer compared to 4 in the control arm ($p=0.7563$). [6] This difference was not statistically significant suggesting that the effect of the retinoid was not durable. [6] The mechanism of action of 4-HPR's cancer chemoprevention is unclear. It may act partly through modulation of gene expression via retinoid receptors although modulation of retinoid receptors is still controversial. [8-14] Retinoid receptors are members of the steroid hormone receptor superfamily. Two types of receptors have been identified: retinoic acid receptors (RARs) and retinoid X receptors (RXRs). Each type includes three subtypes with distinct amino- and carboxyl-terminal domains. The RARs bind to all-trans-

retinoic acid (ATRA) and 9-cis-retinoic acid (9cRA), a natural retinoic acid isomer, whereas the RXRs bind only to 9cRA. [15-18] RARs can form heterodimers with RXRs and bind to retinoic acid response elements (RARE), specific DNA sequences that are characterized by direct repeats of (A/G)GGTCA separated by two or five nucleotides that act as ligand-dependent transcriptional regulators for retinoic acid-responsive genes. Some investigators hypothesize that both *all-trans* retinoic acid (ATRA) and 4-HPR bind to retinoic acid response element (RARE) and regulate gene expression (Zou and Lotan unpublished data). [19, 20]

DNA microarray is widely used in identifying gene expression in normal and cancer cells, and in evaluating molecular changes before and after treatment with drugs. [21-24] Use of array technology allows simultaneous evaluation of expression of many (up to thousands) genes. The challenge of such a powerful technique is to develop rigorous, quantitative methods for interpretation of such a wealth of data to identify the expression profile providing maximal biologic information.

Techniques based on quantitative optical fluorescence spectroscopy have shown promise to improve detection of epithelial lesions in the colon, cervix, bladder, head and neck, esophagus and other epithelial surfaces. [25-28] Certain molecules within a cell can be excited using light in the visible and UV range. This principle can be used to optically interrogate endogenous fluorophores with quasi monochromatic excitation light. Natural intra cellular fluorophores include electron carriers nicotinamide adenine dinucleotide (NADH) and flavin adenine dinucleotide (FAD) and the aromatic amino acids tryptophan, tyrosine and phenylalanine, as well as structural proteins, each of which have a characteristic wavelength for excitation with an associated characteristic emission. [29] In particular, FAD and NADH can provide an estimate of mitochondrial metabolic activity through an estimate of cellular redox. [30] Fluorescence

spectroscopy of endogenous fluorophores has been used as a marker for both early detection and chemoprevention. [31-33]

Identification of biomarkers is important to detect abnormal cells so that invasive cancer can be prevented through chemoprevention. Furthermore, intermediate end point biomarkers are valuable in timely evaluation of the drug efficacy during chemoprevention trials. However, potentially useful biomarkers for evaluating ovarian cancer and 4-HPR's effect on the ovary are currently limited. To identify biomarkers in response to 4-HPR treatment and to investigate the mechanism of its action in ovarian cancer treatment and/or prevention, we used the *in vitro* model of normal cells (IOSE cells) and ovarian cancer OVCA433 cells. Ovarian surface epithelial (OSE) cells originated from ovarian epithelial carcinomas in which women with a strong family history of ovarian carcinomas or with a mutation in one of the two known cancer suppressor genes – BRCA1 and BRCA2. [34, 35] Since OSE cells are thought to be the site of origin of epithelial ovarian cancer, these cells are important to study their molecular and cellular properties compared to ovarian cancer cells to enhance our understanding of malignancy in ovarian cancer.

We compared changes in gene expression from treatment with 4-HPR in normal and malignant ovarian cells by microarray and examined 4HPR action in the context of growth inhibition, apoptosis induction, and mitochondrial permeability transition changes. The gene expression changes were verified further by real-time RT-PCR and Western blot while the metabolic status was evaluated with fluorescence spectroscopy.

MATERIALS AND METHODS

Cell Lines and Retinoids

Immortalized ovarian surface epithelial cells (IOSE) and ovarian cancer OVCA433 cells were grown as previously described. [8] The cells were incubated for 3 days with 4-HPR with different concentration of 4-HPR (1, 5 and 10 μM). Control cultures contained DMSO. N-(4-hydroxyphenyl) retinamide (4-HPR) was purchased from the Sigma Chemical Co. (St. Louis, MO), dissolved in dimethylsulfoxide (DMSO) at stock solutions of 10^{-2}M, and stored in an atmosphere of N_2 at -80^{o} C.

RNA Preparation and Microarray

Total RNA was extracted as previously described. [8] We used DNA chip technology to identify gene expression in the Genomics Core Laboratory at the University of Texas Health Sciences Center. The cDNA chips (Agilent Technologies, Palo Alto, CA) with 8,000 human cDNA's, which had dual-labeled cDNA hybridization for use in high density cDNA microarrays. IOSE and OVCA433 cells were treated with 1 μM 4-HPR for 3 days. The RNA samples were evaluated for degradation and DNA contamination on an Agilent 2100 Bioanalyser (Agilent) using a RNA 6000 NanoKit. RNA from the control and the treated cells were submitted for comparison to each microarray chip. These RNA's were used with a Micromax TSA Labeling Kit (Perkin Elmer Life Sciences, Boston, MA) and Cyanine-3 or Cyanine-5 dyes. The recommended wash and labeling procedures for the Perkin Elmer TSA kit were followed except for increasing the post Cyanine 5 Tyramide labeling washes to 10 min each. The washed chips were read on a ScanArray Lite (Perkin Elmer) and the digital image output analyzed using their software (QuantArray). The resulting values were then compiled using either Excel or File Maker Pro macros written for the Microarray Core Laboratory.

Effect of 4-HPR on Cell Proliferation in Monolayer Cultures

IOSE and OVCA433 cells were placed in 96-well plates at 10^5 cells per well and grown for 24 hrs. The cells were incubated for 5 days with 4-HPR in 1, 5, and 10 μM concentrations. Growth inhibition was determined using the crystal violet method as previously described [8]. All experiments were performed in triplicate and the mean ± standard deviations calculated.

Analysis of Apoptosis Induced by 4-HPR

Terminal deoxynucleotidyl transferase (TdT)-mediated fluorescein-deoxyuridine-triphosphate (dUTP) nick-end labeling (TUNEL) assay was used (8). Flow cytometry used a FACScan flow cytometer (Epics Profile, Coulter Corp., Hialeah, FL) with a 15 mW Argon laser used for excitation at 488 nm. Fluorescence was measured at 570 nm. Computer analysis of the data provided information on the percentage of apoptotic cells. All experiments were performed in triplicate and the mean ± standard deviations calculated.

Caspase 3 Activity Assay and Protein Analysis

The cells were plated in 96-well tissue culture plates at densities ranging from 0.5-1 x 10^5 cells per well and treated with 4-HPR in 1, 5, and 10 μM concentrations for 12, 24, 48, and 72 hours. Control cultures and treated cultures contained the same amount of DMSO. The method for analysis of Caspase 3 activity as previously described [8].

Mitochondrial Permeability Transition (MPT) Assay

IOSE and OVCA433 cells were treated with 4-HPR in 1, 5, and 10 μM concentrations for 3 days to determine the time of maximal mitochondrial permeability transition. Cells were washed and resuspended in 40 nM MitoFluor medium, then incubated at 37^{o}C for 30-45 min.

Cells were visualized under the fluorescence microscope at 490 nm excitation, 576 nm emission. A field of 20-30 cells was chosen using a photo amplifier to measure light intensity. Once the time of maximal mitochondrial permeability was determined, the remainder of the experiments were carried out using the pre-determined times of incubation.

Western Analysis of p53, p21, and p16 Gene Expression Modulated by 4-HPR

Genes showing alterations in expression by 4-HPR (> 2 fold increase or >2-fold decrease) were validated by real-time Q-RT-PCR or Western blotting. Nuclear and cytoplasmic protein extracts were prepared as previously described [8].

Real time Q RT-PCR Analysis for mRNA Expression of RARs and BRCA Genes

Real time Q RT-PCR performed in the University of Arizona Core facility by utilizing the 7700 sequence detector (Applied Biosystems, Foster City, CA) with a similar protocol as previously described. [8].

Optical Spectroscopic Analysis of Redox Ratio FAD/(FAD+NADH)

Fluorescence emission was measured on IOSE cells and OVCA433 cells. Cells were treated with 1 μM, 5 μM, or 10 μM 4-HPR 24 hr before fluorescence measurements, described previously. [36]

Results

Expression of Genes Altered by 4-HPR in IOSE and OVCA433 Cells Detected by Microarray

Microarray analysis was performed using total RNA purified from treated and untreated cells. The expression of genes modulated by 4-HPR was evaluated. Genes with a change of

expression >2 fold were recorded in Table 1a and b. In IOSE cells, there was up-regulation of apoptotic related genes and differentiation genes, as well as genes on chromosome 3 and 9. Cancer cells showed up-regulation of fewer genes associated with apoptosis and showed similar effects on up-regulation of the anti-oncogene segment on chromosome 9**.** Mitochondrial, NAD, NADH, and NADPH genes were modulated by 4-HPR in both IOSE and OVCA433 cells (Table 2).

Growth Inhibition and Apoptosis Induction by 4-HPR in Ovarian Cell Lines

IOSE and OVCA433 cells treated with different concentrations of 4-HPR, the growth inhibitory effect were compared in monolayer culture. Increasing the concentration of 4-HPR resulted in dose-dependent growth inhibition (Fig 1).

Apoptosis Induction by 4HPR in Ovarian Cells

Apoptosis induction in IOSE and OVCA433 cells were analyzed by TdT-labeling and flow cytometry after 3 days of treatment. Results showed 4-HPR apoptosis induction was dose-dependent (Fig 2). Cell cycle analysis demonstrated that 4-HPR increased the percentage of cells in the G_1 phase in OVCA433 cells, also in a dose-dependent manner (Fig 2).

Effect of 4-HPR on Caspase 3 Activity and Caspase 3 and 9 Protein Expression

Caspase 3 activity is a central mediator of apoptosis. Caspase 3 activity was measured in IOSE and OVCA433 cells at different time points with different concentration of 4-HPR. Caspase 3 enzyme activity was slightly increased at day 3 in the different concentration groups in OVCA433 cells (Fig 3a), which correlated with maximal apoptosis and growth inhibition in

these cells. However, Caspase 3 and Caspase 9 protein were not changed by 4-HPR in either IOSE or OVCA433 cells (Fig 3a and b).

Effect of 4-HPR on Mitochondrial Permeability Transition (MPT)

Mitochondrial permeability transition (MPT) changes are associated with mitochondrial mediated apoptosis. To investigate the mechanism of 4-HPR induced apoptosis in ovarian cancer cells, experiments were carried out to investigate the effect of 4-HPR in mitochondrial potential in IOSE and OVCA433 cells. 4-HPR decreased mitochondrial inner-membrane potential, which increased MPT in IOSE and OVCA433 cells (Fig 4). An inverse relationship in mitochondrial potential correlated in a dose-dependent manner with the increase in apoptosis and growth inhibition by 4-HPR in IOSE and OVCA433 cells (Figs 1 and 4), suggesting that these activities were mediated by changes in the mitochondrial membrane.

Expression of Apoptosis-associated Genes Modulated by 4-HPR

The effect of 4-HPR on the expression of the apoptosis-associated genes p53, p21, p16 and Rb were examined along with BRCA genes with Western blot and real-time PCR method. The expression of these genes was detected in both IOSE and OVCA433 cells (Fig 5). 4-HPR increased expression after 3 days of treatment in a dose-dependent manner in OVCA433 cells (Fig 5), which correlated with the microarray results, showing an increase in human p53 binding protein mRNA in these cells (Table 1a).

4-HPR Modulating Rtinoid Receptors and BRCA Genes Detected by Q RT-PCR

Microarray data showed that retinoid receptors were modulated by 4-HPR. Some receptors were induced by 4-HPR and others were suppressed by 4-HPR. We verified the effect of 4-HPR

on receptor expression and induction by Q RT-PCR. RARs were not significantly changed by 4-HPR in either cell line (data not shown); however, RXRs were modulated by 4-HPR in IOSE cells. 4-HPR increased RXRα and RXRβ expression and decreased RXRγ expression in IOSE cells (Fig 6a). The expression of RARs and RXRs were not altered by 4-HPR in cancer cells (Fig 6a).

BRCA1 and BRCA2 gene expression were decreased by 4-HPR in both IOSE and OVCA433 cells (Fig 6b). Real time RT-PCR result was consistent with microarray analysis (Table 1b and Fig 6b).

Redox Ratio Changed by 4-HPR Detected by Optical Spectroscopic Analysis

As shown in Fig 7a, the IOSE cell line exhibited a highly variable redox related fluorescence ratio compared to the OVCA433 cell line in which the estimated redox increased in a linear fashion. The OVCA433 cells demonstrated a strong sensitivity to 4-HPR treatment and Fig 7a illustrates that dose dependence as a linear increase with a slope of 0.0059 / μM 4-HPR ($p<0.001$). An increased redox ratio suggests less oxidative metabolism indicating the cells may be entering quiescence. When considering the relative ratios to untreated cells, as shown in the Fig 7b, the OVCA433 cells had a higher value at each drug dosage. At higher concentrations of 4-HPR the redox related fluorescence ratio increased for the IOSE cells but never reached the level of the OVCA433 cells. This is consistent with the result that the IOSE cell line was variable in response to 4-HPR treatment.

Discussion

The goal of chemoprevention is to prevent the progression of pre-cancerous cells to cancer. In practice, to achieve this goal, surrogate endpoint biomarkers are needed, because the biologic

endpoint (cancer development) may take many years and may be difficult to detect precisely. Large numbers of patients would have to be entered into such a trial to reach statistically significant conclusions. Using biomarkers that reliably predict progression and differentiation, a study can be completed with fewer patients in a reasonable length of time. [37, 38] Unfortunately, only a limited number of potentially useful biomarkers for chemoprevention studies in ovarian cancer have been described. [39-48]

An Italian trial that evaluated 4-HPR for prevention of secondary breast cancers demonstrated a decreased incidence of ovarian cancer in women receiving 4-HPR, suggesting that retinoids prevented the development of ovarian cancer. [5-7] After cessation of 4-HPR treatment, new ovarian cancers occurred in the treatment group, suggesting that this prevention was not durable [7]. Experimental studies have demonstrated that retinoids can affect human ovarian cancer cell growth by inhibiting proliferation and inducing apoptosis [4, 11-13], which are thought to be important mechanisms in cancer prevention, as well as in cancer treatment. However, the detailed mechanism of retinoid activity, including 4-HPR, in cancer chemoprevention has remained unclear. We have used DNA microarray to examine genes whose expression is modulated by 4-HPR in immortalized normal ovarian epithelial and ovarian cancer cells. The results are verified by real-time RT-PCR and western blot to further strengthen our conclusions.

P53, a tumor suppressor protein and transcription factor, is deleted or altered in many human cancers. P53 binds to DNA of cell cycle related genes to induce G1 arrest and allows cells to repair DNA damage or undergo apoptosis if DNA damage is too large for repair. P53 binds to DNA in response to DNA damage, a process that is redox sensitive and is inhibited by oxidizing conditions. Mutation of the p53 protein decreases DNA binding and inhibits activity in induction of apoptosis of genetically altered cells. [49] In our study, microarray data

demonstrated that 4-HPR increases human p53 binding protein mRNA expression and Rb binding protein in both normal and cancer cells (Table 1a), and p53/Rb expression were found in both IOSE and ovarian cancer cells. However, Western blot analysis showed p53 expression increased in OVCA433 cells only. In OVCA433 cells, p53 as well as downstream p21 and p16 proteins increase in a dose-dependent manner, suggesting the cells carry wild-type p53 (Fig 5). The concentration of 1 μM 4-HPR was chosen in microarray study and western analysis because most of clinical trials used this concentration.[5-7] A concentration of 1 μM is approximately equivalent to the plasma concentration when a dose of 200mg/day is administered. However, our results suggested that this dose may not be effective for ovarian cancer prevention. Although microarray results showed increasing gene expression, there were few changes at the protein level (table 1 and fig 5).

In OSE cells however, immortalized IOSE cells with catalytic subunit of telomerase (hTERT) and a SV40 Large T antigen inactivity of the p53/Rb pathway, the expression of p53 were detected but diminished when the temperature increased to 39^{o}C for 5 and 7 days [50], supporting our findings. In downstream genes, p21 expression showed increased expression with the higher temperature but p16 expression was not changed by temperature. [50] The hTERT and a SV40 Large T antigen affected not only expression of p53, but also p16 in OSE cells. [50] 4-HPR treatment increased p21 expression in IOSE cells but the expression of p53 and p16 were not changed by 4-HPR, further confirming that the large T antigen affects p53 expression and thus is not modulated by 4-HPR (Fig. 5). This is a limitation of this cell line. However, primary cell cultures give highly variable results, limiting their usefulness.

p53/Rb mediates the action of 4-HPR on ovarian cancer cells which carry a functional or wild type p53. Up-regulation of p53, p21, and other downstream genes may be one of the mechanisms of retinoid-response in ovarian cancer cells, as is seen in other cell lines. [51, 52] A

previous study has reported [52] that ovarian cancer cell lines that are sensitive to retinoic acid have a higher expression of p53, p27, p21, and p16 compared to the retinoid resistant lines [52], which are concordant with our data. In OVCA433, which is sensitive to 4-HPR, there is an increase in p53, p21, and p16 expression in a dose-dependent manner, which correlates with growth inhibition and apoptosis. In early cancers, wild type p53 may still be present because p53 mutations may be a late event in carcinogenesis, specifically in ovarian cancer, suggesting one of the major effects of 4-HPR may require an intact p53 gene. This would also suggest that 4-HPR may be more active as a preventive agent rather than a treatment agent if a p53 mutation has occurred.

There is thought to be a role for nuclear retinoid receptors in mediating the retinoid regulation of growth, apoptosis, and gene expression. [15-18] RAR and RXR expression have different patterns in different tissues and organs. Retinoid treatment increased certain RAR mRNA levels in several normal and cancer cell lines [9-14] including several ovarian cancer cell lines. [4, 11, 12, 19, 20, 53] However, 4-HPR modulation of expression of retinoid receptors in ovarian cancer is still controversial. In this study, 4-HPR increased RXRα and RXRβ expression and decreased RXRγ expression in IOSE cells. Formelli's group reported that RARβ basal level expression and induction by 4-HPR play an important role in mediating 4-HPR response in ovarian cancer cells. [53] The over expressing RARα clone and RARβ clone increased the tumor-suppressive effect in ovarian tumors. [53] They also found that the most sensitive cell lines had RARβ expression and the highest levels of RARα and RARγ expression.[4] Moreover, ATRA inhibited ovarian cancer cell growth through RARα and RXRα [54, 55], with RXRα playing a critical role in mediating the growth inhibition in ovarian cancer cells. [54] In this study, the RXRs were regulated by 4-HPR in IOSE, but not in ovarian cancer cells, suggesting ovarian carcinogenesis may block some of the receptor expression and induction, and further study on

blocking these receptors to evaluate whether the effect of 4-HPR is altered will be forthcoming.

Retinoids, particularly 4-HPR, have been shown to increase aerobic glycolysis by increasing mitochondrial permeability to the co-enzymes NADH and FAD, as well as activity of the electron transport chain characterized by an increase in reactive oxygen species and cytochrome oxidase. [56, 57] There has been an increased interest in mitochondrial function in both normal and cancer cells; in particular, the mitochondria may be the site of induction of apoptosis by many preventive agents. 4-HPR induces a change in the mitochondrial permeability of the membrane permeability transition [57-59], which we hypothesize is one of the mechanisms of its suppressive activity in growth inhibition. Permeability of the mitochondrial inner membrane is increased by thiol agents and oxidative stress-inducing agents and is thought to be dependent on the opening of a non-selective pore [58]; intracellular redox potential increased along with increases in 4-HPR induced growth inhibition and apoptosis. [59] A shift towards a more oxidized condition increases membrane permeability, while the opposite occurs with reducing agents. Change in mitochondrial permeability allows cytochrome c to be released into the cytosol and is thought to initiate the Caspase system, ultimately with activation of Caspase 3 activity. [58, 60] Caspase 3 activity was investigated in this study because it is a pivotal step in both Caspase 9 and mitochondrial-induced apoptosis. We could not detect any significant change in Caspase genes after treatment with 4-HPR in our microarray and western analysis. Other Caspase genes besides Caspase 3 and 9 may be involved in 4-HPR induced apoptosis in ovarian cells and this requires further investigation.

The redox ratio of a cell defines the level of free radicals divided by the level of anti-oxidants. It is an indirect measure of the cells metabolic activity and functional ability of the electron transport chain. An increase in the ratio suggests a reduced metabolic activity under normoxic conditions. It is hypothesized that chemopreventive treatments reduce growth rate and

induce apoptosis which should result in reduced metabolic activity and an increased redox ratio. [32] The availability of free radical versus anti-oxidants within a cell can be measured by determining the ratio of FAD versus $FADH_2$ or NAD versus NADH. NADH is fluorescent but its oxidized complement NAD is only minimally fluorescent. On the other hand, $FADH_2$ is minimally fluorescent while FAD is fluorescent. Because both fluorophores are oxidized in the electron transport chain, measuring changes in the fluorescence intensity related to FAD serves as an estimate of changes in NAD. Given that the fluorescence from NADH and FAD can be measured non-invasively, a measure approximating the redox ratio can be obtained in vitro on cell cultures without the need for fixation and staining and chemical preparation. This may be an important non-invasive biomarker for the activity of chemopreventive agents *in vivo*.

Our results suggest the optically approximated redox status of the cells provides evidence of differences between the responses to 4-HPR treatment in the two ovarian cell lines. The IOSE cells exhibited a higher redox ratio that did not significantly increase with 4-HPR treatment while the redox ratio estimated from the OVCA433 cells increased in a dose dependant manner.

The BRCA family of genes regulates apoptosis and often has germ-line mutations in familial breast and ovarian cancer. [34, 35] 4-HPR down-regulated BRCA1 in the IOSE cells and decreased BRCA2 gene expression in OVCA433 cells detected by both microarray and real-time RT-PCR (Tables 1b and 3b). Both BRCA1 and BRCA2 function as tumor suppressor genes in the breast and ovary. [34, 35, 61] IOSE cells used in the study are thought to carry a BRCA mutation and originated from a woman with a strong family history of ovarian cancer [34, 61], The ovarian cancer cells OVCA433 had altered expression of BRCA genes, moreover, the expression of BRCA2 transcript in-frame exon 12 deletion (BRCA2Δ12) mRNA was also reported in these cells by Ho, et al. [61] 4-HPR could directly affect mutant BRCA gene to suppress the ovarian carcinogenesis, which is a very important finding in this study and has significant implications

for BRCA-related cancer prevention and merits further study.

Our study suggests that 4-HPR may be active in ovarian cancer cells through growth inhibition and apoptosis induction which is mediated by multiple mechanisms. We use both ovarian cancer cells and immortalized normal ovarian epithelium cells in the study. The IOSE cells represent a cell that has been immortalized as a premalignant cell. Although a true premalignant model in the ovary is still unclear, immortalized cells have been used from lung, cervical, and other cell lines to mimic premalignant cells. [8, 50] In immortalized normal ovarian cells, 4-HPR regulated RXR receptor pathways which increased RXRα and RXRβ expression and decreased RXRγ expression as well as down-regulating the anti-apoptotic genes ras and cyclin-dependent kinase and up-regulating the pro-apoptotic pathways p53 and BCL, although Western blot did not confirm an increase in p53 protein. However, in OVCA433 cells, 4-HPR mediated mitochondrial permeability and induced the pro-apoptotic p53 and downstream pathway. Early changes that have not undergone p53 mutations, for example, may have a response to 4-HPR with induction of the p53 pathway, while cells that have undergone p53 mutations may not be as responsive to drugs such as 4-HPR. Using biomarkers, such as RXR receptors and p53 up-regulation and downstream protein production as well as fluorescence spectroscopy, to evaluate patient response may be helpful to monitoring 4-HPR or other chemopreventive agents' activity as a preventive agent for ovarian cancer. Hence, this drug merits further study in the ovary, both as a preventive agent and as an agent which might aid in preventing future recurrences.

Natural and synthetic retinoids have been used in many different types of cancers for prevention and treatment. However, the mechanism is still not well studied and the suitable concentration of 4-HPR and/or retinoid has not been determined. [62-64] Negative trials were reported for bladder cancer and cervical cancer. [61, 64] A key result from our previous *in vitro*

studies suggested the concentration is important when applying retinoids to different cell types, correlating with different concentrations for various cell populations *in vivo*, i.e. normal and high risk patients as well as cancer patients need to use specifics concentrations. [8, 63, 65-67] Most of the clinical trials for prevention use the dose of 200 mg/day based on a breast cancer chemoprevention trial. [68] Compared with the bladder, cervix, and ovary, the breast is fat tissue that stores retinoids; consequently, the local concentration of 4-HPR in the breast is conceivably higher than that in other organs and this local concentration varies from organ to organ. Therefore, it is imperative that the concentration of 4-HPR in different type of cancer needs to be studied carefully before initiating a clinical trial.

Acknowledgements

Supported by grant from Arizona Disease Control Research Commission (ADCRC), RFP 1-700, grant from Ovarian Cancer Research Foundation, NY, and Department of Defense, DAMD 17-99-1-9505.

References

1. Greenlee RT, Hill-Harmon MB, Murray T, Thun M. Cancer statistics, 2001. CA. Cancer J. Clin. 2001; 51: 15-36.
2. Scully RE. Pathology of ovarian cancer precursors. J Cell Biochem Suppl 1995; 23: 208-18.
3. Kelloff GJ, Boone CW, Crowell JA, Nayfield SG, Hawk E, Steele VE, Lubet RA, Sigman CC. Strategies for phase II cancer chemoprevention trials: cervix, endometrium, and ovary. J Cell Biochem Suppl 1995; 23: 1-9.
4. Supino R, Crosti M, Clerici M, Warlters A, Cleris L, Zunino F, Formelli F. Induction of apoptosis by fenretinide (4HPR) in human ovarian carcinoma cells and its association with retinoic acid receptor expression. Int. J. Cancer 1996; 65: 491-7.
5. Veronesi U, De Palo G, Marubini E, Costa A, Formelli F, Mariani L, Decensi A, Camerini T, Del Turco MR, Di Mauro MG, Muraca MG, Del Vecchio M, Pinto C, D'Aiuto G, Boni C, Campa T, Magni A, Miceli R, Perloff M, Malone WF, Sporn MB. Randomized trial of fenretinide to prevent second breast malignancy in women with early breast cancer. J. Natl. Cancer Inst. 1999; 91: 1847-56.
6. De Palo G, Mariani L, Camerini T, Marubini E, Formelli F, Pasini B, Decensi A, Veronesi U. Effect of fenretinide on ovarian carcinoma occurrence. Gynecol Oncol 2002; 86: 24-7.
7. De Palo G, Veronesi U, Camerini T, Formelli F, Mascotti G, Boni C, Fosser V, Del Vecchio M, Campa T, Costa A, et al. Can fenretinide protect women against ovarian cancer? J. Natl. Cancer Inst. 1995; 87: 146-7.
8. Zou CP, Kurie JM, Lotan D, Zou CC, Hong WK, Lotan R. Higher potency of N-(4-hydroxyphenyl)retinamide than all-trans-retinoic acid in induction of apoptosis in non-small cell lung cancer cell lines. Clin. Cancer Res. 1998; 4: 1345-55.
9. Sun SY, Kurie JM, Yue P, Dawson MI, Shroot B, Chandraratna RA, Hong WK, Lotan R. Differential responses of normal, premalignant, and malignant human bronchial epithelial cells to receptor-selective retinoids. Clin. Cancer Res. 1999; 5: 431-7.
10. Wu S, Zhang D, Donigan A, Dawson MI, Soprano DR, Soprano KJ. Effects of conformationally restricted synthetic retinoids on ovarian tumor cell growth. J Cell Biochem 1998; 68: 378-88.
11. Zhang D, Holmes WF, Wu S, Soprano DR, Soprano KJ. Retinoids and ovarian cancer. J Cell Physiol 2000; 185: 1-20.
12. Sabichi AL, Hendricks DT, Bober MA, Birrer MJ. Retinoic acid receptor beta expression and growth inhibition of gynecologic cancer cells by the synthetic retinoid N-(4-hydroxyphenyl) retinamide. J. Natl. Cancer Inst. 1998; 90: 597-605.
13. Sun SY, Li W, Yue P, Lippman SM, Hong WK, Lotan R. Mediation of N-(4-hydoxyphenyl)retinamide-induced apoptosis in human cancer cells by different mechanisms. Cancer Res. 1999; 59: 2493-8.
14. Clifford JL, Menter DG, Wang M, Lotan R, Lippman SM. Retinoid receptor-dependent and -independent effects of N-(4-hydroxyphenyl)retinamide in F9 embryonal carcinoma cells. Cancer Res. 1999; 59: 14-8.
15. Lotan R, Clifford JL. Nuclear receptors for retinoids: mediators of retinoid effects on normal and malignant cells. Biomed Pharmacother 1991; 45: 145-56.
16. Chambon P. The retinoid signaling pathway: molecular and genetic analyses. Semin. Cell Biol. 1994; 5: 115-25.

17. DeLuca LM. Retinoids and their receptors in differentiation, embryogenesis and neoplasia. FASEB J 1991; 5: 2924-33.
18. Pfahl M. Vertebrate receptors: molecular biology, dimerization and response elements. Semin. Cell Biol. 1994; 5: 95-103.
19. Fanjul AN, Delia D, Pierotti MA, Rideout D, Yu JQ, Pfahl M, Qiu J. 4-Hydroxyphenyl retinamide is a highly selective activator of retinoid receptors. J. Biol. Chem. 1996; 271: 22441-6.
20. Soprano DR, Chen LX, Wu S, Donigan AM, Borghaei RC, Soprano KJ. Overexpression of both RAR and RXR restores AP-1 repression in ovarian adenocarcinoma cells resistant to retinoic acid-dependent growth inhibition. Oncogene 1996; 12: 577-84.
21. Wu Q, Kirschmeier P, Hockenberry T, Yang TY, Brassard DL, Wang L, McClanahan T, Black S, Rizzi G, Musco ML, Mirza A, Liu S. Transcriptional regulation during p21WAF1/CIP1-induced apoptosis in human ovarian cancer cells. J. Biol. Chem. 2002; 277: 36329-37.
22. Kim JH, Skates SJ, Uede T, Wong KK, Schorge JO, Feltmate CM, Berkowitz RS, Cramer DW, Mok SC. Osteopontin as a potential diagnostic biomarker for ovarian cancer. JAMA 2002; 287: 1671-9.
23. Rokudai S, Fujita N, Kitahara O, Nakamura Y, Tsuruo T. Involvement of FKHR-dependent TRADD expression in chemotherapeutic drug-induced apoptosis. Mol Cell Biol 2002; 22: 8695-708.
24. Hardwick JC, van Santen M, van den Brink GR, van Deventer SJ, Peppelenbosch MP. DNA array analysis of the effects of aspirin on colon cancer cells: involvement of Rac1. Carcinogenesis 2004; 25: 1293-8.
25. Sokolov K, Follen M, Richards-Kortum R. Optical spectroscopy for detection of neoplasia. Curr Opin Chem Biol 2002; 6: 651-8.
26. Ramanujam N. Fluorescence spectroscopy of neoplastic and non-neoplastic tissues. Neoplasia (N Y) 2000; 2: 89-117.
27. Wagnieres GA, Star WM, Wilson BC. In vivo fluorescence spectroscopy and imaging for oncological applications. Photochem. Photobiol. 1998; 68: 603-32.
28. Richards-Kortum R, Sevick-Muraca E. Quantitative optical spectroscopy for tissue diagnosis. Annu. Rev. Phys. Chem. 1996; 47: 555-606.
29. Lakowicz JR. Principles of fluorescence spectroscopy, vol. New York: Plenum Press, 1983.
30. Chance B, Schoener B, Oshino R, Itshak F, Nakase Y. Oxidation-reduction ratio studies of mitochondria in freeze-trapped samples. NADH and flavoprotein fluorescence signals. J. Biol. Chem. 1979; 254: 4764-71.
31. Brewer M, Utzinger U, Satterfield W, Hill L, Gershenson D, Bast R, Wharton JT, Richards-Kortum R, Follen M. Biomarker modulation in a nonhuman rhesus primate model for ovarian cancer chemoprevention. Cancer Epidemiology, Biomarkers & Prevention 2001; 10: 889-93.
32. Brewer M, Utzinger U, Li Y, Atkinson EN, Satterfield W, Auersperg N, Richards-Kortum R, Follen M, Bast R. Fluorescence spectroscopy as a biomarker in a cell culture and in a nonhuman primate model for ovarian cancer chemopreventive agents. J. Biomed. Opt. 2002; 7: 20-6.
33. Schantz SP, Alfano RR. Tissue autofluorescence as an intermediate endpoint in cancer chemoprevention trials. J Cell Biochem Suppl 1993; 17F: 199-204.

34. Wong AS, Auersperg N. Ovarian surface epithelium: family history and early events in ovarian cancer. Reprod Biol Endocrinol 2003; 1: 70.
35. Blackwood MA, Weber BL. BRCA1 and BRCA2: from molecular genetics to clinical medicine. J. Clin. Oncol. 1998; 16: 1969-77.
36. Kirkpatrick ND, Zou C, Brewer MA, Brand WR, Drezek RA, Utzinger U. Endogenous fluorescence spectroscopy of cell suspensions for chemopreventive drug monitoring. Photochemistry and Photobiology 2005; 81: In press.
37. Hong WK, Sporn MB. Recent advances in chemoprevention of cancer. Science 1997; 278: 1073-7.
38. Boone CW, Bacus JW, Bacus JV, Steele VE, Kelloff GJ. Properties of intraepithelial neoplasia relevant to cancer chemoprevention and to the development of surrogate end points for clinical trials. Proc Soc Exp Biol Med 1997; 216: 151-65.
39. Berchuck A, Soisson AP, Olt GJ, Soper JT, Clarke-Pearson DL, Bast RC, Jr., McCarty KS, Jr. Epidermal growth factor receptor expression in normal and malignant endometrium. Am J Obstet Gynecol 1989; 161: 1247-52.
40. Bast RC, Jr., Jacobs I, Berchuck A. Malignant transformation of ovarian epithelium. J. Natl. Cancer Inst. 1992; 84: 556-8.
41. Berchuck A, Boente MP, Bast RC, Jr. The use of tumor markers in the management of patients with gynecologic carcinomas. Clin. Obstet. Gynecol. 1992; 35: 45-54.
42. Bast RC, Jr., Boyer CM, Xu FJ, Wiener J, Dabel R, Woolas R, Jacobs I, Berchuck A. Molecular approaches to prevention and detection of epithelial ovarian cancer. J Cell Biochem Suppl 1995; 23: 219-22.
43. Berchuck A, Rodriguez GC, Kamel A, Dodge RK, Soper JT, Clarke-Pearson DL, Bast RC, Jr. Epidermal growth factor receptor expression in normal ovarian epithelium and ovarian cancer. I. Correlation of receptor expression with prognostic factors in patients with ovarian cancer. Am J Obstet Gynecol 1991; 164: 669-74.
44. Kohler M, Janz I, Wintzer HO, Wagner E, Bauknecht T. The expression of EGF receptors, EGF-like factors and c-myc in ovarian and cervical carcinomas and their potential clinical significance. Anticancer Res 1989; 9: 1537-47.
45. Rodriguez GC, Berchuck A, Whitaker RS, Schlossman D, Clarke-Pearson DL, Bast RC, Jr. Epidermal growth factor receptor expression in normal ovarian epithelium and ovarian cancer. II. Relationship between receptor expression and response to epidermal growth factor. Am J Obstet Gynecol 1991; 164: 745-50.
46. Yee D, Morales FR, Hamilton TC, Von Hoff DD. Expression of insulin-like growth factor I, its binding proteins, and its receptor in ovarian cancer. Cancer Res. 1991; 51: 5107-12.
47. Henriksen R, Funa K, Wilander E, Backstrom T, Ridderheim M, Oberg K. Expression and prognostic significance of platelet-derived growth factor and its receptors in epithelial ovarian neoplasms. Cancer Res. 1993; 53: 4550-4.
48. Di Blasio AM, Cremonesi L, Vigano P, Ferrari M, Gospodarowicz D, Vignali M, Jaffe RB. Basic fibroblast growth factor and its receptor messenger ribonucleic acids are expressed in human ovarian epithelial neoplasms. Am J Obstet Gynecol 1993; 169: 1517-23.
49. Polyak K, Xia Y, Zweier JL, Kinzler KW, Vogelstein B. A model for p53-induced apoptosis. Nature 1997; 389: 300-5.

50. Davies BR, Steele IA, Edmondson RJ, Zwolinski SA, Saretzki G, von Zglinicki T, O'Hare MJ. Immortalisation of human ovarian surface epithelium with telomerase and temperature-sensitive SV40 large T antigen. Exp Cell Res 2003; 288: 390-402.
51. Shin DM, Xu XC, Lippman SM, Lee JJ, Lee JS, Batsakis JG, Ro JY, Martin JW, Hittelman WN, Lotan R, Hong WK. Accumulation of p53 protein and retinoic acid receptor beta in retinoid chemoprevention. Clin. Cancer Res. 1997; 3: 875-80.
52. Zhang D, Vuocolo S, Masciullo V, Sava T, Giordano A, Soprano DR, Soprano KJ. Cell cycle genes as targets of retinoid induced ovarian tumor cell growth suppression. Oncogene 2001; 20: 7935-44.
53. Pergolizzi R, Appierto V, Crosti M, Cavadini E, Cleris L, Guffanti A, Formelli F. Role of retinoic acid receptor overexpression in sensitivity to fenretinide and tumorigenicity of human ovarian carcinoma cells. Int. J. Cancer 1999; 81: 829-34.
54. Wu S, Zhang D, Zhang ZP, Soprano DR, Soprano KJ. Critical role of both retinoid nuclear receptors and retinoid-X-receptors in mediating growth inhibition of ovarian cancer cells by all-trans retinoic acid. Oncogene 1998; 17: 2839-49.
55. Wu S, Zhang ZP, Zhang D, Soprano DR, Soprano KJ. Reduction of both RAR and RXR levels is required to maximally alter sensitivity of CA-OV3 ovarian tumor cells to growth suppression by all-trans-retinoic acid. Exp Cell Res 1997; 237: 118-26.
56. Oridate N, Suzuki S, Higuchi M, Mitchell MF, Hong WK, Lotan R. Involvement of reactive oxygen species in N-(4-hydroxyphenyl)retinamide-induced apoptosis in cervical carcinoma cells. J. Natl. Cancer Inst. 1997; 89: 1191-8.
57. Suzuki S, Higuchi M, Proske RJ, Oridate N, Hong WK, Lotan R. Implication of mitochondria-derived reactive oxygen species, cytochrome C and caspase-3 in N-(4-hydroxyphenyl)retinamide-induced apoptosis in cervical carcinoma cells. Oncogene 1999; 18: 6380-7.
58. Tafani M, Schneider TG, Pastorino JG, Farber JL. Cytochrome c-dependent activation of caspase-3 by tumor necrosis factor requires induction of the mitochondrial permeability transition. Am J Pathol 2000; 156: 2111-21.
59. Halestrap AP, McStay GP, Clarke SJ. The permeability transition pore complex: another view. Biochimie 2002; 84: 153-66.
60. Tiwari BS, Belenghi B, Levine A. Oxidative stress increased respiration and generation of reactive oxygen species, resulting in ATP depletion, opening of mitochondrial permeability transition, and programmed cell death. Plant Physiol. 2002; 128: 1271-81.
61. Rauh-Adelmann C, Lau KM, Sabeti N, Long JP, Mok SC, Ho SM. Altered expression of BRCA1, BRCA2, and a newly identified BRCA2 exon 12 deletion variant in malignant human ovarian, prostate, and breast cancer cell lines. Mol Carcinog 2000; 28: 236-46.
Decensis, A., Torrisi, R., Bruno, R., Costantini, M., Curotto, A., Nicolò, A., Malcangi, B., Baglietto, L., Bruttini, G.P., Gatteschi, B., Rondanina, G., Varaldo, M., Perloff, M., Malone W.F., Bruzzi, P. (2000) Randomized Trial of Fenretinide in Superficial Bladder Cancer Using DNA Flow Cytometry as an Intermediate End Point. Cancer Epi Biomaker Prevention **9**, 1071-1078.
63. Brewer, M., Wharton, J.t., Wang, J., Auersperg, N., Gershenson, D., Bast, R., and Zou, C.P**.** *In vitro* model of normal, immortalized ovarian surface epithelium cells and ovarian cancer cells for chemoprevention of ovarian cancer. Gyn Oncology, 98(2):182-92, 2005.
64. Follen, M., Atkinson, E.N., Schottenfeld, D., Malpica, A., West, L., Lippman, S., Zou, C., Hittelman, W.N., Lotan, R., and Hong, W.K. (2001) A randomized clinical trial of 4-

hydroxyphenylretinamide for high-grade squamous intraepithelial lesions of the cervix. Clin. Cancer Res. **7**, 3356-3365.

65. Zou, CP., Liebert, M., Zou, C. C., Grossman, H.B., and Lotan, R. Identification of effective retinoids for inhibition growth and inducing apoptosis in bladder cancer cells. J of Urology, 165: 986-992, 2001.
66. Zou C, Vlastos AT, Yang L, Wang J, Brewer M, Follen M. Effect of 4-hydroxyphenyl retinamide on human cervical epithelial and cancer cell lines. J Soc Gynecol Investig, 10(1):41-8, 2003.
67. Russell Broaddus, Susu Xie, Ching-Ju Hsu, Sui Zhang, Jian Wang, and **Changping Zou.** The chemopreventive agents 4-HPR and DFMO inhibit growth and induce apoptosis in uterine leiomyomas. Am J of OBGYN,190:686-692,2004.
68. Veronesi U, De Palo G, Marubini E, Costa A, Formelli F, Mariani L, Decensi A, Camerini T, Del Turco MR, Di Mauro MG, Muraca MG, Del Vecchio M, Pinto C, D'Aiuto G, Boni C, Campa T, Magni A, Miceli R, Perloff M, Malone WF, Sporn MB. (1999) Randomized trial of fenretinide to prevent second breast malignancy in women with early breast cancer. J Natl Cancer Inst. 3; **91**, 1847-56.

Figure Legends

Fig 1. *Effect of 4-HPR on growth and apoptosis in OVCA433 and IOSE cells*. Cells were grown in the absence (control) or presence of 4-HPR in concentrations of 1, 5, 10 μM. Growth inhibition assay were performed with crystal violet on day 5. The percentage of growth inhibition was calculated, as described in Materials and Methods. The data was presented as the mean ± SE of triplicate determinations.

Fig 2. *Effect of 4-HPR on apoptosis induction in OVCA433 and IOSE cells*. Cells were treated with the indicated 4-HPR concentrations for 3 days. The cells were then stained with fluorescein-labeled dUTP to label DNA fragments by the TUNEL method, as described in Materials and Methods. The percentage of apoptosis cell population and DNA contents, including cell cycle, were calculated.

Fig 3. *Effect of 4-HPR on Caspase 3 Activity in OVCA433 and IOSE cells*. Cells were grown in 96-well plate with absence (control) or presence of 4-HPR in concentrations of 1, 5, and 10 μM for 12, 24, 48 and 72 hrs and incubated in Caspase 3 buffer, as described previously in Materials and Methods. The plates were read at 400 nm excitation, 505 nm emission using a fluorescence plate reader immediately after adding Caspase 3 fluorescent substrate conjugate. The Western blot on Caspase 3 and 9 expression shown in the upper right corner were treated with same concentration of 4-HPR for 3 days.

Fig 4. *Effect of 4-HPR on Mitochondrial Permeability Transition in IOSE and OVCA433 cells*. Cells were treated with 4-HPR in concentrations of 1, 5, and 10 μM for 3 days and resuspended in 40 nM MitoFluor™ medium. Cells were visualized under the fluorescence microscope at 490 nm excitation, 516 nm emission. A field of 20-30 cells was chosen using a spectrophotometer to measure light intensity.

Fig 5. *Effect of 4-HPR on p53, p21, and other protein levels in IOSE and OVCA433 cells*. Nuclear proteins were extracted from cells treated with 1 μM 4-HPR for 3 days. Thirty microgram/lane of nuclear proteins were subjected to SDS-PAGE. The p53, p21, p16, and Rb proteins were identified by blotting with monoclonal antibodies. Immunoreactive bands were visualized using the enhanced chemiluminescence method described in Materials and Methods. The blots were stripped and reblotted to mouse anti-β-actin antibody for assessment of loading in each lane.

Fig 6. a. Estimated fluorescence redox ratios are presented from the OVCA433 and IOSE cells with increasing concentrations of 4-HPR. Standard error bars are shown and the value above each bar represents the number of times the treatment group was measured. **b**. Comparisons relative redox fluorescence ratio between the control and treatment measurements for both cell lines. The mean ratios for the treatment groups are normalized to the control group's mean ratio.

Table 1. *Microarray analysis of all genes induced by retinoid (greater than 2-fold changes).* Ovarian cells were grown in 10% FBS and DMEM/F12 medium treated with 1 μM of 4-HPR. Total RNA was purified and microarray was analyzed. The genes up- and down- regulated by 4-HPR were reported.

Table 2. *Microarray analysis of all genes related to NADH and NAD modulated by 4-HPR*.

Table 3. *Expression of RXR receptors and BRCA in ovarian cell lines determined by real-time RT-PCR analysis*. IOSE and OVCA433 cells were grown in 10% FBS and DMEM/F12 medium treated with 1 μM of 4-HPR for 3 days. The cells were then harvested and the total RNA was extracted and analyzed by real time RT-PCR. The number represented the fold changes. If fold change > 1.0, the gene is up-regulated relative to the control (equal to 1). If fold change is <1.0, the gene is down-regulated relative to the control.

Photochemistry and Photobiology, 2005, 81: 125–134

Endogenous Fluorescence Spectroscopy of Cell Suspensions for Chemopreventive Drug Monitoring¶

Nathaniel D. Kirkpatrick[1], Changping Zou[2], Molly A. Brewer[1,2], William R. Brands[2], Rebekah A. Drezek[3] and Urs Utzinger*[1,2]

[1]Division of Biomedical Engineering, University of Arizona, Tucson, AZ
[2]Department of Obstetrics and Gynecology, University of Arizona, Tucson, AZ
[3]Department of Bioengineering, Rice University, Houston, TX

Received 6 August 2004; accepted 27 October 2004

ABSTRACT

Cancer chemopreventive agents such as *N*-4-(hydroxyphenyl)-retinamide (4HPR) are thought to prevent cancers by suppressing growth or inducing apoptosis in precancerous cells. Mechanisms by which these drugs affect cells are often not known, and the means to monitor their effects is not available. In this study endogenous fluorescence spectroscopy was used to measure metabolic changes in response to treatment with 4HPR in ovarian and bladder cancer cell lines. Fluorescence signals consistent with nicotinamide adenine dinucleotide (NADH), flavin adenine dinucleotide (FAD) and tryptophan were measured to monitor cellular activity through redox status and protein content. Cells were treated with varying concentrations of 4HPR and measured in a stable environment with a sensitive fluorescence spectrometer. Results suggest that redox signal of all cells changed in a similar dose-dependant manner but started at different baseline levels. Redox signal changes depended primarily on changes consistent with NADH fluorescence, whereas the FAD fluorescence remained relatively constant. Similarly, tryptophan fluorescence decreased with increased drug treatment, suggesting a decrease in protein production. Given that each cell line has been shown to have a different apoptotic response to 4HPR, fluorescence redox values along with changes in tryptophan fluorescence may be a response as well as an endpoint marker for chemopreventive drugs.

INTRODUCTION AND BACKGROUND

Fluorescence spectroscopy can be used to measure endogenous fluorescence in various systems. It has been applied *in vitro* to characterize cell cultures, *ex vivo* to assess tissue biopsies and *in vivo* to measure tissue (1–4). Over the last decade many promising applications for autofluorescence spectroscopy have been reported mainly in the area of minimally invasive disease diagnosis and also in drug monitoring (5,6). By measuring endogenous signals, no additional dyes or contrast agents are necessary to determine the native characteristics of tissues *in vivo*. When considering an autofluorescence signal from tissue, all the contributing fluorophores and chromophores must be accounted for because excitation, emission and absorption spectra overlap. Signals corresponding to aromatic amino acids, structural proteins, metabolic cofactors and blood products are known to produce a fluorescence signature in bulk tissue samples. Some of these signatures arise from intracellular structures and can provide information about the metabolic state within the sampled cells. Landmark studies have established experimental links between cellular autofluorescence and metabolic changes (7–9). This study takes advantage of such alterations in fluorescence emission from epithelial cancer cell lines to monitor metabolic responses in the presence of *N*-4-(hydroxyphenyl)retinamide (4HPR).

If cells are measured in suspension, there are little effects of absorption and morphology on fluorescence emission. The sole contributors are intracellular fluorophores. In the case of endogenous fluorescence, there are several key fluorophores that correlate specifically with cellular activity including reduced nicotinamide adenine dinucleotide (NADH), reduced nicotinamide adenine dinucleotide phosphate (NADPH) and flavin adenine dinucleotide (FAD). Although NADH and NADPH are distributed throughout the cytosol, studies have shown that the predominant fluorescence signal originates from the mitochondria, consistent with NADH fluorescence (10–12). This article will refer to NAD(P)H fluorescence as NADH fluorescence, attributed mainly to the mitochondrial NADH concentrations. NADH and FAD are metabolic cofactors that act as electron donors and acceptors in the electron transport chain of the mitochondria. Electrons are transported down the chain, providing the necessary energy to generate a proton gradient and the corresponding adenosine triphosphate production. When oxidized, NADH and $FADH_2$ (reduced FAD) release electrons, and then NAD^+ and FAD return to their reduced forms by accepting electrons by way of the citric acid cycle (13). Of particular optical interest is the reduced NADH, which exhibits a strong fluorescence signal with a maximum at 350 nm excitation and 450 nm emission, whereas the oxidized form, NAD^+, does not elicit fluorescence (14). Conversely, the oxidized FAD fluoresces at a maximum at 450 nm excitation and 535 nm emission, whereas $FADH_2$ fluorescence is minimal. It has

¶Posted on the website on 9 November 2004.

*To whom correspondence should be addressed: Arizona Health Science Center 8319, 1501 North Campbell Avenue, Tucson, AZ 85724, USA. Fax: 520-626-8726; e-mail: utzinger@u.arizona.edu

Abbreviations: CCCP, carbonyl cyanide *m*-chloro phenyl hydrazone; DMSO, dimethylsulfoxide; DPBS, Dulbecco phosphate-buffered saline; EEM, excitation/emission matrix; FAD, flavin adenine dinucleotide; $FADH_2$, reduced FAD; 4HPR, *N*-4-(hydroxyphenyl)retinamide; NaCN, sodium cyanide; NADH, nicotinamide adenine dinucleotide; NADPH, nicotinamide adenine dinucleotide phosphate; PI, propidium iodide.

been shown that flavin fluorescence is predominantly attributed to electron transfer flavoprotein and lipoamide dehydrogenase, a molecule that associates with $FADH_2$ (15). In this article fluorescence consistent with flavin fluorescence will be referred in general as FAD-related signal.

As a cell changes its metabolic activity, the balance between NADH and NAD^+ shifts correspondingly as the reduction–oxidation (redox) state of the cell fluctuates. Similarly, the complementary pair of $FADH_2$ and FAD forms a redox potential that deviates depending on cellular metabolism. To determine the redox potential of sampled cells *in vivo* using fluorescence signals, an ideal approach would be to compare the NAD^+ concentration to the total concentration of NAD^+ and NADH or use the FAD and $FADH_2$ concentrations correspondingly. However, because only NADH and FAD exhibit significant fluorescence signals, the redox potential can be estimated through a ratio of the peak emission values from these molecules assuming their concentrations are inversely linked to the nonfluorescing counterparts.

Among aromatic amino acids, tryptophan contributes to most of the observed intrinsic fluorescence signal (14). In cell suspensions signals attributed to tryptophan typically exhibit fluorescence intensities orders of magnitude greater than those from other endogenous fluorophores. Although not typically a focus in spectroscopic studies, tryptophan-related fluorescence can serve as an additional marker for monitoring cellular status (1) and has demonstrated different signal intensities in metastatic and nonmetastatic cells (16). It can be hypothesized that cellular protein production can be estimated with tryptophan-related fluorescence signals.

In this study, fluorescence spectra resulting from the combination of tryptophan, NADH and FAD were analyzed to characterize cellular response *in vitro* to a chemopreventive drug treatment regimen. 4HPR, a vitamin A derivative, is a known chemopreventive agent in head and neck, bladder, ovary and other epithelial cancers but its mechanisms are not fully understood (17–22). Although 4HPR targets nuclear retinoic acid receptors, it has also been shown to exhibit apoptotic effects independent of receptor mediation (17,23). One hypothesis is that 4HPR modulates the mitochondria and the electron transport chain, releasing reactive oxygen species and initiating apoptosis (24). Changes in the mitochondrial permeability affect the electron transport chain and subsequently alter the balance between reduced and oxidized state of molecules. As described previously, fluorescence spectroscopy can be used to monitor molecular concentrations, which reflect the redox state of the cell (6) because NADH and FAD are directly linked to mitochondrial activity and cellular metabolism. The inclusion of FAD-related fluorescence in a redox calculation increases the precision of the metabolic state estimation compared with analyzing changes of NADH-related signals alone (25). We conducted spectroscopic studies on four different epithelial cancer cell lines with the goal to determine fluorescence properties and redox states as well as the dose response between established epithelial cell lines.

MATERIALS AND METHODS

Epithelial cell suspension. Two ovarian cancer cell lines, OVCA 420 (420) and OVCA 433 (433) (26) (M.D. Anderson Cancer Center, Houston, TX, G. Mills laboratory), along with two bladder cancer cell lines, UM-UC-6 (U6) (27) (M.D. Anderson Cancer Center, HB Grossman Laboratory) and T24 (28) (American Type Culture Collection, Manassas, VA), were used for this study. These cell lines were studied because of their hypothesized susceptibility to 4HPR. The T24 cells have a p53 mutation, and the U6 cells have a wild-type p53 gene (29,30). Previous experiments suggest that T24 epithelial cells are less sensitive to 4HPR treatments compared with the U6 cells. The epithelial cell lines were cultured until they had reached approximately 5×10^6 cells per culture dish in a mixture of 90% volume Dulbecco modified Eagle medium (Invitrogen, GIBCO, Grand Island, NY) and 10% fetal bovine serum (Mediatech Inc., Herndon, VA) at 37°C in a humidified atmosphere of 95% air and 5% CO_2. 4HPR was purchased from Sigma Chemical Co. (St. Louis, MO), dissolved in dimethylsulfoxide (DMSO) (Sigma) at stock solutions of 10^{-2} *M* and stored in an atmosphere of N_2 at −80°C.

Exposure of cell cultures to a 4HPR drug regimen over time results in an increasing number of nonviable cells. To measure live cells during the initiation of apoptosis, they were measured 24 h after treatment before any significant cell death had occurred. Although previous studies have shown that 3 days of treatment produces maximal apoptosis, initiation of apoptosis occurs within the first 24 h. All cell lines were exposed to three concentrations of 4HPR (1, 5 and 10 μ*M*) for 24 h, and the control group received only the vehicle DMSO. The cells were trypsinized, washed in Dulbecco phosphate-buffered saline (DPBS) (Mediatech Inc.) and resuspended in DPBS and 5% glucose (EMD Chemicals, Gibbstown, NJ). The cell concentration was determined manually in a standard manner with a hemocytometer and light microscope and readjusted to achieve a concentration of 1.5×10^6 cells per mL for each measurement. After preparation, the cell suspensions were placed on ice, awaiting measurement. For spectroscopic readings the temperature was increased and maintained at 37°C in a temperature-controlled sample chamber because fluorescence efficiency as well as metabolism are affected by temperature (14). During spectroscopic examination, the suspension was constantly stirred (approximately 10 rps) with a micro stir bar to ensure a uniform cell concentration in the chamber.

Fluorescence spectroscopy. The fluorescence properties of this suspension were measured in a standard 1 cm path length quartz cuvette using a double excitation emission fluorometer (Fluorolog 3-22, JY Horiba, Edison, NJ). For each spectroscopic experiment, excitation and emission wavelengths were varied to obtain fluorescence data matrices. Excitation wavelengths varied from 270 to 600 nm in increments of 10 nm while collecting emission data from a range starting 20 nm above the excitation wavelength and extending to 20 nm less than twice the excitation wavelength with 700 nm as the maximum measured emission wavelength. A full measurement took about 15 min to complete. A background scan was performed using the same batch of DPBS–5% glucose media in which the cells were suspended.

Cell viability. Several factors could have affected cell viability besides drug treatment. First, the motion created by the stir bar and the stir bar itself may both cause cellular injury. Second, cell suspensions were measured as quickly as possible, but the time required for a measurement could lead to cell death once they were removed from the incubator. After spectroscopic interrogation, cell viability was evaluated with a manual viability count after addition of 0.2% volume Trypan Blue (Sigma) and DPBS. Additional cell viability assessments of cells before and after measurement on the first several experiments were conducted to test whether the measurement conditions were inducing cell injury and death.

Data preprocessing. All the data assembly and basic analysis were completed in Matlab (Mathworks, Natick, MA). Data were corrected for the excitation source's power and the wavelength-dependent detector efficiency with manufacturer-supplied correction factors. All data were background subtracted for both the fluorescence of the medium as well as detector background. Spectra from each measurement were assembled into an excitation/emission matrix (EEM). Average fluorescence emission was extracted from EEM and compared between the groups at emission peaks consistent with NADH, FAD and tryptophan. The intensity values corresponding to FAD were calculated from the emission spectra at λ_{ex} = 450 nm as an average of the emission wavelengths spanning the 530–540 nm emission range. The NADH-related fluorescence intensity values were determined from the emission spectra at $\lambda_{ex} = 350$ nm as an average of emission wavelengths ranging from 445 to 455 nm. Tryptophan-related signal was calculated from the emission spectra at λ_{ex} = 280 nm by determining the average fluorescence emission at wavelengths ranging from 320 to 340 nm. The redox ratio was computed on the basis of the NADH- and FAD-related signals using the following equation:

$$\mathrm{REDOX}_{\mathrm{ratio}} = \frac{\mathrm{FAD}_{\mathrm{Intensity}}}{\mathrm{FAD}_{\mathrm{Intensity}} + \mathrm{NADH}_{\mathrm{Intensity}}} \quad (1)$$

Statistical methods. Multiple linear regression was applied to the data with generalized linear model fitting to evaluate dose dependence and to statistically determine differences between the cell lines. All statistical modeling was completed with JMP Software (SAS, Cary, NC). Multiple tests were performed starting with a rich model fit with all possible

interactions and progressively reducing the model by removing non-significant parameters. The full model had the form:

$$\text{Redox} = \alpha_{433,420,U6,T24} + \beta_{433,420,U6,T24}C_{4HPR}, \quad (2)$$

where

$$\alpha_{433} = \alpha_0, \quad \alpha_{420} = \alpha_0 + \Delta\alpha_{420}, \quad \alpha_{U6} = \alpha_0 + \Delta\alpha_{U6}, \quad \alpha_{T24} = \alpha_0 + \Delta\alpha_{T24}$$

and

$$\beta_{433} = \beta_0, \quad \beta_{420} = \beta_0 + \Delta\beta_{420}, \quad \beta_{U6} = \beta_0 + \Delta\beta_{U6}, \quad \beta_{T24} = \beta_0 + \Delta\beta_{T24},$$

with the 433 cell line used as the reference for the model. The intercept α terms represent the initial contribution from each cell line with no treatment, and the β coefficients describe the contributions that varied with the concentration of the drug 4HPR (C_{4HPR}). The $\Delta\alpha$ and $\Delta\beta$ terms refer to cell line differences in baselines and slopes (interactions), respectively. Statistically, α_0, β_0, and the Δ variables were compared with zero to evaluate each parameter's significance in the model. Insignificant terms were removed until the simplest model explained the data. Similar models were fit for the NADH-, FAD- and tryptophan-associated values, with the given response variable replacing redox ratio in the model. NADH-, FAD- and tryptophan-related signals can be affected by cell concentration in the sampled populations, whereas the redox ratio is less sensitive to these fluctuations. The appropriateness of each linear model was assessed by ensuring that residuals from the fit displayed equal variation and did not show a trend.

Dynamic range measurements. On a subset of 4HPR-treated cell suspensions, a series of additional experiments was performed to drive the cells into maximal and minimal fluorescence emission. In brief, two chemicals were used to either increase or decrease the redox potential of the cells, as described previously by Eng *et al*. (12). To drive the NADH-related fluorescence signal to its maximum, 4 m*M* sodium cyanide (NaCN) (BD Biosciences, San Jose, CA) was added to the cell suspension. NaCN affects the mitochondrial transport by blocking the transfer of electrons from the electron donors. This maximizes mitochondrial NADH concentration and a corresponding maximal fluorescence signal because the oxidation of NADH is prohibited. To minimize NADH-related fluorescence signals, 66.7 μM carbonyl cyanide *m*-chloro phenyl hydrazone (CCCP) (BD Biosciences), a mitochondrial uncoupler, was used. CCCP increases exchange through mitochondrial membrane, releasing NADH to the cytosol and thus allowing NADH to be rapidly oxidized. Previously, these methods were used to study the effects on the NADH signal (12). We also observed FAD-related dynamics. Because the fluorescence generated by FAD occurs in its oxidized state, an increase of the FAD-related signal hypothetically corresponds to CCCP addition, whereas a decrease would result from the addition of NaCN. These biologic range measurements followed immediately after a full excitation/emission scan on a subset of 433 and T24 cell suspensions. NaCN was added, and three emission spectra at $\lambda_{ex} = 280$ nm, $\lambda_{ex} = 350$ nm and $\lambda_{ex} = 450$ nm were collected rapidly (<1 min). After 5 min of exposure to NaCN, another set of measurements was performed at those wavelengths. A similar experiment was conducted using CCCP.

Cell cycle analysis. For comparison with the optical data, changes in cell cycle due to 4HPR treatment were determined using cell cycle analysis with propidium iodide (PI) staining. In brief, cells were grown and treated with 1, 5 and 10 μM 4HPR for 24 h, as described previously in Epithelial Cell Suspension. Cells were fixed in 4% paraformaldehyde (pH 7.4) at room temperature then washed and incubated in 70% ethanol containing 1% HCl at –20°C for 10 min. Next, cells were stained in 500 μL of PI–ribonuclease A solution in the dark for 30 min at room temperature and analyzed by flow cytometry using a FACScan flow cytometer (BD Biosciences). Fluorescence was excited at 488 nm, and emission was collected through a bandpass filter (585/42 nm). Data were preprocessed using Cellquest Pro. (BD Biosciences) and analyzed using ModFit LT (Verity Software, Topsham, ME). Results of interest were the proportion of cells in G1 (Gap 1 phase), S (Synthesis phase) and G_2 (Gap 2 phase) phases of the cell cycle.

RESULTS

Fluorescence data of cell suspension

Fluorescence data from multiple, independently grown batches of the four different cancer cell lines were obtained and analyzed. Results presented in this study are based on seven batches of 420 ovarian cancer cell line experiments, five batches of the 433 ovarian cancer cell line, four batches of the U6 bladder cancer cell line and four batches of the T24 bladder cancer cell line. A measurement session consisted of a series of four measurements of the same batch of cultured cells treated at the four different drug concentrations (control, 1, 5 and 10 μM). Data from one control group of the U6 cell line were excluded because of experimental error.

An average EEM from all five 433 cell line measurements is illustrated in Fig. 1. The ordinate of the EEM corresponds to the excitation wavelengths and abscissa corresponds to the emission wavelengths. Fluorescence intensities in calibrated but arbitrary units are given in a gray scale with the lightest level corresponding to the strongest emission. EEM provide quantitative fluorescence information analogous to a contour map, with peaks qualitatively corresponding to fluorescence maximums and valleys corresponding to low fluorescence or absorption. The average fluorescence emission of the 433 cell line shows a large peak located at 280/340 nm (excitation/emission) consistent with tryptophan fluorescence and a smaller peak at 350/450 nm consistent with NADH fluorescence as shown in Fig. 1A. Because of the substantially larger fluorescence signal from tryptophan, many of the more subtle fluorescence peaks are masked when looking at a full EEM scale. A subset of the EEM shown in Fig. 1B provides a more sensitive view of the NADH- and FAD-related signal. The NADH-associated peak at 350/450 nm is prominent, but a peak at 450/535 nm consistent with FAD fluorescence becomes visible. Water Raman scattering from the PBS and glucose media was removed when the background was subtracted. The PBS and glucose media exhibited minimal autofluorescence, on average less than 1% of the maximal cell fluorescence signal.

Besides minimal background signal, another important experimental condition was to maintain cell viability during measurement. Cells remained viable through the experimental procedure as shown in Table 1. Typically, the viability exceeded 90%, which is an acceptable value in a normal population of cultured cells. Cell viability values before and after measurement showed little or no difference (data not shown), confirming that the measurement conditions did not affect cell viability.

Redox ratio

The fluorescence redox ratio was calculated to approximate the metabolic status of the cell suspensions. Figure 2 shows the redox ratios of the four cell lines and four drug concentrations with mean and standard errors. As shown in Fig. 2A, the 433 cell line exhibited an increase in the redox ratio as the drug concentration increased. Results from our linear model show a 0.006 increase per micromole of 4HPR (β_{433}, Table 2). The 433 cell line was chosen as the reference cell line in the multiple regression model and is the only one depicted because there was no evidence of difference between the rate of increased redox ratio in any of the cell lines ($F_{3,71} = 1.08$, $P = 0.364$, Extra Sum of Squares F-test). These data suggest that the drug affects each cell line through a similar mechanism. Further examination of the redox state in the control group (Fig. 2B) revealed that the T24 cells generally had a lower metabolic status than the 433 cells (higher redox ratio), whereas the 420 cells had the highest baseline metabolic status (α_{T24} and α_{420}, respectively, Table 2). However, the predicted baseline value of the U6 cells in our linear model was not statistically different from that of the 433 cells (α_{U6}, Table 2). These baseline redox values may

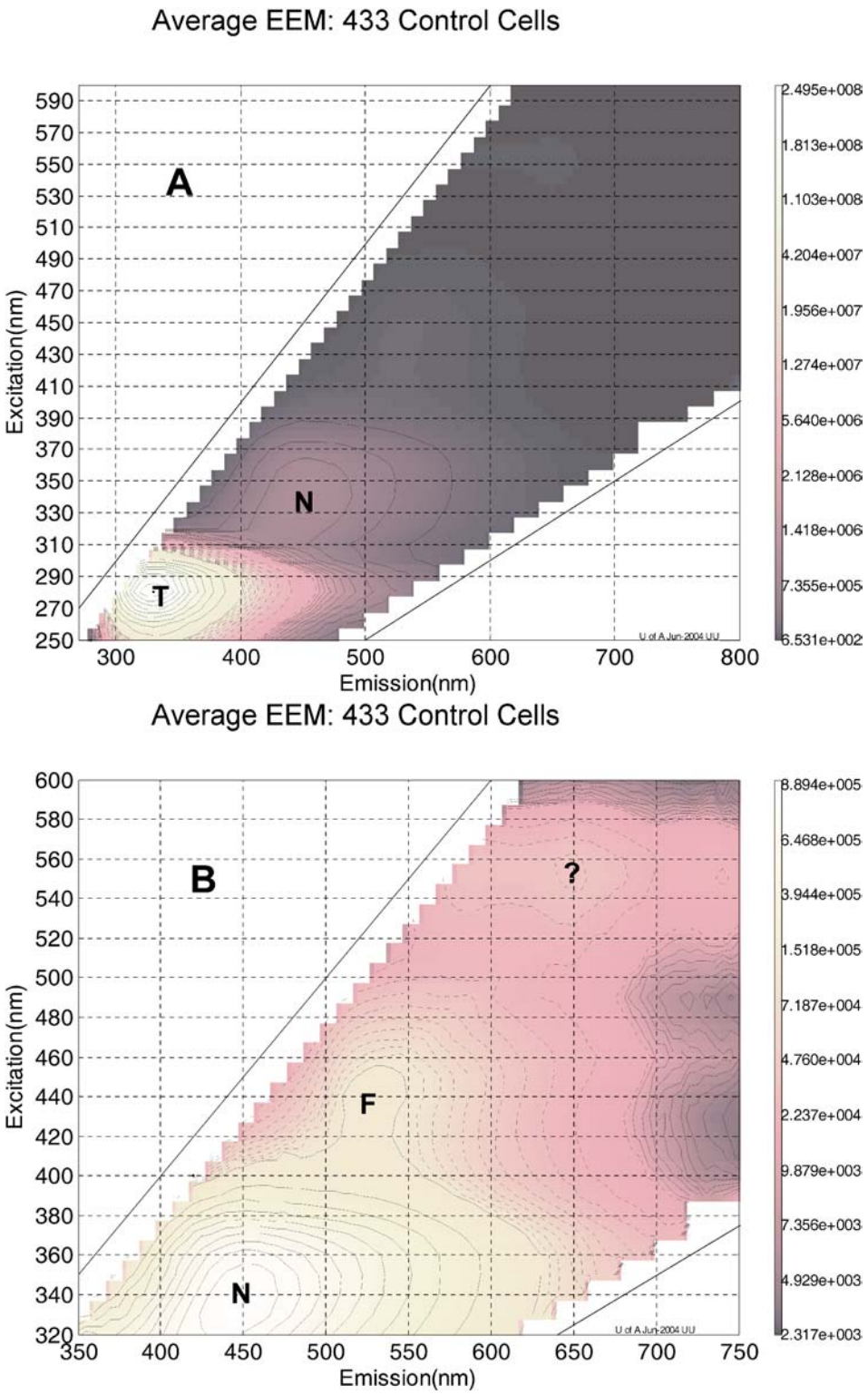

Figure 1. Average excitation/emission matrices (EEM) for the 433 control cells. A: A full EEM is shown with a prominent peak at 280/340 nm associated with tryptophan (T) and a smaller peak consistent with NADH (N) at 350/450 nm. B: By excluding the strong fluorescence peak of tryptophan, the same data seen in Fig. 1A reveal a peak at 450/530 nm associated with FAD (F) along with the NADH peak. Some additional autofluorescence is present at higher wavelengths but the origins are unknown.

provide information regarding cell line sensitivity to chemopreventive drug treatment and initiation of apoptosis.

Fluorophore contributions

To understand the individual contributions of NADH and FAD to the redox ratio, fluorescence data were specifically evaluated for both fluorophores. Figure 3A illustrates average emission spectra at 350 nm excitation for the 433 cell line. With increasing drug concentration, an intensity decrease is observed. There is also a redshift of the fluorescence slope at 400 nm emission wavelength and minimal intensity decrease at 550 nm. This redshift may be because of changes in the mitochondrial electrochemical environment. An FAD-related shoulder is observed at 530 nm that does

Table 1. Average postmeasurement cell viabilities with standard deviations for the four different drug concentrations and the four different cell lines

Treatment	420 Cell line	433 Cell line	T24 Cell line	U6 Cell line
Control	91.4 ± 5.9%	90.9 ± 7.6%	79.4 ± 20.0%	89.9 ± 7.1%
1 μ*M* 4HPR	91.3 ± 6.3%	92.8 ± 4.6%	86.4 ± 3.8%	89.3 ± 7.1%
5 μ*M* 4HPR	91.2 ± 5.1%	91.4 ± 5.3%	92.0 ± 2.3%	93.1 ± 3.7%
10 μ*M* 4HPR	91.2 ± 6.1%	91.0 ± 3.9%	90.2 ± 4.0%	91.1 ± 6.9%

not change. The NADH-related intensity was extracted between 445 and 455 nm and showed the largest signal decrease that was the least affected by spectral shape changes. Figure 3B illustrates that NADH-related signal decreased as the 4HPR concentration increased ($\beta_{433} = -2.84 \times 10^4$ au per μ*M* of 4HPR, Table 3). As was the case for the redox analysis, there were no significant interactions between cell lines ($F_{3,71} = 0.25$, $P = 0.861$, Extra Sum of Squares *F*-test). Thus, the slope of the 433 cell line in Fig. 3B represents the NADH decrease for all the cell lines. Statistically significant differences between cell lines were observed (Table 3, Fig. 3C), with the 420 and U6 cell lines exhibiting larger NADH-related contributions compared with the 433 cell line. All the parameter estimates for the linear model are shown in Table 3, with comparisons made to the 433 cell line. Baseline NADH-related values were similar between the T24 cell line and the 433 cell line, as suggested by the nonsignificant α_{T24} estimate in Table 3, unlike the redox parameter, which indicated a similarity between 433 cells and U6 cells.

Compared with the significant decrease in NADH-related signal, the FAD-related signal exhibited minimal change at each treatment level, as illustrated in Fig. 4A,B. Figure 4A shows no perceivable change in spectral shape at 450 nm excitation, the emission spectra used to extract the FAD-related signal between 530 and 540 nm emission. Figure 4B shows there was no significant increase or decrease in the peak FAD-related signal in the 433 cell line as 4HPR dose increased (β_{433}, $P = 0.463$, Table 4). Interaction between cell lines was minimal ($F_{3,71} = 0.44$, $P = 0.725$, Extra Sum of Squares *F*-test), but baseline FAD-related signal for the control groups differed (Fig. 4C). The FAD-related signal for the 420 cell line was not significantly different from the 433 cell line. As shown in Table 4, the bladder cancer cell lines had higher predicted baseline values than the ovarian cancer cell lines, but the statistical analysis showed significance only for the predicted baseline of the U6 cells (α_{U6}).

Tryptophan variation was also analyzed to investigate changes in protein-related fluorescence. Figure 5A shows representative average fluorescence emission spectra at 280 nm excitation for the 433 cell line. Fluorescence intensity decreased with increased drug dose, and no spectral shape change can be discerned. A tryptophan-related signal was extracted at the emission peak between 320 and 340 nm. Initially, it was hypothesized that the tryptophan signal correlated with the number of sampled cells and should be treated as a covariate in the linear model to remove potential variability in sample size. However, despite similar cell concentrations, we found that the tryptophan-related signal decreased ($\beta_{433} = -7.70 \times 10^6$ au per μ*M* 4HPR, Table 5) with increased 4HPR concentration, as seen for the 433 cell line (Fig. 5B), suggesting that these changes may correlate with a decrease in protein synthesis in the cells treated with 4HPR. As with the other

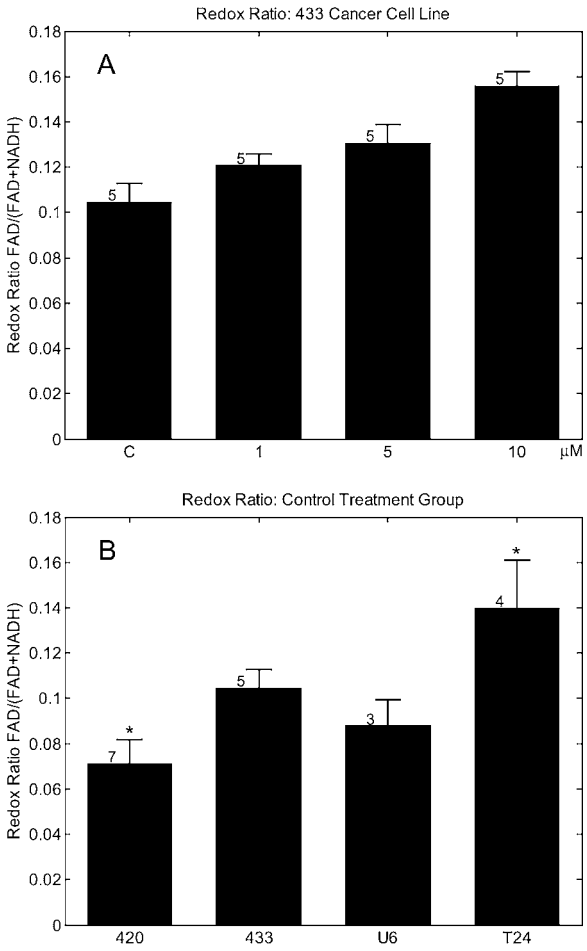

Figure 2. A: Mean redox ratios with their standard errors are graphed for the 433 cell line. The numbers on each bar represent the sample size for every cell line. The ''C'' stands for the control group, and it was treated as a 4HPR concentration of zero for the statistical models. With increasing drug concentration, the redox ratio linearly increases corresponding to a decrease in metabolic state in the cells. This linear increase was similar for all the measured cell lines. B: For each cell line the mean redox ratio is plotted along with the standard error bar for the control group. The T24 cells exhibit a higher redox ratio, whereas the 420 cells demonstrate the lowest redox state. An asterisk (*) denotes a significant difference ($P < 0.05$) of the predicted intercepts of the multiple regression model compared with the predicted reference cell line intercept (433 cells).

extracted parameters, this decrease was independent of cell line, with interaction terms not explaining additional variation ($F_{3,71} = 0.034$, $P = 0.992$, Extra Sum of Squares *F*-test). Tryptophan levels were similar for the U6 and T24 cell lines in the control groups,

Table 2. Redox parameter estimates from multiple regression fit of a simple model with no interactions. α_{433} and β_{433} represent the 433 cell line intercept and redox slope, respectively. α_{420}, α_{U6} and α_{T24} are estimates for the intercept of the 420, U6 and T24 cell lines. *P* values for the 433 intercept and slope are low because they are compared with zero making them the reference values for the other cell lines

	Redox estimate	$F_{1,74}$	*P* value
α_{433}	0.104	169	<0.0001
β_{433}	0.006	43.5	<0.0001
α_{420}	0.075	9.87	0.0024
α_{U6}	0.108	0.173	0.68
α_{T24}	0.148	16.9	0.0003

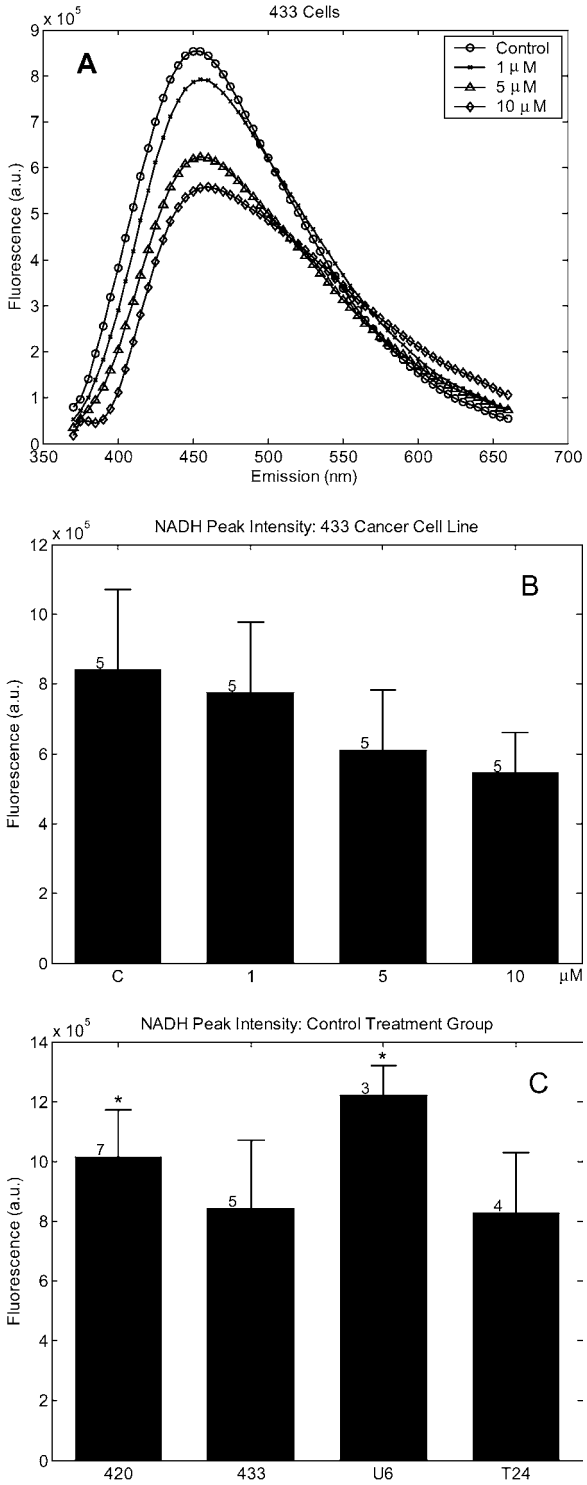

Figure 3. A: Average emission spectra excited at 350 nm are plotted for each treatment group with the 450 nm peak corresponding to the data in Fig. 3B. With increased drug concentration the peak intensity decreases and a redshift at 400 nm can be observed. At 530 nm, the fluorescence intensity does not decrease in a similar pattern as at 450 nm. B: The changes in mean NADH-associated fluorescence are graphed for the 433 cell line with standard error bars and sample size indicators. The "C" stands for the control group, and it was treated as a 4HPR concentration of zero for the statistical models. There was a linear decrease in the NADH signal with no significant difference in decrease between cell lines. C: The NADH-associated fluorescence is compared between cell lines for the control groups with significant differences ($P < 0.05$) of the predicted intercepts from the multiple regression model in relation to the reference cell line (433 cells) indicated with an asterisk (*).

Table 3. NADH-related fluorescence signal parameter estimates from multiple regression fit of a simple model with no interactions. α_{433} and β_{433} represent the 433 cell line intercept and NADH slope, respectively. α_{420}, α_{U6} and α_{T24} are estimates for the intercept of the 420, U6 and T24 cell lines

	NADH estimate	$F_{1,74}$	P value
α_{433}	6.59×10^5	9230	<0.0001
β_{433}	2.83×10^4	7.55	0.0075
α_{420}	9.29×10^5	4.46	0.038
α_{U6}	1.02×10^6	0.173	0.024
α_{T24}	7.16×10^5	0.202	0.65

with the ovarian cancer cell lines manifesting lower fluorescence intensity (Fig. 5C). A summary of the statistics for the tryptophan model is shown in Table 5. The tryptophan-related signal from the bladder cells can be statistically differentiated from that of the 433 cells. The 420 cells are not statistically different from the 433 cells.

Effects of metabolic blocker and mitochondrial uncoupler

Because metabolic blockers and mitochondrial uncouplers provide a good estimate for the dynamic range of the sampled cells fluorescence emission, an additional set of measurements were completed on one batch of 433 cells as well as two batches of T24 cells. Figure 6 illustrates fluorescence spectra at 350 nm excitation before and after the addition of NaCN. The NADH-related signal in the 433, 5 μ*M* treated cells immediately increased after adding NaCN, and over a period of 5 min, the intensity increased by 125%. This increase was the largest observed in all measurements.

To illustrate the combined effect of CCCP and 4HPR, spectra from T24 cell lines treated with 5 and 10 μ*M* 4HPR are shown in Fig. 7. Figure 7A shows a sharp signal decrease when CCCP was added to the 5 μ*M* treated cells, and after 5 min the NADH-related signal was decreased by 26%. In this cell line the depletion of NADH-related emission leads to an observed fluorescence shoulder at wavelengths consistent with FAD emission (535 nm), indicating that the relative FAD contribution to the spectral shape increased. Figure 7B depicts the same cell line treated with the highest dose of 4HPR before and after the addition of CCCP. A dramatic depletion of NADH manifests itself in an FAD-dominant spectrum of the pre-CCCP cells, suggesting a dysfunctional state of the cells. However, an NADH pool still exists, as seen in the decrease after CCCP addition, which shifts the emission maximum to 530 nm. On average, regardless of the 4HPR dose, after introducing NaCN, the NADH peak signal strongly increased (79.7% ± 30%), and the peak signal decreased by a substantial amount (36.8% ± 9.59%) after CCCP treatment. These data suggest that the fluorescence values used to estimate NADH signal after each 4HPR treatment were neither the minimal nor maximal NADH-related fluorescence that could be achieved by the cells.

When examining the FAD-related fluorescence from the 450 nm emission spectra for the same set of experiments, little change was seen, which was inconsistent with the expected decrease and increase after the addition of NaCN and CCCP, respectively. Regardless of the 4HPR concentration, after treatment with CCCP, the FAD-related signal, on average, slightly increased (8.57 ± 5.90%), whereas the signal after NaCN also increased (5.51 ± 7.15%). It was assumed that the mitochondrial agents NaCN and CCCP would have the opposite effect on the FAD-related signal than on the NADH-related signals, but our data indicate that the

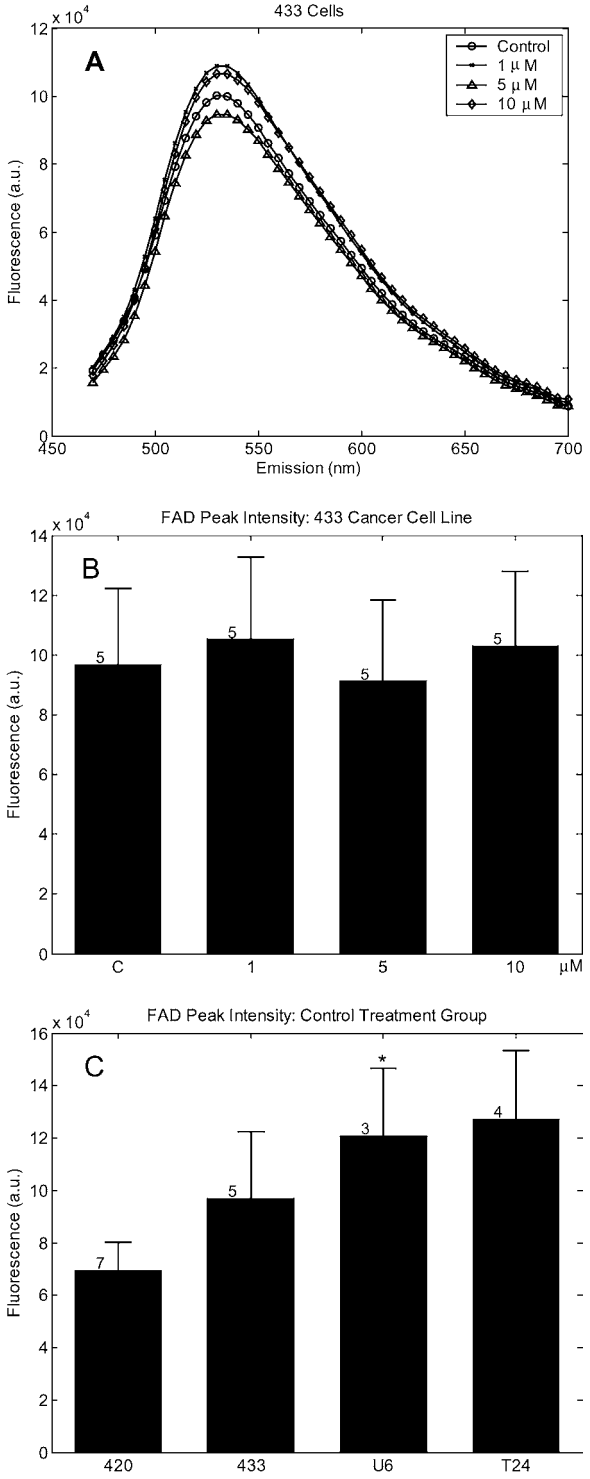

Figure 4. A: Average emission spectra excited at 450 nm are shown for each treatment group. The 530 nm peak is analogous to the data depicted in Fig. 4B. Spectral line shape as well as intensity does not seem to depend on drug concentration. B: FAD-associated fluorescence of the 433 cells remained unchanged with a higher drug concentration and the same trend was observed in the other cell lines. Mean FAD-associated fluorescence signal is graphed with corresponding standard error bars. The control group is denoted by ''C'' and was treated as a 4HPR concentration of zero. The numbers on each bar represent the sample size for every cell line. C: FAD-associated fluorescence varied among the control groups for each cell line. An asterisk (*) indicates a significant difference ($P < 0.05$) between the predicted intercepts of the cell lines and the intercept of the 433 cell line in the multiple regression model.

Table 4. FAD-related fluorescence signal parameter estimates from multiple regression fit of a simple model with no interactions. α_{433} and β_{433} represent the 433 cell line intercept and FAD slope, respectively. α_{420}, α_{U6} and α_{T24} are estimates for the intercept of the 420, U6 and T24 cell lines

	FAD estimate	$F_{1,74}$	P value
α_{433}	9.51×10^4	65.8	<0.0001
β_{433}	985	0.545	0.46
α_{420}	8.58×10^4	0.476	0.49
α_{U6}	1.29×10^5	4.52	0.037
α_{T24}	1.20×10^5	2.55	0.11

FAD-related signal is unaffected by these agents as was found for the 4HPR treatment (Table 4, Fig. 4B).

Cell cycle analysis

To verify whether the optical changes observed in cell suspensions correlated with traditional cell cycle assays, we measured the changes in cell cycle 24 h after treatment, a similar time point to the spectroscopic measurements, using a flow cytometry cell cycle analysis with PI staining. Changes in the cell cycle can be used as early indicators of growth inhibition and apoptosis. Data presented in this study were measured on one batch of cells for each cell line. Figure 8 illustrates cell cycle distributions for the T24 and U6 cells at each treatment level. The S phase decreased with increased treatment, and this decrease was more substantial in the U6 cells than in the T24 cells. Correspondingly, the G1 phase increased with increased 4HPR concentration. A decrease in the S phase and an increase in the G1 phase is consistent with growth inhibition and an early sign of apoptosis. At 10 μM 4HPR concentration, the S phase for both cell lines was practically nonexistent at 0% for the U6 cells and 10.1% for the T24 cells, indicating substantial effects induced by 4HPR. Results from the 433 and 420 cell cycle measurements also showed similar trends, with substantial decrease in the S phase and increase in the G1 phase with increased 4HPR treatment (data not shown).

DISCUSSION

For each cell line, it was observed that redox ratio increased at a similar rate with increased 4HPR concentration. A lower metabolic status of the cell is consistent with a higher redox ratio and one thought is that less metabolically active cells are less likely to undergo apoptosis (31). Although all the cell lines responded with similar changes in the redox ratio, their absolute redox state differed at each level of drug concentration. Our findings are in agreement with parallel studies examining molecular markers for mitochondrial membrane potential, caspase activity, growth inhibition and gene expression (32). Those studies suggest that, in the bladder cancer cell lines, the U6 cells are more sensitive to 4HPR than the T24 cells in apoptosis and growth inhibition. Although cells with the wild-type (U6) and mutated p53 tumor-suppressor gene (T24) can both mediate apoptosis (33), the p53 mutation might factor into the decrease in sensitivity to 4HPR treatment. In addition, the results from cell cycle analysis suggested that the cell cycle was altered by 4HPR treatment with increasing G1 phase and decreasing S phase of the cell cycle in all the cell lines. An increase in the G1 and a decrease in the S phase indicates cell cycle arrest and is an early marker for apoptosis. The U6 cell line demonstrated a larger decrease in the S phase, particularly at

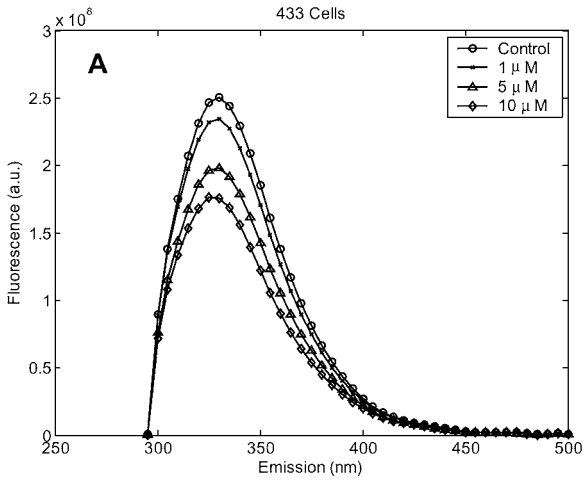

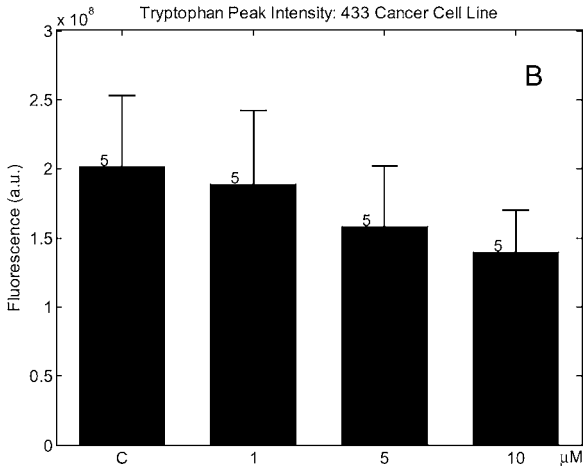

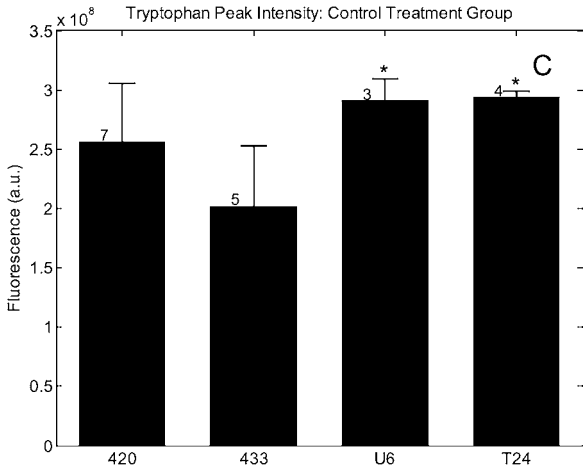

Figure 5. A: Average emission spectra excited at 280 nm are shown for each treatment group. The 340 nm peak is homologous to the data illustrated in Fig. 5B. Fluorescence intensity seems to depend on drug concentration, and spectral line shape indicates that a single fluorophore is involved. B: Tryptophan-associated fluorescence decreased with an increase in 4HPR concentration for the 433 cell line, and this decrease was found to be consistent with changes in the other cell lines. The mean fluorescence signal is plotted with standard error bars and sample size indicators. The "C" represents the control group, and it was treated as zero drug concentration for the statistical models. C: In the control group, differences of the predicted intercepts of the multiple regression model were detected between cell lines. Significant differences in predicted intercepts ($P < 0.05$) compared with the 433 cell line are represented with an asterisk (*).

Table 5. Tryptophan (TRY)-related fluorescence signal parameter estimates from multiple regression fit of a simple model with no interactions. α_{433} and β_{433} represent the 433 cell line intercept and tryptophan slope, respectively. α_{420}, α_{U6} and α_{T24} are estimates for the intercept of the 420, U6 and T24 cell lines

	TRY estimate	$F_{1,74}$	P value
α_{433}	2.08×10^8	105	<0.0001
β_{433}	7.70×10^6	11.1	0.0013
α_{420}	2.45×10^8	2.4	0.12
α_{U6}	2.69×10^8	4.94	0.029
α_{T24}	2.68×10^8	4.94	0.029

low 4HPR concentrations, suggesting a higher sensitivity to 4HPR and supporting differences observed in the optical data. Results from the cell cycle studies also showed a decrease in the S phase for the ovarian cancer cell lines after 4HPR treatment. These changes in the cell cycle suggested that both ovarian cell lines also undergo growth arrest and early apoptosis after 24 h of 4HPR treatment, consistent with sensitivity to the drug. These results are consistent with apoptosis and growth-inhibition data collected in our laboratory, highlighting a sensitivity difference between the T24 and U6 cells while suggesting 4HPR induces growth inhibition and apoptosis in all the cell lines. After several days of drug treatment at low drug concentration (1 μ*M*), the T24 cells undergo less growth inhibition and apoptosis than the U6, 420 and 433 cells. Optically, we found that the T24 cells had the highest redox states and the U6, 420 and 433 cells had lower redox states, which correlated with their sensitivity to 4HPR treatment.

When examining the main source of 4HPR-induced change within the estimated redox ratio, the NADH-related signal demonstrated the greatest amount of change, decreasing over the treatment groups, whereas the FAD-related signal remained at a relatively constant level. However, both NADH- and FAD-related signals varied between the cell lines, supporting a biological variance. Although FAD-related fluorescence may not be affected by drug treatment, these data suggest ratiometric calculations based on FAD and NADH data provide a normalized redox estimate, correcting for cell type heterogeneities. NADH-related fluorescence

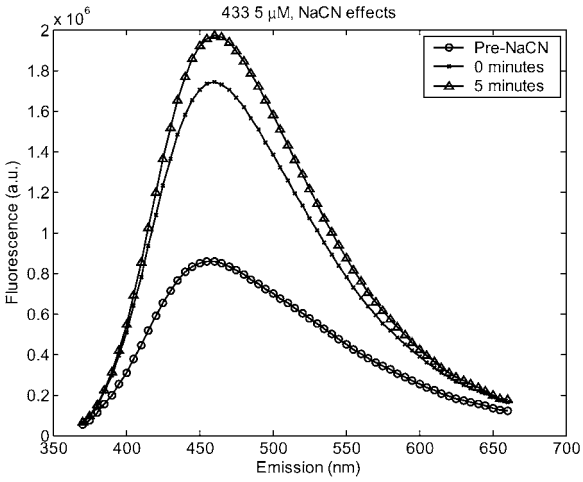

Figure 6. The emission spectra at 350 nm excitation after the addition of NaCN to one sample of 5 μ*M* 4HPR-treated 433 cells are shown. An increase in fluorescence was immediately observed, reaching an even higher level after 5 min.

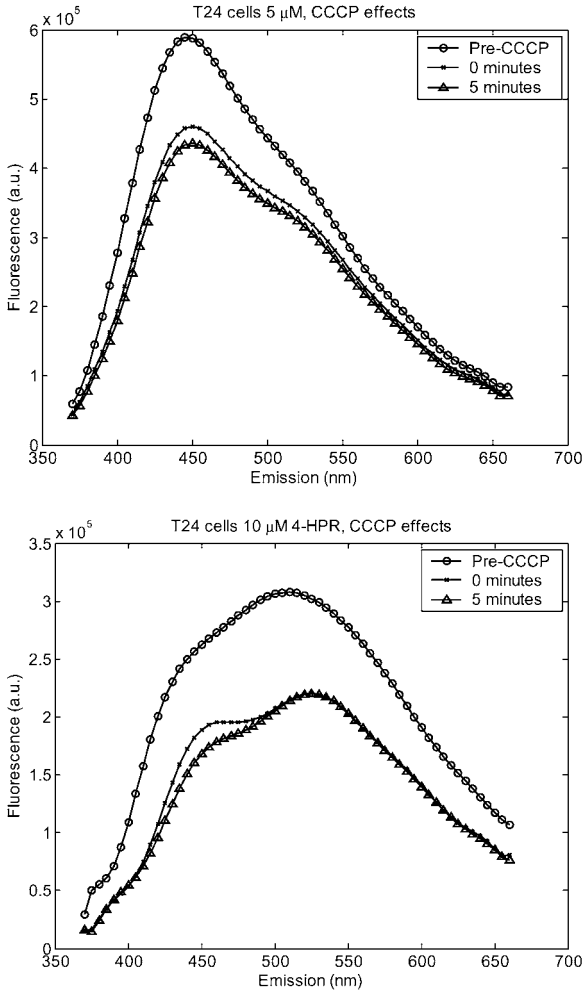

Figure 7. Emission spectra at 350 nm excitation of two samples of T24 cells as shown. A: A representative sample of the 5 μ*M* 4HPR-treatment group after the addition of CCCP shows a rapid decrease in fluorescence that leveled off after 5 min of exposure. A fluorescence shoulder consistent with FAD fluorescence can be easily observed at 530 nm after 5 min because of the large decrease in NADH-related fluorescence. B: The spectra for the 10 μ*M* treatment group of T24 cells exhibits an FAD shoulder before treatment, indicating a depletion of the NADH pool because of 4HPR treatment. After 5 min CCCP treatment distinctly decreases NADH-related fluorescence even further.

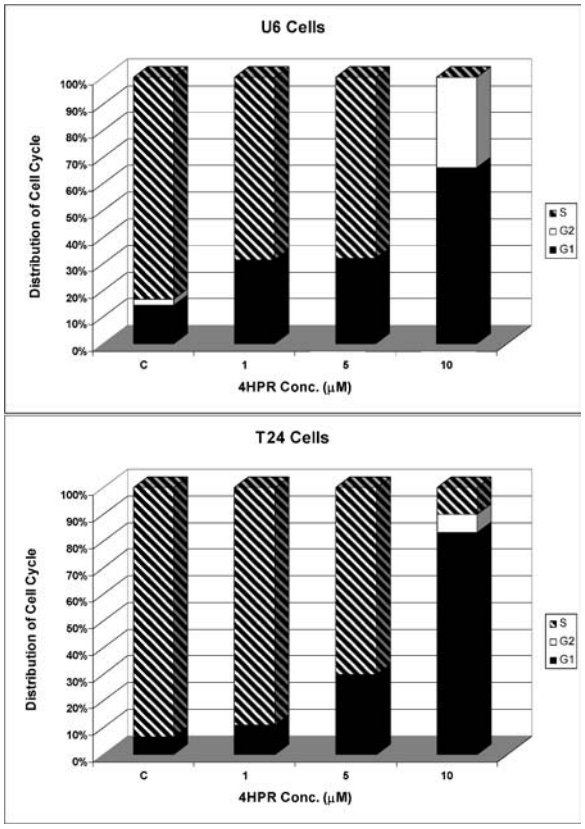

Figure 8. The percent of cells in different cell cycle stages at each treatment level are depicted for the T24 and U6 bladder cancer cell lines. The ''C'' treatment level refers to the control group that did not receive 4HPR. In both cell lines the cell cycle distribution is affected with increased drug concentration. An initial cell cycle change at 1 μ*M* is more noticeable in the U6 cells than the T24 cells.

changes explain drug activity, but the baseline redox estimate seems to be necessary to predict cell susceptibility to 4HPR treatment.

Similarly, the NADH-related signal was strongly affected by CCCP and NaCN treatment, whereas the FAD-related signal remained unaffected. Similar results have been reported by Huang *et al*. in myocytes, where the NADH signal was principally affected by mitochondrial blockers and uncouplers, whereas the FAD-related signal only changed 12% and –3%, respectively (15). In general, these findings suggest that FAD-related fluorescence is not a dynamic component of the redox estimate but serves as a reference level in calculating the ratio. We also observed that the CCCP addition seems to affect the existing NADH pool regardless of the previously administrated 4HPR treatment. This is further supported by the results from our experiments with NaCN addition.

Tryptophan-related fluorescence also decreased with 4HPR treatment, suggesting an additional fluorophore that may change with altered cellular function. This change in tryptophan signal could be due to changes in protein synthesis or protein degradation, or both. Similar findings have been reported by Pradhan *et al*. (16). Further studies are warranted to better understand how tryptophan levels may be altered in relation to metabolic changes; these changes may have both diagnostic and prognostic potential.

This study has shown that a noninvasive optical method can be used to sensitively monitor cellular metabolism in response to a chemopreventive drug treatment. Of particular interest, the redox ratio increased at a similar rate for each cell line, with the drug-induced changes mainly affecting NADH- and tryptophan-related fluorescence, whereas FAD-related fluorescence only varied at the baseline level between cell lines. In general, we have shown that spectroscopy of endogenous fluorophores is a complementary tool for drug–response studies and in this specific case could be a biomarker for apoptosis with the potential to be expanded to *in vivo* applications of monitoring the response to a chemopreventive agent.

Endogenous fluorescence spectroscopy has been extensively evaluated as a biomarker for carcinogenesis, and results on living tissue models suggested an increase of NADH-related fluorescence and a statistically insignificant change in FAD-related fluorescence in dysplastic epithelial tissue (34). In this study we have shown that our method of detecting quiescence is based on opposite effects in the cells' fluorescence signature and that this technology can serve as a sensitive marker not only for detection but also for treatment of carcinogenesis.

Acknowledgements—The optical spectroscopy work was sponsored by the Arizona Disease and Research Commission (Contract 7003). Cell cycle analysis was supported by NIH/NCI CA75966 and Ovarian Cancer Research Fund. The authors would like to thank Drs. Jian Wang and Rongyu Zang (Obstetrics and Gynecology) for their support in growing cells. We are grateful to Dr. Ron Lynch (Physiology) who provided excellent support and useful discussions. The authors also thank Dr. Margaret Briehl (Pathology) for her helpful and open discussions.

REFERENCES

1. Ramanujam, N. (2000) Fluorescence spectroscopy of neoplastic and non-neoplastic tissues. *Neoplasia (NY)* **2**, 89–117.
2. Wagnieres, G. A., W. M. Star and B. C. Wilson (1998) In vivo fluorescence spectroscopy and imaging for oncological applications. *Photochem. Photobiol.* **68**, 603–632.
3. Sokolov, K., M. Follen and R. Richards-Kortum (2002) Optical spectroscopy for detection of neoplasia. *Curr Opin Chem Biol* **6**, 651–658.
4. Richards-Kortum, R. and E. Sevick-Muraca (1996) Quantitative optical spectroscopy for tissue diagnosis. *Annu. Rev. Phys. Chem.* **47**, 555–606.
5. Sacks, P. G., H. E. Savage, J. Levine, V. R. Kolli, R. R. Alfano and S. P. Schantz (1996) Native cellular fluorescence identifies terminal squamous differentiation of normal oral epithelial cells in culture: a potential chemoprevention biomarker. *Cancer Lett.* **104**, 171–181.
6. Brewer, M., U. Utzinger, Y. Li, E. N. Atkinson, W. Satterfield, N. Auersperg, R. Richards-Kortum, M. Follen and R. Bast (2002) Fluorescence spectroscopy as a biomarker in a cell culture and in a nonhuman primate model for ovarian cancer chemopreventive agents. *J. Biomed. Opt.* **7**, 20–26.
7. Chance, B. (1991) Optical method. *Annu. Rev. Biophys. Biophys. Chem.* **20**, 1–28.
8. Galeotti, T., G. D. V. van Rossum, D. H. Mayer and B. Chance (1970) On the fluorescence of NAD(P)H in whole-cell preparation of tumors and normal tissues. *Eur. J. Biochem.* **17**, 485–496.
9. Thorell, B. and B. Chance (1959) Localization and kinetics of reduced pyridine nucleotide in living cells by microfluorometry. *J. Biol. Chem.* **234**, 3044–3050.
10. Huber, R., M. Buchner, H. Li, M. Schlieter, A. D. Speerfeld and M. W. Riepe (2000) Protein binding of NADH on chemical preconditioning. *J. Neurochem.* **75**, 329–335.
11. Nuutinen, E. M. (1984) Subcellular origin of the surface fluorescence of reduced nicotinamide nucleotides in the isolated perfused rat heart. *Basic Res. Cardiol.* **79**, 49–58.
12. Eng, J., R. M. Lynch and R. S. Balaban (1989) Nicotinamide adenine dinucleotide fluorescence spectroscopy and imaging of isolated cardiac myocytes. *Biophys. J.* **55**, 621–630.
13. Lodish, H. (1999) *Molecular Cell Biology.* W.H. Freeman, New York.
14. Lakowicz, J. R. (1983) *Principles of Fluorescence Spectroscopy.* Plenum Press, New York.
15. Huang, S., A. A. Heikal and W. W. Webb (2002) Two-photon fluorescence spectroscopy and microscopy of NAD(P)H and flavoprotein. *Biophys. J.* **82**, 2811–2825.
16. Pradhan, A., P. Pal, G. Durocher, L. Villeneuve, A. Balassy, F. Babai, L. Gaboury and L. Blanchard (1995) Steady state and time-resolved fluorescence properties of metastatic and non-metastatic malignant cells from different species. *J. Photochem. Photobiol. B: Biol.* **31**, 101–112.
17. Sun, S. Y., W. Li, P. Yue, S. M. Lippman, W. K. Hong and R. Lotan (1999) Mediation of N-(4-hydoxyphenyl)retinamide-induced apoptosis in human cancer cells by different mechanisms. *Cancer Res.* **59**, 2493–2498.
18. Sabichi, A. L., S. P. Lerner, H. B. Grossman and S. M. Lippman (1998) Retinoids in the chemoprevention of bladder cancer. *Curr. Opin. Oncol.* **10**, 479–484.
19. Sporn, M. B., R. A. Squire, C. C. Brown, J. M. Smith, M. L. Wenk and S. Springer (1977) 13-cis-retinoic acid: inhibition of bladder carcinogenesis in the rat. *Science* **195**, 487–489.
20. Supino, R., M. Crosti, M. Clerici, A. Warlters, L. Cleris, F. Zunino and F. Formelli (1996) Induction of apoptosis by fenretinide (4HPR) in human ovarian carcinoma cells and its association with retinoic acid receptor expression. *Int. J. Cancer* **65**, 491–497.
21. Kurie, J. M., J. S. Lee, F. R. Khuri, L. Mao, R. C. Morice, J. J. Lee, G. L. Walsh, A. Broxson, S. M. Lippman, J. Y. Ro, B. L. Kemp, D. Liu, H. A. Fritsche, X. Xu, R. Lotan and W. K. Hong (2000) N-(4-hydroxyphenyl)retinamide in the chemoprevention of squamous metaplasia and dysplasia of the bronchial epithelium. *Clin. Cancer Res.* **6**, 2973–2979.
22. Clifford, J. L., A. L. Sabichi, C. Zou, X. Yang, V. E. Steele, G. J. Kelloff, R. Lotan and S. M. Lippman (2001) Effects of novel phenylretinamides on cell growth and apoptosis in bladder cancer. *Cancer Epidemiol. Biomarkers Prev.* **10**, 391–395.
23. Sun, S. Y., P. Yue and R. Lotan (1999) Induction of apoptosis by N-(4-hydroxyphenyl)retinamide and its association with reactive oxygen species, nuclear retinoic acid receptors, and apoptosis-related genes in human prostate carcinoma cells. *Mol. Pharmacol.* **55**, 403–410.
24. Suzuki, S., M. Higuchi, R. J. Proske, N. Oridate, W. K. Hong and R. Lotan (1999) Implication of mitochondria-derived reactive oxygen species, cytochrome C and caspase-3 in N-(4-hydroxyphenyl)retinamide-induced apoptosis in cervical carcinoma cells. *Oncogene* **18**, 6380–6387.
25. Chance, B., B. Schoener, R. Oshino, F. Itshak and Y. Nakase (1979) Oxidation-reduction ratio studies of mitochondria in freeze-trapped samples. NADH and flavoprotein fluorescence signals. *J. Biol. Chem.* **254**, 4764–4771.
26. Bast Jr., R. C., J. S. Berek, R. Obrist, C. T. Griffiths, R. S. Berkowitz, N. F. Hacker, L. Parker, L. D. Lagasse and R. C. Knapp (1983) Intraperitoneal immunotherapy of human ovarian carcinoma with Corynebacterium parvum. *Cancer Res.* **43**, 1395–1401.
27. Grossman, H. B., G. Wedemeyer, L. Ren, G. N. Wilson and B. Cox (1986) Improved growth of human urothelial carcinoma cell cultures. *J. Urol.* **136**, 953–959.
28. Bubenik, J., M. Baresova, V. Viklicky, J. Jakoubkova, H. Sainerova and J. Donner (1973) Established cell line of urinary bladder carcinoma (T24) containing tumour-specific antigen. *Int. J. Cancer* **11**, 765–773.
29. Cooper, M. J., J. J. Haluschak, D. Johnson, S. Schwartz, L. J. Morrison, M. Lippa, G. Hatzivassiliou and J. Tan (1994) p53 mutations in bladder carcinoma cell lines. *Oncol. Res.* **6**, 569–579.
30. Zou, C., Y. Guan, J. Wang, L. E. Wang, M. Liebert, H. B. Grossman and Q. Wei (2002) N-(4-hydroxyphenyl)retinamide (4-HPR) modulates GADD45 expression in radiosensitive bladder cancer cell lines. *Cancer Lett.* **180**, 131–137.
31. Lutz, N. W., M. E. Tome, N. R. Aiken and M. M. Briehl (2002) Changes in phosphate metabolism in thymoma cells suggest mechanisms for resistance to dexamethasone-induced apoptosis. A 31P NMR spectroscopic study of cell extracts. *NMR Biomed.* **15**, 356–366.
32. Zou, C., M. Liebert, H. B. Grossman and R. Lotan (2001) Identification of effective retinoids for inhibiting growth and inducing apoptosis in bladder cancer cells. *J. Urol.* **165**, 986–992.
33. Chipuk, J. E., T. Kuwana, L. Bouchier-Hayes, N. M. Droin, D. D. Newmeyer, M. Schuler and D. R. Green (2004) Direct activation of Bax by p53 mediates mitochondrial membrane permeabilization and apoptosis. *Science* **303**, 1010–1014.
34. Drezek, R., C. Brookner, I. Pavlova, I. Boiko, A. Malpica, R. Lotan, M. Follen and R. Richards-Kortum (2001) Autofluorescence microscopy of fresh cervical-tissue sections reveals alterations in tissue biochemistry with dysplasia. *Photochem. Photobiol.* **73**, 636–641.

Minireview

Prevention of Ovarian Cancer: Intraepithelial Neoplasia

Molly A. Brewer,[1] Karen Johnson, Michele Follen, David Gershenson, and Robert Bast Jr.

Department of Obstetrics and Gynecology, Division of Gynecologic Oncology, Arizona Cancer Center, University of Arizona, Tucson, Arizona 85724 [M. A. B.]; Division of Cancer Prevention, National Cancer Institute, Bethesda, Maryland 20892 [K. J.]; Departments of Gynecologic Oncology [M. A. B., M. F., D. G.] and Translational Research [R. B.], The University of Texas M. D. Anderson Cancer Center, Houston, Texas 77030; and Department of Obstetrics, Gynecology and Reproductive Science, University of Texas Medical School, Houston, Texas 77030 [M. F.]

Abstract

To reduce the incidence and mortality associated with invasive cancers, the Intraepithelial Neoplasia (IEN) Task Force recommends that carcinogenesis be viewed as a disease that requires treatment. This publication outlines the current knowledge of IEN of the ovary and reviews chemoprevention possibilities for ovarian cancer. Ovarian cancer has the highest mortality of all of the gynecological cancers and is the fourth leading cause of death from cancer in women. The IEN Task Force has defined precancer as a noninvasive lesion that has genetic abnormalities, loss of cellular control functions, and some phenotypic characteristics of invasive cancer with a substantial likelihood of developing invasive cancer. The IEN Task Force recommends targeting moderate to severe dysplasia for new IEN treatment agents in clinical trials. Ovarian cancer does not have a clear preinvasive lesion yet merits considerable study for new prevention strategies because of the high mortality associated with ovarian cancer. There is a great unmet clinical need for treatments that can prevent ovarian cancer by providing nonsurgical options that treat the entire epithelial layer. New prevention strategies hold significant promise to reduce the mortality from ovarian cancer.

Introduction

Carcinogenesis must be viewed as a disease and disequilibrium that requires treatment to dramatically reduce the incidence and mortality associated with invasive cancers. The IEN[2] Task Force has defined precancer as a noninvasive lesion that has genetic abnormalities, loss of cellular control functions, some phenotypic characteristics of invasive cancer, and predicts a substantial likelihood of developing invasive cancer. In demonstrating effectiveness and patient benefit of new IEN treatment agents in clinical trials, the IEN Task Force recommends targeting moderate to severe dysplasia, which is close in stage of progression to invasive cancer and thus substantially elevates the risk of developing cancer.

Epithelial ovarian cancer has the highest mortality rate of any of the gynecological cancers; the 5-year survival is no more than 30% despite aggressive treatment. Seventy percent of these cancers are diagnosed with widespread intra-abdominal disease or distant metastases, which partially accounts for the poor prognosis associated with ovarian cancer. Although up to 90% of stage IA tumors and 70% of stage II tumors can be cured by current management, the cure rate drops below 30% for Stage III and IV tumors. Even ovarian cancer limited to the pelvis has a 5-year survival of only 50% (1). This dismal overall prognosis for women with ovarian cancer results from an inability to detect ovarian cancers at an early, curable stage, from the lack of effective therapy for advanced disease, and from our incomplete understanding of both the early changes in the ovary that predate the development of cancer and the initiators of these changes. Although radical surgery, radiation therapy where appropriate, and new methods of chemotherapy have improved survival times, cure rates have stayed essentially the same over the last 20 years. Thus, early intervention with chemopreventive agents merits serious consideration as a desirable alternative to suboptimal treatment of invasive disease.

Cancer chemoprevention is a rapidly growing area of research because of the possibility to prevent disease and to restore cancer-suppressing cellular functions. Chemopreventives are micronutrients or medications that prevent or delay cancer in at-risk populations. Fundamental elements for chemoprevention studies include (*a*) a suitable cohort of patients with sufficient incidence to establish an acceptable risk:benefit ratio; (*b*) appropriate agents that are safe and whose use is supported by both epidemiological and mechanistic data; and (*c*) measurable biomarkers that are likely to be affected by the agent and whose modulation is predictive of the postulated chemopreventive activity (2). Biomarkers are important because they can be used in lieu of following patients prospectively until a cancer occurs, if they indicate a protective response to a chemopreventive agent. Several criteria must be met for biomarkers to be useful: (*a*) they are relevant to the development of neoplasia either phenotypically (proliferation, angiogenesis, or nuclear morphometry) or mechanistically (molecular markers); (*b*) they

Received 4/22/02; revised 8/6/02; accepted 8/8/02.
The costs of publication of this article were defrayed in part by the payment of page charges. This article must therefore be hereby marked *advertisement* in accordance with 18 U.S.C. Section 1734 solely to indicate this fact.

[1] To whom requests for reprints should be addressed, at Department of Obstetrics and Gynecology, Division of Gynecologic Oncology, The University of Arizona, Arizona Cancer Center, 1515 North Campbell Avenue, Salmon Building, Room 1968, Tucson, AZ 85724-5024. Phone: (520) 626-9283; Fax: (520) 626-9287; E-mail: mbrewer@azcc.arizona.edu.

[2] The abbreviations used are: IEN, intraepithelial neoplasia; OSE, ovarian surface epithelial; EGFR, epidermal growth factor receptor; TGF, transforming growth factor; 4-HPR, (4-hydroxyphenyl) retinamide; TKI, tyrosine kinase inhibitor; COX, cyclooxygenase; PI3K, phosphatidylinositol 3′-kinase; OCP, oral contraceptive; RA, retinoic acid; RAR, RA receptor; KGF, keratinocyte growth factor; NOE, normal ovarian epithelial; HGF, hepatocyte growth factor.

are modulated by chemopreventive agent; and (*c*) they should predict a decrease in carcinogenesis (3).

Epidemiology

High Epidemiological Risk. The etiology of ovarian cancer remains unknown; low prevalence rates, low participation rates, small sample sizes, and potential bias in the selection of control groups have limited the interpretation of results from epidemiological studies. However, multiple epidemiological studies agree that an increased risk of epithelial ovarian cancer has been linked to advancing age, family history of breast or ovarian cancer, and frequency of ovulation (4–15). Reproductive factors have been extensively studied, but interpreting these results has been complicated by the intercorrelation of reproductive characteristics (4–15). Despite these limitations, several factors related to ovulation have been consistently associated with increased or decreased risk of developing ovarian cancer. Risk is increased with uninterrupted ovulation (nulliparity), larger number of lifetime ovulatory cycles (early age at menarche and late age at menopause), and possibly hyperovulation (fertility drugs), whereas risk is reduced by factors that suppress ovulation [pregnancy, breast feeding, and OCP use (4–15)].

High-Risk Population

High Genetic Risk. Premenopausal women with a family history of breast and/or ovarian cancer constitute an important high-risk group and are excellent candidates for prevention strategies. Although only 10% of ovarian cancers are attributable to germ-line mutations, this high-risk population is an ideal patient population to target for preliminary chemoprevention studies because of the higher prevalence of ovarian cancer as compared with that seen in the general population. Women from a cohort of high-risk families carrying the BRCA1 mutation were observed to have an approximately 40–60% risk of developing ovarian cancer and an 85% chance of developing breast cancer (15). Multiple methods of calculating risk are available. The Parmigiani method (16) uses Bayes theorem and calculates likelihood ratios. The probability of a mutation in the general population is 0.04%–0.20%, with part of the variation attributable to the ethnic mix of the population. A family history of breast and/or ovarian cancer determines the risk calculation in a particular patient. High-risk family histories with an elevated risk of developing ovarian cancer include >2 breast cancers and 1 or more cases of ovarian cancer at any age, >3 cases of breast cancer before age 50 years, sister pairs with cancers less than age 50 years, cases of breast cancer occurring at or before age 40 years, Ashkenazi Jewish descent (which carries a 2% or greater risk of mutation; Ref. 17), or 1 or more cases of breast/ovarian cancer.

The ideal design for a chemoprevention trial includes a high-risk population with an identifiable and easily accessible preinvasive lesion (*e.g.*, IEN), a safe and effective chemopreventive agent, and surrogate end point biomarkers that have been validated as markers of regression of such lesions. For ovarian cancer chemoprevention trials, the targeted population should include high-risk women with a strong family history of breast/ovarian cancer, with or without a BRCA mutation, or with Ashkenazi Jewish descent. Although there is as yet no identifiable preinvasive lesion of ovarian cancer (18), there is strong evidence for one based on the increased numbers of inclusion cysts and areas of proliferation noted in the ovaries of high-risk women seen in some studies (19); thus, this has the potential for use as a biomarker.

Pathology

IEN in the Ovary. We hypothesize that there is an IEN precursor to ovarian cancer; however, the natural history of ovarian cancer and the location of the ovary have made it difficult to characterize precursor lesions. The ovary is not routinely biopsied because of the inaccessibility of the ovary in its i.p. location and concern about the effect on fertility that might result from biopsy. Scully (20) has qualitatively described early histological changes in the ovary, whereas Deligdesch *et al.* (21, 22) have described them quantitatively with the use of nuclear texture analysis. These studies support the concept that ovarian cancer behaves in a similar manner to other epithelial cancers with an identifiable precursor. Other authors (23, 24) have described a pathological process in the ovary consistent with the IEN seen in other organ systems that occurred adjacent to existing cancers. Although progression from IEN to cancer has not yet been validated, there is accumulating evidence including a chain of underlying molecular events that supports the ovarian IEN concept.

The cell of origin of epithelial ovarian cancer remains controversial, although most investigators think it is the OSE cell. Many ovarian cancers are thought to arise from OSE cell-lined inclusion cysts (see Fig. 1); these small, subsurface cysts are hypothesized to arise from involution of ovarian surface epithelium at ovulation (20), but some inclusion cysts are thought to antecede ovulation because they are often present in fetal and juvenile ovaries (25). Small collections of malignant cells contiguous with normal ovarian epithelium suggestive of an IEN but not involving underlying tissues can be found in: (*a*) ovaries removed from women who eventually develop primary peritoneal carcinomatosis (19); (*b*) high-risk women who undergo prophylactic oophorectomy (19), particularly those with the BRCA1 mutations (24); and (*c*) in areas adjacent to stage I cancers that show a transition from malignant to normal epithelium (23, 24). However, a characteristic histological precursor lesion for ovarian cancer is not apparent in all prophylactic oophorectomy specimens (26–29). Whether these contradictory findings are due to differences in patient populations or differences in pathological techniques is not clear. However, these findings underscore the discrepancies present in our understanding of IEN of the ovary and suggest that the ovarian surface epithelium is probably the precursor for most epithelial ovarian cancers. OSE cells differ from peritoneal mesothelial cells because they overlie the ovarian stroma and are in close contact with the hormones secreted by the ovary. The chronic repair after ovulation and/or the influence of ovarian hormones are thought to increase the propensity of the OSE cells to undergo tumorigenesis and may account for the higher incidence of ovarian cancer compared with primary peritoneal cancer.

The molecular mechanisms leading to the initiation and progression of ovarian cancer remain elusive, partly because of the ovary's location and the consequent difficulty in identifying

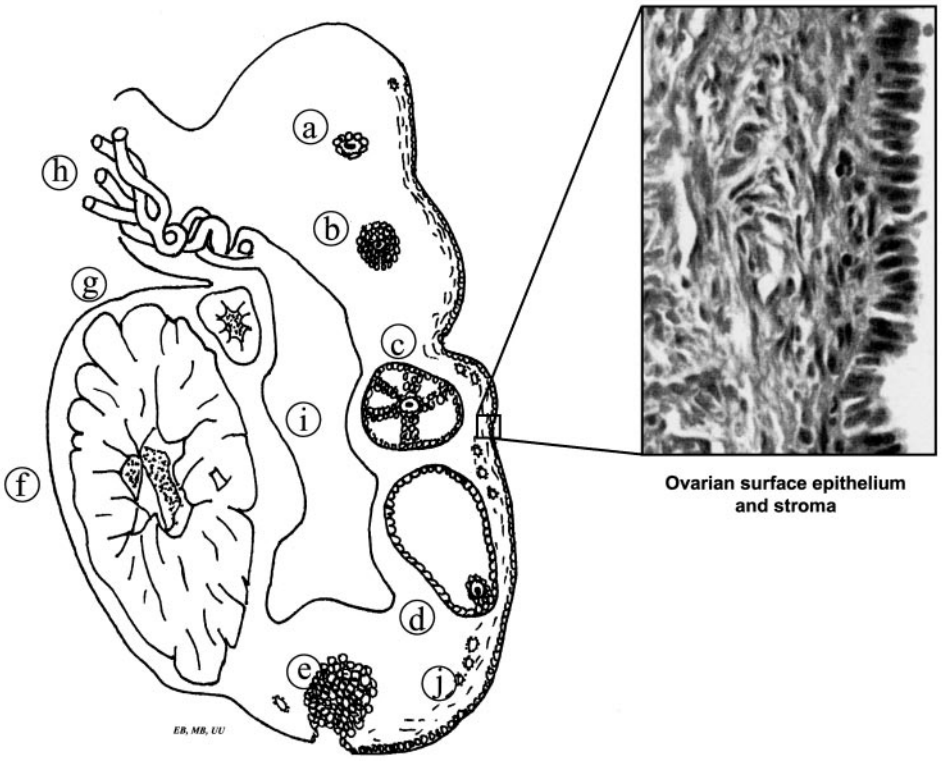

Fig. 1 Normal ovarian structures. *a*, primary follicle; *b*, secondary follicle; *c*, tertiary follicle; *d*, ovulatory follicle; *e*, hemorrhagic cyst; *f*, corpus luteum; *g*, corpus albicans; *h*, ovarian artery and vein; *i*, medulla; *j*, inclusion cyst.

early or precursor lesions. In contrast, analysis of colon, cervix, and head and neck cancers have resulted in a rapidly emerging understanding of the genetic events underlying the initiation and progression of these diseases and of the biological events that result from these genetic changes.

As with all cancers, ovarian cancer is a consequence of either germ-line or acquired somatic changes in genetic function. The acquired changes in gene expression or function can result from mutations or epigenetic alterations such as changes in methylation. Therefore, one important challenge is to link the genotypic changes that occur in ovarian cancer cells to the phenotypic and biological changes observed in human tumors and cell lines.

Although the association between ovulation and ovarian cancer is well accepted, little is known about the underlying biological mechanisms of this association. Ovulation is thought to be important for the development of inclusion cysts from which ovarian cancers may arise. In addition, ovulation, and particularly the high estrogen associated with ovulation, may provide a stimulus for proliferation of ovarian surface epithelium. Ovaries removed prophylactically from women with a strong family history of ovarian cancer demonstrate increased frequency of occult carcinomas, epithelial hyperplasia and atypia, and increased stromal activity (30). Epithelial hyperplasia and increased number of crypts (which are deep indentations of the ovary covered with surface epithelial cells) with an associated increase in proliferation may contribute to tumorigenesis by increasing the risk that a genetic alteration will occur.

OSE cells are generally quiescent but proliferate after ovulation to repair the defect created by the release of an oocyte from a mature follicle. Increased proliferation may contribute to the accumulation of genetic defects in the OSE cells. Furthermore, growth factors produced during wound healing may promote the survival of OSE cells with accumulated mutations. Alternatively, ovulation may be important for the development of inclusion cysts from which ovarian cancers may arise. Entrapment of ovarian epithelium in the stroma of the ovary may disrupt the normal relationship between the ovarian surface epithelium and the underlying stroma. Disruption of normal epithelial stromal interactions can increase mutation rates, directly contributing to ovarian cancer development. Furthermore, growth factors normally produced by the ovarian epithelium that would diffuse into the large potential space of the peritoneal cavity may be present at higher levels in the microenvironment of entrapped ovarian epithelium. Finally, ovarian epithelium in the stroma may be exposed to higher concentrations of paracrine growth factors produced by the stroma or to higher hormone levels than are present on the surface of the ovary. In support of the concept of increased ovulation conferring increased risk are the pathobiological data that show a strong correlation between the lifetime number of ovulations and the frequency of p53 mutations (19, 30). One biological hypothesis is that ovulation may result in genomic instability that occurs as a result of the repeated turnover of cells that renders cells sensitive to the high levels of gonadotropins or gonadotropin-releasing factors present postmenopausally.

Animal Models

A reliable animal model is invaluable in providing optimal flexibility for examining mechanistic, dose-response relationships and comparative efficacy. Ovarian chemoprevention studies of specific molecular targets could be accomplished with greater efficiency if an accepted rodent model of ovarian cancer were available. Under current circumstances, the opportunity to test the many hypotheses being generated by a growing list of potential agents with activity against targets implicated by the new molecular technologies is limited. Research to evaluate several candidate rodent models is being supported by the National Cancer Institute and its Mouse Consortium, and there has been investigation of both syngeneic models (31) by injecting malignant cells or by transfecting epithelial cells with oncogenes (32) to simulate development of a tumorigenic phenotype with variable success. In the meantime, the most widely accepted animal model for ovarian cancer prevention is the domestic white Leghorn chicken (33). Although investigators at The University of Texas M. D. Anderson Cancer Center (Houston, TX) are performing primate studies because of their close similarity to humans, the absence of tumor formation is a drawback, and little is known about primate ovarian carcinogenesis. The chicken, however, has an extremely high rate of Müllerian cancer, of which 30–50% are oviductal in origin. The spontaneous rate of ovarian cancers was approximately 19% in hens ranging from age 2–7 years (33). The potential utility of immunohistochemical markers in the chicken has been investigated to further develop the chicken (*Gallus domesticus*) as a model for spontaneous ovarian carcinoma. Antibodies used to characterize human tumors that were cross-reactive in chicken carcinomas included cytokeratin AE1/AE3, pan-cytokeratin, EGFR, HER-2, Lewis Y, carcinoembryonic antigen, TAG 72, proliferating cell nuclear antigen, p27, and TGF-α (34). Antibodies that were not cross-reactive included CA125, Ki67, Muc-1, and Muc-2. Oviductal cancers were not differentiated from ovarian cancers, which could limit the applicability of these markers. However, the white leghorn chicken model has considerable merit and is being investigated as a model for chemoprevention with the University of Illinois collaborating with Duke University.

Advantages of the chicken model include a high incidence of epithelial cancers. Disadvantages include a high incidence of oviductal cancers and lower correlation with humans than in primates. A study of progestin and 4-HPR in the chicken model is currently in progress. It will be interesting to see if marker modulation in this system corresponds to observations in humans and in cynomolgus macaques.

TKIs. Although the role of the EGFR family in ovarian carcinogenesis is not fully documented, it has been appreciated for some time that growth regulation and differentiation, in response to these receptors in normal ovarian surface epithelium, follow a complex system of interactions that are tissue specific. EGFR, along with the other three members of this receptor family (HER-2, HER-3, and HER-4), is detected immunohistochemically in normal OSE cells at low or moderate intensity (35, 36). Under normal conditions, epidermal growth factor, TGF-α, and amphiregulin provide growth-stimulatory signals to EGFR, and growth inhibition is mediated by TGF-β autocrine feedback (36).

Expression of the various EGFRs in ovarian cancer has been studied extensively by immunohistochemistry. Abnormal expression implying abnormal signaling through EGFR pathways is a common finding in ovarian malignancy. In contrast to the levels observed in normal ovarian surface epithelium, EGFR may be overexpressed in 50–70% of ovarian cancers (37–40). HER-2 is intensely expressed in approximately 10–20% of ovarian cancers and moderately expressed in another 20–40% more cases (41). Because of heterodimer formation among EGFR family members, multiplex expression of certain receptors may be of particular biological relevance. For instance, coexpression of EGFR and HER-2 has been reported in 30–50% of some case series (38, 39). Although intense expression of EGFR and HER-2 is not seen in normal cells and appears to confer a negative prognosis in malignancy, conflicting results regarding prognostic implications are found in the literature. This confusion should resolve as the understanding of EGFR dysregulation in ovarian cancer is updated. For instance, EGFR overexpression is reported to be associated with serous histology (40), and amphiregulin expression is reported to be associated with mucinous histology (42). These observations suggest that histological heterogeneity of ovarian cancer may contribute to the complexity of interpreting the results of growth factor pathway analysis.

A model of the expression patterns underlying EGFR dysregulation has been developed on the basis of EGFR-mediated signals in human ovarian cancer cell lines (43). In brief, the major observation is that coexpression of EGFR and HER-2 facilitates transactivation by epidermal growth factor and produces a strong mitogenic signal. Coexpression of *Her-2* gene product and EGFR was present in 68% of ovarian cancers (44). Two other observations include: (*a*) heregulin activates HER-4, either on its own or with HER-3; and (*b*) HER-3 and HER-4 do not cross-react with EGFR and HER-2 after stimulation with heregulin. Activation of the EGFR and HER-2 heterodimer may be the predominant growth-stimulatory signal in ovarian epithelium, as suggested by the commonly observed overexpression of these two receptors in ovarian cancer (45). If unattenuated, it is plausible that this signal could be a critical driving force in ovarian carcinogenesis. This hypothesis is the basis for testing the potential usefulness of TKIs for preventing the abnormal proliferation of ovarian epithelium that is postulated to precede malignant transformation (see "New Agents").

COX-2 Expression. Abnormal COX-2 expression is found in ovarian cancer. Matsumoto *et al.* (46) have reported a series of 28 ovarian carcinomas, of which 79% were positive for COX-2 expression overall, with 61% strongly positive and 18% weakly positive. In contrast, COX-2 expression was not found in the surface epithelium or inclusion cysts of the uninvolved ovaries in this series (46). In these samples, COX-2 expression was correlated with vascular endothelial growth factor expression. Ovarian cancer cell lines that express COX-2 include SKOV3, CAOV3, and OVCAR3, all of which undergo growth suppression by a COX-2 inhibitor *in vitro* (47).

PI3K. PI3K represents a node in a pathway downstream to the proliferation signals originating from the EGFR family. The potential importance of PI3K in the malignant process is

suggested by its position in signal transduction between EGFR and AKT2, which has been identified as another site of oncogene abnormality in ovarian cancer (48). PI3K has become a focus of attention because amplification of PI3K activity is observed in approximately 40% of ovarian tumors confined to the subset of tumors with serous histology (49, 50). PTEN mutations predominate in endometrioid ovarian cancers. In addition to increased proliferation, decreased apoptosis is also found in association with increased PI3K activity (51). Amplification of PI3K activity is observed in several ovarian cancer cell lines, including OVCAR3. Mechanistic studies have shown that enzyme activity of PI3K is reduced more than 80% by specific inhibitor LY294002 (52). LY294002 causes a dose-dependent reduction in growth of OVCAR3 cells in culture and reduces tumor burden in nude mice inoculated with OVCAR3 (52).

Agents

Well-known agents are being considered for use in reducing the risk of developing ovarian cancer. One of these is the OCP. The OCP reduces the risk of developing ovarian cancer with odds ratios ranging from 0.25 to 0.8 (12–14, 53–55). Its protective effect is independent of study design (case-control or cohort study) and study population (population based or hospital based). The reduction in risk appears to persist for up to 10 or more years after discontinuation of OCP. Based on epidemiological findings and assuming a lifetime protective effect and similar protection by all formulations of OCP, it is estimated that more than half of all ovarian cancers in the United States could be prevented by the use of OCP for at least 4 years (53, 54). A recent case control study (56) that compared high-dose OCP with mid-dose OCP showed greater protection from the high-dose OCP. Both progestin and estrogen concentrations are higher in the high-dose pill, but the greater protective effect is attributed to the progestin component. There have not been studies comparing the mid-dose pill with the low-dose pill, but it would be important to determine the effectiveness of the low-dose pill. In monkey studies using both progestins and OCP (57), the progestin arm had more apoptosis of the OSE cells than the OCP arm, suggesting that progestin may be the active component in the OCP, although variances were large, and median values were used because of the large variability. A reanalysis of the data from the cancer and steroid hormone study (58), which examined the strength of OCP components taken by 390 women diagnosed with ovarian cancer compared with controls, found the greatest reduction in ovarian cancer risk associated with the highest progestin potency. In addition to this information, a recent report has explored the relationship between progestin, TGF-β expression, and apoptosis in the ovarian epithelium of cynomolgus macaques. Exposure to progestin changed the expression of TGF-β, lowering TGFβ-1 with a corresponding increase in TGF-β2/3, correlating closely with induction of substantial apoptosis in the ovarian epithelium (59). Consequently, the progesterone receptor is a prime candidate as a preventive target. Definitive mechanistic and clinically based studies are of great importance in refining the opportunity to specify a role for progestins, agent/dose/schedule, in ovarian cancer risk management. This body of evidence makes the OCP (and potentially the progestin component) an excellent candidate chemopreventive agent for ovarian cancer, although more needs to be learned about the mechanism of its protective effect.

Use of the OCP for 5 years decreases the risk of ovarian cancer by 50% (53–55) but reduces the number of ovulatory cycles by approximately 15 percent. Consequently, there is not a linear correlation between the duration of OCP use and the impact on ovarian oncogenesis, suggesting that more complex mechanisms other than just ovulation suppression may be at work in the chemopreventive activity of OCP. Inhibition of gonadotropin release from the pituitary, one of the effects of OCP use, or other unknown effects of estrogens and progestins may also play a role in this chemopreventive activity.

Retinoids. As with OCP, the antineoplastic effect of 4-HPR is not completely understood. In the laboratory, the activity of retinoids in ovarian cancer has been studied in various ways. In four different ovarian cancer cell lines, 4-HPR was the most effective at suppressing growth compared with all-*trans*-RA, 9-*cis*-RA, and 13-*cis*-RA (60). Studied in more detail in cell line OVCAR3, 4-HPR was found to weakly activate only RARγ, with induction of apoptosis appearing to occur independent of retinoid receptors. This result is consistent with the classification of 4-HPR as a receptor-independent apoptotic retinoid. In addition to retinoid receptors, several other targets have been suggested to mediate their effect. They include the destruction of the mitochondrial membrane by reactive oxygen species and stabilization of the Rb2/p120 protein that mediates retinoid induced growth arrest (61).

Epidemiological and laboratory data suggest that retinoids may have a role as preventive or therapeutic agents for ovarian cancer (58, 62, 63). Fenretinide or 4-HPR has few side effects compared with other vitamin A derivatives and is currently being used in chemoprevention studies of other organ sites, including lung, head and neck, cervix, and bladder. Experimental studies have demonstrated that retinoids can affect human ovarian cancer cell growth by inhibiting proliferation and inducing apoptosis (58, 62); preliminary data from our laboratory show that 4-HPR induces apoptosis in immortalized OSE cells and in normal OSE cells (64). Some cells respond to 2 μM/ml 4-HPR, which might be achievable by oral administration, but others require as high as 10 μM/ml to have an effect. The 10 μM/ml dose would not be achievable by an oral dose because of side effects, particularly skin and ophthalmic effects (nyctaglia). Because epithelial ovarian cancer is thought to arise from a neoplastic process that results from a series of mutations in the OSE cells, the probability of developing a neoplasm would decrease if premalignant or genetically altered cells were eliminated by apoptosis.

In Italy, a randomized trial for the prevention of breast cancer has provided preliminary evidence that retinoids, specifically 4-HPR, may prevent or delay the development of ovarian cancer (63). After surgical treatment for breast cancer, 2972 patients were assigned to treatment with 4-HPR (1422) or placebo (1427) to prevent development of new primary breast cancers. After a median follow-up of 51.9 months, no overall difference in the development of new primary breast cancers was evident; however, there was a significant difference in the numbers of ovarian cancers that developed. During the treatment period, six new cases of ovarian cancer were diagnosed in

the placebo group *versus* none in the 4-HPR group ($P = 0.0162$). After cessation of treatment, there were four additional cancers in the control group and six in the 4-HPR group, suggesting that the effect was not durable. There was also a difference in the characteristics between groups: the control group was more likely to have a BRCA mutation than the 4-HPR group, which suggests that the difference may be due to the BRCA status rather than drug effect (65). However, when combined with the cell work, there is the suggestion that retinoids may have chemopreventive activity in the ovary but may need to be administered for long periods of time or to have a different dosing developed so that higher doeses could be achieved without toxicity.

Some low-toxicity retinoids, known as heteroarotinoids, share the receptor-independent apoptotic profile of 4-HPR and may be candidates for development as chemopreventive agents (61). In addition to this group of retinoids, AHPN/CD437, a conformationally restricted retinoid engineered to bind selectively to RARγ, also shares the apoptotic profile of 4-HPR. In ovarian tumor cell cultures, exposure to AHPN was associated with increased expression of *BAX* and decreased expression of *Bcl*-2 (66, 67). Agent development for ovarian risk reduction will benefit from mechanistic studies of apoptotic induction by 4-HPR and functionally similar compounds such as AHPN. Retinoids that suppress both growth and survival of abnormal cells hold more promise as chemopreventive agents. Prioritizing retinoids for ovarian cancer prevention will ultimately depend on the overall interrelationship among antiproliferative, differentiating, and apoptotic properties of these compounds.

Although there are still too little data to definitively guide chemopreventive studies, there is compelling evidence that as many as 50% of ovarian cancers may be prevented with OCP, and possibly even more may be prevented if a combination of the active ingredients (presumably progesterone) and a vitamin A derivative could be combined for use in high-risk women. Likewise, a similar reduction might be obtained if the active component of OCP could be administered to low-risk women, the group that develops 90% of the ovarian cancers.

Biomarkers

Biomarkers need to be identified that are predictive of drug or micronutrient activity and pharmacodynamics because the modulation and utility of particular biomarkers will depend on the drug-specific mechanism of action and conditions of use for any given agent. At the current time, little is known about effective biomarkers for drug activity in ovarian cancer chemoprevention. Markers of proliferation and apoptosis are key biomarkers in prevention. Apoptosis is hypothesized to be one of the major mechanisms by which cells with genetic alterations are eliminated (68). In a pivotal trial, primates were treated for 2 years with OCP, estrogen, progestin, or placebo (69). After this period, ovaries were removed, and their surface epithelia were assessed for apoptosis. OCP and progestin significantly increased apoptosis in OSE cells from 5% (baseline) to 25%, whereas estrogen had no effect. If OCP increased the rate of apoptosis in epithelial cells from human ovaries, as they have been found to do in primate ovaries, apoptotic elimination of aberrant cells might be one of the mechanisms underlying the chemopreventive effects of OCP. In the primate, the high rate of apoptosis (25%) also indicates that either a very large proportion of OSE cells had underlying genetic abnormalities or a number of NOE cells underwent apoptosis in response to components of the OCP. This 25% frequency of apoptosis in the primates appears particularly high when it is considered that it represents a "snapshot" in time and that many cells may already have undergone apoptosis and been cleared from the system. One possible explanation may be the use of a Triphasil pill that has the highest concentration of the progestin in the third week. These monkeys were sacrificed in the third week of their OCP use.

In cell culture, different retinoids (including 4-HPR and all-*trans*-RA) inhibit proliferation and induce apoptosis in a number of tumor cell types [including ovarian cancer cell lines (57, 70–74)]. In at least some cell lineages, 4-HPR is more effective than other retinoids at inducing apoptosis (57) and can induce apoptosis in cells resistant to conventional retinoids. However, the mechanism by which 4-HPR and other retinoids induce growth inhibition and apoptosis is unclear. Most, but not all, studies indicate a correlation between RARβ expression or the ability to induce its expression and the ability of 4-HPR to induce growth inhibition and apoptosis (70–72). However, in ovarian cancer cells, 4-HPR effect appears to be receptor independent (61). Induction of reactive oxygen species is another proposed mechanism (74) of 4-HPR, but there are no data available on OSE cells or ovarian cancer cells. These biomarkers of retinoid activity warrant further exploration.

Growth Factor Specific. TGF-β is another potential biomarker of chemoprevention. It can induce growth arrest and apoptosis of ovarian cancer cell lines, as well as ovarian cancer cells isolated directly from patients (73, 74). In several cell types, including ovarian stroma, steroid hormones can increase TGF-β production and activation (75–79). Whether TGF-β, in concert with retinoids or steroids, induces apoptosis in ovarian epithelial cells *in vitro* or, more importantly, *in vivo* remains to be assessed. A recent histochemical evaluation of the primate ovary from primates receiving either progestin alone or the Triphasil OCP found an increase in expression of TGF-β2, but not TGF-β1, suggesting that TGF-β2 may be modulated by OCP, serving as a marker of progestin activity (59). Thus, TGF-β and its receptors definitely merit exploration. Other potential biomarkers include proliferative markers, such as Ki67, which are currently being used to evaluate the antiproliferative effects of progesterone.

Stromal cells may play an important role in epithelial carcinogenesis. Both types of cells contribute to the extracellular matrix (80), and stromal cells may influence some of the premalignant changes that occur in the epithelial cells (81). Epithelial ovarian cells express both cytokeratin and vimentin, suggesting a dual phenotype consistent with a multipotential stem cell origin. These epithelial cells produce both epithelial and mesenchymal components of extracellular matrix in tissue culture, which is consistent with their dual phenotype (80). KGF, a mesenchymal growth factor that mediates epithelial-stromal interaction, has been recently studied as a factor in early carcinogenesis (82). Fresh NOE cells, but not stromal cells, were found to highly express KGF, which subsequently growth-stimulated NOE cells in an autocrine manner (83). HGF and its

receptor, Met, have also been studied. HGF and KGF, as well as Kit ligand, have been found to interact and promote NOE cell growth and growth factor expression, suggesting that these may play a role in the growth stimulation that accompanies the carcinogenic process (84). Wong *et al.* (85) found that NOE cells from women without a family history of ovarian cancer down-regulated the HGF receptor with increasing passage, whereas the NOE cells from women with a family history of ovarian cancer did not, suggesting that HGF may be a growth regulator, particularly in cells destined to develop cancers (85). Telomerase may be an additional marker warranting both study and targeting. These biomarkers need further study to understand their role in modulating growth and to determine which growth modulators might be a target for prevention.

Optical Spectroscopy

One of the more exciting prospects for an early marker of ovarian cancer is optical spectroscopic signatures. In the last decade, substantial research has lead to useful optical methods of diagnosing early cancers (86–92). Fluorescence spectroscopy is being used to detect cancers noninvasively in many organ systems using a probe that can interrogate the tissue. The system utilizes redox potential (ratio), which is calculated by (FAD/(FAD + NADH) and is, in part, a measure of the relative hypoxia of the tissue (93). FAD and NAD(P) are reduced in the citric acid cycle (anaerobic glycolysis) to FADH and NAD(P)H, which are used as coenzymes in the electron transport chain. In tumors, these coenzymes will accumulate in their reduced states (NADH and FADH) and produce a unique fluorescence signature (NADH high, FAD low) as a result of alterations in blood flow, decreases in tissue pH, and abnormalities in mitochondria and in transport of electron carrier molecules into the mitochondria (93, 94), where the electron transport chain functions. In a pilot study (95), patterns of fluorescence called excitation/emission matrices differed between normal ovaries and areas of invasive cancer and thus are promising for early detection of ovarian cancer. As anticipated, redox potentials were 50% lower in the cancer than in the normal ovary with peaks at 350 nm (excitation) and 460 nm (emission), representing both collagen and NADH. Even more exciting, however, was our recent primate study of fluorescence spectroscopy as a marker for drug activity in the ovary (96). Unlike cancer, where redox potentials are reduced, redox potentials were increased in response to both OCP and 4-HPR. Changes in fluorescence signatures were hypothesized to be due to a decrease in NAD(P)H and an increase in FAD in response to the drugs. 4-HPR had the least effect on the fluorescence signature of NAD(P)H and the greatest effect on the area corresponding to FAD, in contrast to OCP, suggesting that each agent has a unique effect on cellular metabolism. These agents also produced an increase in the redox-related potential of the target organ, suggesting that hypoxia was less extensive and that the system was more quiescent. Thus, optical spectroscopic signatures may serve as an early marker of drug activity.

Cell culture data (97) show that retinoids can induce apoptosis or inhibit growth in both normal and immortalized OSE cells. Cell studies measuring fluorescence emission compared with percentage of apoptosis and growth inhibition showed that both apoptosis and growth inhibition correlated with redox ratio ($P = 0.0274$), FAD fluorescence intensity correlated with apoptosis ($P < 0.001$), and NAD(P)H fluorescence intensity correlated with cell survival ($P = 0.04$; Ref. 68).

New Agents

Given the preponderance of evidence that OCP and/or retinoids have a role to play in ovarian cancer prevention, an initial consideration for the development of new agents would be optimizing the effect of these two categories of agents on ovarian cancer risk reduction. In general, recent progress in pharmacological intervention has been achieved by identifying a specific target that is critical to a pathological process. Disruption of a critical pathological signal by eliminating target function can be the key to disease prevention as well as disease control. Evidence reviewed above suggests that OCPs disrupt a critical pathway in early ovarian carcinogenesis in a substantial proportion of women at risk, but a specific target has not been clearly identified. A recent study supports the theory that the progesterone component of OCPs is responsible for reducing ovarian cancer risk.

In addition to the targets suggested by the observation of ovarian cancer risk reduction associated with the use of OCP or 4-HPR, the molecular analysis of malignant ovarian tumors has identified other candidate prevention targets. Selected oncogenes, growth factors, and signal transduction pathways are connected with ovarian carcinogenesis. The focus on targets related to the EGFR family, P13K, and COX2 is guided not only by preclinical studies but also by the presumption that relatively nontoxic oral agents in these categories are either available or about to become available.

TKIs. TKIs are of interest to ovarian cancer prevention because of their effect on the activation of EGFRs. In general, the dose-limiting toxicities for TKIs are skin rash and/or diarrhea. In the prevention setting, it may be possible to identify conditions of use that will avoid these toxicities. Alternatively, if preclinical concepts of prevention are demonstrated with compounds like these, it may be possible to identify less toxic versions of these agents that reduce cancer risk. Beyond EGFR-selective agents, there are TKIs in development with a different range of activity. For instance, CI-1033 is a potent inhibitor of kinase activity across the entire EGFR family. Agents selective for HER-2 are also in development.

Examples of TKIs that are of theoretical interest for testing in ovarian cancer prevention studies are ZD1839 (Iressa), OSI774, and PKI-166 (98, 99). As a pyrolopyrimidine, PKI-166 is structurally different, but like ZD1839 and OSI774, targets EGFR. All of these agents have been used in clinical trials and could be studied in model systems to generate preclinical data relevant to ovarian cancer prevention. EGFR, HER-2, and HER-4 all have a tyrosine kinase domain that can be activated when particular EGFR dimer-ligand complexes are formed. As members of a structural class of compounds known as quinazolines, ZD1839 and OSI774 are structurally similar and selectively deactivate the tyrosine kinase of EGFR. These agents might be particularly useful if it could be demonstrated that an EGFR-selective drug deactivates abnormal EGFR/HER-2 heterodimer expression in ovarian epithelium. In breast cancer cells

that overexpress HER-2, blocking transmodulation through EGFR with an EGFR-specific TKI is known to halt growth (100).

PI3K Inhibition. Because of the position downstream to the proliferation signals originating from the EGFR family, agents targeting PI3K might have chemopreventive activity on the basis of an antiproliferative effect. P13K inhibitors have not reached clinical trials, so future use of agents in this class for chemoprevention awaits their further pharmacological development.

COX-2 Inhibition. Another target of chemopreventive interest is COX-2 (101). COX-2 is an inducible enzyme of inflammation, mediating the conversion of arachidonic acid to prostaglandins. Attention has been called to the role that inflammation might play in ovarian carcinogenesis (102). It remains to be seen whether COX-2 inhibitors can be used to modulate COX-2 expression in ovarian epithelium and whether such modulation has a role early in carcinogenesis. As with the other agents mentioned in this review, it would be helpful to have a valid animal model of ovarian carcinogenesis to use in the development of preclinical data.

Clinical Trials

There are currently ongoing trials of both high low- and high-risk women for investigating chemopreventive agents in the ovary. Fox Chase Cancer Center has a trial using 4-HPR in high-risk women undergoing oophorectomy. The University of Texas M. D. Anderson Cancer Center and the University of Arizona have chemoprevention trials in both low- and high-risk women using OCPs and 4-HPR alone and in combination for women undergoing oophorectomy. This is early exploratory work, and findings from these trials will serve as templates for additional trials. Markers that are elucidated as a result of these trials will help determine which are the best biomarkers for drug activity. Following the results of these and other trials that may be starting in the next decade, larger randomized prospective trials will be important to determine the true preventive activity of these and other agents.

Discussion

Of the four criteria given in the opening definition of IEN, the most difficult to pinpoint in ovarian cancer is the abnormal phenotype. Although access to early ovarian neoplasia is limited by anatomical circumstance, there may, in fact, be biological reasons why an understanding of ovarian IEN is elusive. Ovarian cancer has been described as diseases (37), and, in fact, more than 40 histological entities contribute to the WHO classification of epithelial tumor types. Heterogeneity in ovarian cancer histology suggests a corresponding complexity in IEN. Also, it is recognized that malignant cells with a specific and identifying molecular fingerprint are not always histologically unidentifiable in seemingly normal epithelium adjacent to tumor (34). Given these observations, it may ultimately be necessary to rely on the genetic and consequent functional abnormalities to identify the precursor population of cells that gives rise to invasive ovarian cancer. In addition to the spectroscopic technique described above, genomic and proteomic methods are now being developed that may facilitate the definition of localized precursors of ovarian cancer (103). The possibility of analyzing proteins characteristic of cancer risk and shed from ovarian IEN into serum (104–107) appears to offer an attractive alternative to the direct assessment of the ovarian epithelium by microlaparotomy for examination by spectroscopy or biopsy and subsequent microdissection.

References

1. Hoskins, W. J. Prospective on ovarian cancer: why prevent? J. Cell. Biochem. Suppl., *23:* 189–199, 1995.

2. Kelloff, G. J., Boone, C. W., Crowell, J. A., Nayfield, S. G., Hawk, E., Steele, V. E., Lubet, R. A., and Sigman, C. C. Strategies for Phase II cancer chemoprevention trials: cervix, endometrium, and ovary. J. Cell. Biochem. Suppl., *23:* 1–9, 1995.

3. Dhingra, K. A Phase II chemoprevention trial design to identify surrogate endpoint biomarkers in breast cancer. J. Cell. Biochem. Suppl., *23:* 19–24, 1995.

4. Casagrande, J. T., Pike, M. C., Ross, R. K., Louise, E. W., Roy, S., and Henderson, B. E. Incessant ovulation and ovarian cancer. Lancet, *2:* 170–172, 1979.

5. Greene, M. H., Clark, J. W., and Blayney, D. W. The epidemiology of ovarian cancer. Semin. Oncol., *11:* 209–226, 1984.

6. Hartge, P., Schiffman, M. H., Hoover, R., McGowan, L., Lesher, L., and Norris, H. J. A case-control study of epithelial ovarian cancer. Am. J. Obstet. Gynecol., *161:* 10–16, 1989.

7. Hildreth, N. G., Kelsey, J. L., LiVolsi, V. A., Fischer, D. B., Holford, T. R., Mostow, E. D., Schwartz, P. E., and White, C. An epidemiologic study of epithelial carcinoma of the ovary. Am. J. Epidemiol., *114:* 398–405, 1981.

8. Joly, J. D., Lilienfeld, A. M., Diamond, E. L., and Borss, I. D. J. An epidemiologic study of the relationship of reproductive experience to cancer of the ovary. Am. J. Epidemiol., *99:* 190–209, 1974.

9. Kvale, G., Heuch, I., Nilssen, S., and Beral, V. Reproductive factors and risk of ovarian cancer. A prospective study. Int. J. Cancer, *42:* 246–251, 1988.

10. Mori, M., Harabuchi, I., Miyake, H., Casagrande, J. T., Henderson, B. E., and Ross, R. K. Reproductive, genetic, and dietary risk factors for ovarian cancer. Am. J. Epidemiol., *128:* 771–777, 1988.

11. Whittemore, A. S., Harris, R., and Itnyre, J. Collaborative Ovarian Cancer Group. Characteristics relating to ovarian cancer risk: collaborative analysis of 12 U.S. case-control studies. II. Invasive epithelial ovarian cancers in white women. Am. J. Epidemiol., *136:* 1184–1203, 1992.

12. Franceschi, S., Parazzini, F., Negri, E., Booth, M., La Vecchia, C., Beral, V., Tzonou, A., and Trichopoulos, D. Pooled analysis of 3 European case-control studies of epithelial ovarian cancers. III. Oral contraceptive use. Int. J. Cancer, *49:* 61–65, 1991.

13. Centers for Disease Control Cancer and Steroid Hormone Study. Oral contraceptive use and the risk of ovarian cancer. J. Am. Med. Assoc., *249:* 1596–1599, 1983.

14. Rosenberg, L., Shapiro, S., Slone, D., Kaufman, D. W., Helmrich, S. P., Miettinen, O. S., Stolley, P. D., Rosenshein, M. B., Schottenfeld, D., and Engle, R. L., Jr. Epithelial ovarian cancer and combination oral contraceptives. J. Am. Med. Assoc., *247*: 3210–3212, 1982.

15. Easton, D. F., Ford, D., and Bishop, D. T. Breast and ovarian cancer incidence in BRCA-1 mutation carriers. Breast Cancer Linkage Consortium. Am. J. Hum. Genet., *56:* 265–271, 1995.

16. Berry, D., Parmigiani, G., Sanchez, J., Schildkraut, J., and Winer, E. Probability of carrying a mutation of breast-ovarian cancer gene BRCA-1 based on family history. J. Natl. Cancer Inst. (Bethesda), *89:* 227–238, 1997.

17. Struewing, J., Hartge, P., Wacholder, S., Baker, S., Berlin, M., McAdams, M., Timmerman, M., Brody, L., and Tucker, M. The risk of cancer associated with specific mutations of BRCA1 and BRCA2 among Ashkenazi Jews. N. Engl. J. Med., *336:* 1401–1408, 1997.

18. Gershenson, D. M., Tortolero-Luna, G., Malpica, A., Baker, V. V., Whittaker, L., Johnson, E., and Mitchell, M. F. Ovarian intraepithelial neoplasia and ovarian cancer. Obstet. Gynecol. Clin. N. Am., *23:* 475–543, 1996.

19. Salazar, H., Godwin, A. K., Daly, M. B., Laub, P. B., Hogan, W. M., Rosenblum, N., Boente, M. P., Lynch, H. T., and Hamilton, T. C. Microscopic benign and invasive malignant neoplasms and a cancer-prone phenotype in prophylactic oophorectomies. J. Natl. Cancer Inst. (Bethesda), *88*: 1810–1820, 1996.

20. Scully, R. E. Pathology of ovarian cancer precursors. J. Cell. Biochem. Suppl., *23:* 208–218, 1995.

21. Deligdisch, L., Miranda, C., Barba, J., and Gil, J. Ovarian dysplasia: nuclear texture analysis. Cancer (Phila.), *72:* 3253–3257, 1993.

22. Deligdisch, L., Gil, J., Kerner, K., Wu, H. S., Beck, D., and Gershoni-Baruch, R. Ovarian dysplasia in prophylactic oophorectomy specimens, cytogenetic and morphometric correlations. Cancer (Phila.), *86:* 1544–1550, 1999.

23. Puls, L., Powell, D., DePriest, P. D., Gallion, H. H., Hunter, J. E., Kryscio, R. J., and van Nagell, J. R., Jr. Transition from benign to malignant epithelium in mucinous and serous ovarian cystadeno-carcinoma. Gynecol. Oncol., *47:* 53–57, 1992.

24. Plaxe, S. C., Deligdisch, L., Dottino, P. R., and Cohen, C. J. Ovarian intraepithelial neoplasia demonstrated in patients with stage I ovarian carcinoma. Gynecol. Oncol., *38:* 367–372, 1990.

25. Blaustein, A. Surface cells and inclusion cysts in fetal ovaries. Gynecol. Oncol., *12:* 222–233, 1981.

26. Blaustein, A., Kantius, M., Kaganowicz, A., Pervez, N., and Well, J. Inclusions in ovaries of females aged day 1–30 years. Int. J. Gynecol. Pathol., *1:* 145–153, 1982.

27. Lu, K., Garber, J., Cramer, D., Welch, W., Niloff, J., Schrag, D., Berkowitz, R., and Muto, M. Occult ovarian tumors in women with BRCA1 or BRCA2 mutations undergoing prophylactic oophorectomy. J. Clin. Oncol., *18:* 2728–2732, 2000.

28. Stratton, J. F., Buckley, C. H., Lowe, D., Ponder, B. A. J., and UKCCCR Familial Ovarian Cancer Study Group. Comparison of prophylactic oophorectomy specimens from carriers and non-carriers of a *BRCA1* or *BRCA2* gene mutation. J. Natl. Cancer Inst. (Bethesda), *91:* 626–628, 1999.

29. Barakat, R. R., Federici, M. G., Saigo, P. E., Robson, M. E., Offit, K., and Boyd, J. Absence of premalignant histologic, molecular or cell biologic alterations in prophylactic oophorectomy specimens from BRCA1 heterozygotes. Cancer (Phila.), *89:* 383–390, 2000.

30. Casey, M. J., Bewtra, C., Hoehne, B. S., Tatpati, A. D., Lynch, H. T., and Watson, P. Histology of prophylactically removed ovaries from BRCA1 and BRCA2 mutation carriers compared with non-carriers in hereditary breast ovarian cancer syndrome kindreds. Gynecol. Oncol., *78*: 278–287, 2000.

31. Roby, K. E., Taylor, C. C., Sweetwood, J. P., Cheng, Y., Pace, J. L., Tawfik, O., Persons, D. L., Smith, P. G., and Terranova, P. E. Development of a syngeneic mouse model for events related to ovarian cancer. Carcinogenesis (Lond.), *21:* 585–591, 2000.

32. Davies, B. R., Auersperg, N., Worsley, S. D., and Ponder, B. A. J. Transfection of rat ovarian surface epithelium with *erb*-B2/*neu* induces transformed phenotypes *in vitro* and the tumorigenic phenotype *in vivo*. Am. J. Pathol., *152:* 297–306, 1998.

33. Fredrickson, T. N. Ovarian tumors of the hen. Environ. Health Perspect., *73:* 35–51, 1987.

34. Rodriguez-Burford, C., Barnes, M. N., Berry, W., Partridge, E. E., and Grizzle, W. E. Immuno-histochemical expression of molecular markers in an avian model: a potential model for preclinical evaluation of agents for ovarian cancer chemoprevention. Gynecol. Oncol., *81:* 373–379, 2001.

35. Berchuck, A., Rodriguez, G. C., Kamel, A., Dodge, R. K., Soper, J. T., Clarke-Pearson, D. L., and Bast, R. C., Jr. Epidermal growth factor receptor expression in normal ovarian epithelium and ovarian cancer. I. Correlation of receptor expression with prognostic factors in patients with ovarian cancer. Am. J. Obstet. Gynecol., *164:* 669–674, 1991.

36. Berchuck, A., Kamel, A., Kerns, W. B., Kinney, R., Soper, R., Dodge, D. L., Clarke-Pearson, P., McKenzie, S., Yin, S., and Bast, R. C., Jr. Overexpression of HER-2/neu is associated with poor survival in advanced epithelial ovarian cancer. Cancer Res., *50:* 4087–4091, 1990.

37. Auersperg, N., Edelson, M. I., Mok, S. C., Johnson, S. W., and Hamilton, T. C. The biology of ovarian cancer. Semin. Oncol., *25:* 281–304, 1998.

38. Henzen-Logmans, A. C., van der Burg, M. E. L., Foekens, J. A., Berns, P. M. J. J., Brussee, R., Fieret, J. H., Klijn, J. G. M., Chadha, S., and Rodenburg, C. J. Occurrence of epidermal growth factor receptors in benign and malignant ovarian tumors and normal ovarian tissues: an immunohistochemical study. J. Cancer Res. Clin. Oncol., *118:* 303–307, 1992.

39. Harlozinska, A., Bar, J. K., Sobanska, E., and Goluda, M. Epidermal growth factor receptor and c-*erb*B-2 oncoproteins in tissue and tumor effusion cells of histopathologically different ovarian neoplasms. Tumor Biol., *19:* 364–373, 1998.

40. Simpson, B. J. B., Phillips, H. A., Lessells, A. M., Langdon, S. P., and Miller, W. R. C-*erb* B growth-factor-receptor proteins in ovarian tumors. Int. J. Cancer, *64:* 202–206, 1995.

41. Bartlett, J. M. S., Langdon, S. P., Simpson, B. J. B., Stewart, M., Katsaros, D., Sismondi, P., Love, S., Scott, W. N., Williams, A. R. W., Lessells, A. M., Macleod, K. G., Smyth, J. F., and Miller, W. R. The prognostic value of epidermal growth factor receptor mRNA expression in primary ovarian cancer. Br. J. Cancer, *73:* 301–306, 1996.

42. Ross, J. S., Yang, F., Kallakury, B. V., Sheehan, C. E., Ambros, R. A., and Muraca, P. J. HER-2/neu oncogene amplification by fluorescence *in situ* hybridization in epithelial tumors of the ovary. Am. J. Clin. Pathol., *11:* 311–316, 1999.

43. Niikura, H., Sasano, H., Sato, S., and Yajima, A. Expression of epidermal growth factor-related proteins and epidermal growth factor receptor in common epithelial ovarian tumors. Int. J. Gynecol. Pathol., *16:* 60–68, 1997.

44. Bast, R. C., Puztai, L., Kerns, B. J., MacDonald, J. A., Jordan, P., Daly, L., Boyer, C. M., Mndolson, J., and Berchuk, A. Coexpression of the HER-2/*neu* (c-*erb*B2) gene product (p185) and the epidermal growth factor receptor (p170) on epithelial ovarian cancers and normal tissues. Hybridoma, *17:* 313–321, 1998.

45. Campiglio, M., Ali, S., Knyazev, P. G., and Ullrich, A. Characteristics of EGFR family-mediated HRG signals in human ovarian cancer. J. Cell. Biochem., *73:* 522–532, 1999.

46. Matsumoto, Y., Ishiko, O., Deguchi, M., Nadagawa, E., and Ogita, S. Cyclo-oxygenase-2 expression in normal ovaries and epithelial ovarian neoplasms. Int. J. Mol. Med., *8:* 31–36, 2001.

47. Rodriguez-Burford, C., Barnes, M. N., Oelschlager, D. K., Myers, R. B., Talley, L. I., Partridge, E. E., and Grizzle, W. E. Effects of nonsteroidal anti-inflammatory agents (NSAIDs) on ovarian carcinoma cell lines: Preclinical evaluation of NSAIDs as chemopreventive agents. Clin. Cancer Res. *8:* 202–209, 2002.

48. Bellacosa, A., De Feo, D., Godwin, A. K., Bell, D. W., Cheng, J. Q., Altomare, D. A., Wan, M., Dubeau, L., Scambia, G., Masciullo, V., Ferrandina, G., Benedetti Panici, P., Mancuso, S., Neri, G., and Testa, J. R. Molecular alterations of the AKT2 oncogene in ovarian and breast carcinomas. Int. J. Cancer, *64:* 280–285, 1995.

49. Iwabuchi, H., Sakamoto, M., Sakunaga, H., Ma, Y. Y., Carcangiu, M. L., Pinkel, D., Yang-Feng, T. L., and Gray, J. W. Genetic analysis of benign, low-grade, and high-grade ovarian tumors. Cancer Res., *55:* 6172–6180, 1995.

50. Bast, R. C., and Mills, B. F. Alterations in oncogenes, tumor suppressor genes, and growth factors associated with epithelial ovarian cancers. *In*: J. M. S. Bartlett (ed.), Ovarian Cancer, Methods and Protocols, Methods in Molecular Medicine, pp. 37–48. Totowa, NJ: Humana Press, Inc., 2000.

51. Shayesteh, L., Lu, Y., Kuo, W-L., Baldocchi, R., Godfrey, T., Collins, C., Pinkel, D., Powell, B., Mills, G. B., and Gray, J. W. PIK3CA is implicated as an oncogene in ovarian cancer. Nat. Genet., *21:* 99–102, 1999.

52. Hu, L., Zaloudek, C., Mills, G. B., Gray, J., and Jaffe, R. B. *In vivo* and *in vitro* ovarian carcinoma growth inhibition by a phophatidylinositol 3-kinase inhibitor (LY294002). Clin. Cancer Res., *6:* 880–886, 2000.

53. Berchuck, A., Kohler, M. F., Marks, J. R., Wiseman, R., Boyd, J., and Bast, R. C., Jr. The p53 tumor suppressor gene frequently is altered in gynecologic cancers. Am. J. Obstet. Gynecol., *170:* 246–252, 1994.

54. Centers for Disease Control Cancer and Steroid Hormone Study. The reduction in risk of ovarian cancer associated with oral contraceptive use. N. Engl. J. Med., *316:* 650–655, 1987.

55. Weiss, N. S., Lyon, J. L., Liff, J. M., Vollmer, W. M., and Daling, J. R. Incidence of ovarian cancer in relation to the use of oral contraceptives. Int. J. Cancer, *28:* 669–671, 1981.

56. The WHO Collaborative Study of Neoplasia and Steroid Contraceptives. Epithelial ovarian cancer and combined oral contraceptives. Int. J. Epidemiol., *8:* 538–545, 1989.

57. Rodriguez, G. C., Walmer, D. K., Cline, M., Krigman, H., Lessey, B. A., Whitaker, R. S., Dodge, R., and Hughes, C. L. Effect of progestin on the ovarian epithelium of macaques: cancer prevention through apoptosis? J. Soc. Gynecol. Invest., *5:* 271–276, 1998.

58. Schildkraut, J. M., Calingaert, B., Marchbanks, P. A., Moorman, P. G., and Rodriguez, G. C. Impact of progestin and estrogen potency in oral contraceptives on ovarian cancer risk. J. Natl. Cancer Inst. (Bethesda), *94:* 32–38, 2002.

59. Hughes, D. E., Dai, A., Tiffee, J. C., Li, H. H., Mundy, G. R., and Boyce, B. F. Estrogen promotes apoptosis of murine osteoclasts mediated by TGF-β. Nat. Med., *2:* 1132–1136, 1996.

60. Um, S-J., Lee, S-Y., Kim, E-J., Han, H-S., Koh, Y-M., Hong, K-J., Sin, H-S., and Park, J-S. Anti-proliferative mechanism of retinoid derivatives in ovarian cancer cells. Cancer Lett., *174*: 127–134, 2001.

61. Zhang, D., Holmes, W. F., Wu, S., Soprano, D. R., and Soprano, K. J. Retinoids and ovarian cancer. J. Cell. Physiol., *185:* 1–20, 2000.

62. Formelli, F., and Cleris, L. Synthetic retinoid fenretinamide is effective against a human ovarian carcinoma xenograft and potentiates cisplatin activity. Cancer Res., *53:* 5374–5376, 1993.

63. Taylor, D. D., Taylor, C. G., Black, P. H., Jiang, C. G., and Chou, I. N. Alterations of cellular characteristics of a human ovarian teratocarcinoma cell line after *in vitro* treatment with retinoids. Differentiation, *43:* 123–130, 1990.

64. DePalo, G., Veronesi, U., Camerini, T., Formelli, F., Mascotti, G., and Boni, C. Can fenretinamide protect women against ovarian cancer. J. Natl. Cancer Inst. (Bethesda), *87:* 146–147, 1995.

65. De Palo, G., Mariani, L., Camerini, T., Marubini, E., Formelli, F., Pasini, B., Decensi, A., and Veronesi, U. Effect of fenretinide on ovarian carcinoma occurrence. Gynecol. Oncol., *86:* 24–27, 2002.

66. Guruswamy, S., Lightfoot, S., Gold, M. A., Hassan, R., Berlin, D., Ivey, R. T., and Benbrook, D. M. Effects of retinoids on cancerous phenotype and apoptosis in organotypic cultures of ovarian carcinoma. J. Natl. Cancer Inst. (Bethesda), *93:* 516–525, 2001.

67. Wu, S., Zhang, D., Donigan, A., Dawson, M. I., Soprano, D. R., and Soprano, K. J. Effects of conformationally restricted synthetic retinoids on ovarian tumor cell growth. J. Cell. Biochem., *68:* 378–388, 1998.

68. Brewer, M., Utzinger, U., Li, Y., Atkinson, E. N., Satterfield, W., Auersperg, N., Richards-Kortum, R., Follen, M., and Bast, R. Fluorescence spectroscopy as a biomarker in a cell culture and in a nonhuman rhesus primate model for ovarian cancer chemopreventive agents. J. Biomed. Opt., *7:* 20–26, 2002.

69. Wyllie, A. H. Apoptosis and carcinogenesis. Eur. J. Cell. Biol., *73:* 189–197, 1997.

70. Zou, C. P., Kurie, J. M., Lotan, D., Zou, C. C., Hong, W. K., and Lotan, R. Higher potency of *N*-(4-hydroxyphenyl) retinamide than all-*trans*-retinoic acid in induction of apoptosis in non-small cell lung cancer cell lines. Clin. Cancer Res., *4:* 1345–1355, 1998.

71. Supino, R., Crosti, M., Clerici, M., Warlters, A., Cleris, L., Zunino, F., and Formelli, F. Induction of apoptosis by fenretinide (4-HPR) in human ovarian carcinoma cells and its association with retinoic acid receptor expression. Int. J. Cancer, *65:* 491–497, 1996.

72. Fanjul, A. N., Delia, D., Pierotti, M. A., Rideout, D., Yu, J. Q., Pfahl, M., and Qiu, J. 4-Hydroxyphenyl retinamide is a highly selective activator of retinoid receptors. J. Biol. Chem., *271:* 22441–22446, 1996.

73. Sheikh, M. S., Shao, Z. M., Li, X. S., Ordonez, J. V., Conley, B. A., Wu, S., Dawson, M. I., Han, Q. X., Chao, W. R., and Quick, T. *N*-(4-Hydroxyphenyl) retinamide (4-HPR)-mediated biological actions involve retinoid receptor-independent pathways in human breast carcinoma. Carcinogenesis (Lond.), *16:* 2477–2486, 1995.

74. Dabal, R., Boyer, C. M., Berchuck, A., Roberts, A., Roche, N., Sporn, M., and Bast, W. Synergistic inhibition of ovarian cancer cell proliferation by TGFβ and retinoic acid (RA) derivatives. Proc. Am. Assoc. Cancer Res., *36:* 635, 1995.

75. Oridate, N., Suzuki, S., Higuchi, M., Mitchell, M., Hong, W., and Lotan, R. Involvement of reactive oxygen species in *N*-(4-hydroxyphenyl) retinamide-induced apoptosis in cervical carcinoma cells. J. Natl. Cancer Inst. (Bethesda), *89:* 1191–1198, 1997.

76. Berchuck, A., Rodriguez, G., Olt, G. J., Whitaker, R., Boente, M. P., Arrick, B. A., Clarke-Pearson, D. L., and Bast, R. C., Jr. Regulation of growth of normal ovarian epithelial cells and ovarian cancer cell lines by transforming growth factor-β. Am. J. Obstet. Gynecol., *166:* 676–684, 1992.

77. Jakowlew, S. B., Moody, T. W., and Mariano, J. M. Transforming growth factor-β receptors in human cancer cell lines: analysis of transcript, protein and proliferation. Anticancer Res., *17:* 1849–1860, 1997.

78. Schneider, S. L., Gollnick, S. O., Grande, C., Pazik, J. E., and Tomasi, T. B. Differential regulation of TGF-β 2 by hormones in rat uterus and mammary gland. J. Reprod. Immunol., *32:* 125–144, 1996.

79. Lindstrom, P., Bergh, A., Holm, I., and Damber, J. E. Expression of transforming growth factor-β 1 in rat ventral prostate and Dunning R3327 PAP prostate tumor after castration and estrogen treatment. Prostate, *29:* 209–218, 1996.

80. Rodriguez, G. C., Nimesh, N. P., Lee, K. L., Bentley, R. C., Walmer, D. K., Cline, M., Whitaker, R. S., Isner, P., Berchuck, A., Dodge, R. K., and Hughes, C. L. Progestin-induced apoptosis in the macaque ovarian epithelium: differential regulation of transforming growth factor-β. J. Natl. Cancer Inst. (Bethesda), *94:* 50–60, 2002.

81. Auersperg, N., Maclaren, I. A., and Kruk, P. A. Ovarian surface epithelium: autonomous production of connective tissue-type extracellular matrix. Biol. Reprod., *44:* 717–724, 1991.

82. Parrott, J. A., Nilsson, E., Mosher, R., Magrane, G., Albertson, D., Pinkel, D., Gray, J., and Skinner, M. K. Stroma-epithelial interactions in the progression of ovarian cancer: influence and source of stromal cells. Mol. Cell. Endocrinol., *175:* 29–39, 2001.

83. Parrott, J. A., Kim, G., Mosher, R., and Skinner, M. K. Expression and action of keratinocyte growth factor (KGF) in normal ovarian surface epithelial and ovarian cancer. Mol. Cell. Endocrinol., *167:* 77–87, 2000.

84. Parrott, J. A., Mosher, R., Kim, G., and Skinner, M. K. Autocrine interactions of keratinocyte growth factor, hepatocyte growth factor, and kit-ligand in the regulation of normal ovarian surface epithelial cells. Endocrinology, *141:* 2532–2539, 2000.

85. Wong, A. S. T., Pelech, S. L., Woo, M., Yim, G., Rosen, B., Ehlen, T., Leung, P., and Auersperg, N. Coexpression of hepatocyte growth factor-Met: an early step in ovarian carcinogenesis? Oncogene, *20:* 1318–1328, 2000.

86. Auersperg, N., Maines-Bandiera, S., Dyck, H. G., and Kruk, P. A. Characterization of cultured human ovarian surface epithelial cells: phenotypic plasticity and premalignant changes. Lab. Investig., *71:* 510–518, 1994.

87. Mourant, J. R., Bigio, I. J., Boyer, J., Conn, R. L., Johnson, T., and Shimada, T. Spectroscopic diagnosis of bladder cancer with elastic light scattering. Lasers Surg. Med., *17:* 350–357, 1995.

88. Ge, Z., Schomacker, K. T., and Nishioka, N. S. Identification of colonic dysplasia and neoplasia by diffuse reflectance spectroscopy and pattern recognition techniques. Appl. Spectrosc., *52:* 833–345, 1998.

89. Koenig, F., Larne, R., Enquist, H., McGovern, F. J., Schomacker, K. T., Kollias, N., and Deutsch, T. F. Spectroscopic measurement of diffuse reflectance for enhanced detection of bladder carcinoma. Urology, *51:* 342–345, 1998.

90. Backman, V., Wallace, M., Perelman, L. T., Arendt, J. T., Gurjar, R., Müller, M. G., Zhang, Q., Zonios, G., Kline, E., McGillican, T., Shapshay, S., Valdez, T., Badizadegan, K., Crawford, J. M., Fitzmaurice, M., Kabani, S., Levin, H. S., Seiler, M., Dasari, R. R., Itzkan, I., Van Dam, J., and Feld, M. S. Detection of preinvasive cancer cells. Nature (Lond.), *406:* 35–36, 2000.

91. Richards-Kortum, R., and Sevick-Muraca, E. Quantitative optical spectroscopy for tissue diagnosis. Annu. Rev. Phys. Chem., *47:* 555–606, 1996.

92. Mahadevan-Jansen, A., and Richards-Kortum, R. Raman spectroscopy for the detection of cancers and precancers. J. Biomed. Opt., *1:* 31–70, 1996.

93. Bigio, I. J., and Mourant, J. R. Ultraviolet and visible spectroscopies for tissue diagnostics: fluorescence spectroscopy and elastic-scattering spectroscopy. Phys. Med. Biol., *42:* 803–814, 1997.

94. Chance, B. Metabolic heterogeneities in rapidly metabolizing tissues. J. Appl. Cardiol., *4:* 207–221, 1989.

95. Gulledge, C. J., and Dewhirst, M. W. Tumor oxygenation: a matter of supply and demand. Anticancer Res., *16:* 741–750, 1996.

96. Brewer, M., Utzinger, U., Silva, E., Gershenson, D., Bast, R. C., Jr., Follen, M., and Richards-Kortum, R. Fluorescence spectroscopy for *in vivo* characterization of ovarian tissue. Lasers Surg. Med., *29:* 128–135, 2001.

97. Brewer, M., Utzinger, U., Silva, E., Gershenson, D., Bast, R. C., Jr., Follen, M., Wharton, J. T., and Richards-Kortum, R. Biomarker modulation in a nonhuman rhesus primate model for ovarian cancer chemoprevention. Cancer Epidemiol. Biomark. Prev., *10:* 889–893, 2001.

98. Blume-Jensen, P., and Hunter, T. Oncogenic kinase signaling. Nature (Lond.), *411:* 355–365, 2001.

99. Slichenmyer, W. J., and Fry, D. W. Anticancer therapy targeting the ErbB family of receptor tyrosine kinases. Semin. Oncol., *28:* 67–79, 2001.

100. Moulder, S. L., Yakes, M., Muthuswamy, S. K., Bianco, R., Simpson, J. F., and Arteaga, C. L. Epidermal growth factor receptor (HER1) tyrosine kinase inhibitor ZD1839 (Iressa) inhibits HER2/*neu* (*erb*B2)-overexpressing breast cancer cells *in vitro* and *in vivo*. Cancer Res., *61:* 8887–8895, 2001.

101. Steinbach, G., Lynch, P. M., Phillips, R. K., Wallace, M. H., Hawk, E., Gordon, G. B., Wakabayashi, N., Saunders, B., Shen, Y., Fujimura, T., Su, L. K., and Levin, B. The effect of celecoxib, a cyclooxygenase-2 inhibitor, in familial adenomatous polyposis. N. Engl. J. Med., *342:* 1946–1952, 2000.

102. Ness, R. B., and Cottreau, C. Possible role of ovarian epithelial inflammation in ovarian cancer. J. Natl. Cancer Inst. (Bethesda), *91:* 1459–1467, 1999.

103. Williams, A. R. W. Pathological assessment of ovarian cancer. *In*: J. M. S. Bartlett (ed.), Ovarian Cancer, Methods and Protocols, Methods in Molecular Medicine, pp. 49–60. Totowa, NJ: Humana Press, Inc., 2000.

104. Zheng, J., Benedict, W. F., Xu, H. J., Hu, S. X., Kim, T. M., Velicescu, M., Wan, M., Cofer, K. F., and Dubeau, L. Genetic disparity between morphologically benign cysts contiguous to ovarian carcinomas and solitary cystadenomas. J. Natl. Cancer Inst. (Bethesda), *87:* 1146–1153, 1995.

105. Liotta, L., and Petricoin, E. F. Molecular profiling of human cancer. Nat. Rev. Genet., *1:* 48–56, 2000.

106. Petricoin, E. F., Ardekani, A. M., Hitt, B. A., Levine, P. J., Fusaro, V. A., Steinberg, S. M., Mills, G. B., Simone, C., Fishman, D. A., Kohn, E. C., and Liotta, L. A. Use of proteomic patterns in serum to identify ovarian cancer. Lancet, *359:* 572–577, 2002.

107. Liotta, L., Kohn, L. C., and Petricoin, E. F. Clinical proteomics, personalized molecular medicine. J. Am. Med. Assoc., *286:* 2211–2214, 2001.

Biomarker Modulation in a Nonhuman Rhesus Primate Model for Ovarian Cancer Chemoprevention[1]

Molly Brewer,[2] Urs Utzinger, William Satterfield, Lori Hill, David Gershenson, Robert Bast, J. Taylor Wharton, Rebecca Richards-Kortum, and Michele Follen

Departments of Gynecologic Oncology [M. B., D. G., J. T. W., M. F.], Veterinary Sciences Science Park [W. S., L. H.], and Medicine [R. B.], University of Texas M. D. Anderson Cancer Center, Houston, Texas 77030; Department of Obstetrics, Gynecology and Reproductive Science, University of Texas Medical School, Houston, Texas 77030 [M. B., M. F.]; and Biomedical Engineering Program, University of Texas at Austin, Austin, Texas 78712 [U. U., R. R-K.]

Abstract

Objective: The objective of this study was to explore *whether a nonhuman primate model could be developed to test drugs for the prevention of ovarian cancer.*

Methods: Nineteen adult female Rhesus macaques were given fenretinide (4HPR), oral contraceptives (OCP), the combination (4HPR + OCP), or no medication for 3 months. Exploratory laparotomy was done pre- and postdrug to assess intermediary biomarkers of neoplastic phenotype, proliferation, response pathways, and growth-regulatory and metabolic markers. Fluorescence emission spectra were plotted for each group pre- and postdrug and means were overlaid on these plots and normalized. Fluorescence intensities were compared using the 2-tailed Student *t* test, ($P = 0.1–0.01$).

Results: **All monkeys tolerated drugs and surgeries without difficulty. Histochemical markers showed no significant trend. However, fluorescence spectroscopy showed increased intensity at 450 nm excitation, 550 nm emission correlating with increased FAD presence. The 4HPR group ($P = 0.01$) showed higher intensity than the OCP group ($P = 0.05–0.07$) when compared with the controls. Decreased emission was seen at 350 nm excitation, 450 nm emission correlating with decreased NAD(P)H presence. The OCP group showed the largest change ($P < 0.01$), and the control group showed the smallest change.**

Conclusions: **The nonhuman primate is an excellent model to test drug effect on the ovarian surface epithelium and merits additional study. Fluorescence spectroscopy was the most sensitive marker for drug activity and the apparent increase in NAD and FAD in the 4HPR group is consistent with the effect of 4HPR observed in cell culture. The differences between the OCP and the 4HPR groups suggest a different mechanism of activity of these drugs.**

Introduction

Epithelial ovarian cancer has the highest mortality rate of any of the gynecological cancers, with a 5-year survival rate of 30% or less, despite aggressive treatment. Seventy percent of these cancers are diagnosed with widespread intra-abdominal disease or distant metastases, which accounts for the dismal prognosis for ovarian cancer. Even ovarian cancer limited to the pelvis has a 5-year survival rate of only 50% (1). Thus, cancer prevention merits at least as much attention as does treatment of disease that has already occurred. Cancer chemoprevention is a rapidly growing area of research because of the difficulties in treating advanced cancers. Chemoprevention refers to the administration of chemical agents that prevent or delay cancer in normal or undiseased people. Necessary elements for chemoprevention studies include appropriate agents that are safe and which have both epidemiological and mechanistic data that support their use; a suitable cohort with adequate incidence of disease and in which the risk:benefit ratio is acceptable; and measurable biomarkers that are likely to be affected by the agent and whose modulation supports the postulated chemopreventive activity (2). Biomarkers are important because they are relevant to the development of neoplasia, either phenotypically (proliferation, angiogenesis, or nuclear morphometry) or mechanistically (molecular markers), they are likely to be required for a response to the chemopreventive agent, or they are relevant to carcinogenesis (3).

Two drugs that have received attention as agents that can prevent ovarian cancer are OCPs[3] and retinoids. There are multiple epidemiological studies that show that OCP use of at least 5 years' duration is associated with a 50% or greater reduction in the odds of developing ovarian cancer (4–8). The mechanism of this prevention is unclear; ovulation suppression may be one factor, but other mechanisms are hypothesized. A single prospective study showed that OCP and progesterone increased the rate of apoptosis of ovarian surface epithelial cells in primates (9). Premenopausal women with a family history of breast cancer, ovarian cancer, or both are excellent candidates for prevention strategies; however, in premenopausal women the potential teratogenicity of retinoids is a concern (10). Epidemiological and laboratory data suggest that retinoids may have a role as preventive or therapeutic agents for ovarian cancer (11–12). 4-HPR has the fewest side effects of the vita-

Received 12/1/00; revised 5/25/01; accepted 5/31/01.
The costs of publication of this article were defrayed in part by the payment of page charges. This article must therefore be hereby marked *advertisement* in accordance with 18 U.S.C. Section 1734 solely to indicate this fact.
[1] Supported by the Sandra G. Davis Ovarian Cancer Research Program and Dr. J. Taylor Wharton.
[2] To whom requests for reprints should be addressed, at Department of Gynecologic Oncology, The University of Texas M. D. Anderson Cancer Center, Houston, TX 77030. Phone: (713) 500-6391; Fax: (713) 500-0796; E-mail: Molly.Brewer@uth.tmc.edu.

[3] The abbreviations used are: OCP, oral contraceptive; 4-HPR, fenretinide; EEM excitation and emission matrix.

min-A derivatives and is currently being used in chemoprevention studies in other organ sites including lung, head and neck, cervix, and bladder. Preliminary results from the 2972 women in the Italian randomized chemoprevention trial for prevention of secondary breast cancers suggest that retinoids have preventive activity against ovarian cancer (12). Ovarian cancer developed in six women in the placebo arm, but there were no cancers in the 4HPR arm. Although this response was not durable, it suggested retinoid activity in the ovary. Experimental studies have demonstrated that retinoids can affect human ovarian cancer cell growth by inhibiting proliferation and inducing apoptosis (13–15). Preliminary data from our laboratory shows that 4HPR induces a rate of 40–95% apoptosis in immortalized ovarian surface epithelial cells and 30–90% in normal ovarian surface epithelial cells,[4] compared with the baseline rate of 1–3% in untreated cells. The probability of developing a neoplasm will decrease with increasing apoptosis.

Substantial research has been done to develop optical methods as early diagnostic tools for cancers in the last decade (16–19). Optical spectroscopy has the potential to decrease the necessity for pathological diagnosis; to aid in early, near-real-time diagnosis; and to identify abnormal areas that may not have a visible lesion for localization of biopsy. Fluorescence spectroscopy uses energy in the form of a light photon to activate certain molecules within a cell; the subsequent radiative relaxation of the molecule and the release of a reemission photon is the process called fluorescence. It is an optical method of illuminating tissue with monochromatic light and exciting the natural fluorophores within tissue, which then emits fluorescent light when a paired electron in an excited state returns to a lower or ground state. Natural fluorophores in tissue include NADH; FAD; structural proteins such as collagen, elastin, and their cross-links; and the aromatic amino acid tryptophan, each of which has a characteristic wavelength for excitation with an associated characteristic emission. Fluorophore concentrations change as tissue progresses from normal to a preneoplastic state to cancer (20). Theoretically, different changes in the fluorescent signature should occur in response to an agent that induces quiescence or apoptosis.

It is difficult to study the ovary because its intraperitoneal location makes access difficult; therefore, the development of an animal model to study these drugs is appealing. Small animal models (mice, chicken, and guinea pigs) are being developed for ovarian cancer that are useful for understanding basic mechanisms, but these animals differ from the human reproductively. Primates, however, are much closer to humans in reproductive function and anatomy, hormonal and menstrual patterns (9, 21), and histochemistry and will be a better model with which to develop strategies for prevention of ovarian cancer in the future. This study describes the use of the *Macaca mulatta* as a nonhuman primate model to test drugs for the prevention of ovarian cancer.

Materials and Methods

Initially, a pilot study was done with three animals to test drug tolerance, tolerance for two surgical procedures, and the feasibility of the model. After this pilot, 19 female adult *M. mulatta* were brought together for this preliminary exploratory study. This protocol was approved by the Animal Care Use Committee at The University of Texas M.D. Anderson Cancer Center and was conducted at the Department of Veterinary Sciences in Bastrop, Texas, an Association for the Assessment and Accreditation of Laboratory Animal Care International-accredited facility, in accordance with the *Guide for the Care and Use of Laboratory Animals*. Numbers were chosen based on cost and availability of animals: five animals were initially placed in each drug group, and four were placed in the control group. This study was a pilot study designed to generate measurements so that future studies could be designed with adequate numbers.

The animals were given 4HPR (five monkeys), OCP (five monkeys), the combination of 4HPR+OCP (five monkeys), or no medication (four monkeys) daily for 3 months. Doses of 4HPR and OCP were calculated by allometric scaling, which calculates a dose based on both weight and basal metabolic rate (22). This is derived from the equation $Y + K(W_{kg}^{0.75})$, where *Y* is the resting animal's energy output in kcal/24 h (also termed the minimum energy cost), K is a constant based on core temperature, which is specific for each species, and W is mass in kilograms. Monkeys ranged in weight from 6–8 kg, but doses were calculated for a 7 kg monkey. The OCP used was Ortho-Novum 1/35, a medium-dose OCP known to suppress cyst formation, which has 1 mg of norethindrone and 35 μg of ethinyl estradiol in each pill. The 4-HPR dose was calculated in the same manner from the human dose of 200 mg daily. The OCP dose was 0.2 mg norethindrone/0.07 mg of ethinyl estradiol, and the 4HPR dose was 35 mg.

Before starting medication and after 90 days of medication, monkeys underwent laparotomy and ovarian biopsies. Two to three 2-mm samples were taken from the left ovary at the time of the first surgery and from the right ovary at the time of the second surgery. Fluorescence measurements were taken from each site before biopsy. Biopsy and healing of the ovary was hypothesized to interfere with the spectroscopic signature because of the increased collagen associated with healing as well as with histochemical assessment. Thus, to avoid this bias, one ovary was biopsied on the first surgery and the other ovary was biopsied on the second surgery.

Biomarkers. Biomarkers chosen for this trial include markers of neoplastic phenotype (p53), proliferative markers (Ki67), markers of intact response pathways (estrogen, progesterone, and nuclear retinoid receptors), or inducible growth-regulatory molecules (TGF-β and receptors HER-2, BAX, and BCLx). Apoptosis was evaluated with Apotag. The remainder of the markers were either mouse or rabbit antibodies that were evaluated by immunohistochemistry in the standard manner. The choice of these markers was based on previous studies (apoptotic, proliferative, neoplastic, and retinoid markers), known pathways (retinoid markers), and hypothesized mechanisms (TGFβ and receptors and p21).

Complete characterization of the fluorescence properties of an unknown sample requires measurement of a fluorescence EEM, with the fluorescence intensity recorded as a function of both excitation and emission wavelengths (23). Our custom-made system records EEMs in $<$1.5 min and consists of a xenon arc lamp coupled to a scanning spectrometer that provides excitation light between 300–480 nm. A fiber optic probe directs excitation light to the tissue and collects emitted fluorescence light, which it delivers to an imaging spectrograph and CCD camera. Fig. 1 shows the probe placed on a monkey ovary. Fluorescence emission spectra ranging from 320–850 nm were collected sequentially at 19 excitation wavelengths ranging from 300–480 nm. Before assembling the data into fluorescence EEMs, system-dependent response and background signals were removed. Tissue exposure to broadband UV radiation from this device is below the total exposure limits

[4] Unpublished data.

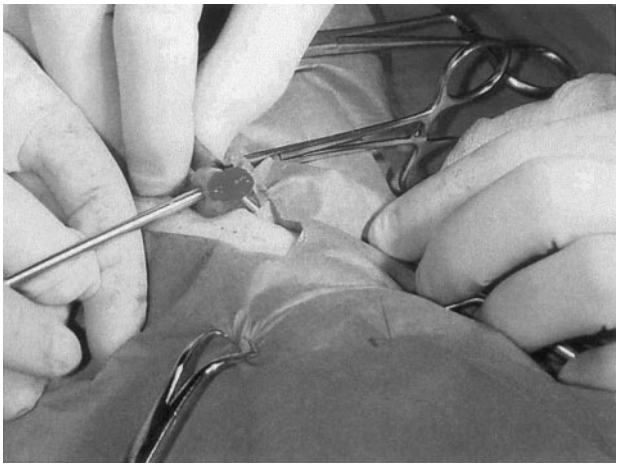

Fig. 1. Fast EEM probe placed on the monkey ovary at the time of laparotomy.

developed by the American Conference of Governmental Industrial Hygienists (ACGIH) for epithelial tissues.

Data Analysis. A visual analytic tool was developed to explore fluorescence differences grouped by monkey, drug, and time (pre- and postdrug), and emission spectra were plotted for each group pre- and postdrug at each excitation wavelength measured. Means were calculated and overlaid on these plots to view the relationship. The data were examined in two fashions: the raw intensities were compared, and emission spectra were normalized to a common wavelength to enhance relative spectral contributions. Using this information, we compared all fluorescence measurements between the first and second measurements using the two-tailed Student *t* test. *P*s were between 0.1 and 0.01 for this exploratory study. Areas where statistically significant differences were observed between the first (predrug) and second (postdrug) measurements were identified in the EEM and plotted as contour lines.

Animal Care. Monkeys used in this study were culled from the specific pathogen free rhesus colony because they developed herpes-B-indeterminate status, they were poor breeders, or they had chronic diarrhea. The monkeys were prevented from eating for 12 h before surgery. Anesthesia was induced with an i.m. injection of tiletamine HCl/zolazepam HCl (Telazol; Fort Dodge Laboratories, Inc., Fort Dodge, IA). When the monkey was sedated, she was removed from the cage and intubated, and anesthesia was maintained on 2–2.5% isoflurane gas with oxygen. After each initial procedure, monkeys were maintained in separate housing and were fed the drug in a flavored treat. Menses were recorded daily, and progesterone levels were measured 2 weeks apart to evaluate ovulatory status.

Pathology. Biopsy specimens were fixed in 10% neutral buffered formalin, embedded in paraffin, cut into 4-mm sections, and stained with H&E for light microscopic examination. Sections were evaluated for morphological characteristics and pathological changes.

Results

Animal Tolerance. The pilot study showed that the three animals tolerated the drugs and two surgeries without difficulty. Rhesus monkey ovaries are easily accessible through a midline laparotomy incision and are 1–1.5 cm in length and 0.75–1 cm in the other two dimensions (see Fig. 1). At the time of the second surgery, the scar from the previous biopsy was completely healed and there was a small visible area <1 mm where the defect had filled in. In the larger study, there was one death of a monkey in the 4HPR group that was not related to this study. She was a 9-year-old obese macaque with severe amyloidosis on necropsy.

Fluorescence Measurements. There were consistent differences in the absolute fluorescence intensities and relative contributions noted between the pre- and postdrug measurements in each drug group as well as in the controls. However, the differences noted in the control group that were attributable to a time effect were much smaller than those seen in the three drug groups. Fig. 2 shows areas of significant differences between the pre- and postdrug measurements for all 4 groups. To the right of each graph is the *P*, from 0.01–0.1. Two main areas of change can be identified. The center of the first area is located at 450 nm excitation and 550 nm emission wavelength, consistent with the FAD emission peak. This area of fluorescence intensity is increased in the three postdrug groups, which correlates with increased FAD presence and decreased FADH. The 4HPR group ($P = 0.01$) shows a larger area of difference in pre and postdrug intensity than the OCP group ($P = 0.05$–0.07), whereas the combination group is in between the 4HPR and OCP groups. There were no differences attributable to treatment seen in the control group in this area of the EEM. The second area is located in the 350 nm excitation, 450 nm emission wavelength, which is consistent with the NAD(P)H emission peak. All four groups show decreases in these intensities that correlate with a decreased NAD(P)H presence and thus an increase in NAD(P) (the oxidized form). However, the OCP group shows the largest change ($P < 0.01$), the control group shows the smallest change (very small area of significant change), followed by the 4HPR and OCP group; and, again, the drug combination lies in between the 4HPR and OCP groups.

Other Biomarkers. Markers were evaluated visually in a 2×2 table. Missing data in the 4HPR as well as the OCP group precluded any data analysis, inasmuch as there were only two monkeys with histochemical marker data in the 4HPR group and four in the OCP group because of difficulties in slide preparation. The markers did not show consistent changes in response to drug group, but there were trends noted in marker expression. EGFR was consistently present, in both pre- and postdrug measurements; Her-2, p21, and p53 were rarely present in either group, whereas BAX was usually present in both groups. Estrogen receptors were absent, whereas progesterone receptors were usually present and did not change in response to drug exposure. Two monkeys in the OCP group showed apoptosis and TGFβ declining after exposure to drug. However, there were two monkeys that did not show either marker present before or after drug exposure; However, if trends were actually present, they were not large enough, given our numbers, to have adequate power to detect a difference statistically.

Discussion

The pilot study of three monkeys was done to assess and plan the feasibility of developing a primate model for a chemoprevention study. After that, we did a larger study to develop additional expertise in administering the drugs for a longer period of time, in multiple surgical procedures on a larger number of animals, and in handling and processing the ovary. The primate was chosen because of the close association with humans, and the rhesus monkeys were chosen because of their availability, their cost, and their ease of handling. A "before and

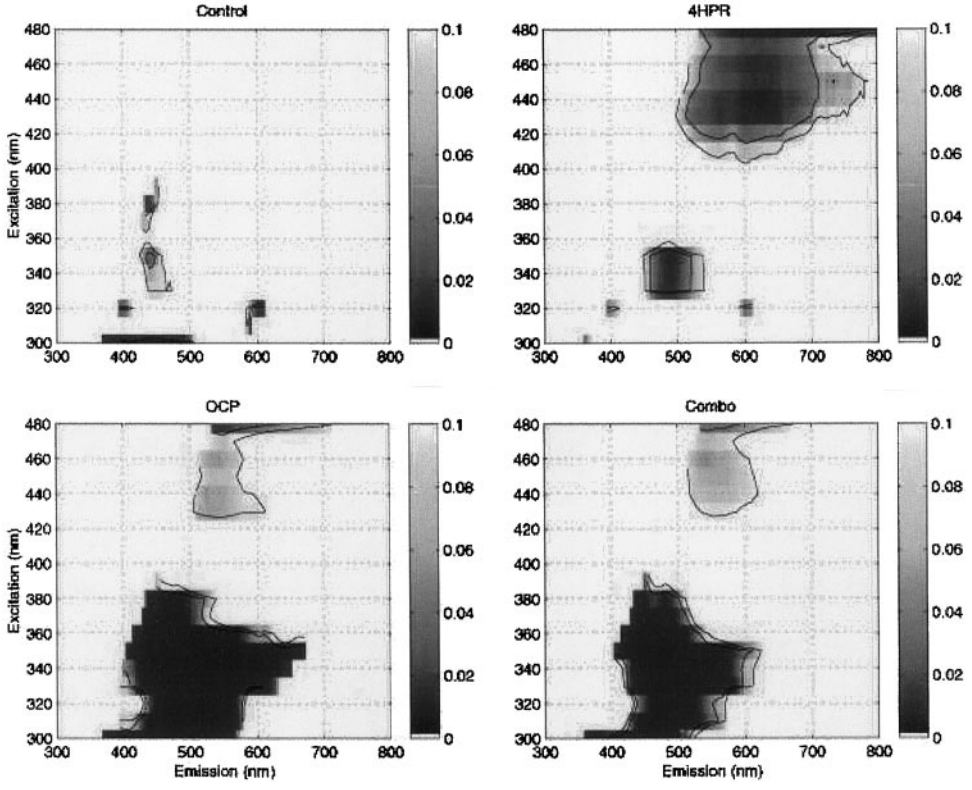

Fig. 2. Results from a two-tailed Student *t* test of pre- and postdrug measurements are presented for the control group (*top left*), the 4HPR group (*top right*), the OCP group (*bottom left*), and the combination group (*bottom right*). Each graph illustrates *P*s between 0 and 0.1 at all measured fluorescence intensities. *Abscissa*, the fluorescence emission wavelength; *ordinate*, the fluorescence excitation wavelength. *P*s are color coded, and a low *P* is represented by a *dark* color, indicating an area where the drug treatment has affected significantly the average fluorescence emission.

after" drug study has the advantage of controlling for intraspecies variation as well as variations attributable to time—things that historical controls or separate control groups cannot account for.

Animal models are developed to reconcile biological phenomena between species (24) and to allow for extrapolation of knowledge from one species to another. Humans are difficult to use as an experimental model because of ethical limitations, cost limitations, and lack of volunteers. Transgenic mice are commonly used because of their availability and cost, but, in addition to their different reproductive physiology (21) from all primates, their compromised immune systems cannot approximate a normal host for chemoprevention. The nonhuman primate more closely approximates the human in its reproductive physiology and thus remains an important model that needs additional development. The cost of procuring and caring for rhesus monkeys and their low reproductive rates, long developmental periods, and relative scarcity have limited their use as animal models for human diseases. However, the close genetic similarity and, thus, the high probability of producing results that can be extrapolated to humans more than overcomes the above limitations (25). Histochemical analysis (26) and hormone activity (21) of the nonhuman primate ovary show remarkable similarities to that of humans, and the microanatomy of all primates, both human and nonhuman, is almost identical, which is consistent with their close phylogenetic linkage. The fact that all animals in this study were not "reproductively healthy" should not affect our results, and in fact should make this study population more analogous to the diversity seen in women, rather than the selection seen in most breeding colonies.

Fluorescence spectroscopy is being used to noninvasively detect cancers in many organ systems. In this study, we evaluated it as a marker for drug activity in the ovary. Redox potential can be calculated by $(FAD/(FAD + NADH)$ and is a measure of the relative hypoxia of the tissue (20). FAD and NAD(P) are reduced in the citric acid cycle (anaerobic glycolysis) to FADH and NAD(P)H, which are used as coenzymes in the electron transport chain. In tumors, these coenzymes will accumulate in their reduced state (NADH or FADH) with a unique fluorescence signature (NADH, high, and FAD, low) as a result of alterations in blood flow, decreased pH of the tissue, and abnormal mitochondria as well as abnormal transport of electron carrier molecules into the mitochondria (27), where the electron transport chain takes place. Although these coenzymes have a unique signature, there is considerable overlap in tissue from other fluorophores, such as structural proteins, and reabsorption of emitted fluorescence by blood. Therefore, results in living tissue are affected by several factors and not these coenzymes alone. This study shows that the opposite occurs in response to the chemopreventive agents. NAD(P)H is reduced consistently by the drugs, and FAD is increased. 4HPR decreases NAD(P)H less than does OCP or the combination of the two drugs, and it increases FAD more than either OCP or the combination, suggesting that each agent has a unique effect on cellular metabolism. These agents show an increase in the redox potential of the target organ, suggesting that less hypoxia is present and that the system is more quiescent. Although numbers were small in this study, variances were also small, suggesting that there is a consistent effect of these drugs on the fluorescence signature of the ovary. By measuring fluorescence from endogenous fluorophores with this system, we were able to identify two areas in the EEM that are affected by these drugs. Thus, a system could be constructed easily to interrogate the entire ovary

and to potentially quantify the drug effect on the ovary as well as to identify areas of occult cancer, which are thought to be more common in BRCA1-positive women (28). The use of fluorescence as a biomarker has a distinct advantage over the repeat biopsy of the ovary and, with the additional development of algorithms, could be used for an "optical biospy," in lieu of a tissue biopsy, to reassess biomarkers in the original field of investigation.

Although the histochemical marker data were not definitive, some data were gathered regarding the ability to test these histochemical methods in the monkey as well as some data on markers that are present or absent in the rhesus. One of the hypotheses of our group and others is that both progesterone and 4HPR induce apoptosis in the ovarian surface epithelial cells. This may be by a direct effect on the epithelial cells or by induction of TGFβ by the stromal cells. Preliminary data from our laboratory suggests that 4HPR and TGFβ act synergistically in induction of apoptosis in normal ovarian epithelial cells. We did not document this effect with histochemistry. TGFβ1 was the marker tested, and there is evidence from Rodriquez (9) that TGFβ1 may be decreased, whereas TGFβ2 and -3 are increased. BAX and BCLx are proteins produced by the *bcl2* gene family that are thought to be modulated by retinoids, with BAX being proapoptotic and BCLx being antiapoptotic. The 4HPR group did not have enough data to evaluate this effect on either protein. The numbers in this pilot were not adequate to show a statistically significant drug effect in any of the categories, if such an effect exists.

The nonhuman primate is an excellent model for investigating the effects of chemopreventive agents for ovarian cancer. There is evidence that OCP and 4HPR have different effects on the ovary that merit additional study. Although there was no rationale for the sample size except cost and the availability of monkeys, the results of this study will allow us to plan for additional animal studies with better power. In addition, changes caused by the chemopreventive agents have the potential to be followed optically, and this may prove helpful in assessing responses to the drugs. The clear difference in activity in the ovary as a result of 4HPR activity suggests that this is a drug meriting additional study in both monkeys and women. The largest effect consistent with decreased NADH presence was seen in the monkeys who were given OCP, the largest effect consistent with increased FAD presence was seen in the monkeys given 4HPR, whereas a combination of effects was seen in the monkeys given both OCP and 4HPR. The additional development of this nonhuman primate model for assessing chemopreventive agents for ovarian cancer will allow us to make significant progress in understanding how these drugs affect the ovary and in developing rational chemoprevention strategies for this devastating disease.

References

1. Hoskins, W. J. Prospective on ovarian cancer: why prevent? J. Cell. Biochem., *23* (Suppl.)*:* 189–199, 1995.

2. Kelloff, G. J., Boone, C. W., Crowell, J. A., Nayfield, S. G., Hawk, E., Steele, V. E., Lubet, R. A., and Sigman, C. C. Strategies for Phase II cancer chemoprevention trials: cervix, endometrium, and ovary. J. Cell. Biochem., *23* (Suppl.)*:* 1–9, 1995.

3. Dhingra, K. A Phase II chemoprevention trial design to identify surrogate endpoint biomarkers in breast cancer. J. Cell. Biochem., *23* (Suppl.)*:* 19–24, 1995.

4. Whittemore, A. S., Harris, R., Itnyre, J., and the Collaborative Ovarian Cancer Group. Characteristics relating to ovarian cancer risk: collaborative analysis of 12 U. S. case-control studies. II. Invasive epithelial ovarian cancers in white women. Am. J. Epidemiol., *136:* 1184–1203, 1992.

5. Franceschi, S., Parazzini, F., Negri, E., Booth, M., La Vecchia, C., Beral, V., Tzonou, A., and Trichopoulos, D. Pooled analysis of 3 European case-control studies. III. Oral contraceptive use. Int. J. Cancer, *49:* 61–65, 1991.

6. Centers for Disease Control, Cancer, and Steroid Hormone Study. Oral contraceptive use and the risk of ovarian cancer. JAMA, *249:* 1596–1599, 1983.

7. Rosenberg, L., Shapiro, S., Slone, D., Kaufman, D. W., Helmrich, S. P., Miettinen, O. S., Stolley, P. D., Rosenshein, N. B., Schottenfeld, D., and Engle, R. L. Epithelial ovarian cancer and combination oral contraceptives. JAMA, *247:* 3210–3212, 1982.

8. Rosenberg, L., Palmer, J. R., Zauber, A. G., Warshauer, M. E., Lewis, J. L., Jr., Strom, B. L., Harlap, S., and Shapiro, S. A case-control study of oral contraceptive use and invasive epithelial ovarian cancer. Am. J. Epidemiol., *139:* 654–661, 1994.

9. Rodriguez, G. C., Walmer, D. K., Cline, M., Krigman, H., Lessey, B. A., Whitaker, R. S., Dodge, R., and Hughes, C. L. Effect of progestin on the ovarian epithelium of macaques: cancer prevention through apoptosis? J. Soc. Gynecol. Investig., *5:* 271–276, 1998.

10. Hendrickx, A. G., and Dukelow, W. R. Reproductive biology. *In:* Nonhuman Primates in Biomedical Research. Academic Press, Inc., 1995.

11. Mori, M., Harabuchi, I., Miyake, H., Casagrande, J. T., Henderson, B. E., and Ross, R. K. Reproductive, genetic, and dietary risk factors for ovarian cancer. Am. J. Epidemiol., *128:* 771–777, 1988.

12. De Palo, G., Veronesi, U., Camerini, T., Formelli, F., Mascotti, G., Boni C., Fosser, V., Del Vecchio, M., Campa, T., and Costa, A. Can fenretinamide protect women against ovarian cancer. J. Natl. Cancer Inst. (Bethesda), *87:* 146–147, 1995.

13. Taylor, D. D., Taylor, C. G., Black, P. H., Jiang, C. G., and Chou, I. N. Alterations of cellular characteristics of a human ovarian teratocarcinoma cell line after *in vitro* treatment with retinoids. Differentiation, *43:* 123–130, 1990.

14. Dabal, R., Boyer, C. M., Berchuck, A., Roberts, A., Roche, N., Sporn, M., and Bast, R. Synergistic inhibition of ovarian cancer cell proliferation by TGFβ and retinoic acid (RA) derivatives. Proc. Am. Assoc. Cancer Res., *36:* 635, 1995.

15. Supino, R., Crosti, M., Clerici, M., Warlters, A., Cleris, L., Zunino, F., and Formelli, F. Induction of apoptosis by fenretinide (4HPR) in human ovarian carcinoma cells and its association with retinoic acid receptor expression. Int. J. Cancer, *65:* 491–497, 1996.

16. Marchesini, R., Brambilla, M., Pignoli, E., Bottiroli, G., Croce, A. C., Dal Fante, M., Spinelli, P., and di Palma, S. Light-induced fluorescence spectroscopy of adenomas, adenocarcinomas and non-neoplastic mucosa in human colon. Photochem. Photobiol., *14:* 219–230, 1992.

17. Cothren, R. M., Richards-Kortum, R. R., Rava, R. P., Boyce, G. A., Doxtader, M., Blackman, R., Ivanc, T. B., and Hayes, G. B. Gastrointestinal tissue diagnosis by LIF spectroscopy at endoscopy. Gastrointest. Endosc., *36:* 105–111, 1990.

18. Hung, J., Lam, S., LeRiche, J. C., and Palcic, B. Autofluorescence of normal and malignant bronchial tissue. Lasers Surg. Med., *11:* 99–105, 1991.

19. Lam, S., Hung, J. Y. C., Kennedy, S. M., LeRiche, J. C., Vedal, R., Nelems, B., Macaulay, C. E., and Palcic, B. Detection of dysplasia and carcinoma *in situ* by ratio fluorometry. Am. Rev. Respir. Dis., *146:* 1458–1461, 1992.

20. Chance, B. Metabolic heterogeneities in rapidly metabolizing tissues. J. Appl. Cardiol., *4:* 207–221, 1989.

21. Hild-Petito, S., Stouffer, R. L., and Brenner, R. M. Immunocytochemical localization of estradiol and progesterone receptors in the monkey ovary throughout the menstrual cycle. Endocrinology, *123:* 2896–2905, 1988.

22. Sedgwick, C. J. and Pokras, M. A. Extrapolating rational drug doses and treatment by allometric scaling. Proceedings of the 55th Annual Meeting of the AAHA, 1988.

23. Gillenwater, A., Jacob, R., and Richards-Kortum, R. Fluorescence spectroscopy: a technique with potential to improve the early detection of aerodigestive tract neoplasia. Head Neck, *20:* 556–562, 1998.

24. Bourne, G. H. Nonhuman primates and medical research. New York and London: Academic Press, 1973.

25. Lewis, S. M., and Carraway, J. H. Large animal models of human disease. Animal Model, January 22–29, 1992.

26. Khan-Dawood, F. S., Dawood, M. Y., and Tabibzadeh, S. Immunohistochemical analysis of the microanatomy of primate ovary. Biol. Reprod., *54:* 734–774, 1996.

27. Gulledge, C. J. and Dewhirst, M. W. Tumor oxygenation: a matter of supply and demand. Anticancer Res., *16:* 741–750, 1996.

28. Lu, K., Garber, J., Cramer, D., Welch, W., Niloff, J., Schrag, D., Berkowitz, R., and Muto, M. Occult ovarian tumors in women with BRCA1 or BRCA2 mutations undergoing prophylactic oophorectomy. JCO, *18:* 2728–2732, 2000.